UNIVERSIDAD NACIONAL AUTÓNOMA DE MÉXICO

Maestría y Doctorado en Ciencias Bioquímicas

Identificación de posibles biomarcadores pronóstico asociados con la expresión de los oncogenes E6 y E7 del Virus del Papiloma Humano tipo 16 en cáncer cervical

TESIS

QUE PARA OPTAR POR EL GRADO DE:

Doctor en Ciencias

PRESENTA:
Leslie Olmedo Nieva

Dra. Marcela Lizano Soberón
Unidad de Investigación Biomédica en Cáncer, Instituto Nacional de Cancerología; Departamento de Medicina Genómica y Toxicología Ambiental, Instituto de Investigaciones Biomédicas.

Dra. Elizabeth Langley McCarron
Instituto Nacional de Cancerología

Dr. Vicente Madrid Marina
Facultad de Medicina (Instituto Nacional de Salud Pública)

Ciudad de México. Mayo 2023

CGEP/PMDCBQ/320
047259-63CCA04C88F2C
Asunto: Jurado de examen

SINODALES DESIGNADOS
Presente

Estimado académico:

Los miembros del Subcomité Académico en reunión ordinaria del **16 de enero de 2023**, conocieron la solicitud de asignación de **JURADO DE EXAMEN** para optar por el grado de **Doctora en Ciencias** del/la estudiante **OLMEDO NIEVA LESLIE**, con la tesis **"Identificación de posibles biomarcadores pronóstico asociados con la expresión de los oncogenes E6 y E7 del Virus del Papiloma Humano tipo 16 en cáncer cervical"**, dirigida por el/la Dr(a). **LIZANO SOBERÓN MARCELA .**

De su análisis se acordó nombrar el siguiente jurado en el que se encuentra usted incluido:

			ACEPTA	FECHA	FIRMA
GONZÁLEZ ESPINOSA CLAUDIA	PMDCBQ	PRESIDENTE	SI X NO	07 / 02 / 2023	
VALVERDE RAMÍREZ MAHARA ANGÉLICA	PMDCBQ	SECRETARIO	SI X NO	7 / 2 / 2023	
GARCÍA SAINZ JESÚS ADOLFO	PMDCBQ	VOCAL	SI X NO	7 / 2 / 2023	
GÓMORA MARTÍNEZ JUAN CARLOS	PMDCBQ	VOCAL	SI X NO	09 / 02 / 2023	
ROCHA ZAVALETA LETICIA	PMDCBQ	VOCAL	SI X NO	10 / 02 / 2023	

Sin otro particular por el momento, aprovecho la ocasión para enviarle un cordial saludo.

A t e n t a m e n t e
"POR MI RAZA HABLARÁ EL ESPÍRITU"
Cd. Universitaria, Cd. Mx., a 20 de enero de 2023

Coordinadora
Dra. Claudia Lydia Treviño Santa Cruz

AGRADECIMIENTOS

A la Universidad Nacional Autónoma de México, y su Posgrado en Ciencias Bioquímicas, por forjar mi formación como Maestra y Doctora en Ciencias durante los últimos años de mi vida.

Al Instituto Nacional de Cancerología, por permitirme desarrollar mi trabajo de doctorado en sus instalaciones, en el Laboratorio de Epidemiología y Biología Molecular de Virus Oncogénicos en la Unidad de Investigación Biomédica en Cáncer.

A la Dra. Marcela Lizano, a cargo del Laboratorio de Epidemiología y Biología Molecular de Virus Oncogénicos, por toda la confianza en mí, la continua ayuda y los consejos que siempre me alientan a seguir adelante.

A la Dra. Elizabeth Langley McCarron y el Dr. Vicente Madrid Marina, por formar parte de mi comité tutoral y siempre compartir todo su conocimiento conmigo, así como su gran disposición y comprensión en todo momento.

A Dra. María Alexandra Rodríguez Sastre del Instituto de Investigaciones Biomédicas de la UNAM, por la asesoría técnica prestada.

A los diferentes programas que apoyaron parcialmente el presente trabajo: Programa de Apoyo en Proyectos de Investigación e Innovación Tecnológica, Universidad Nacional Autónoma de México PAPIIT-UNAM (IN200219); Instituto Nacional de Cancerología (017/007/IBI)(CEI/1144/17); PRONAII-7-Virus y Cáncer #303044 y Paradigmas y Controversias de la Ciencia #320812; CF-2019-51488 del Consejo Nacional de Ciencia y Tecnología (CONACyT), México. A los programas que me apoyaron permitiendo mi formación a lo largo del doctorado: Programa de Apoyo a los Estudios del Posgrado (PAEP), PAPIIT-UNAM (IN200219) y CONACyT (404293).

RESUMEN

La infección con el Virus de Papiloma Humano de alto riesgo (VPH-AR) es la principal causa para el desarrollo de cáncer cervical (CC), en el que la continua expresión de las oncoproteínas virales E6 y E7 mantiene el fenotipo maligno de las células del epitelio cervical. En México, alrededor del 70% de los casos de CC son diagnosticados en etapas avanzadas, impactando en la supervivencia de las pacientes. El objetivo de este estudio fue identificar biomarcadores afectados por las oncoproteínas E6 y E7 de VPH-16 que impacten en el pronóstico de las pacientes con cáncer cervical. Los perfiles de expresión dependientes de las oncoproteínas E6 y E7, al igual que su relación con diversos procesos biológicos y vías de señalización, fueron analizados en líneas celulares de CC. Por otro lado, la comparación entre los perfiles de expresión de las células con E6 y E7 con una cohorte de pacientes obtenida de The Cancer Genome Atlas (TCGA), demostraron que la expresión de 13 genes, compartidos entre las líneas celulares y las muestras de pacientes, impacta la supervivencia global (SG). Una regresión de Cox reveló que la disminución en la expresión de RIPOR2 está fuertemente asociada con una peor SG en los pacientes del TCGA, pero además, todas las variantes transcripcionales de RIPOR2 detectadas en las líneas celulares, fueron fuertemente disminuidas en presencia de E6 y de E7. Finalmente, en una cohorte de población mexicana, encontramos que en lesiones cervicales premalignas, la expresión de RIPOR2 también se encontró disminuida, y que la disminución de esta expresión estuvo asociada con una peor SG en pacientes mexicanas con CC.

ABSTRACT

High-risk human papillomavirus (HPV) infection is the main risk factor for cervical cancer (CC) development, where the continuous expression of E6 and E7 oncoproteins maintain the malignant phenotype. In Mexico, around 70% of CC cases are diagnosed in advanced stages, impacting the survival of patients. The aim of this work was to identify biomarkers affected by HPV-16 E6 and E7 oncoproteins that impact the prognosis of CC patients. Expression profiles dependent on E6 and E7 oncoproteins, as well as their relationship with biological processes and cellular signaling pathways, were analyzed in CC cells. A comparison among expression profiles of E6- and E7-expressing cells and that from a CC cohort obtained from The Cancer Genome Atlas (TCGA) demonstrated that the expression of 13 genes impacts the overall survival (OS). A multivariate analysis revealed that the downregulated expression of RIPOR2 was strongly associated with a worse OS. RIPOR2, including its transcriptional variants, were overwhelmingly depleted in E6- and E7-expressing cells. Finally, in a Mexican cohort, it was found that in premalignant cervical lesions, RIPOR2 expression decreases as the lesions progress; meanwhile, decreased RIPOR2 expression was also associated with a worse OS in CC patients.

ÍNDICE

INTRODUCCIÓN

El Cáncer Cervical y el Virus del Papiloma Humano

De acuerdo con las más recientes estadísticas del GLOBOCAN 2020 y la Agencia Internacional para la Investigación en Cáncer, el cáncer cervical (CC) ocupa el cuarto lugar en incidencia y mortalidad por cáncer en mujeres del mundo. La incidencia global fue de alrededor de 604 000 nuevos casos en el 2020, mientras que la mortalidad por CC representó el 7.7% de las muertes en mujeres con cáncer (Ferlay et al., 2020; Sung et al., 2021) (Figura 1).

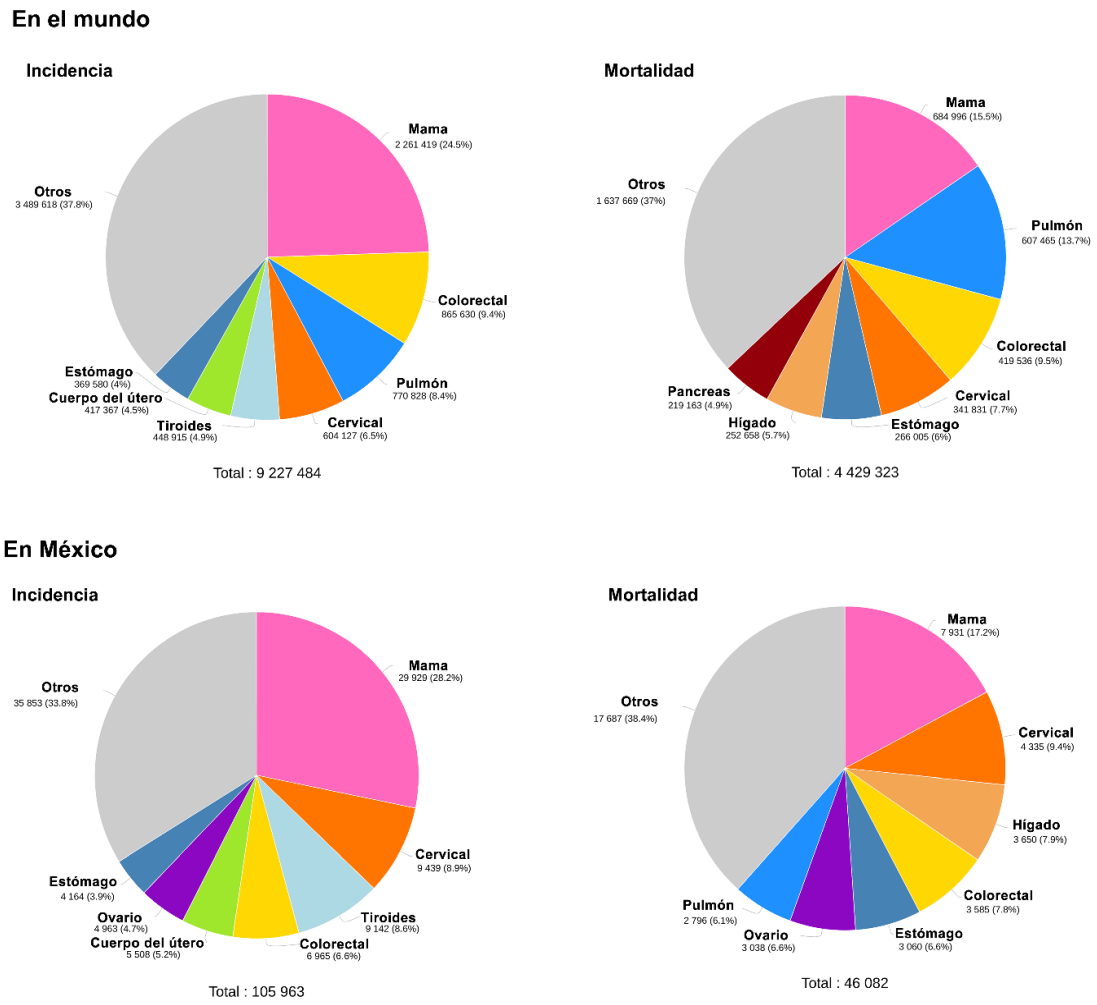

Figura 1. Incidencia y mortalidad por tipo de cáncer en mujeres de México y el mundo. Figura modificada de GLOBOCAN 2020/IARC (Ferlay et al., 2020).

Las estrategias de diagnóstico oportuno permiten detectar lesiones precancerosas, lo que favorece mejores opciones de tratamiento y la posibilidad de no desarrollar CC. También ha sido documentado que alrededor del 90% de las muertes por cáncer en mujeres a nivel mundial suceden en países en vías de desarrollo, principalmente debido al acceso limitado a las medidas preventivas de detección. La identificación del CC en etapas avanzadas, provoca que los tratamientos disponibles sean menos eficientes y/o los costos sean muy elevados (Sung et al., 2021).

En México, el CC es la segunda causa de muerte por cáncer en mujeres y continúa siendo un problema de salud pública; en 2012 se estimaron 3357 muertes por cáncer cervical en nuestro país, mientras que para el año 2020 esta estimación aumentó a 4335 muertes (Ferlay et al., 2020). En países en vías de desarrollo, como México, una alta proporción de los casos de CC son diagnosticados en etapas clínicamente avanzadas, resultando en una menor sobrevivencia y una alta tasa de muerte (Singh et al., 2012). Se ha observado que en México más del 70% de los pacientes con cáncer cervical son diagnosticados en etapas avanzadas (Isla-Ortiz et al., 2020), lo que afecta notablemente a la supervivencia global del paciente (Torreglosa-Hernández et al., 2022).

Es importante tomar en cuenta que el principal factor de riesgo atribuido al desarrollo de CC es la infección persistente por el Virus de Papiloma Humano (VPH) de alto riesgo (AR), cuyo genoma ha sido encontrado en la mayoría de los casos de cáncer cervical (más del 90%) (Li et al., 2011). Hoy en día, se han identificado alrededor de 220 tipos virales capaces de infectar al humano (*PaVE: The Papillomavirus Episteme*, 2022; Van Doorslaer et al., 2017), de los cuales, alrededor de 40 infectan la zona genital y 15 se determinan como de AR (16, 18, 21, 33, 35, 39, 45, 51, 52, 56, 58, 59, 68, 73, y 82) (Yu et al., 2022). Dentro de los tipos de alto riesgo, el VPH-16 y el VPH-18 causan alrededor del 70% de los casos de CC, siendo el VPH-16 el más prevalente y encontrándose en alrededor del 50% de los casos (Alfaro et al., 2016; Szymonowicz & Chen, 2020).

Este virus se transmite principalmente por contacto sexual y alrededor del 80% de las personas con vida sexual activa presentarán una infección con VPH en algún momento de sus vidas. La mayoría de estas infecciones son eficientemente eliminadas por el sistema inmune, sin embargo, alrededor del 10% persiste y el desarrollo de cáncer se presentará en menos del 1% (Sasagawa et al., 2012). Se ha calculado que alrededor del mundo, cerca del 13% de los casos de cáncer se asocian con infecciones. Dentro de estos factores infecciosos se encuentran *Helicobacter pylori*, VPH, Virus de Hepatitis C, Hepatitis B, Epstein-Barr, etc., relacionados principalmente con cáncer gástrico, cervical, hepático, nasofaringe, etc (de Martel et al., 2020; Plummer et al., 2016). Para el caso específico de Latinoamérica, el VPH es el agente más relacionado con cáncer (de Martel et al., 2020; Plummer et al., 2016) y globalmente, se ha calculado que causa poco más del 30% del total de los casos de cáncer causados por agentes infecciosos (Szymonowicz & Chen, 2020). Además del CC, el VPH se asocia con el desarrollo de otros tipos de cáncer en hombres y mujeres, siendo el CC el más frecuente en mujeres y el cáncer de orofaringe el más común en hombres. En la Figura 2 se puede observar el número estimado de casos anuales para cada uno de los tipos de cáncer asociados a VPH tanto en hombres como en mujeres, así como los tipos virales con los que se asocian.

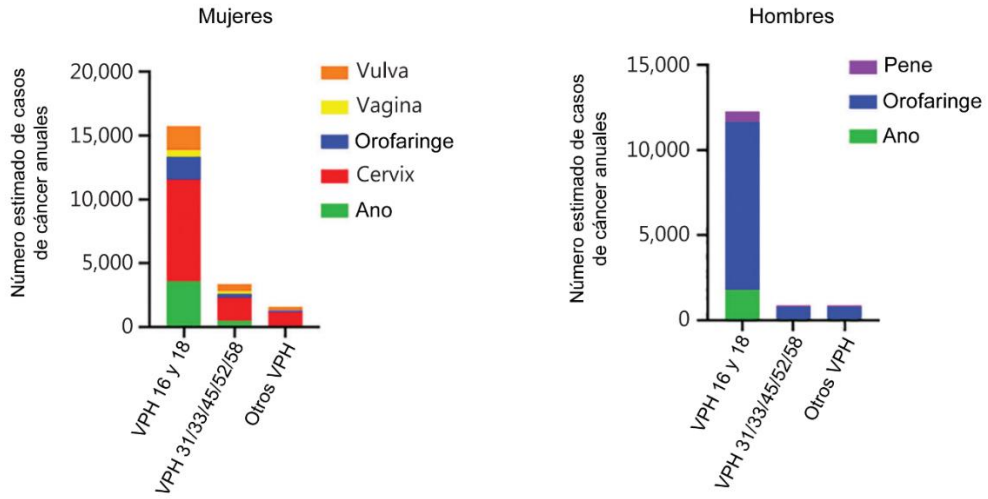

Figura 2. Tipos de cáncer asociados con la infección del VPH en hombres y mujeres. Se muestran los casos anuales estimados para cáncer de vulva, vagina, orofaringe, cérvix, ano y pene en hombres y mujeres alrededor del mundo, así como los tipos virales con los que se asocia cada uno de estos. Imagen modificada de (Szymonowicz & Chen, 2020).

El genoma del VPH

El VPH es un virus pequeño que oscila entre los 52-55 nm, contiene un genoma de DNA de doble cadena dentro de una cápside icosaédrica que no posee envoltura (Yu et al., 2022). La longitud del DNA viral es de alrededor de 8000 pb y se distribuye en tres regiones que pueden identificarse en la Figura 3 como: 1) URR o LCR por Upstream Regulatory Region o Long Control Region, que no posee marcos abiertos de lectura, pero se encarga de la regulación de la replicación y transcripción virales; 2) una región de expresión temprana (E), que codifica para las proteínas E1, E2, E1ˆE4, E5, E6, E7 y E8ˆE2; 3) la región tardía (L) que codifica para las dos proteínas de la cápside viral L1 y L2 (Tabla 1). Dos promotores principales regulan la transcripción de los marcos de lectura temprano y tardío, aunque otros promotores han sido identificados (Yu et al., 2022).

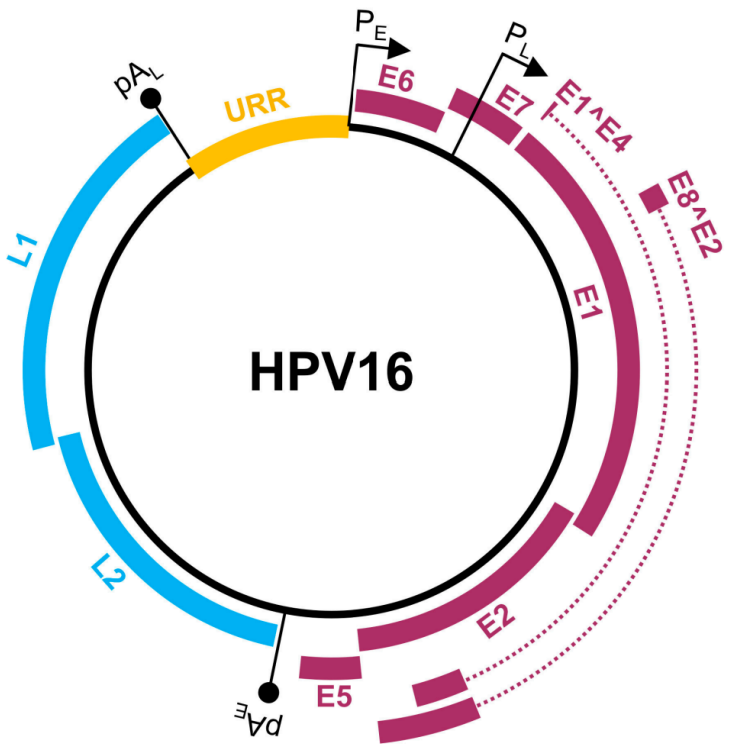

Figura 3. Estructura general del genoma del VPH tipo 16. En Amarillo muestra la upstream regulatory región (URR), en color vino las proteínas de expresión tempranas y en color azul las proteínas de expresión tardía. P_E y P_L denotan los promotores para los transcritos tempranos y tardíos, respectivamente, así como pA_E y pA_L las secuencias de poliadenilación de las mismas. Imagen tomada de (Yu et al., 2022).

Tabla 1. Funciones principales de las proteínas del VPH.	
Proteína	**Papel en el ciclo de vida viral**
E1	Replicación del genoma, DNA helicasa dependiente de ATP.
E2	Replicación del genoma, transcripción, segregación, encapsidación, regulación de la expresión génica celular, ciclo celular y regulación de la apoptosis.
E4	Remodelación de las redes de citoqueratina, arresto del ciclo celular, ensamblaje del virión.
E5	Control del crecimiento celular y diferenciación, modulación inmune.
E6	Inhibición de la apoptosis y diferenciación, regulación de la forma celular, polaridad, movilidad y señalización.
E7	Control del ciclo celular, controla la duplicación de centrosomas.
L1	Proteína mayor de la cápside.
L2	Proteína menor de la cápside, recluta L1, ensamblaje del virión.

Se describen las principales funciones de las proteínas tempranas y tardías codificadas en el genoma del VPH-16. Modificada de (Bhat, 2022).

La oncogenicidad de los VPH-AR recae principalmente en la expresión continua de dos de sus oncogenes tempranos E6 y E7, los cuales son suficientes para promover la transformación celular (Münger et al., 1989) mediante diversos mecanismos (Figura 4). Los productos proteicos de estos genes, interaccionan con diferentes blancos celulares que promueven procesos asociados con cáncer, tales como proliferación, migración, invasión, inhibición de la apoptosis, evasión del sistema inmune, entre otros (Pal & Kundu, 2020). Una de las funciones más estudiadas de las oncoproteínas virales, es que promueven la degradación de proteínas supresoras de tumores. E6 interacciona con p53 y con la ubiquitina ligasa E6AP, promoviendo la degradación de p53 a través del proteosoma, evento que permite la inhibición de la apoptosis, la promoción de la inestabilidad genómica y la acumulación de mutaciones (Martinez-Zapien et al., 2016; Scheffner et al., 1993). La proteína E7 interacciona con pRb y con la ubiquitina ligasa Culina 2, favoreciendo la degradación proteosomal de pRb. Este evento promueve la translocación del factor transcripcional E2F al núcleo y de la transcripción de genes relacionados con

la transición de la fase G1 a la fase S, favoreciendo la continuidad del ciclo celular (Huh et al., 2007).

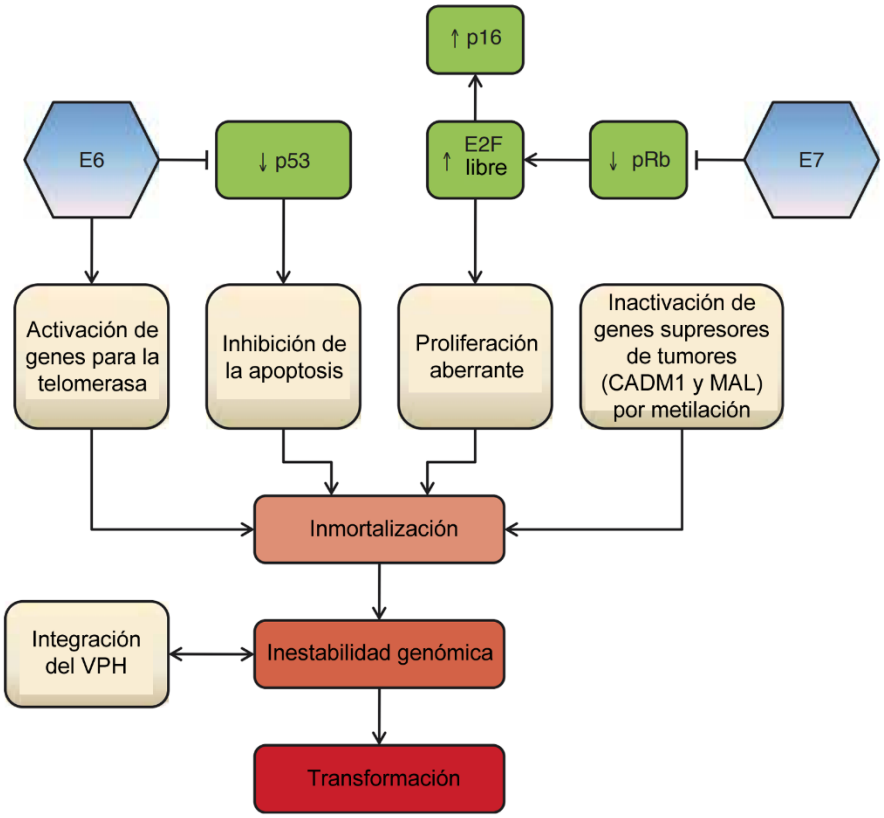

Figura 4. Diagrama que muestra los principales procesos celulares afectados por E6 y E7 durante la infección con VPH de AR en células del epitelio cervical. E6 promueve la degradación de p53 resultando en la inhibición de la apoptosis y E7 inactiva pRb, favoreciendo la proliferación. En combinación con otros procesos, se promueve la transformación celular. Aún continúa en estudio si la promoción de la inestabilidad genómica lleva a la integración viral o si el proceso de integración facilita la inestabilidad. Imagen modificada de (World Health Organization, 2020).

Ciclo viral y el desarrollo de cáncer cervical

Como se ha mencionado anteriormente, el genoma viral se compone de una región temprana y otra tardía; la expresión de dichas regiones se regula por la diferenciación del epitelio una vez que este ha sido infectado por el VPH mediante microabrasiones (Cosper et al., 2021).

El VPH posee tropismo por epitelios escamosos, ya sean mucosos o cutáneos dependiendo del tipo viral. Dichos epitelios poseen una capa basal compuesta por células indiferenciadas, seguida de una capa suprabasal, una granular y finalmente una capa de células en descamación. A través de endocitosis mediada por receptores, el VPH infecta las células basales, las cuales se encuentran en división y proveen un ambiente idóneo para la replicación viral inicial. Una vez que se da la infección, el ciclo viral productivo consta de tres principales etapas: a) Establecimiento, en la que se da una amplificación inicial muy regulada hasta alcanzar alrededor de 100 copias virales; b) Mantenimiento, donde el número de copias se conserva constante y el virus puede persistir en esta etapa hasta por décadas; c) Amplificación, en la cual las células basales infectadas comienzan a diferenciarse, proceso que promueve el incremento de la replicación en los estratos superiores (mediada principalmente por la expresión de E6 y E7) que culminará con la generación y liberación de partículas virales en las últimas capas (Figura 5 A) (Cosper et al., 2021).

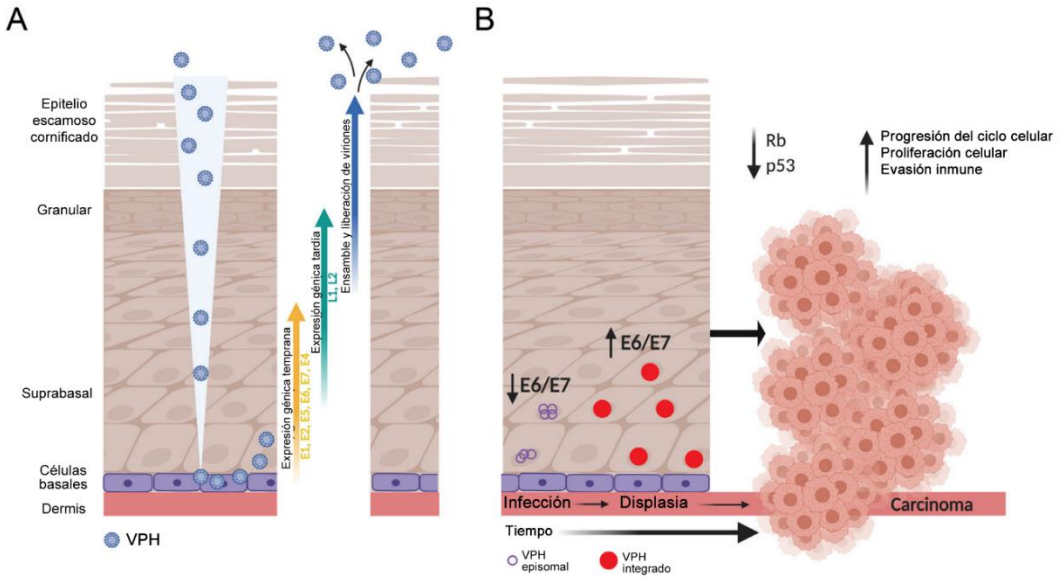

Figura 5. Ciclo de vida del Virus de Papiloma Humano. A) Se muestra el ciclo viral reproductivo en el que a través de una micro lesión el virus infecta la capa basal y posteriormente su genoma se expresa de acuerdo con la capa del epitelio en el que se encuentre hasta que en las capas superiores se ensamblan y liberan nuevas partículas virales por descamación; B) Integración del genoma viral que aumenta los niveles de E6 y E7, la degradación de blancos celulares como p53 y pRb, y puede promover el desarrollo de cáncer. Imagen tomada de (Cosper et al., 2021).

Cuando se da una larga etapa de mantenimiento y el virus persiste, el DNA del VPH puede integrarse en el genoma celular, proceso que no es considerado como parte del ciclo natural de infección; debido a que dicha integración ya no permitirá la síntesis de genomas virales extra-cromosomales que puedan ser empaquetados y transmitidos a un nuevo hospedero (Cosper et al., 2021; McBride & Warburton, 2017). La integración viral en el genoma celular es comúnmente observada en CC y en algunas lesiones premalignas, donde una de secuencias virales en las que el genoma del VPH se rompe frecuentemente es la del gen E2. Debido a que la proteína E2 actúa como represor transcripcional de E6 y E7, al ser interrumpido, se promueve un incremento de las oncoproteínas y entre otros eventos, la degradación de sus blancos proteicos p53 y pRb, favoreciendo el establecimiento del CC (Figura 5 B) (Cosper et al., 2021; McBride & Warburton, 2017). Es importante destacar que conforme la lesión cervical es más cercana a cáncer se detecta mayor integración viral (Cosper et al., 2021), sin embargo, se estas lesiones premalignas e incluso algunos casos de CC pueden llegar a desarrollarse sin que se detecte integración (Rossi et al., 2023).

Una vez que el VPH ha infectado el epitelio, pueden desarrollarse lesiones de diversos grados que pueden llevar o no al desarrollo de cáncer cervical escamoso (CCE). Estas lesiones se denominan neoplasias intraepiteliales cervicales (NIC), las cuales representan etapas precancerosas y normalmente revierten por sí solas en pocos años. Las infecciones cervicales que progresan pueden generar un NIC I o también llamadas lesiones intraepiteliales escamosas de bajo grado (LIEBG), caracterizadas por una displasia moderada con la presencia de coilocitos; posteriormente puede generarse un NIC II, que consiste en una lesión que afecta dos tercios del epitelio; finalmente encontramos al NIC III, que representa una displasia severa afectando más de dos tercios del epitelio. Tanto el NIC II como el NIC III se engloban en las lesiones intraepiteliales escamosas de alto grado (LIEAG), que cuando progresan, pueden generar cáncer invasor (Burmeister et al., 2022) el cual se estratifica en estadios I, II, III y IV (Tabla 2) de acuerdo con la guía

de la FIGO (Fédération Internationale de Gynécologie et d'Obstétrique, por sus siglas en francés) (FIGO Committee on Gynecologic Oncology, 2014).

Tabla 2. Estadios clínicos del cáncer cervical.	
Estadio	**Descripción**
I	El carcinoma está estrictamente confinado al cérvix (extensión al cuerpo uterino debe descartarse).
IA	Cáncer invasivo identificado sólo microscópicamente (toda lesión macroscópica incluso con invasión superficial es estadio IB). La invasión está limitada a una invasión estromal con una profundidad máxima de 5 mm y de no más de 7mm de ancho.
● IA1	Invasión al estroma ≤3 mm de profundidad y ≤7 mm de ancho.
● IA2	Invasión al estroma >3 mm y <5mm* de profundidad y ≤7 mm de ancho.
IB	Lesiones clínicas confinadas al cérvix o lesiones preclínicas mayores a estadio IA.
● IB1	Lesiones clínicas no mayores a 4 cm.
● IB2	Lesiones clínicas mayores a 4 cm.
II	El carcinoma se extiende a través del útero, pero no se extiende en la pared pélvica o al tercio inferior de la vagina.
IIA	Se involucra los 2/3 superiores de la vagina. Sin afección parametrial evidente.
● IIA1	Lesión clínicamente visible ≤4 cm.
● IIA2	Lesión clínicamente visible >4 cm.
IIB	Afección parametrial evidente pero no hacia la pared lateral pélvica.
III	El carcinoma se ha extendido hacia la pared lateral pélvica. En la examinación rectal, no hay espacio libre entre el tumor y la pared lateral pélvica. El tumor involucra el tercio inferior de la vagina. Todos los casos de hidronefrosis o riñón no funcional deben incluirse al menos que se sepa que se deben a otras causas.
IIIA	Se involucra la vagina inferior pero no hay extensión hacia la pared lateral de la pelvis.
IIIB	Extensión hacia la pared lateral pélvica o hidronefrosis/riñón no funcional.
IV	El carcinoma se ha extendido dentro de la pelvis o se encuentra clínicamente involucrada la mucosa de la vejiga y/o el recto.
IVA	Se ha diseminado a los órganos adyacentes a la pelvis.
IVB	Se ha diseminado a órganos distantes.

*La profundidad de la invasión no debe ser mayor a 5mm tomado desde la base del epitelio, cualquier superficie glandular, de la que se origina. La invasión del espacio vascular no debe alterar la tinción. Modificada de (FIGO Committee on Gynecologic Oncology, 2014).

Biomarcadores en el cáncer cervical

Las características de la enfermedad relacionadas con el estadio clínico, tales como el tamaño del tumor, infiltración a nódulos linfáticos y metástasis, están relacionadas con la supervivencia de los pacientes; sin embargo, no todos los pacientes con el mismo estadio clínico tienen el mismo desenlace. Por lo tanto, algunos estudios se han enfocado en la búsqueda de moléculas que pueden predecir la sobrevida de los pacientes. Con respecto a esto, algunas proteínas han sido reportadas como biomarcadores pronóstico para CC, incluyendo los niveles de Ki-67/MIB-1 (Piri et al., 2015), la subunidad catalítica de la glucosa-6-fosfatasa (G6PC) (Zhu et al., 2022) y una cinasa específica de proteína rica en serina/arginina 1 (SRPK1) (Z. Dong et al., 2022), las cuales están relacionadas con una peor sobrevida; mientras los altos niveles de Galectina 9 (Beyer et al., 2022) correlacionan con un mejor pronóstico en pacientes con CC. Además, a través del análisis de perfiles transcripcionales derivados de bases de datos genómicas de pacientes con CC, se han identificado genes relacionados con la sobrevida global (SG) (Campos-Parra et al., 2022; Cui et al., 2022). Por ejemplo, la elevada expresión de BRCA1 (Paik et al., 2021) está asociada con una mejor SG, mientras que los altos niveles transcripcionales de VEGF165 se han asociado con una peor sobrevida libre de enfermedad (Patel et al., 2020) en pacientes con CC. Alteraciones de RNAs no codificantes también han sido propuestos como biomarcadores pronóstico en CC (Chang et al., 2022; Nahand et al., 2019; G. Zhang et al., 2022).

Debido a que las oncoproteínas virales son responsables del mantenimiento del fenotipo maligno, estrategias enfocadas en el descubrimiento de nuevos biomarcadores asociados al desarrollo de CC dependientes del VPH han sido explorados. La detección del genoma del VPH (DNA) así como su expresión (RNA) ha sido utilizada para determinar el riesgo de progresión a cáncer y como un biomarcador pronóstico. Los transcritos de E6 y E7 han mostrado tener alta especificidad comparados con la positividad al DNA viral (Coquillard et al., 2011; Gupta et al., 2022) y un alto valor predictivo positivo de progresar a LEIAG o cáncer cervical. Además, ha sido demostrado que la presencia, así como los niveles de los

transcritos de E6, incrementan el riesgo de progresar a cáncer (Ho et al., 2010). En cáncer cervical, la alta expresión del oncogén E6 y de su isoforma E6* están asociadas con una pobre sobrevida global (Ruiz et al., 2021). Por otro lado, el uso del mRNA del VPH ha sido propuesto como un marcador molecular para la propagación metastásica del cáncer cervical (Dürst et al., 2015; Rose et al., 1994). En el ganglio centinela de los pacientes con nódulos linfáticos libres de metástasis, se ha demostrado que la presencia de mRNA del VPH tiene valor pronóstico independiente del tamaño del tumor, donde la supervivencia libre de recurrencia fue significativamente mayor para pacientes con ganglios centinelas negativos al mRNA de VPH (Dürst et al., 2015).

Debido al efecto de E6 y E7 sobre la transformación celular, los perfiles de expresión génicos dependientes de los oncogenes virales en CC, ofrecen una alternativa para la búsqueda de biomarcadores con valor pronóstico. Una clasificación más precisa de los casos de CC de acuerdo con sus perfiles moleculares y considerando la expresión de los oncogenes, podría ser útil para identificar a los pacientes con tumores más agresivos que requieran un seguimiento más estrecho.

Resultan de gran relevancia los estudios enfocados en el establecimiento de nuevos biomarcadores de progresión y pronóstico de sobrevida global en cáncer cervical, algunas evidencias han mostrado la actividad de proteínas como PFKFB4 y RIPOR2 con expresión alterada en cáncer cervical. Particularmente se ha observado aumento de PFKFB4 y disminución de RIPOR2 en la neoplasia antes mencionada. Estas moléculas están involucradas en la regulación de procesos tales como metabolismo, migración, proliferación, reparación del DNA y procesos de suma importancia para mantener la homeostasis celular.

ANTECEDENTES

PFKFB4 y RIPOR2 en cáncer cervical

La 6-fosfofructo-2-cinasa/fructosa-2,6-bifosfatasa 4, también conocida como PFKFB4, es una de las cuatro isoenzimas de PFKFB (Yalcin et al., 2009), las cuales generan fructosa-2, 6-bifosfato, un activador alostérico de la 6-fosfofructo-1-cinasa, enzima limitante en la glucólisis, la gluconeogénesis y que regula la vía de las pentosas fosfato. Estudios recientes han demostrado que la alta expresión de PFKFB4 predice un mal pronóstico en varios tipos de cáncer, incluyendo cáncer de mama (Cai et al., 2021), gástrico (Wang et al., 2021), de pulmón (Zhou et al., 2022), melanoma (Trojan et al., 2018) y de tiroides (Lu et al., 2020). En CC se han realizado trabajos recientes que muestran la sobreexpresión de PFKFB4 en este cáncer y lo asocian con procesos carcinogénicos (Hsin et al., 2021; Sun & Jin, 2022; Wu et al., 2022), aunque la relación de su incremento aún no se ha ligado con la actividad de las oncoproteínas virales.

RIPOR2 pertenece a la familia RIPOR (RHO family interacting cell polarization regulators), compuesta por 3 distintas proteínas: RIPOR1, RIPOR2 y RIPOR3, las cuales se codifican por los genes FAM65A, FAM65B y FAM65C, respectivamente. Las proteínas RIPOR se unen directamente a las GTPasas RHO (A, B y C) a través de su motivo de unión a RHO, inhibiendo la actividad de RHO e influenciando negativamente las funciones celulares reguladas por estas GTPsas, tales como tráfico mediado por receptores, migración, crecimiento y polarización celulares (Lv et al., 2022). A lo largo del tiempo, se han dado distintos nombres a RIPOR2 (PL48, C6orf32, FAM65B) y se han reportado con un número distinto de nucleótidos y aminoácidos. Las primeras variantes de RIPOR2 identificadas en citotrofoblastos en diferenciación fueron tres mRNAs de 2.8, 3.5 y 4.8 kb (Dakour et al., 1997; Morrish et al., 1996). Posteriormente, diversas isoformas de la proteína RIPOR2 fueron detectadas mediante inmunoblot (Yoon et al., 2007).

Por otro lado, la expresión de la proteína RIPOR2 se ha visto disminuida en cáncer, aunque existe muy poca información sobre el papel que tiene en este padecimiento.

Dakour *et al*., en 1997, describieron la falta de expresión de RIPOR2 en una amplia variedad de líneas celulares de cáncer de pulmón, retinoblastoma, glioma, vejiga y colon (Dakour et al., 1997), aunado a esto, en diversas líneas de cáncer cervical, se observa una muy baja o nula expresión (*FANTOM. Functional Annotation of the Mammalian Genome*, 2014; Lizio et al., 2015, 2019). La línea celular PC3, derivada de tumores de cáncer de próstata, también muestra bajos niveles de RIPOR2, sin embargo, las subpoblaciones de esta línea PC3 con características de células troncales cancerosas (CSC), poseen un fenotipo contrario con altos niveles de RIPOR2. Sorprendentemente, los tumores generados en ratones a partir de estas CSC, nuevamente poseen baja expresión de RIPOR2 (K. Zhang & Waxman, 2010), haciendo pensar que la formación del tumor requiere de la disminución de este transcrito en algún punto del desarrollo tumoral. De forma interesante, también se ha observado que cuando RIPOR2 se sobre-expresa en las líneas celulares de CC SiHa y HeLa, la viabilidad celular y la migración, disminuyen significativamente (Xu et al., 2022). Estos hallazgos sugieren que RIPOR2 podría actuar como un supresor tumoral.

Hasta el momento, dos estudios han reportado una relación entre los niveles de expresión de RIPOR2 y la SG de las pacientes con cáncer cervical, ambos asociando a este mensajero con la expresión de una firma compuesta por 4 genes. El primero de estos estudios reveló que la firma compuesta por RIPOR2, DAAM2, SORBS1, CXCL8, se asocia con la SG de las pacientes con cáncer cervical; siendo el grupo de alto riesgo donde RIPOR2 se encontró disminuido y las pacientes poseen peor pronóstico (Mei et al., 2020). Concordando con los resultados antes mencionados, un estudio reciente identificó que las pacientes con CC que presentan mayor expresión de RIPOR2 poseen una mejor SG, concluyendo que RIPOR2 es un factor protector en CC (Xu et al., 2022).

De manera relevante, al dividir a las pacientes con cáncer cervical en dos grupos, de acuerdo con la alta o baja infiltración de ciertas células del sistema inmune en el tumor (pej. T CD8, Treg, Macrófagos), se observó que la alta expresión de RIPOR2

correlaciona con la elevada infiltración de estas células en tumores cervicales (Mei et al., 2020; Xu et al., 2022). En relación con estos resultados, los pacientes con alta infiltración también poseen una elevada expresión los transcritos para proteínas de muerte celular programada como PD-1, PD-L1, PD-L2, y CTLA-4, haciéndolos candidatos para terapia con inhibidores de estos puntos de control (Mei et al., 2020).

PLANTEAMIENTO DEL PROBLEMA Y JUSTIFICACIÓN

El cáncer cervical es la cuarta causa de muerte por cáncer en mujeres del mundo y la segunda en mujeres mexicanas. En países en vías de desarrollo como México, este padecimiento es comúnmente detectado en etapas avanzadas, lo que disminuye la esperanza de vida de las pacientes.

La expresión de los genes E6 y E7 del virus del papiloma humano (VPH) ha demostrado estar asociada con el pronóstico de las pacientes con cáncer cervical, sin embargo, los estudios que evidencian este efecto son pocos y no permiten concluir la participación de las oncoproteínas sobre otros probables biomarcadores pronóstico. Enriquecer esta información ayudaría en el entendimiento de los mecanismos que promueven el desarrollo del cáncer cervical, mejoraría la estratificación de las pacientes y, en un futuro, podría apoyar en la elección de tratamientos más adecuados para este grupo de pacientes con mal pronóstico.

PREGUNTA DE INVESTIGACIÓN

¿Cuáles de los transcritos celulares que se alteran por la presencia de los oncogenes E6 y E7 afectan la sobrevida global de las pacientes con cáncer cervical?

HIPÓTESIS

Las proteínas E6 y E7 del VPH-16 modifican la expresión de genes relacionados con la sobrevida global de las pacientes con cáncer cervical.

OBJETIVOS

Objetivo General

Evaluar el efecto de las proteínas E6 y E7 del VPH-16 sobre la expresión de genes celulares que afectan la sobrevida global de las pacientes con cáncer cervical.

Objetivos Específicos

1. Establecer modelos de expresión estable de los oncogenes E6 y E7 del VPH-16 en la línea celular de cáncer de cérvix C-33 A.
2. Caracterizar el transcriptoma de los modelos de expresión estable alterados por las oncoproteínas E6 y E7.
3. Determinar mediante herramientas bioinformáticas los procesos biológicos y vías de señalización asociados a la expresión de las oncoproteínas virales.
4. Evaluar la expresión génica diferencial entre muestras de cáncer cervical y tejido normal a partir de bases de datos públicos de una cohorte proveniente del TCGA.
5. Identificar los transcritos cuya expresión es modificada por las proteínas virales en líneas celulares, y que también se encuentran alterados en muestras de cáncer cervical.
6. Analizar la asociación de los niveles de expresión de los transcritos seleccionados con la sobrevida global en la cohorte de TCGA.
7. Validar la expresión de los genes involucrados en el desenlace clínico de las pacientes en líneas celulares de cáncer cervical positivas a VPH-16 y en los modelos celulares con expresión estable de E6 y E7.
8. Analizar la expresión de los genes seleccionados en muestras cervicales de pacientes con epitelio normal, lesiones precancerosas y cáncer.
9. Determinar el efecto de los niveles de expresión de los genes de interés en la supervivencia global de las pacientes con cáncer cervical.

MÉTODOS

Clonación de E6 y E7

Los marcos de lectura abiertos (ORFs) para E6 y E7 de VPH-16 fueron amplificados a partir de DNA extraído de células Ca Ski utilizando Reacción en Cadena de la Polimerasa (PCR). Las secuencias virales, fusionadas a la secuencia del tag HA, fueron amplificadas utilizando los primers específicos EcoRI-HA-E616 Fwd/BglII-E616 Rev, así como EcoRI-HA-E716-Fwd/BglII-E716-Rev (mostrados en la Tabla 3) y clonados en el vector de expresión p3x-FLAG CMV-10 (Sigma, Burlington, MA, EUA). Para llevar a cabo dicha clonación, se utilizaron las enzimas de restricción EcoRI y BglII, así como la enzima Ligasa T4 (Invitrogen, Waltham, MA, EUA), de acuerdo con las recomendaciones del proveedor. Las construcciones fueron verificadas mediante secuenciación Sanger. Los plásmidos generados se nombraron: vector vacío p3x-FLAG (VV), p3x-FLAG-HA-E616 (E616) y p3x-FLAG-HA-E716 (E716). Las distintas electroforesis fueron llevadas a cabo en genes de agarosa al 1% utilizando un marcador o estándar de DNA de 100pb Thermo Scientific, Waltham, MA, EUA.

Tabla 3. Oligonucleótidos utilizados en el presente trabajo.

Blanco	Nombre del primer	Secuencia 5´→ 3’	Tamaño del producto
VPH-16 E6	EcoRI-HA-E616 Fwd	GGGGAATTCATACCCATACGATGTTCCAGATTACGCT TTTCAGGACCCACAGGAGC	499 pb
	BglII-E616 Rev	GGGAGATCTTTACAGCTGGGTTTCTCTACGTG	
VPH-16 E7	EcoRI-HA-E716-Fwd	GGGGAATTCATACCCATACGATGTTCCAGATTACGCT C ATGGAGATACACCTACA	340 pb
	BglII-E716-Rev	GGGAGATCTTTATGGTTTCTGAGAACAGAT	
VPH-16 E6	E616 Fwd	TTTCAGGACCCACAGGAGCGA	130 pb
	E616 Rev	AGTCATATACCTCACGTCGCAGTA	
VPH-16 E7	E716 Fwd	CAAGTGTGACTCTACGCTTCGG	82 pb
	E716 Rev	TGTGCCCATTAACAGGTCTTCCAA	
18S	18S Fwd	AACCCGTTGAACCCCATT	149 pb

	18s Rev	CCATCCAATCGGTAGTAGCG	
PFKFB4	PFKFB4 Fwd	CAACATCGTGCAAGTGAAACTG	111 pb
	PFKFB4 Rev	GACTCGTAGGAGTTCTCATAGCA	
RIPOR2 pool	RIPOR2 pool Fwd	GAGCTTCAAGGAGTACACAGAG	96 pb
	RIPOR2 pool Rev	CCAGCCAGACCTTTCATCTT	
RIPOR2 VAR 1	RIPOR2 VAR 1 Fwd	CTGTCTGTCTTGAGTGCCTTG	136 pb
	RIPOR2 VAR 1 Rev	AGATGTCATCAGGTAGATTTGAATAGAG	
RIPOR2 VAR 2	RIPOR2 VAR 2 Fwd	GGATGATATTCTAAAAAAGTAGAGAAG	121 pb
	RIPOR2 VAR 2 Rev	GAAGTCAGCAGGTTGAAGAATAGG	
RIPOR2 VAR 3	RIPOR2 VAR 3 Fwd	AGTGTGACTGCTGAGACTG	133 pb
	RIPOR2 VAR 3 Rev	GTCGGTAGTCCTTCACCAAA	
RIPOR2 VAR 4	RIPOR2 VAR 4 Fwd	TGGTGTTACCTTCGCGATTAC	87 pb
	RIPOR2 VAR 4 Rev	TGGTCGGTAGTCGGTTGA	
RIPOR2 VAR 5-4	RIPOR2 VAR 5-4 Fwd	GGATGATATTCTAAAAGATGCTAAACAC	149 pb
	RIPOR2 VAR 5-4 Rev	ACTCAAGATGGCACAAAAGC	
RIPOR2 VAR 6-1	RIPOR2 VAR 6-1 Fwd	ATTGGTGCGGAGGCTTT	91 pb
	RIPOR2 VAR 6-1 Rev	GAGTCTGGTCGGTAGTCCTAA	
RIPOR2 VAR 7	RIPOR2 VAR 7 Fwd	GGTACGGTCGGGAAGTTG	99 pb
	RIPOR2 VAR 7 Rev	GTAGTCCTTGGCCCGTTC	

Líneas celulares y cultivo

Las líneas de cáncer cervical C-33 A, SiHa y Ca Ski fueron adquiridas en ATCC (Manassas, VA, EUA) y mantenidas a 37 °C con 5% de CO_2. De acuerdo con el proveedor, C-33 A es una línea celular de cáncer cervical proveniente de una mujer de 66 años, adherente y negativa tanto a DNA como a RNA del VPH. Las células SiHa, provienen de un tumor primario de una paciente de 55 años con cáncer cervical escamoso, adicionalmente se menciona que son células adherentes que contienen entre una y dos copias de HPV-16. La línea Ca Ski fue generada a partir

de una mujer de 40 años con un tumor de origen cervical con metástasis al mesenterio del intestino delgado; las células son adherentes y de acuerdo con el proveedor, contienen alrededor de 600 copias de VPH-16 y secuencias relacionadas con VPH-18. Las células SiHa y C-33 A fueron crecidas en medio Dulbecco's modified Eagle's medium (DMEM) de ATCC, VA, EUA, mientras que las células Ca Ski en medio Roswell Park Memorial Institute (RPMI) de GIBCO, Thermo Scientific, Waltham, MA, EUA. Todos los medios se suplementaron con 10% de Suero Fetal Bovino (SFB) de GIBCO, Thermo Scientific, Waltham, MA, EUA.

Las células C-33 A fueron transfectadas de forma estable con los plásmidos generados anteriormente, utilizando Lipofectamine™ 2000 (Invitrogen, Waltham, MA, EUA) de acuerdo con las indicaciones del fabricante y seleccionadas utilizando 2 g/L de G418 (ChemCruz Bio, Dallas, TX, EUA) durante alrededor de un mes y medio. Una vez que solo quedaron las células resistentes al antibiótico en cada una de las tres transfecciones (VV, E616 y E716), una mezcla de dichas células fue congelada y otra parte fue diluida para obtener colonias aisladas provenientes de una sola célula. Cuando algunas de las colonias fueron lo suficientemente grandes, estas células fueron despegadas y divididas en 3 placas distintas que se utilizaron para: extracción de DNA, congelar el pase 0 de cada colonia y continuar con el cultivo de células.

Western Blot

Las células C33-VV, C33-E616 y C33-E716 fueron cultivadas en placas de 60 mm y 24 h después, fueron lisadas utilizando 300 µL de buffer RIPA (100 mM Tris pH 8.0, 50 mM NaCl2, 0.5% Nonidet P-40) adicionado con un coctel de inhibidores de proteasas de acuerdo a las instrucciones del proveedor (Roche, Basilea, Suiza). Un total de 20 µg de extractos proteicos fueron analizados mediante geles SDS-PAGE al 10 y 12% que fueron posteriormente transferidos a una membrana de nitrocelulosa de 22 µm (Bio-Rad, Hercules, CA, EUA). Las membranas fueron bloqueadas con 10% de leche disuelta en TBS con 0.1% Tween 20 (Biorad, CA, EUA) durante 1 h a temperatura ambiente y seguida de una incubación con

anticuerpos primarios anti-HA (Cell Signaling, Danvers, MA, EUA) y anticuerpo anti-H4 (Cell Signaling, Danvers, MA, EUA) diluidos 1:1000 y 1:20 000, respectivamente.

Después de lavar tres veces con Tween 20 al 0.1% en TBS, las membranas fueron incubadas con anticuerpo secundario anti-ratón conjugado con HRP (Santa Cruz, Bio., Dallas, TX, EUA) a una dilución 1:10 000. Las proteínas fueron visualizadas utilizando el Clarity™ Western ECL Substrate (Bio-Rad, Hercules, CA, EUA), de acuerdo con las instrucciones del fabricante. Posteriormente, las membranas fueron visualizadas y analizadas en el iBright FL1500 imagining system (Invitrogen, Waltham, MA, EUA).

Inmunofluorescencia

Las células estables C-33 A fueron sembradas sobre cubreobjetos en placas de seis pozos. Después de 24 h, las células fueron fijadas utilizando paraformaldehído al 3.7% en PBS con 0.1% de Tritón-X100. Después, las células fueron bloqueadas utilizando una solución de BSA al 0.3% y se incubaron durante toda la noche a 4°C con anticuerpo anti-HA (Cell Signaling, Danvers, MA, EUA) diluido 1:50. Las células fueron lavadas con PBS e incubadas con anticuerpo secundario anti-conejo conjugado a Alexa-488 (Invitrogen, Waltham, MA, EUA) diluido 1:700. Los portaobjetos fueron lavados con PBS y montados con medio de montaje Vectashield antifade adicionado con DAPI (Vector laboratories, Burlingame, CA, EUA). Las células fueron analizadas con el microscopio de fluorescencia EVOS FL (Invitrogen, Waltham, MA, EUA).

RNAseq y análisis de datos

El RNA total fue extraído a partir de células C33-VV, C33-E616, y C33-E716 utilizando RNeasy mini kit (Qiagen, Hilden, Alemania) de acuerdo con las instrucciones del fabricante. Tres experimentos independientes fueron realizados para cada una de las distintas líneas estables. Una vez verificada la integridad del RNA utilizando el equipo Bioanalyzer 2100 system (Agilent, Santa Clara, CA, EUA), la preparación de bibliotecas y secuenciación fue llevada a cabo por Novogene Bioinformatics Technology Co., Ltd. (Sacramento, CA, EUA). Los resultados

obtenidos fueron alineados contra el genoma humano de referencia GRCh38 y los análisis de expresión diferencial fueron obtenidos comparando C33-VV contra C33-E616, así como C33-VV contra C33-E716 utilizando DESeq2 R package (1.16.1). Los genes con p ajustada < 0.05 fueron considerados como diferencialmente expresados. Los análisis de enriquecimiento a partir de los genes diferencialmente expresados fueron implementados mediante clusterProfiler en R para Gene Ontology (GO) (Carbon et al., 2021; *Gene Ontology Resource*, 1999), las vías de señalización de la Encyclopedia of Genes and Genomes (KEGG) (*KEGG: Kyoto Encyclopedia of Genes and Genomes*, 1995) y para Reactome (*Reactome Pathway Database*, 2023). Procesos con p ajustada < 0.05 fueron considerados como significativamente enriquecidos con genes diferencialmente expresados.

Análisis de datos de The Cancer Genome Atlas

Datos obtenidos a partir de 309 muestras cervicales de The Cancer Genome Atlas (TCGA) fueron obtenidos usando Bioconductor package TCGABiolinks (Colaprico et al., 2016). El análisis de expresión diferencial fue realizado comparando entre tejido normal y muestras de tumores usando DESeq2 package (Love et al., 2014) y considerando a aquellos transcritos con una p ajustada < 0.05 como estadísticamente significativa.

RT-qPCR

Las células fueron sembradas en placas de 60 mm y 24 h después, el RNA total fue extraído utilizando RNeasy mini kit (Qiagen, Hilden, Alemania). El RNA obtenido fue tratado con el kit DNase-Free DNA removal (Ambion, Austin, TX, USA) y 1000 µg de RNA fueron reverso-transcritos con hexámeros aleatorios usando GeneAmp RNA PCR Core Kit (Applied Biosystems, Waltham, MA, EUA). Los oligonucleótidos utilizados para la amplificación de los distintos blancos analizados se muestran en la Tabla 3. Para la reacción de PCR cuantitativa (qPCR), se utilizó Maxima SYBR green/ROX qPCR Master Mix (2×) (Thermo Scientific, Waltham, MA, EUA). Los resultados se presentan como cuantificación relativa utilizando el método de $\Delta\Delta$Ct.

Muestras cervicales

Una cohorte de muestras obtenidas de pacientes mexicanas con epitelio normal y con lesiones cervicales premalignas fueron utilizadas para evaluar la expresión de RIPOR2. Dicha cohorte se compone de 17 muestras cervicales normales negativas a VPH, 7 muestras con epitelio normal pero positivas a VPH, 20 lesiones premalignas de bajo grado y 15 de alto grado, todas provistas por el Instituto Nacional de Salud Pública (INSP). Además de esto, 19 muestras de cáncer cervical obtenidas del banco de tumores del Instituto Nacional de Cancerología (INCan) de la CDMX fueron incluidas. El protocolo fue revisado y aceptado en febrero de 2017 por el comité Científico y de Ética del INCan Ref. (017/007/IBI)(CEI/1144/17).

Análisis estadístico

Los datos mostrando los efectos de E6 y E7 de VPH-16 sobre los niveles transcripcionales de RIPOR2 se presentan como la media ± DS. Los análisis fueron realizados utilizando el software GraphPad Prisma 5; la p fue calculada mediante la prueba de t de student y las diferencias fueron determinadas como significativas cuando $p < 0.05$. Para determinar la expresión de RIPOR2 en lesiones premalignas comparadas con muestras cervicales normales, el análisis estadístico fue realizado utilizando la prueba U de Mann-Whitney. Para el análisis de sobrevida, los datos clínicos y de seguimiento de 309 pacientes del TCGA fueron obtenidos utilizando TCGABiolinks package. Para cada gen evaluado, los pacientes fueron divididos en dos grupos, alta o baja expresión, a partir de la mediana de expresión. La supervivencia global de los pacientes, dependiente del gen analizado, fue calculada utilizando el estimador Kaplan-Meier. La comparación de las curvas de sobrevivencia para ambos grupos fue realizada utilizando la prueba de log-rank. Después, realizamos un análisis de regresión de Cox univariado y multivariado utilizando el R survival package. Una $p < 0.05$ fue considerada como significativa.

RESULTADOS

Desarrollo de un modelo celular de cáncer cervical con expresión estable de las proteínas E6 y E7 de VPH-16

Para generar el modelo celular con expresión de las proteínas E6 y E7 de VPH-16, se clonaron los ORFs correspondientes a los genes virales E6 y E7 en un vector de expresión. Las secuencias de los genes virales fueron amplificadas a partir de DNA proveniente de línea celular Ca Ski, utilizando los primers EcoRI-HA-E616 Fwd/ BglII-E616 Rev para la amplificación de E6 y EcoRI-HA-E716-Fwd/ BglII-E716-Rev para E7. Es importante resaltar que en la secuencia de los oligonucleótidos Fwd (5´) se agregó la secuencia específica para la endonucleasa EcoRI y la secuencia codificante del tag HA, lo que permitió obtener proteínas virales con fusión a HA en el extremo amino terminal y su detección mediante anticuerpos anti-HA. Por otro lado, los primers Rev (3´) contenían la secuencia para el corte con la enzima BglII. Los primers diseñados, así como el tamaño del amplificado obtenido mediante PCR se muestran en la Tabla 3.

Los productos amplificados de E6 y E7 fueron clonados en el vector p3XFLAG-CMV-10 (Figura 6), utilizando las enzimas de restricción EcoRI y Bglll así como una enzima ligasa, de acuerdo con lo especificado en la sección de métodos. Los plásmidos obtenidos fueron denominados p3x-FLAG-HA-E616 (E616) y p3x-FLAG-HA-E716 (E716). El control, correspondiente al vector vacío, se denominó VV.

Los tres diferentes vectores fueron transfectados por separado en células C-33 A, las cuales se seleccionaron con G418 y se diluyeron para obtener colonias provenientes de una sola célula y así generar líneas celulares clonales. Cada una de las clonas utilizadas fue identificada con las coordenadas del pozo de la placa en la que crecieron (A.2, C.4, D.3, etc) y cuando fueron lo suficientemente grandes, se extrajo DNA.

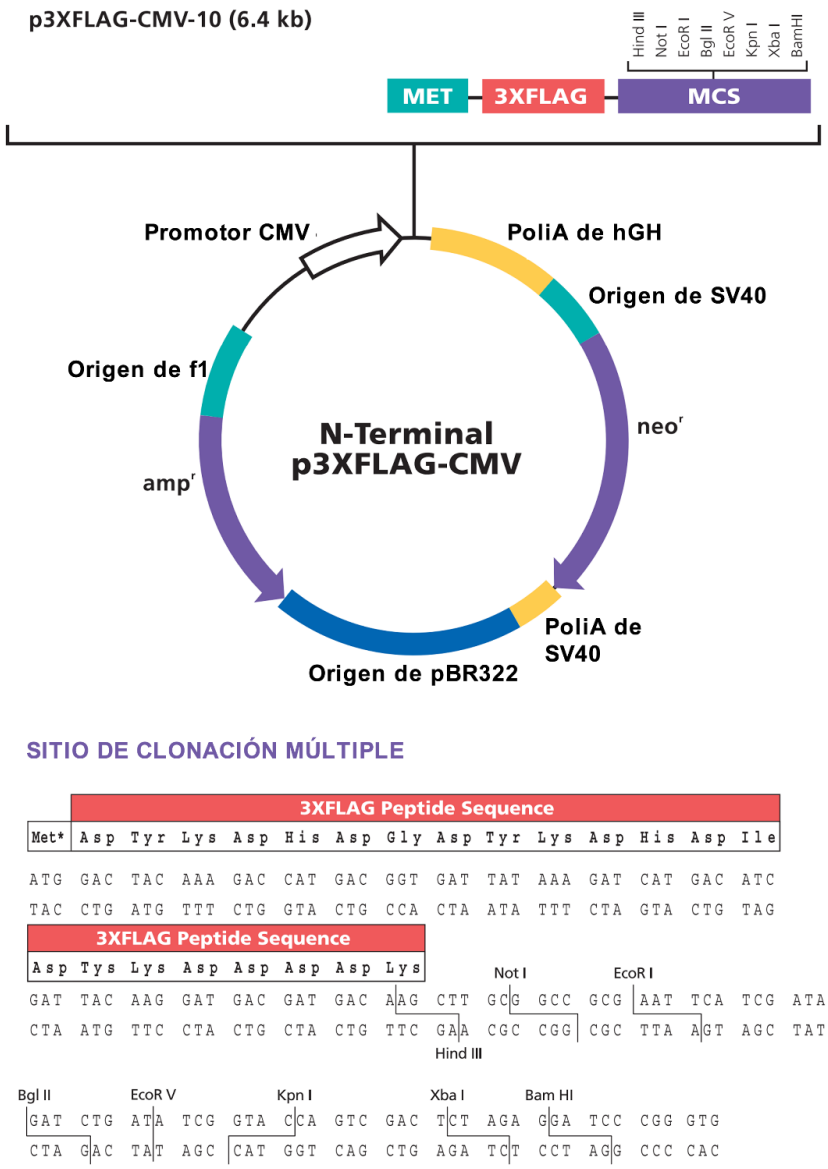

Figura 6. Vector p3XFLAG-CMV-10. Se muestra el mapa del vector donde se identifican las secuencias de origen de replicación, poliadenilación, promotora y de resistencia a antibióticos. Sobre la secuencia del sitio de clonación múltiple, se identifican la secuencia codificante del péptido tag 3XFLAG y el sitio de corte para las enzimas de restricción. Imagen modificada del proveedor.

A partir del DNA genómico obtenido de cada colonia y utilizando los primers para la amplificación de los ORFs E6 y E7, se realizó una PCR punto final para evaluar la presencia de los genes virales en tres colonias con el VV, tres con E616 y dos con E716. Los resultados demostraron que todas las células transfectadas con E616 contenían sólo el gen E6, que las células transfectadas con E716 solo contenían

secuencias del gen E7, mientras que las células con el VV no mostraron amplificación para ninguno de los ORFs virales (Figura 7).

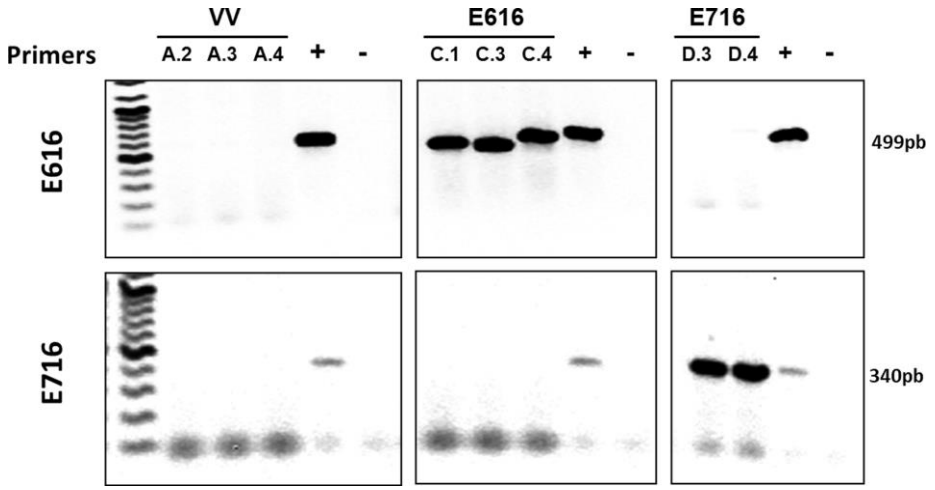

Figura 7. Amplificación de E6 y E7 a partir del DNA de las colonias resistentes. Se muestran los resultados de una PCR punto final visualizada en un gel de agarosa al 1%. La PCR a partir de DNA genómico de tres colonias resistentes para VV, tres para E616 y 2 para E716. Las columnas (p.e. A.2, C.1, D.3, etc.) indican la posición en la placa de 24 pozos en la que creció la colonia resistente. El control positivo (+) corresponde a DNA genómico obtenido de la línea celular Ca Ski, mientras que el control negativo (-) corresponde a una reacción sin DNA y utilizando agua para completar el volumen final de la reacción. El marcador de peso molecular corresponde a 100 pb. VV denota al vector vacío.

Una vez que se verificó la presencia de las secuencias virales en las colonias correspondientes, comprobamos la expresión de los genes de VPH a nivel de RNA y de proteína en dos colonias con VV, dos con E616 y dos con E716 (Figura 8). Debido a que se ha comprobado el efecto de factores de crecimiento sobre la regulación del splicing del mRNA para E6, modulando la proporción de E6/E6* (Rosenberger et al., 2010), evaluamos la expresión de los transcritos y proteínas virales en presencia y ausencia de suero. Los resultados obtenidos mediante RT-PCR (Figura 8 A), mostraron patrones similares a simple vista en los transcritos para las isoformas de E6, tanto en presencia como en ausencia de suero. Para el caso de las proteínas virales (Figura 8 B), se observó un ligero incremento en los niveles de expresión de la proteína E6 completa en presencia de suero, comparado con los niveles de esta proteína en ausencia de suero; debido a esto, todos los

experimentos restantes se llevaron a cabo en presencia de suero. Posteriormente, una colonia con cada uno de los vectores (VV, E616 o E716) fue elegida para los experimentos siguientes, en el caso de E6, se eligió la colonia que mostró una mayor presencia de E6* que de E6 completo, patrón que corresponde con lo reportado anteriormente para la línea celular Ca Ski (Rosenberger et al., 2010).

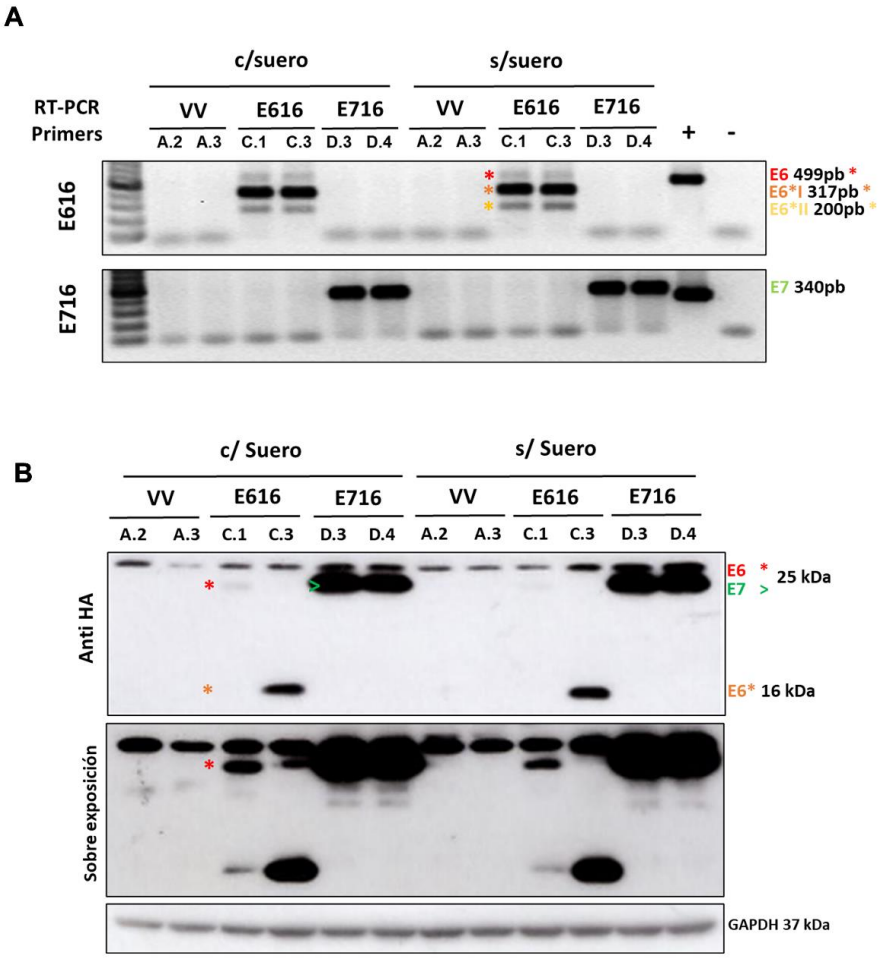

Figura 8. Patrones de expresión de los ORFs para E6 y E7 en células C-33 A en presencia y ausencia de suero. A) A partir del RNA total obtenido de las distintas líneas celulares clonales denotadas como A.2, A.3 (con VV), C.1, C.3 (con E616) y D.3, D.4 (con E716), la retro-transcripción de este RNA y la amplificación del cDNA, se evaluó la expresión de los transcritos generados a partir de los ORFs E6 y E7. El control positivo (+) corresponde a DNA genómico obtenido de la línea celular Ca Ski, mientras que el control negativo (-) corresponde a una reacción sin DNA y utilizando agua para completar el volumen final de la reacción. El marcador de peso molecular utilizado es de 100 pb; B) Western Blot utilizando un anticuerpo anti-HA, tag de fusión a las proteínas E6 y E7, para la identificación de ambas oncoproteínas en las distintas líneas celulares especificadas en la imagen. La detección de la proteína GAPDH mediante un anticuerpo específico fue utilizada como control de carga. VV corresponde al vector vacío.

Finalmente, la expresión de los genes virales se muestra a nivel de RNA (Figura 9 A) y de proteína (Figura 9 B). Como se esperaba, la expresión de E6 completo, así como de sus isoformas E6*I y E6*II fue detectada en la línea celular C33-E616, mientras que las células C33-E716 solo expresaron transcritos para E7. Cabe resaltar que los niveles de la proteína E6 completa fueron poco perceptibles, mientras que la isoforma E6* fue muy abundante. Un análisis de epifluorescencia mostró que tanto E6 como E7 se expresaron en todas las células con E616 y E716, respectivamente, confirmando que el modelo con expresión estable de las oncoproteínas fue desarrollado exitosamente (Figura 9 C).

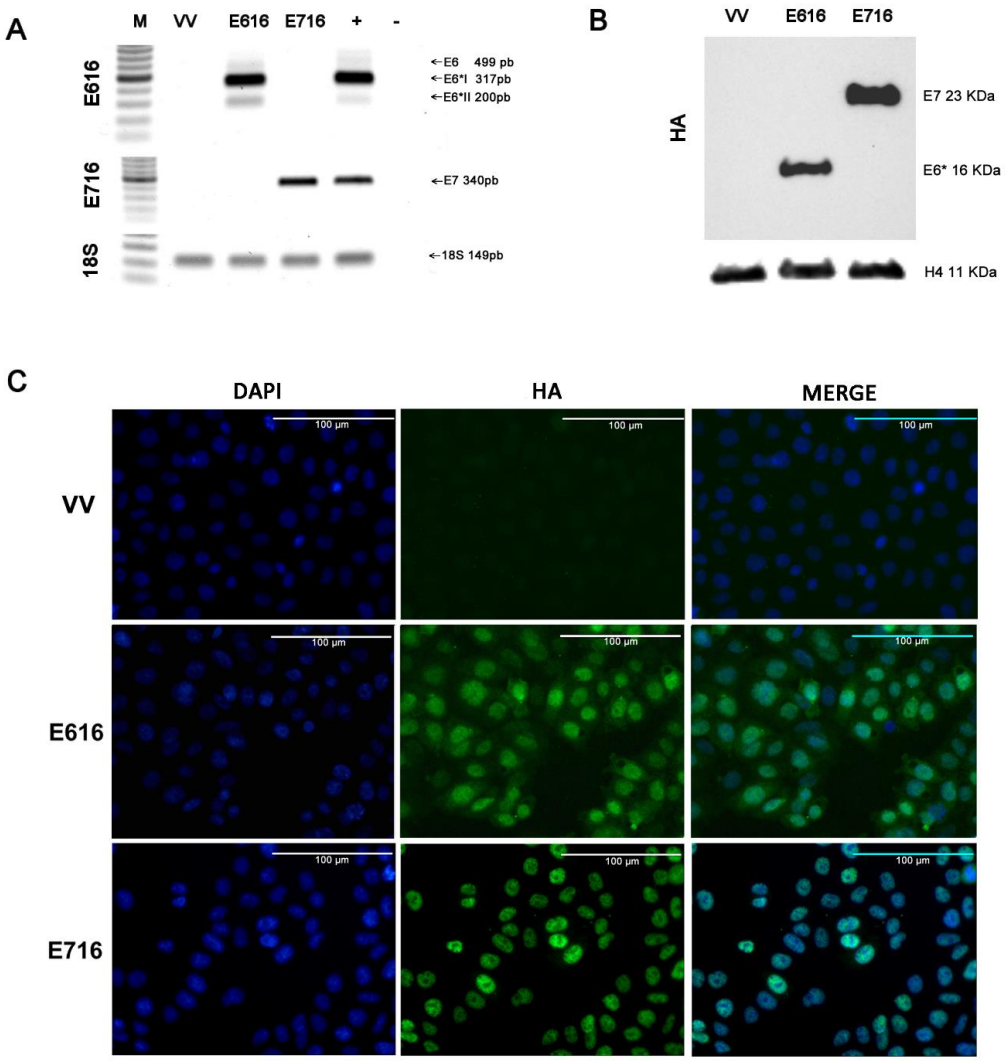

Figura 9. Expresión estable de E616 y E716 en células C-33 A. A) Patrones de expresión generados a partir de los ORFs para E6 y E7. A partir del RNA total obtenido de las distintas líneas celulares evaluadas (C33-VV, C33-E616 y C33-E716), la retro-transcripción de este

RNA y la amplificación del cDNA específico (RT-PCR), pudimos observar la expresión del mRNA de E6, E6*I y E6*II solo las células C33-E616, así como del mRNA de E7 solo en células C33-E716. La expresión de 18S fue utilizada como control interno. El control positivo (+) corresponde a una RT-PCR a partir de RNA obtenido de la línea celular Ca Ski, mientras que el control negativo (-) corresponde a una reacción sin ácidos nucleicos y utilizando agua para completar el volumen final de la reacción. El marcador de peso molecular (M) utilizado corresponde a 100 pb; B) A partir de extractos proteicos de las tres líneas celulares estables (C33-VV, C33-E616 y C33-E716), se realizó un WB utilizando un anticuerpo anti-HA, lo que permitió la detección de las proteínas E616 o E716 fusionadas al tag HA en las dos líneas celulares con expresión de cada una de las oncoproteínas. La expresión de la proteína H4 fue verificada como control de carga utilizando un anticuerpo anti-H4; C) Inmunofluorescencia utilizando un microscopio de epifluorescencia. DAPI fue utilizado para la detección del núcleo (en azul) y anticuerpo anti-HA para la detección de las oncoproteínas E6 y E7 (en verde), la barra de la escala representa 100 µm. Se muestra una imagen representativa de los experimentos.

Las proteínas E6 y E7 de VPH-16 modifican la expresión génica en células de cáncer cervical

Para identificar los perfiles de expresión génica asociados con la presencia de los oncogenes E6 y E7, se montaron tres ensayos independientes a partir de cada una de las líneas celulares generadas: C33-VV, E616 y E617 y se obtuvo RNA total de cada uno de estos ensayos. La integridad de este RNA se verificó mediante un gel de agarosa al 1% (Figura 10 A) y la obtención del RNA Integrity Number (RIN) (Tabla 4). Por otro lado, se corroboró la correcta expresión de los transcritos virales a partir del RNA obtenido (Figura 10 B).

Una vez que la calidad del RNA fue verificada, se realizó un análisis de secuenciación masiva de los transcritos expresados en los tres ensayos con las células C-33 A establemente transfectadas con E616, E717 y VV. El promedio de los resultados de expresión obtenidos por grupo, evidencian las diferencias entre los patrones de expresión de cada una de las tres líneas celulares generadas (Figura 11).

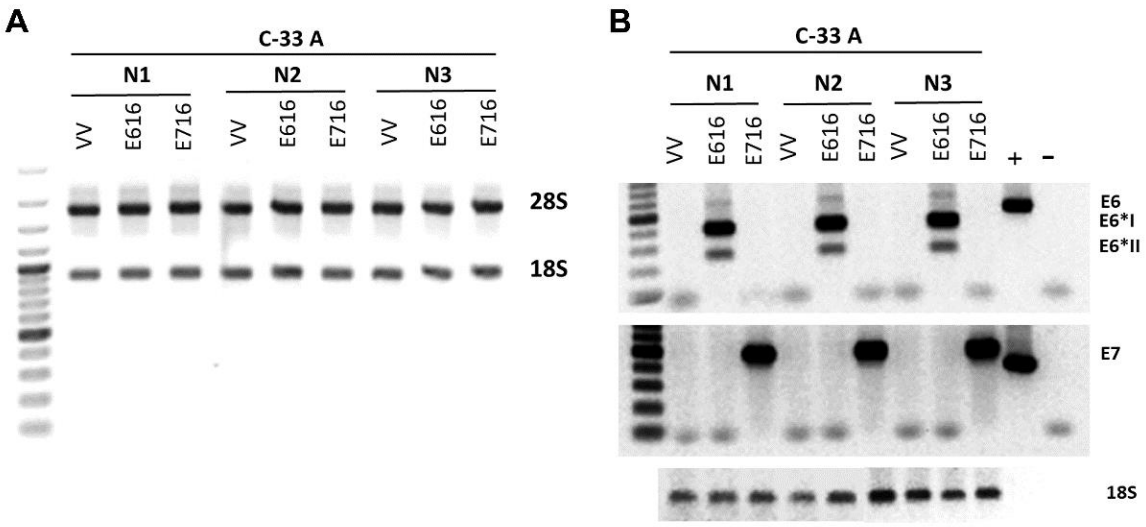

Figura 10. Verificación de la calidad de RNA utilizado para el ensayo de secuenciación de transcritos. A) Electroforesis en gel de agarosa al 1% para el RNA obtenido a partir de cada uno de los ensayos sembrados por triplicado (N1, N2 y N3) para las tres líneas celulares generadas. Se muestra el RNA 28 y 18 S; B) RT-PCR para verificar la correcta expresión de los transcritos para E6 y E7 en las líneas celulares correspondientes. La expresión de 18S fue utilizada como control interno. El control positivo (+) corresponde a DNA genómico obtenido de la línea celular Ca Ski, mientras que el control negativo (-) corresponde a una reacción sin DNA y utilizando agua para completar el volumen final de la reacción. El marcador de peso molecular utilizado corresponde a 100 pb. VV denota al vector vacío.

Tabla 4. RNA Integrity Number o RIN para cada una de las muestras de RNA utilizadas para el análisis de RNAseq.

Muestra de RNA	RIN
VV_N1	9.6
VV_N2	9.7
VV_N3	9.7
E616_N1	9.7
E616_N2	9.9
E616_N3	9.8
E716_N1	10
E716_N2	10
E716_N3	9.9

Después de observar los patrones generales de expresión, se realizó un análisis de expresión diferencial comparando los niveles de expresión génicos (Log2 FC) en C33-E616 y C33-E716 en relación con C33-VV. Un total de 2,689 genes se expresaron diferencialmente de forma significativa (p-adj < 0.05) en presencia de E6. De estos genes, 1,520 fueron incrementados mientras que 1,169 fueron disminuidos (Figura 12 A). Cuando se comparó a las células C33-E716 contra C33-VV, la expresión de 2,018 se mostró desregulada significativamente (p-adj < 0.05), la expresión de 1,108 incrementó y la de 910 disminuyó en presencia de la proteína viral (Figura 12 B).

En la Tabla 5, pueden consultarse los 20 genes cuya expresión fue mayoritariamente incrementada y los 20 genes para los cuales la expresión disminuyó de forma significativa (log2 FC p<0.001) tanto en presencia de la proteína E6 como de E7. Cabe resaltar que varios de los genes afectados son incrementados o disminuidos por ambas proteínas en el mismo sentido, por ejemplo: la expresión de ROBO2 se incrementa por E6 y E7, 5.3097 (p=0) y 4.7807 ($p=1.08^{-222}$), respectivamente; mientras que la expresión de ALDH1A1 disminuye por efecto de ambas proteínas, E6 -6.4088 (p=0) y E7 -8.5927 (p=0).

Estos resultados evidencian el efecto de ambas proteínas en un modelo de cáncer cervical y proveen gran cantidad de valiosa información para el estudio individual de cada una de las proteínas virales o el efecto conjunto que estas podrían tener.

Procesos celulares y vías de señalización modificados por E6 y E7 de VPH-16

Para identificar las vías de señalización y los procesos biológicos significativamente afectados por la expresión de E6 y E7 en células C33-A, se realizó un análisis de enriquecimiento utilizando la información de tres diferentes bases de datos: Gene Ontology (GO), Kyoto Encyclopedia of Genes and Genomes (KEGG) y Reactome.

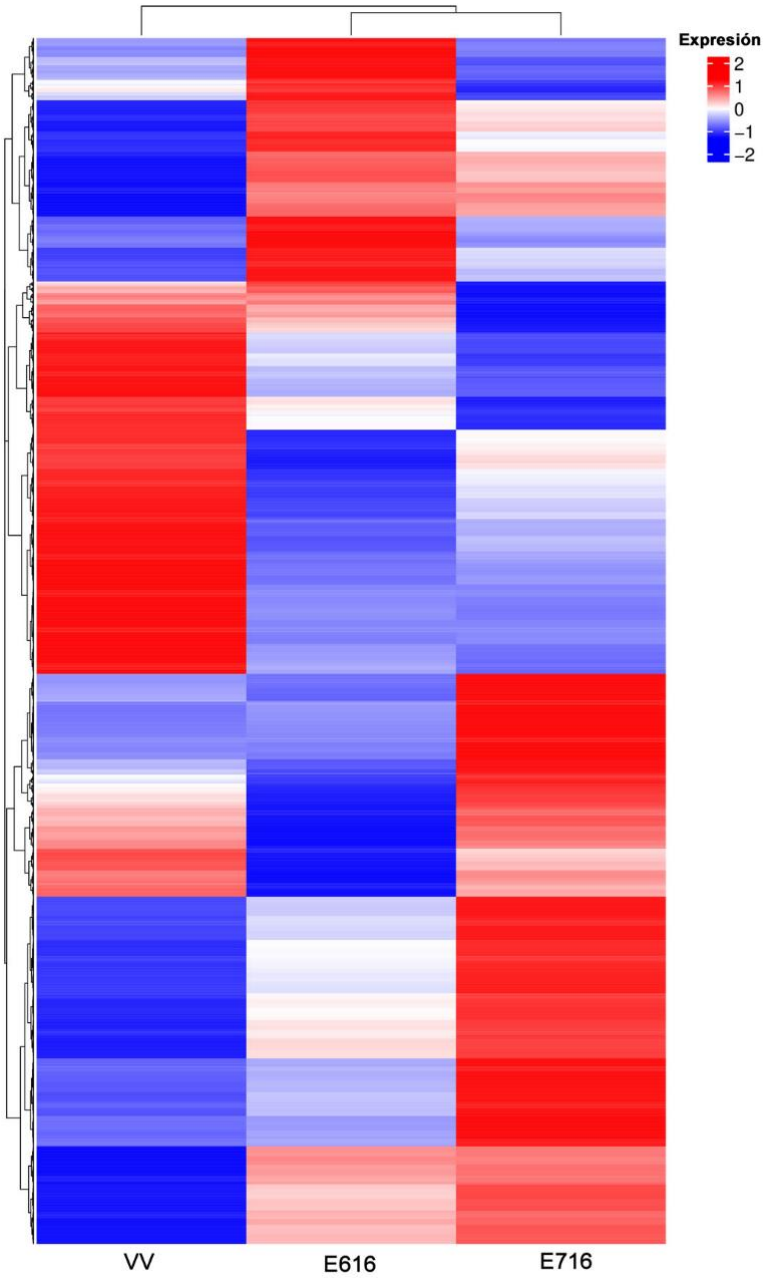

Figura 11. Patrones de expresión de las células C33-VV, C33-E616 y C33-E716. Mapa de calor que muestra la expresión diferencial de los genes Log2(FPKM+1) en las tres distintas condiciones de las columnas: Vector vacío o VV, E616 y E716. Cada fila representa la expresión de un gen. El color rojo indica el incremento en los niveles de expresión y el color azul la disminución de esta, mientras que el blanco refiere ningún cambio significativo o ausencia de datos. La agrupación jerárquica se muestra en la parte superior de la figura de acuerdo con los patrones transcripcionales de cada condición, mostrando que las células que expresan a las oncoproteínas son más cercanas entre ellas que aquellas con el vector vacío. Al lado izquierdo de la imagen se muestra la agrupación de los genes basada en la similitud de sus patrones de expresión.

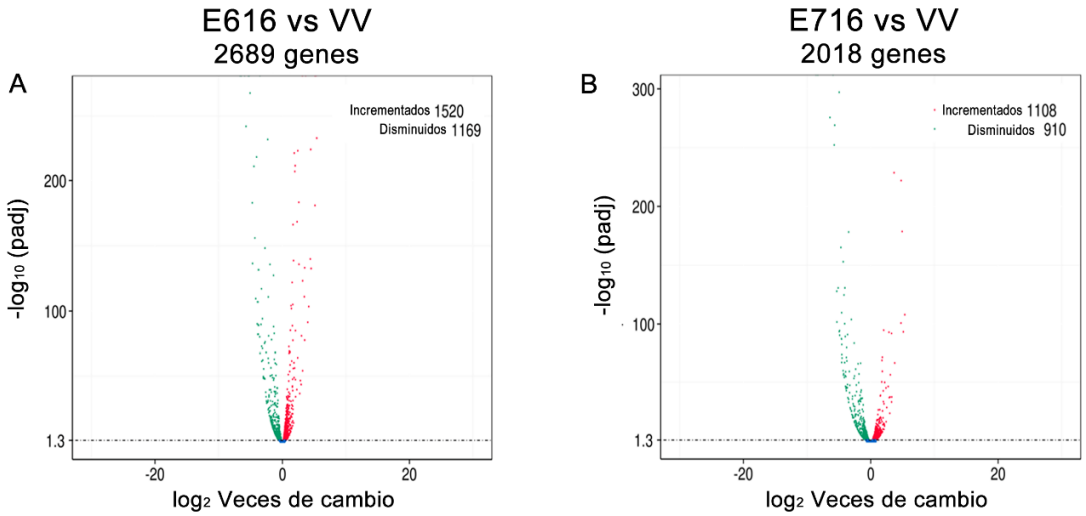

Figura 12. Genes diferencialmente expresados por E616 y E716 en células C-33 A. Gráfico de Volcán que ilustra los genes significativamente (p-adj < 0.05) desregulados en células A) C33-E616 y B) C33-E716, comparados con las células C33-VV. Los genes cuya expresión incrementó se muestran con un punto color rojo, mientras que aquellos genes cuya expresión disminuyó se observan como un punto verde. VV denota al vector vacío.

Tabla 5. Genes cuya expresión mostró más veces de cambio (sobreexpresión y disminución de la expresión) en presencia de E6 y E7 del VPH-16 en células C-33 A.

SOBREEXPRESIÓN							
E616				**E716**			
Gen	**log2 FC**	**p-ajust**	**Producto** proteína/RNA	**Gen**	**log2 FC**	**p-ajust**	**Producto** proteína/RNA
ROBO2	5.30	0	Receptor ROBO2	***HIST1H3I***	5.35	1.24^{-108}	Histona H3.1
HIST1H3I	5.13	1.16^{-181}	Histona H3.1	***KCNQ1OT1***	5.11	4.70^{-94}	RNA antisentido 2 de KCNQ1
RORB	5.12	0	Receptor RORB	***SLC16A3***	4.94	1.91^{-179}	Transportador de monocarboxilato 3
HIST1H2AL	4.51	2.49^{-133}	Histona H2AL	***ROBO2***	4.78	1.08^{-222}	Receptor ROBO2
SLC16A3	4.45	1.38^{-224}	Transportador de monocarboxilato 3	***DMD***	4.75	1.52^{-101}	Distrofina
DMD	4.38	1.28^{-140}	Distrofina	***CASC19***	3.77	1.28^{-67}	LncRNA LINC01245
KCNQ1OT1	4.14	3.43^{-104}	RNA antisentido 2 de KCNQ1	***EEF1A2***	3.66	2.21^{-229}	Factor eucariote de elongación de la traducción 1 α 2
PRSS12	3.65	0	Serina proteasa 12	***CASC8***	3.27	1.94^{-34}	lncRNA CASC8
AK5	3.50	1.75^{-78}	Adenilato cinasa 5	***CPED1***	3.26	1.14^{-92}	CPED1
CASC19	3.45	1.07^{-111}	lncRNA LINC01245	***JAG2***	3.07	1.39^{-57}	Jagged 2 Ligando canónico de Notch
CPED1	3.17	5.88^{-124}	CPED1	***HIST1H2AL***	2.98	7.16^{-25}	Histona H2AL
EEF1A2	3.14	0	Factor eucariote de elongación de la traducción 1 α 2	***FBLN1***	2.91	3.25^{-38}	Fibrilina 1

GREM1	2.99	8.48^{-82}	Gremlin-1	***LAMC3***	2.74	1.25^{-47}	Laminina 3 subunidad gamma
GNAT3	2.60	1.51^{-136}	Proteína G subunidad α transducina 3	***CRACR2B***	2.51	8.78^{-30}	Regulador CRAC 2B
HIST1H1B	2.58	4.54^{-184}	Histona H1.5	***BCAM***	2.41	1.15^{-17}	Molécula de adhesión de células basales
JAG2	2.40	3.29^{-65}	Jagged 2 Ligando canónico de Notch	***ITPR3***	2.39	1.90^{-46}	Receptor de IP3 isoforma 3
SCG2	2.30	3.93^{-169}	Secretogranina II	***FAM171B***	2.19	3.60^{-51}	FAM171B
CRACR2B	2.25	6.80^{-41}	Regulador CRAC 2B	***AK5***	2.15	6.69^{-14}	Adenilato cinasa 5
LAMC3	2.06	1.98^{-35}	Laminina 3 subunidad gamma	***POU5F2***	2.09	7.07^{-16}	Factor de transcripción con dominio POU 2 clase 5
TBC1D4	2.05	8.55^{-86}	TBC1 Domain Family Member 4	***RAB36***	2.07	3.47^{-11}	Proteína relacionada con Ras Rab-36
DISMINUCIÓN DE LA EXPRESIÓN							
E616				**E716**			
Gen	**log2 FC**	**p-ajust**	**Proteína**	**Gen**	**log2 FC**	**p-ajust**	**Proteína**
TFPI2	-6.61	0	Inhibidor 2 de la vía del factor tisular	***ALDH1A1***	-8.59	0	Aldehído Deshidrogenasa miembro de la familia A1
ALDH1A1	-6.40	0	Aldehído Deshidrogenasa miembro de la familia A1	***EMP1***	-8.36	0	Proteína de membrana epitelial 1
ANXA1	-5.86	0	Anexina A1	***ANXA1***	-8.30	0	Anexina A1
SYT1	-5.66	2.74^{-242}	Sinaptotagmina 1	***TFPI2***	-6.41	2.04^{-276}	Inhibidor 2 de la vía del factor tisular
VIM	-5.30	0	Vimentina	***VIM***	-5.92	0	Vimentina
CUBN	-5.15	0	Cubilina	***CAMK2D***	-5.73	5.34^{-253}	Subunidad Delta de la cinasa CaM II
NAV3	-5.02	8.79^{-268}	Neuron Navigator 3	***CUBN***	-5.66	8.03^{-270}	Cubilina
KITLG	-4.67	1.17^{-183}	Liando KIT	***COL11A1***	-5.33	1.33^{-128}	Cadena alfa 1 del colágeno tipo XI
DACH2	-4.63	3.48^{-137}	DACH2	***DACH2***	-5.31	2.06^{-102}	DACH2
SPRY2	-4.42	1.36^{-211}	Sprouty RTK Signaling Antagonist 2	***KITLG***	-5.11	1.92^{-131}	Liando KIT
FRMD3	-4.26	9.58^{-157}	Proteína con dominio FERM 3	***DPPA2***	-4.95	2.49^{-94}	Proteína asociada a desarrollo pluripotencial 2
MARCKS	-4.12	2.76^{-110}	Fosfomiristina	***RGS5***	-4.95	7.96^{-298}	Regulador de la vía de proteínas G 5
F3	-3.98	8.04^{-219}	Factor de Coagulación III	***ANGPT1***	-4.88	4.94^{-95}	Angiopoyetina 1
JAG1	-3.84	1.01^{-107}	Ligando canónico de Noctch 1 Jagged	***PLXDC2***	-4.88	3.83^{-91}	Proteína con dominio plexina 2
ARAP2	-3.79	5.84^{-83}	Proteína adaptadora 2 de Arf y Rho GAP	***F3***	-4.68	6.53^{-166}	Factor de Coagulación III

ARSJ	-3.73	6.86^{-90}	Arilsulfatasa J	***CADM1***	-4.61	3.45^{-88}	Molécula de adhesión celular 1
AC024909.2	-3.72	2.56^{-132}	LncRNA AC024909.2	***JAG1***	-4.58	6.34^{-88}	Ligando canónico de Noctch 1 Jagged
HIST1H2BH	-3.57	4.62^{-81}	Histona H2B tipo 1 H	***FRMD3***	-4.57	2.45^{-110}	Proteína con dominio FERM 3
CAMK2D	-3.54	0	Subunidad Delta de la cinasa CaM II	***ARAP2***	-4.56	4.86^{-68}	Proteína adaptadora 2 de Arf y Rho GAP
TRIM17	-3.51	1.37^{-68}	E3 ubiquitin ligasa TRIM17	***MARCKS***	-4.55	2.18^{-83}	Fosfomiristina

El análisis realizado a partir de datos de GO, mostró que los genes desregulados por E6 están involucrados en diversos procesos que se relacionan con ribosomas y localización de proteínas, así como catabolismo de RNA (Figura 13 A). De forma importante, el análisis de KEGG también mostró que las vías que incluían más genes desregulados fueron aquellas relacionadas con ribosomas, pero también se identificaron vías relacionadas con metabolismo del carbono (Figura 13 C). De forma muy interesante, el análisis a partir de datos de Reactome, también mostró que E6 se involucra principalmente con la desregulación de diversos procesos relacionados con traducción, así como con la vía de señalización SLIT/ROBO (Figura 13 E). Tomando en cuenta los resultados obtenidos, podemos decir que el efecto de E616 sobre diversos genes relacionados con el proceso de traducción a diferentes niveles, fue muy evidente.

Por otro lado, los genes desregulados por la expresión constitutiva de E716 en células C33-A se relacionaron con uniones y motilidad celulares, aunque también un gran número de estos se asociaron con proteínas que tienen actividad cinasa de serina/treonina, esto de acuerdo con el análisis obtenido a partir de datos de GO (Figura 13 B). Mientras tanto, el análisis de KEGG mostró que la expresión constitutiva de E716 en células C33-A desreguló genes relacionados con diversas vías de señalización en cáncer, incluyendo MAPK, PI3K/Akt, entre otras; aunque también se observaron algunos procesos relacionados con uniones celulares (Figura 13 D). Por otro lado, el análisis obtenido a partir de Reactome, evidenció que los procesos modulados significativamente estuvieron relacionados con interacciones de la célula, tanto con sindecano como con la matriz extracelular

(Figura 13 F). Los resultados obtenidos mostraron de forma constante, que E7 tiene un efecto sobre procesos involucrados con las uniones celulares de distintos tipos.

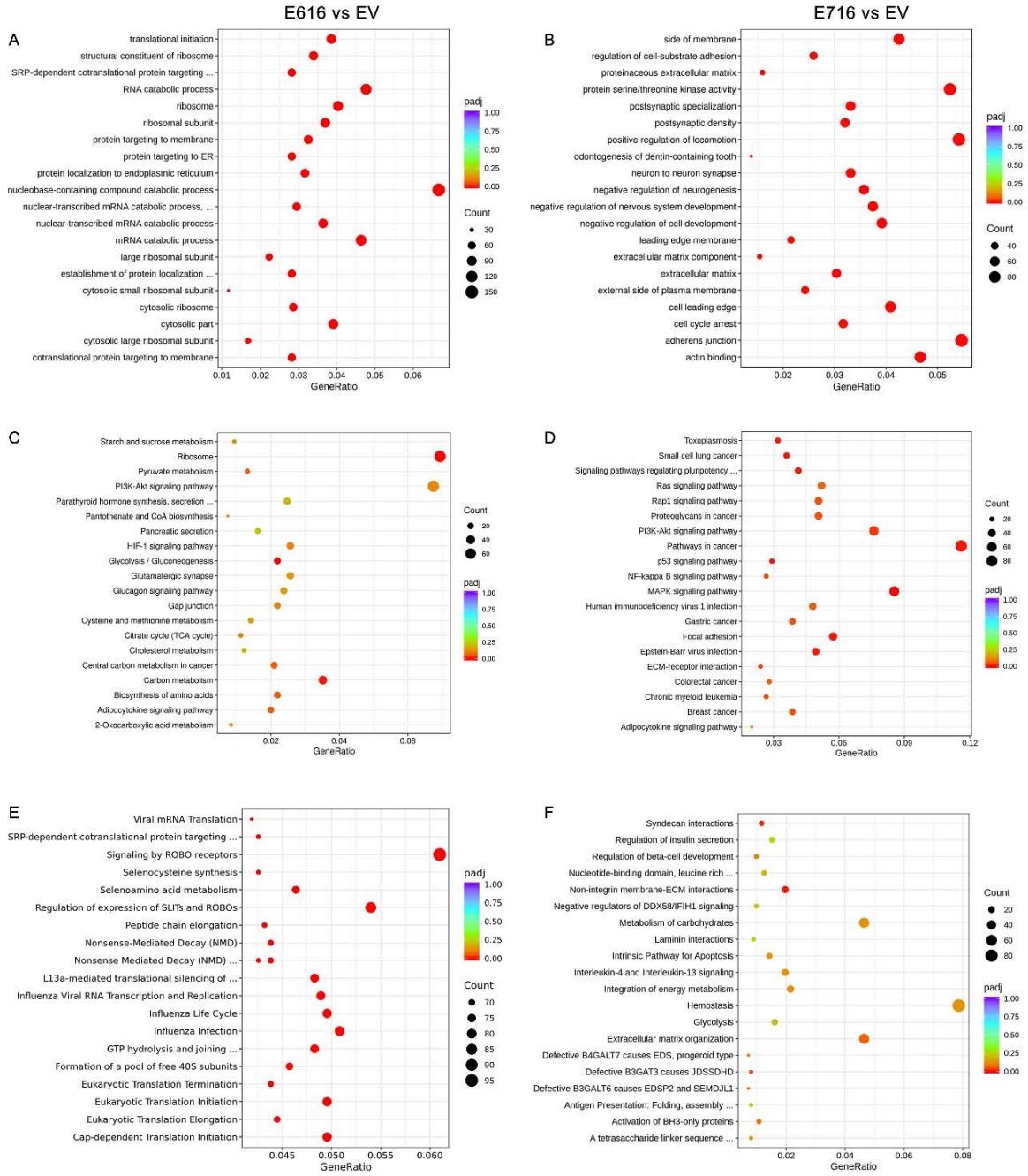

Figura 13. Análisis de enriquecimiento de los genes diferencialmente expresados (GDE) en células que contienen a las oncoproteínas E616 y E716. Se muestran las gráficas de puntos con las 20 funciones biológicas o vías de señalización más significativamente relacionadas con los GDE por E6 y E7. El análisis de enriquecimiento fue

realizado utilizando: datos de GO para células que expresan (A) E6 y (B) E7; dato del KEGG para (C) E616 y (D) E716; Reactome para (E) E6 y (F) E7. Los procesos significativamente (p-adj < 0.05) desregulados se muestran en color rojo. Los conteos se refieren al número de genes asignados a un término. El Radio de gen se refiere al número de GDE dividido entre el número de genes relacionados a cada categoría. Imagen tomada de (Olmedo-Nieva et al., 2022).

Genes desregulados por E6 y E7 que afectan la sobrevida global de pacientes con cáncer cervical

Inicialmente, se determinaron los genes afectados de forma significativa por la expresión de ambas oncoproteínas, es decir, los genes cuya expresión incrementa o disminuye tanto en presencia de E6 como en presencia de E7. Tomando en cuenta los 2,689 genes desregulados significativamente por E6 y los 2,018 por E7, identificamos 1,130 genes que fueron desregulados por ambas proteínas en las líneas celulares estables desarrolladas a partir de C-33 A. Con estos datos, se construyó el diagrama de Venn que se muestra en la Figura 14.

Debido a que ambas oncoproteínas virales se encuentran constitutivamente sobre expresadas en CC, se compararon los 1,130 genes afectados tanto por E6 como por E7 en nuestro modelo celular, con los genes desregulados en muestras de CC. Utilizando datos obtenidos a partir de una cohorte de TCGA compuesta por 309 pacientes, se realizó un análisis de expresión diferencial utilizando la paquetería DESeq2. Los resultados del análisis revelaron que la expresión de 6,667 genes se encontraba desregulada significativamente ($p < 0.05$) en CC y de estos, 335 genes se compartieron con los genes desregulados tanto en células C33-E616 como en C33-E716 (Figura 14).

Tomando en cuenta los 335 genes identificados, los pacientes fueron divididos en alta o baja expresión a partir de la mediana de expresión de cada gen, posteriormente, la sobrevida global de las pacientes fue calculada con el estimador Kaplan-Meier para cada gen y la comparación de sus respectivas curvas de sobrevivencia se realizó con la prueba de log-rank. Con los resultados de este estudio se identificaron 46 genes cuya alta o baja expresión afectó la SG de las

pacientes de forma significativa ($p < 0.05$). Después de esto, se llevó a cabo un análisis de regresión de Cox utilizando el R survival package, para analizar la tasa de riesgos instantáneos o Hazard Ratio (HR) (Tabla 6). Mediante un análisis univariado, se observó que la expresión de 13 de estos genes afectó significativamente ($p < 0.05$) el riesgo de supervivencia.

Debido a que la SG también se vio afectada por el estadio clínico, la dependencia del estadio clínico fue analizada a través de un análisis multivariado para cada uno de los 13 genes identificados. Los resultados mostraron que la expresión de sólo dos de estos 13 genes, moduló el riesgo de supervivencia independientemente del estadio clínico. Los resultados mostraron que la alta expresión de RIPOR2 incrementó la SG (HR = 1.8, CI 1.00–3.25, p = 0.048), mientras que la alta expresión de PFKFB4 disminuyó la SG (HR = 0.50, CI 0.27–0.93, p = 0.029) (Tabla 6).

Los gráficos de Kaplan-Meyer correspondientes al análisis de supervivencia, tomando en consideración la alta y baja expresión de PFKFB4 y de RIPOR2 en las muestras de las pacientes con cáncer cervical de TCGA se muestran en la Figura 15. La alta expresión de PFKFB4 (Figura 15 A) se asoció con una SG no favorable ($p = 0.0075$), evidenciada por la disminución de la mediana de sobrevida de 8.48 años en pacientes con baja expresión de PFKFB4 a 5.57 años en pacientes con alta expresión. De forma contraria, la alta expresión de RIPOR2 mostró un efecto protector ($p = 0.0011$) (Figura 15 B), ya que los pacientes con alta expresión mostraron una mediana de sobrevida de 8.48, comparada con 5.57 años en pacientes que expresan bajos niveles de RIPOR2. Los resultados obtenidos, evidencian que RIPOR2 y PFKFB4 están desregulados en pacientes con CC y en las líneas celulares C33-E616 y C33-E716, sugiriendo que su modulación en CC es al menos parcialmente debido al efecto de las oncoproteínas E6 y E7.

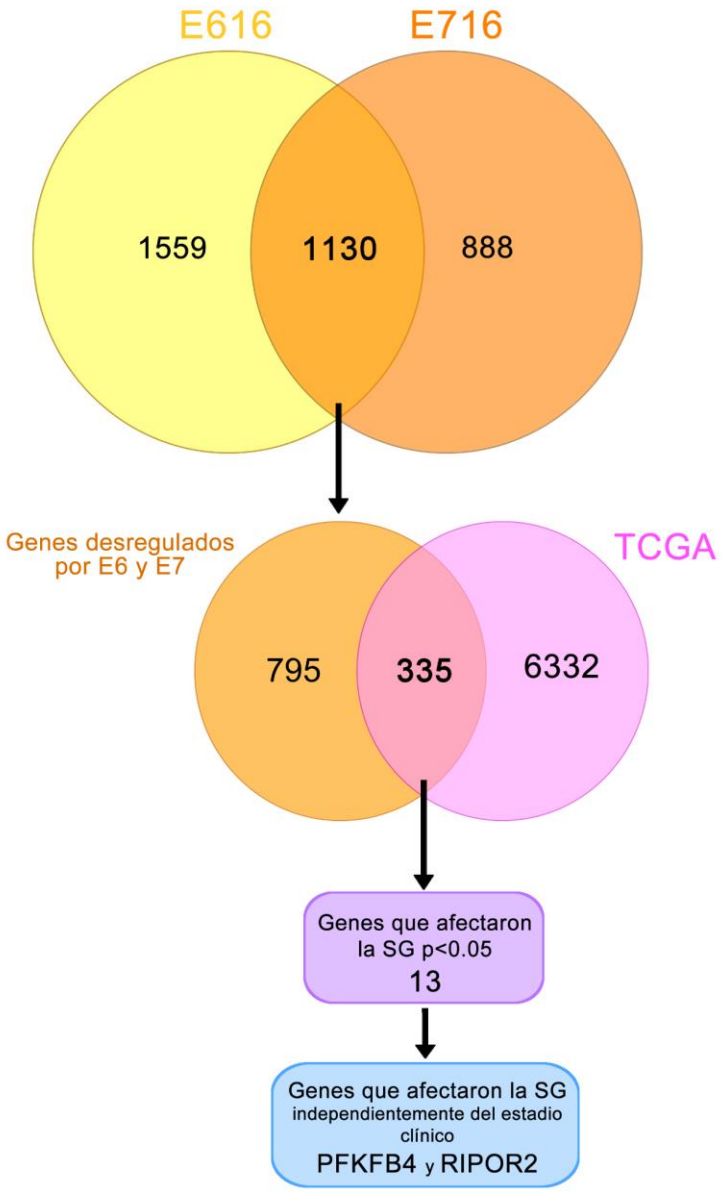

Figura 14. Genes desregulados en biopsias de pacientes con cáncer cervical y en las células C33-A que expresan constitutivamente a las oncoproteínas E6 o E7. El diagrama de Venn de color amarillo y naranja muestra a los genes desregulados por E616 y por E716 en las células C-33 A establemente transfectadas; la intersección de este diagrama muestra 1130 genes significativamente modulados por ambas oncoproteínas. El diagrama de Venn naranja y rosa, muestra 335 genes en la intersección de los genes modulados en CC y los genes desregulados por ambas oncoproteínas en las líneas celulares. A partir de estos datos, un análisis univariado mostró que 13 genes afectan significativamente la SG ($p < 0.05$). El análisis multivariado demostró que la expresión de los genes PFKFB4 y RIPOR2 afectó la SG de las pacientes independientemente del estadio clínico ($p < 0.05$). El análisis de regresión de Cox univariado y multivariado se realizó utilizando el R survival package. TCGA corresponde a The Cancer Genome Atlas.

Tabla 6. Análisis de regresión de Cox univariado y multivariado a partir de los genes que afectaron la sobrevida global de las pacientes con cáncer cervical en la cohorte de TCGA.					
Gen	**Supervivencia Global**	**Análisis univariado**		**Análisis multivariado**	
		HR (95% CI)	**p-value**	**HR (95% CI)**	**p-value**
SLC4A11	Alta vs baja expresión	2 (1.2-3.5)	**0.0081**	1.42 (0.79-2.55)	0.228
NUP188		2 (1.2-3.4)	**0.0097**	1.10 (0.54-2.23)	0.773
CREM		2 (1.2-3.3)	**0.013**	0.80 (0.40-1.62)	0.55
AP1B1		1.9 (1.1-3.1)	**0.016**	0.99 (0.52-1.88)	0.99
RIPOR2		2.4 (1.4-4.1)	**0.0016**	1.80 (1.00-3.25)	**0.048**
PFKFB4		0.5 (0.3-0.84)	**0.0085**	0.50 (0.27-0.93)	**0.029**
CC2D1A		1.9 (1.1-3.2)	**0.015**	1.14 (0.56-2.30)	0.704
BICDL1		1.9 (1.1-3.2)	**0.015**	1.16 (0.62-2.15)	0.629
RHOT2		2 (1.2-3.4)	**0.0073**	1.44 (0.74-2.79)	0.278
NBEAL2		1.9 (1.1-3.2)	**0.016**	1.27 (0.69-2.33)	0.436
CPNE7		2.2 (1.3-3.7)	**0.0033**	1.55 (0.83-2.90)	0.165
FARSA		1.9 (1.1-3.2)	**0.013**	1.15 (0.55-2.40)	0.692
SHTN1		2.2 (1.3-3.7)	**0.0033**	1.46 (0.73-2.91)	0.281
Estadio Clínico		1.5 (1.2-1.9)	**0.0003**	1.40 (1.06-1.83)	**0.014**

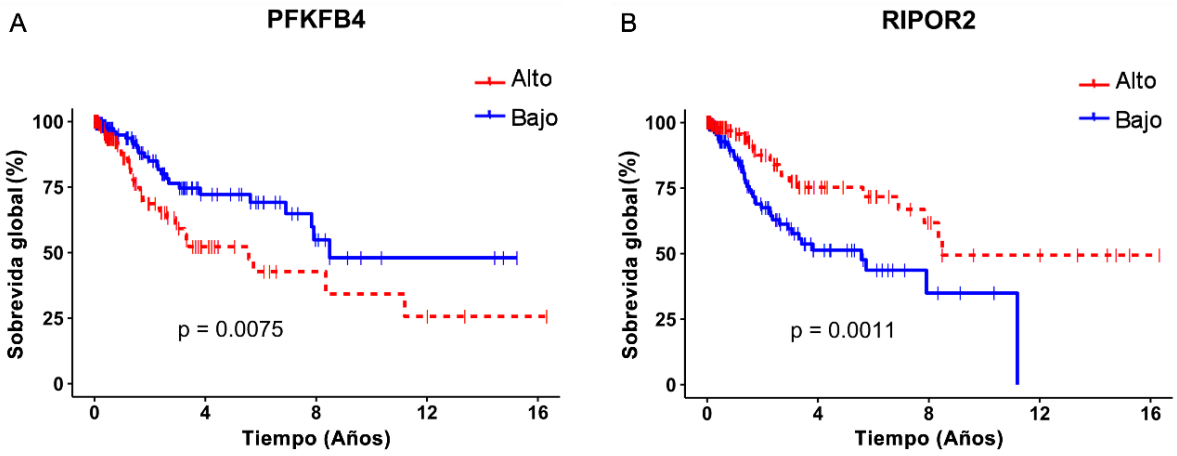

Figura 15. Análisis de sobrevida global (SG) mediante el estimador Kaplan-Meier a partir de la expresión de PFKFB4 y RIPOR2 en las pacientes de la cohorte de TCGA. A) Se observó que las pacientes con alta expresión de PFKFB4 mueren significativamente (p = 0.0075) más rápido que las pacientes con baja expresión de este transcrito; B) Para el caso de RIPOR2, se observó que las pacientes con baja expresión de este transcrito

mueren significativamente más rápido (p = 0.0011) que aquellas que presentaron una mayor expresión de RIPOR2. Los datos obtenidos de pacientes con bajos niveles de mRNA se representan en color azul mientras que aquellos obtenidos de pacientes con altos niveles en color rojo. La comparación de las curvas de sobrevivencia para los grupos de alta y baja expresión se realizó con la prueba de log-rank.

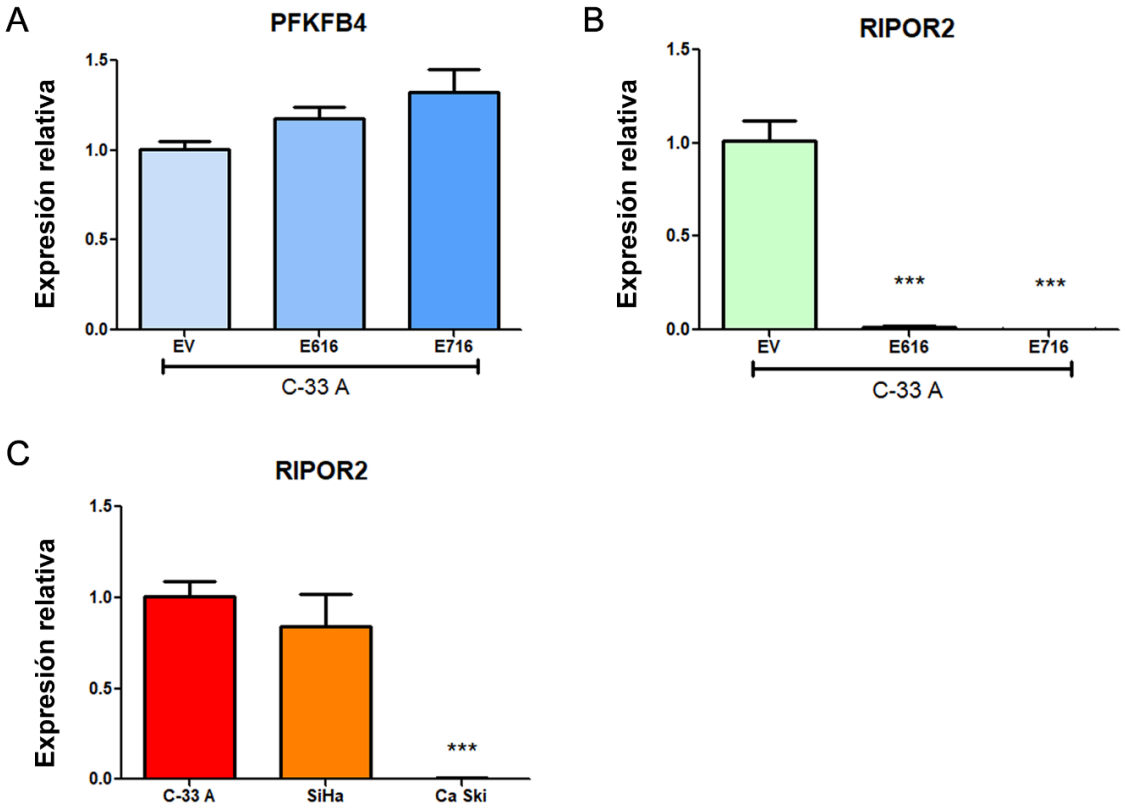

Figura 16. Expresión de PFKFB4 y RIPOR2 en líneas celulares de cáncer cervical. Se muestran los resultados de la expresión de PFKFB4 o RIPOR2 obtenidos a partir de la extracción de RNA total, su retro-trascripción y la amplificación del cDNA específico mediante PCR en tiempo real para distintas líneas celulares de cáncer cervical estudiadas. Niveles de expresión relativa de A) PFKFB4 y B) RIPOR2 en las tres líneas celulares generadas (C33-VV, C33-E616 y C33-E716); C) Niveles de expresión relativa de RIPOR2 en las líneas C-33 A, SiHa y Ca Ski. Cada gráfico es un experimento representativo de tres independientes que fueron realizados. La estadística se realizó comparando los resultados de expresión obtenidos en las células C33-VV o C-33 A, comparados con las demás condiciones experimentales mostradas en cada inciso. El análisis de resultados se llevó a cabo en GraphPad prism, media ± DS, utilizando la prueba de t de Student, *** p < 0.0001. VV. Vector vacío.

Los niveles de expresión de los transcritos para PFKFB4 y RIPOR2 se encuentran afectados en las líneas celulares que expresan E6 y E7

Para validar los resultados obtenidos en el análisis de RNAseq, los niveles transcripcionales de PFKFB4 y de RIPOR2 fueron analizados mediante RT-qPCR en células C-33 A que expresaban E6 y que expresaban E7. Estos valores fueron comparados con células transfectadas con el vector vacío (VV). Para el caso de PFKFB4, se observó un ligero incremento en su expresión en presencia de E6 y de E7, aunque dichos cambios no fueron significativos como se muestra en la Figura 16 A. En contraste, los niveles de RIPOR2 fueron evidentemente abatidos por la expresión de ambas oncoproteínas ($p < 0.0001$) (Figura 16 B). Esos resultados fueron comparables con aquellos obtenidos para la expresión de RIPOR2 en el análisis de RNAseq, ya que los niveles de expresión fueron Log2 FC –2.622 ($p = 7.16^{-39}$) y Log2 FC –3.839 ($p = 4.32^{-44}$) para células que expresan E616 y E716, respectivamente. Estos datos corroboraron el efecto de ambas oncoproteínas en la disminución de los niveles del mRNA de RIPOR2 en células de CC, C-33 A.

A continuación, la expresión de RIPOR2 fue analizada en líneas celulares de CC que contienen secuencias de VPH-16. Como se muestra en la Figura 16 C, las células SiHa, a pesar de mostrar una tendencia a la baja, no mostraron diferencias significativas en los niveles de expresión de RIPOR2 en relación con las células C-33 A; sin embargo, las células Ca Ski prácticamente no expresaron RIPOR 2.

Las oncoproteínas E6 y E7 de VPH-16 disminuyen los niveles de seis variantes transcripcionales de RIPOR2 en células C-33 A

De acuerdo con el National Center for Biotechnology Information (NCBI) (*NCBI. Gene RIPOR2*, 2023), existen al menos siete variantes transcripcionales para RIPOR2 que codifican para seis diferentes isoformas proteicas. A pesar de que el transcrito 6 contiene 5403 pb y el transcrito 7 se compone de 5359 pb, ambos contienen el ORF para la isoforma proteica 6, por lo que codifican para una misma proteína (Tabla 7). Debido a que, hasta el momento, hay poca información disponible sobre estas variantes (Dakour et al., 1997; Yoon et al., 2007), decidimos

investigar el impacto de la expresión de las oncoproteínas E6 y E7 del VPH-16 sobre los niveles de los distintos transcritos de RIPOR2.

Tabla 7. Transcritos y proteínas codificados a partir del gen RIPOR2.

Transcrito	Longitud (nt)	Tipo de transcrito	Isoforma proteica	Longitud (aa)
1	5553	Codificante	1	1068
2	2372	Codificante	2	591
3	5295	Codificante	3	1047
4	3546	Codificante	4	647
5	3548	Codificante	5	613
6	5403	Codificante	6	1018
7	5359	Codificante	6	1018

Para esto, identificamos y descargamos las secuencias nucleotídicas de las 7 variantes transcripcionales y realizamos un alineamiento múltiple de secuencias utilizando Clustal Omega (*Clustal Omega*, 2023). A partir de los resultados de este análisis, identificamos las zonas compartidas y diferenciales entre las secuencias de las distintas variantes y usando estos datos, diseñamos primers para detectar las siete variantes transcripcionales de RIPOR2. Como se puede observar en la Figura 17, los primers utilizados en los experimentos anteriores para la cuantificación de RIPOR2, identificados como “Pool”, detectaron todas las variantes transcripcionales. Por otro lado, debido a la similitud entre algunas de las secuencias de las variantes de RIPOR2, solamente fue posible diseñar primers específicos para las variantes 1, 2, 3, 4 y 7 (Denotados con azul en la Figura 17). Sin embargo, no existen secuencias específicas dentro de los exones o en las uniones exonicas que puedan distinguir a las variantes 5 y 6, debido a esto, se diseñaron primers capaces de detectar a la variante 5 (además de a la variante 4), así como primers que detectan a la variante 6 (pero también a la variante 1), estos primers pueden observarse resaltados en color morado en la Figura 17. Las secuencias de todos los oligonucleótidos utilizados para las variantes de RIPOR2 se especifican en la Tabla 3.

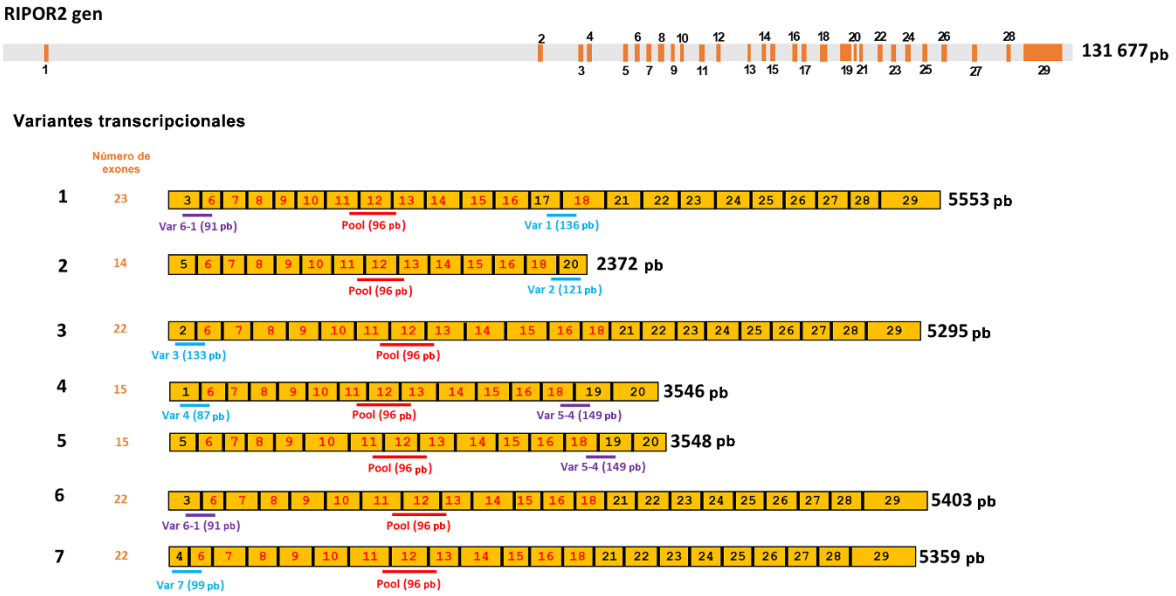

Figura 17. Gen humano de RIPOR2 y sus variantes transcripcionales. La barra superior gris muestra la posición de los intrones en el gen RIPOR2, mientras los cuadros naranjas enumerados denotan a los exones. Siete variantes transcripcionales se enlistan bajo el gen en color amarillo, mostrando los números de los exones que componen cada transcrito. Los exones con números en color rojo son aquellos que se comparten por todos los transcritos. Debajo de la representación de cada variante transcripcional, se muestra la posición de los primers específicos y el tamaño esperado del amplicón. Los primers denominados Pool amplifican una secuencia dentro de la región común entre transcritos (mostrado en rojo). Los exones con los números en negro se comparten solo entre algunos transcritos; por lo tanto, los primers específicos para cada variante fueron diseñados sobre dichas zonas. Los amplicones mostrados en color azul son aquellos que permiten la detección de las variantes específicas, mientras los amplicones en color morado son compartidos por dos variantes (variante 1 y 6; variante 4 y 5).

Una vez diseñados los distintos pares de primers, los niveles basales de expresión de las siete variantes transcripcionales de RIPOR2 fueron determinados en células C-33 A mediante RT-qPCR. La Figura 18 A muestra la expresión de cada variante transcripcional comparada con los niveles totales de los transcritos de RIPOR2, detectados mediante los primers Pool. Los resultados mostraron que las variantes más abundantes fueron la 6 y la 5, las cuales, en relación con los niveles totales de RIPOR2 se detectaron 2.68 y 2.84 veces menos, respectivamente. La variante 3, cuyos niveles fueron 4.95 veces menores que los detectados con los primers Pool,

fue la siguiente variante más abundante. Por otro lado, las variantes 1, 2 y 7 muestran niveles bajos en esta línea celular, los cuales fueron 200, 43.47 y 76.9 veces menores que los totales, respectivamente. De manera interesante, nosotros no fuimos capaces de detectar a la variante 4 en células C-33 A, sin embargo, esta se detectó en leucocitos humanos obtenidos a partir de un donador aparentemente sano (Figura 18 B), demostrando que los primers diseñados amplifican correctamente a la variante 4 y que esta no se expresa en C-33 A.

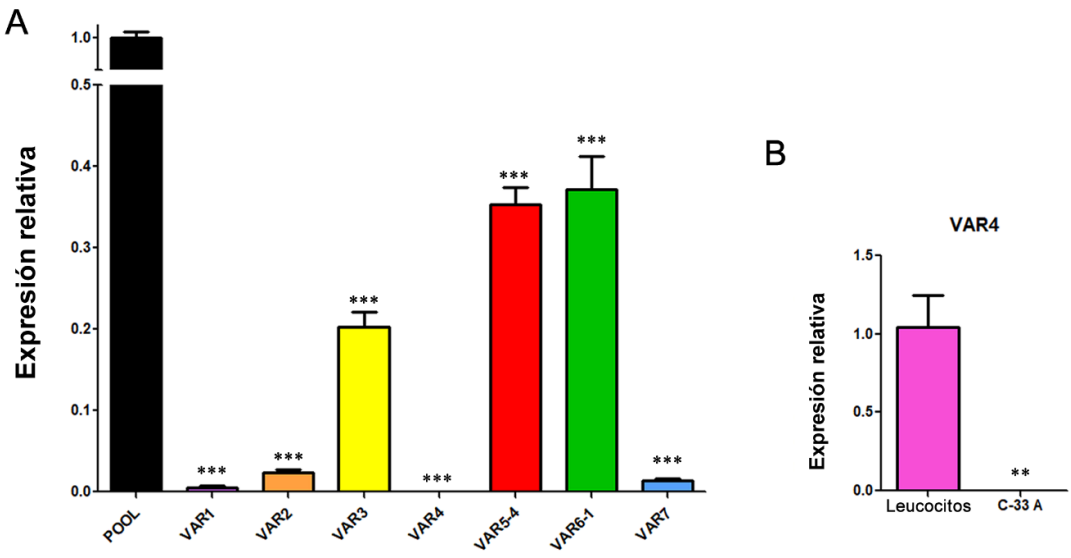

Figura 18. Las variantes transcripcionales de RIPOR2 expresadas en células C-33 A. A) Se muestran los resultados de la expresión de las 7 variantes transcripcionales de RIPOR2 obtenidos a partir de la extracción de RNA total, su retro-trascripción y la amplificación del cDNA específico mediante PCR en tiempo real (RT-qPCR) para la línea celular C-33 A, comparados con los niveles detectados con los primers RIPOR2 Pool en la misma línea celular; (B) Expresión de la variante 4 de RIPOR2 en linfocitos humanos obtenidos a partir de un donador aparentemente sano comparada con la expresión en células C-33 A mediante RT-qPCR. *** $p < 0.0001$, ** $p = 0.0066$.

Posteriormente, investigamos el efecto de la expresión de las proteínas E6 y E7 sobre los niveles de las siete variantes transcripcionales de RIPOR2 en las células C-33 A establemente transfectadas (Figura 19). Al analizar el efecto de las oncoproteínas sobre los niveles totales de los transcritos de RIPOR2 (Pool), detectamos una dramática disminución de su expresión, ocasionados por la expresión de E6 (50 veces) o de E7 (250 veces). Específicamente para las distintas

variantes transcripcionales, la disminución de los niveles del mRNA fue significativa en presencia de cualquiera de las dos proteínas virales y esto, para todas las variantes transcripcionales detectadas (1, 2, 3, 5, 6 y 7), incluso para aquellas variantes que se expresan muy poco en esta línea celular. Las variantes 5 y 6, aquellas con mayor expresión, se redujeron 20 y 29.4 veces, respectivamente, en células con expresión de E6, mientras que se redujeron 76.9 y 500 veces, respectivamente, en células con E7. Notablemente, la variante 3 fue completamente abatida en presencia de cualquiera de las dos oncoproteínas. Como esperábamos, la expresión de la variante 4 no fue detectada en ninguna de las tres líneas celulares.

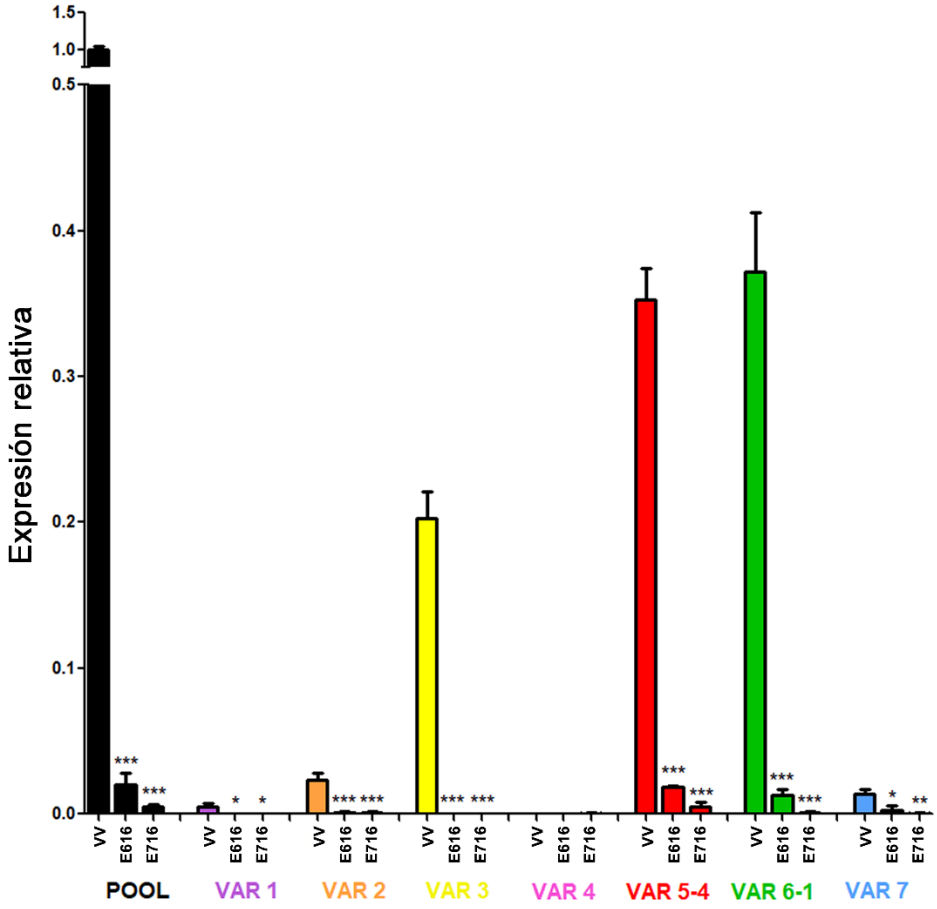

Figura 19. Efecto de las oncoproteínas E616 y E716 sobre los niveles de las variantes transcripcionales de RIPOR2. Los niveles de los transcritos 1-7 de RIPOR2 fueron evaluados en células C33-VV, C33-E616 y C33-E716 mediante la extracción de RNA total, su retro-trascripción y la amplificación del cDNA por PCR en tiempo real, utilizando los primers Pool y los primers específicos para las variantes transcripcionales. Las diferencias estadísticas son *** $p \leq 0.0009$, ** $p = 0.0029$, y * $p \leq 0.0166$ cuando comparas VV contra E616 o E716 para cada uno de los transcritos. VV corresponde al vector vacío.

Una vez evaluados los niveles específicos para cada transcrito de RIPOR2 en presencia de las oncoproteínas virales de forma individual quisimos evaluar los niveles de estas variantes en las líneas celulares con el genoma completo de VPH-16. Concordando con los resultados anteriormente obtenidos para los niveles totales de transcritos de RIPOR2 en C-33 A, SiHa y Ca Ski, algunas de las variantes se expresan en C-33 A y en SiHa, pero ninguna de ellas se expresa en Ca Ski (Figura 20). De manera interesante, observamos que las variantes 5 y 6, anteriormente identificadas como las más abundantes en C-33 A (Figura 18), fueron también las más abundantes en células SiHa, que las variantes 2 y 7 se expresan muy poco en ambas líneas celulares y que la variante 4 no se detecta en ninguna de ellas. En contraste, las variantes 1 y 3, las cuales sí fueron detectadas en C-33 A, no se expresan en la línea celular SiHa (Figura 20). Cabe resaltar, que todas las variantes tienden a expresarse ligeramente menos en las células SiHa que en las C-33 A.

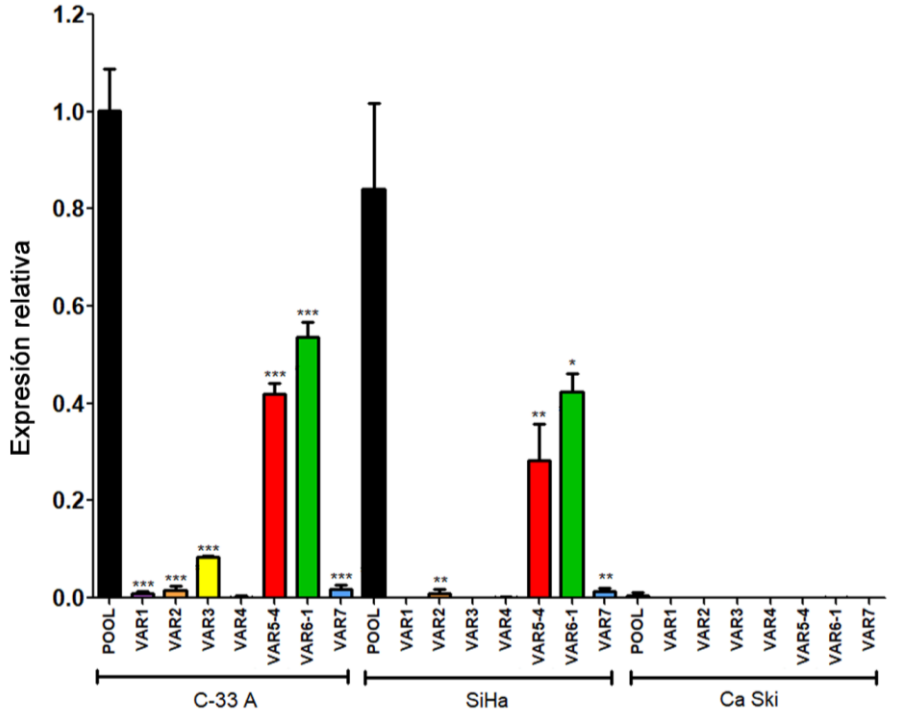

Figura 20. Expresión de las variantes transcripcionales de RIPOR2 en líneas celulares de cáncer cervical. Los niveles de las 7 variantes transcripcionales de RIPOR2 fueron evaluados en las líneas celulares de cáncer cervical C-33 A (sin HPV), SiHa (con 1 a dos copias de HPV-16) y Ca Ski (con 500 copias de HPV-16), a partir de la extracción de RNA total, su retro-trascripción y la amplificación del cDNA específico por PCR en tiempo real,

utilizando los primers Pool y los primers específicos para las variantes transcripcionales. Los datos de expresión relativa fueron obtenidos fueron comparados con los niveles del Pool en cada línea celular, *** $p \leq 0.009$, ** $p \leq 0.0072$, and * $p = 0.0159$. VV corresponde al vector vacío.

La actividad de los promotores de RIPOR2 es menor en células de cáncer cervical comparada con epitelio cervical normal

Debido a que tanto E6 como E7, disminuyen los niveles de todas las variantes transcripcionales detectadas en C-33 A y a que los niveles de todas estas variantes observadas en células SiHa, con 1 o 2 copias de VPH, tienden a ser menores que en C-33 A, mientras que en Ca Ski, con cientos de copias virales, no se expresa ninguna de las variantes, nos preguntamos si el efecto generalizado sobre todos los transcritos podría estarse dando a nivel transcripcional.

Para evaluar esta hipótesis, buscamos la secuencia del promotor del gen RIPOR2 utilizando la base de datos Eukaryotic Promoter Database (EPD) (*EPD The Eukaryotic Promoter Database*, 2023). En la base EPD, identificamos que el gen RIPOR2 posee 4 promotores dentro de su secuencia, cuya posición sobre el genoma puede observarse en el esquema general de la Figura 21, donde además de la localización de los promotores, se muestran las islas CpG establecidas para esta zona y las zonas con enriquecimiento de la marca H3K4me3, comúnmente asociada con activación transcripcional. En la parte inferior de la imagen también se muestran los siete transcritos analizados.

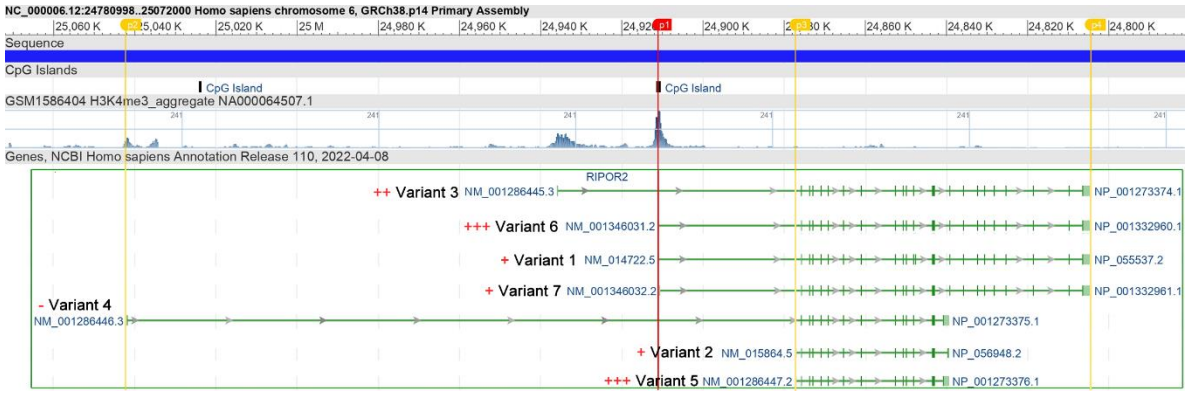

Figura 21. Localización de los promotores de RIPOR2 sobre el genoma humano. Se muestran las posiciones para los cuatro promotores presentes en el gen de RIPOR2,

denotados como p1, p2, p3 y p4. En la imagen también se ejemplifican las posiciones donde se ubican islas CpG y las zonas en las que la marca H3K4me3 se encuentra enriquecida. En la parte inferior de la imagen se muestran los transcritos para las siete variantes transcripcionales de RIPOR2 y con signos + o - en color rojo, se ejemplifica la expresión que se encontró para cada una de estas variantes en el presente estudio. Imagen modificada a partir de (*NCBI. Gene RIPOR2*, 2023).

Interesantemente, la localización del promotor 1 (p1), concuerda con la localización de una isla CpG y con una zona altamente enriquecida con la marca H3K4me3, lo que hace pensar que es un promotor altamente transcrito. Datos obtenidos del proyecto FANTOM5, que contiene información sobre los perfiles completos de expresión en líneas celulares y tejidos de distintas estirpes celulares (*FANTOM. Functional Annotation of the Mammalian Genome*, 2014), concuerdan perfectamente con la información previamente obtenida. Utilizando los datos de FAMTOM5, pudimos observar la expresión a partir de los 4 promotores de RIPOR2 en diversas líneas celulares provenientes de cáncer cervical, en comparación con un pool de tejido cervical normal. Los resultados que se muestran en la Figura 22, muestran que en general, el pool de tejido cervical mostró expresión en los promotores 1, 2 y 4, pero no en el 3, y que la expresión observada en los promotores de tejido normal fue mayor que la expresión observada en cualquiera de las líneas de cáncer cervical. Finalmente, cabe resaltar que el p1 es el que mostró mucha mayor expresión, si se compara con los otros promotores, tanto en el tejido normal como en las células de CC.

La expresión de RIPOR2 está disminuida en lesiones premalignas y su baja expresión en cáncer cervical está asociada con un peor pronóstico

Posteriormente, para poder observar los niveles de expresión de RIPOR2 en pacientes mexicanas, no solo con cáncer cervical, sino también con lesiones intraepiteliales escamosas de bajo y alto grado (LIEBG y LIEAG, respectivamente) así como en muestras normales con y sin infección con VPH, llevamos a cabo una extracción de RNA a partir de las muestras y posteriormente realizamos una RT-qPCR. Como se muestra en la Figura 23 A, la expresión de RIPOR2 es

significativamente más baja en LIEBG, LIEAG y muestras normales con infección de VPH, en comparación con muestras normales sin infección viral.

Figura 22. Niveles de expresión a partir de los promotores de RIPOR2 en CC. Se muestran los niveles de expresión para un pool de tejido adulto de cérvix y 11 líneas celulares de CC a partir de los cuatro diferentes promotores de RIPOR2. Datos obtenidos de FANTOM 5 (*FANTOM. Functional Annotation of the Mammalian Genome*, 2014).

Finalmente, la evaluación de la expresión de RIPOR2 en tejido de cáncer cervical (n=19) mostró que la baja expresión de este gen podría asociarse con un peor pronóstico en la cohorte de mujeres mexicanas (Figura 23 B).

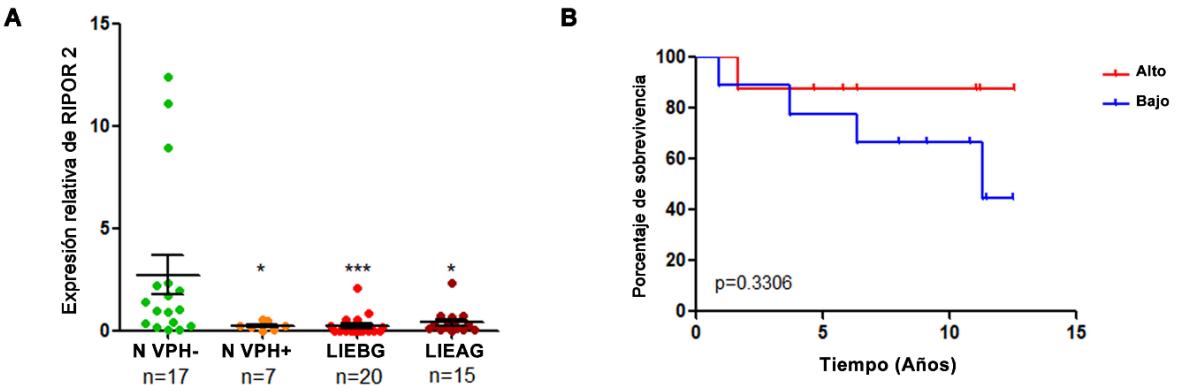

Figura 23. Expresión de RIPOR2 en lesiones cervicales premalignas y cáncer cervical. (A) Niveles de mRNA de RIPOR2 analizados mediante retrotranscripción y posterior amplificación del cDNA obtenido utilizando los primers pool en epitelio normal (N) positivo y negativo a VPH, así como en LIEBG y LIEAG * $p \leq 0.0222$; *** $p = 0.0001$; (B) Análisis de sobrevivencia global comparando los pacientes con baja expresión de RIPOR2 (en azul) contra los pacientes con alta expresión (en rojo), p=0.3306.

DISCUSIÓN

En México, el cáncer cervical continúa siendo un problema de salud importante, donde la gran mayoría de los casos son diagnosticados en etapas localmente avanzadas y avanzadas (Isla-Ortiz et al., 2020). Para estas pacientes, los tratamientos más utilizados actualmente son quimioterapia y radioterapia, administrados de forma individual o empleando terapias combinadas (Arango-Bravo et al., 2022). El fármaco más comúnmente utilizado es el cis-platino, que afecta principalmente la división celular, causando apoptosis en las células cancerígenas; sin embargo, los efectos de este compuesto también afectan a otras células, provocando alta toxicidad en las pacientes (Dasari & Bernard Tchounwou, 2014). Causas como esta, explican que las pacientes diagnosticadas en etapas avanzadas muestren una sobrevida global cercana al 40% (Arango-Bravo et al., 2022). Por lo tanto, estrategias que permitan una estratificación más adecuada de las pacientes en etapas avanzadas permitirá la elección de seguimientos más estrechos en pacientes con mayor riesgo, así como la disminución de tratamiento excesivo en pacientes con menor riesgo. En este sentido, la búsqueda de biomarcadores pronóstico se ha convertido en un área de interés para la identificación de grupos específicos de pacientes.

La expresión continua de las oncoproteínas E6 y E7 del VPH promueve y mantiene el fenotipo maligno en CC. Se ha demostrado que la reducción en la expresión de los oncogenes E6 y E7 revierte el fenotipo maligno. Estudios *in vitro* e *in vivo,* reportaron que la edición de los genes E6/E7 de VPH-16 y VPH-18 mediante el sistema CRISPR-Cas9, disminuye la cantidad de las proteínas virales, incrementa la expresión de los supresores tumorales blancos de estas oncoproteínas (p53 y p21) y promueve la reducción del tamaño tumoral en modelos animales (Ling et al., 2020; Zhen et al., 2020). Adicionalmente, se ha investigado el efecto combinado de la restauración de la expresión de p53 y la inhibición de E7 de VPH-16, mediante el uso de vectores en distintos modelos. Los resultados con este tratamiento fueron inhibición del crecimiento celular en las líneas de cáncer cervical SiHa y Ca Ski, así

como la reducción del tamaño de tumores generados a partir de células SiHa en ratones. En un modelo murino con lesiones cervicales premalignas, esta terapia promovió una evidente regresión de las lesiones cervicales (Xiong et al., 2022). Dichos resultados evidencian la importancia de la expresión de las oncoproteínas en el mantenimiento, tanto de lesiones premalignas como de los tumores cervicales. A pesar de estos resultados, el uso de estrategias como CRISPR-Cas9, dirigidas a la disminución de E6 y E7 en células tumorales sigue siendo limitado, debido principalmente a los posibles blancos inespecíficos y a las dificultades de entrega a las células infectadas (Wei et al., 2022). Tomando en cuenta los obstáculos observados hasta ahora, el estudio paralelo no solo de las oncoproteínas virales, sino también de sus blancos moleculares es de suma importancia, ya que estas moléculas podrían ser utilizadas como objetivos farmacológicos y de forma más inmediata, como biomarcadores pronóstico en las pacientes con cáncer cervical.

En este sentido, se han realizado algunos esfuerzos para identificar moléculas que permitan predecir la sobrevida global de las pacientes con CC, basados en las moléculas desreguladas en este padecimiento (Volkova et al., 2021) y en la presencia o expresión de las secuencias virales (A. Dong et al., 2022). Sin embargo, hay poca información sobre aquellos elementos desregulados específicamente por las oncoproteínas virales y que puedan ser utilizados como biomarcadores asociados con la sobrevida global en CC. Anteriormente, se han estudiado perfiles de expresión de RNA, identificados por secuenciación masiva, que proveen información de las moléculas alteradas en los principales subtipos de CC y que se asocian con el desenlace clínico de las pacientes (Campos-Parra et al., 2022), pero además de estos perfiles, sería de importancia conocer aquellos genes cuya alteración en cáncer es consecuencia de la presencia de los oncogenes virales. Con esto en mente, en el presente estudio analizamos el transcriptoma de las células de cáncer cervical C-33 A establemente transfectadas con los oncogenes E6 y E7 de VPH-16.

A partir de los resultados obtenidos, pudimos identificar tres grupos principales de genes: aquellos modificados solo por E616, los que se alteran únicamente en presencia de E716 y los genes cuya expresión es afectada por ambas proteínas. Aunque el presente trabajo se enfoca en el estudio de los genes alterados por ambas oncoproteínas virales, todos aquellos genes cuya expresión incrementó o disminuyó en presencia de E6 o de E7, representan blancos importantes para el estudio de los mecanismos moleculares relacionados con el VPH.

Entre otros, E6 altera la expresión de genes relacionados con procesos que se han visto desregulados en variados tipos de cáncer, tales como el metabolismo del carbono, la señalización de ROBO/Slit y la traducción, tanto al nivel de la estructura de ribosomas, como a nivel de iniciación, elongación y terminación (Figura 13 A, C y E). Mientras que la desregulación del metabolismo del carbono ha sido ampliamente abordada en CC, existe muy poca información sobre la desregulación de la vía de ROBO, donde se ha reportado hipermetilación en varios genes de la vía, promoviendo la disminución de su expresión (Narayan et al., 2006). Sobre la traducción, se ha observado anteriormente la modulación de este proceso por efecto de E6, quien ha mostrado incrementar la traducción de componentes de la vía de Wnt, promoviendo proliferación celular (Zhao et al., 2019) y también se ha relacionado con el incremento del factor traduccional eIF5A-1, causando migración y proliferación celular (Liu et al., 2018).

El efecto de E7 sobre la expresión génica se asocia principalmente con la modificación de uniones celulares y vías de señalización asociadas a cáncer (Figura 13 B, D y F), modulaciones que han sido relacionadas anteriormente con la oncoproteína viral. Ejemplo de esto es la alteración de la arquitectura celular, la disminución de la expresión de claudinas, el incremento de los espacios entre las células y el aumento de la migración celular mediados por la sobreexpresión de E7 en células adherentes (Uc et al., 2020). Además, los datos obtenidos en este trabajo reafirmaron el efecto de E7 sobre diversas vías de señalización tales como MAPK cinasas, PI3K/AKT, entre otras (Bonab et al., 2021; Hua et al., 2022).

Dentro del grupo de genes desregulados por ambas oncoproteínas (Tabla 5), identificamos algunos que fueron incrementados tanto por E6 como por E7; la expresión del gen ROBO2 por ejemplo, se incrementa 5.3097 veces en presencia de E6 (p=0) y 4.7807 veces en presencia de E7 ($p=1.08^{-222}$). Aunque el efecto de los receptores ROBO ha sido estudiado en cáncer, su expresión se muestra incrementada en ciertos tipos y disminuida en otros (Tong et al., 2019); en CC ha sido muy poco estudiado (Mitra et al., 2012) y muestra discrepancias con los resultados de este estudio. Por otro lado, la expresión de genes como ALDH1A1, disminuyó en presencia de cualquiera de las oncoproteínas, mostrado una expresión de -6.4088 veces ($p< 0.001$) cuando se sobre expresa E6 y de -8.5927 veces ($p< 0.001$) cuando está presente la proteína E7. En contraste con los resultados que obtuvimos, la expresión de ALDH1A1 se ha observado incrementada en NIC II, III y CC, tanto a nivel de mRNA como de proteína (Tulake et al., 2018). La poca información publicada a la fecha sobre estos y otros blancos afectados por ambas oncoproteínas virales que fueron detectados en nuestro estudio, así como las discrepancias encontradas con la información publicada, demuestran que más investigación es necesaria para poder generar conclusiones contundentes.

Con el propósito de identificar cuáles de los genes diferencialmente expresados en presencia de las ambas oncoproteínas virales, podrían estar involucrados en el desarrollo de cáncer cervical, decidimos comparar los genes afectados por E6 y E7 en células C-33 A, con los genes diferencialmente expresados en muestras de CC provenientes de una cohorte de pacientes del TCGA. Los resultados mostraron 335 genes compartidos por ambos análisis y un sucesivo estudio de SG asociada con la alta o baja expresión de estos genes mostró que la expresión de 13 de ellos afectó significativamente el pronóstico de las pacientes, mientras que solo la baja expresión de RIPOR2 y la alta expresión de PFKFB4 disminuyeron la SG de las pacientes independientemente del estadio clínico. Es importante mencionar, que los 13 genes proveen información valiosa en cuanto a blancos terapéuticos, incluso cuando su expresión sea dependiente del estadio clínico, sin embargo, el uso de

RIPOR2 y PFKFB4 plantea un valor agregado y los posiciona como posibles biomarcadores pronóstico.

A la fecha, varios estudios han relacionado la alta expresión de PFKFB4 con el mal pronóstico de los pacientes con distintos tipos de cáncer (Cai et al., 2021; Lu et al., 2020; Trojan et al., 2018; Wang et al., 2021; Zhou et al., 2022). En CC ya se ha reportado la sobreexpresión de PFKFB4 y también se ha asociado con el proceso carcinogénico y un mal pronóstico para las pacientes (Cai et al., 2020; Hsin et al., 2021; Sun & Jin, 2022; Wu et al., 2022); sin embargo, la actividad de las oncoproteínas E7 y E6 no se ha relacionado con dicho incremento de PFKFB4.

Por otro lado, se ha observado baja o nula expresión de RIPOR2 en líneas celulares derivadas de cáncer, incluyendo retinoblastoma, pulmón, glioma, vejiga y colon (Dakour et al., 1997); mientras que su sobreexpresión en células Jurkat (leucemia) disminuyó la proliferación celular (Froehlich et al., 2016). A partir de datos provenientes del TCGA, se observó baja expresión de RIPOR2 en muestras de hepatocarcinoma y esta fue relacionada con el mal pronóstico de los pacientes (Dastsooz et al., n.d.). Específicamente en CC, se identificó una firma compuesta de cuatro genes (RIPOR2, DAAM2, SORBS1, CXCL8) que se asocia con la sobrevida de las pacientes, mostrando que los tumores en los que RIPOR2 se encontró disminuido tienen un peor pronóstico. De acuerdo con con esto, otro estudio identificó una firma compuesta por RIPOR2, CCL22, PAMR1 y FBN1, donde las pacientes con CC que presentan mayor expresión de RIPOR2 poseen una mayor SG, concluyendo que RIPOR2 es un factor protector en CC (Xu et al., 2022), datos que coinciden con lo reportado en el presente trabajo. Además de esto, cuando RIPOR2 fue sobre-expresado en las líneas celulares de CC SiHa y HeLa, la viabilidad celular y la capacidad de migrar de estas células disminuyó significativamente (Xu et al., 2022). En este sentido, RIPOR2 parece actuar como supresor tumoral en varios tipos de cáncer, no obstante, nuestro trabajo provee información valiosa sobre la participación de las oncoproteínas E6 y E7 en la disminución de RIPOR2 específicamente en cáncer cervical.

Posteriormente, verificamos los niveles transcripcionales tanto de PFKFB4 como de RIPOR2 en las células C33-VV, C33-E616 y C33-E716, observando una evidente disminución de los transcritos de RIPOR2 tanto en presencia de E6 como de E7, pero ningún efecto significativo en el caso de PFKFB4. La expresión de RIPOR2 también fue analizada en las líneas celulares de CC SiHa y Ca Ski que contienen secuencias de VPH-16, comparada con su expresión en C-33 A, que a pesar de ser de CC no contiene VPH. Los resultados de dichos experimentos mostraron que las células SiHa, a pesar de mostrar una tendencia a la baja, no tuvieron diferencias significativas en los niveles de expresión de RIPOR2 en relación con las células C-33 A; sin embargo, las células Ca Ski no expresaron RIPOR 2. Estos resultados podrían ser explicados parcialmente por las diferencias en el número de copias de VPH-16 en cada línea celular; mientras que Ca Ski posee 500 copias de VPH, SiHa contiene de 1 a 2 copias (Mincheva et al., 1987), lo que probablemente podría influenciar los niveles de las proteínas virales y por tanto, de RIPOR2.

A lo largo del tiempo, se han dado distintos nombres a los transcritos y proteínas provenientes del gen RIPOR2 (PL48, C6orf32, FAM65B) y estos se han reportado con un número distinto de nucleótidos y aminoácidos. Las primeras variantes de RIPOR2 identificadas en citotrofoblastos en diferenciación fueron tres mRNAs de 2.8, 3.5 y 4.8 kb (Dakour et al., 1997; Morrish et al., 1996). Posteriormente, diversas isoformas de la proteína RIPOR2 fueron detectadas mediante inmunoblot, y estas fueron descritas como isoformas 1 y 2, las cuales se componían de 1018 y 591 aminoácidos, respectivamente (Yoon et al., 2007), que podrían corresponder con las isoformas 6 y 2 más recientemente reportadas en el NCBI (*NCBI. Gene RIPOR2*, 2023). Además, PL48 fue descrito como una isoforma corta de C6orf32, compuesta por 536 aminoácidos (Yoon et al., 2007), que podría tratarse de la actual variante de RIPOR2 descrita como la número 2. Por tanto, no existe una nomenclatura bien descrita para estas isoformas de RIPOR2 y hasta ahora, los roles específicos de cada una de ellas siguen sin conocerse.

En este trabajo, decidimos averiguar cuál o cuáles de las 7 variantes transcripcionales de RIPOR2 (Tabla 7), disminuían en presencia de las oncoproteínas virales. Los resultados mostraron una disminución significativa en la expresión de todas las variantes transcripcionales de RIPOR2, sugiriendo que su modulación podría ser a nivel transcripcional. De acuerdo con la base de datos EPD (*EPD The Eukaryotic Promoter Database*, 2023), cuatro promotores medían la transcripción del gen RIPOR2 (Figura 21) y la expresión de dichos promotores pudo ser observada a partir de información obtenida del proyecto FANTOM5 (*FANTOM. Functional Annotation of the Mammalian Genome*, 2014). La expresión de los transcritos a partir de los promotores 1, 2 y 4 del gen de RIPOR2 se encuentra disminuida en células de CC con infección de VPH-16, -18 y -68, si se compara con su expresión en epitelio cervical normal, mientras que a partir a partir de promotor 3 no se observa expresión alguna (Figura 22). Análisis funcionales de los promotores que regulan la expresión de las variantes transcripcionales de RIPOR2 son necesarios para dilucidar los procesos específicos relacionados y los factores que participan en esto. Sin embargo, no se descarta que la baja expresión de RIPOR2 en células que contienen E6 y E7 de VPH-16 pueda relacionarse con cambios epigenéticos en el promotor de RIPOR2, debido a que las oncoproteínas E6 y E7 han mostrado promover la hipermetilación de varios genes que funcionan como supresores tumorales, lo que se ha asociado con un incremento en la proliferación (Sen et al., 2018).

Por otro lado, se sabe que la expresión de RIPOR2 es regulada a nivel transcripcional por el factor FOXO1 (Rougerie et al., 2013) y en nuestro estudio, datos obtenidos mediante el RNAseq mostraron una disminución en la expresión de FOXO1 de −0.49 y −0.41 log2FC en células que expresaban E6 y E7, respectivamente. Tomando en cuenta estos resultados, podríamos pensar en un eje HPV/FOXO1/RIPOR2, en el que las oncoproteínas virales disminuyan los niveles de FOXO1 en cáncer cervical, promoviendo la disminución de la expresión de RIPOR2, a nivel transcripcional. En relación con esto, se ha reportado que la expresión de FOXO1 está abatida en tumores cervicales si se compara con epitelio

normal, y que dicha expresión disminuye conforme las lesiones precancerosas progresan (Zhang et al., 2015). Sin embargo, algunos estudios generan controversia sobre estos resultados pues muestran que los niveles de FOXO1 están incrementados y disminuidos en NIC y CC, respectivamente (Chen et al., 2020) o que están incrementados tanto en NIC como en CC, disminuyendo la SG de las pacientes con cáncer (Chay et al., 2019). Dichas inconsistencias, generan la necesidad de realizar más estudios que nos pueden llevar a averiguar si la disminución de RIPOR2 mediada por las oncoproteínas virales, se relaciona el factor FOXO1.

Por otro lado, se ha descrito que las oncoproteínas E6 y E7, regulan la activación de la GTPasa RhoA (Charette & McCance, 2007; Hampson et al., 2004). En células C-33 A con sobre expresión de E6, RhoA está más activo que en células control sin la proteína viral, y aunque el mecanismo por el cual esto sucede no ha sido descrito (Hampson et al., 2004), concuerda con la disminución de la expresión de RIPOR2 observada en presencia de E6 en nuestro trabajo, ya que RIPOR2 es un inhibidor de RhoA (Lv et al., 2022). De forma contraria ha sido reportado que E7 atenúa la actividad de RhoA (Charette & McCance, 2007). Aunque aún se requieren más estudios que permitan definir el papel que las oncoproteínas tienen sobre RIPOR2 y las consecuencias que esto genera sobre la actividad de RhoA en CC, podría sugerirse la existencia de un eje FOXO1/RIPOR2/RhoA, controlado por las oncoproteínas del VPH.

Al evaluar los niveles de expresión de RIPOR2 en muestras de pacientes mexicanas con epitelio normal con y sin infección de VPH, LIEBG y LIEAG, observamos que RIPOR 2 se encuentra disminuido en LIEBG, LIEAG y muestras normales con infección de VPH, en comparación con muestras normales sin infección viral (Figura 23A). Estos resultados apuntan a que la expresión de RIPOR2 es disminuida por efecto del VPH y al menos parcialmente, por las oncoproteínas E6 y E7, concordando con los resultados que obtuvimos en las líneas celulares generadas en este estudio. Por otro lado, es importante destacar que la disminución de

RIPOR2 parece ser un evento que sucede desde el inicio de la infección y se mantiene hasta el cáncer cervical. Finalmente, datos de expresión de RIPOR2 que obtuvimos a partir de muestras de cáncer cervical de pacientes mexicanas sugieren que la baja expresión de RIPOR2 está asociada con una sobrevida global poco favorable para los pacientes de nuestra cohorte.

Cabe mencionar que una limitante de este estudio fue el número de muestras analizadas (19) en la cohorte de pacientes mexicanas, por lo que la validación de la expresión de RIPOR2 como potencial biomarcador pronóstico es necesaria en una cohorte más grande que sea representativa de la población de estudio. Por otro lado, sería importante evaluar la expresión de RIPOR2 a nivel de proteína y asociar su expresión con la SG de las pacientes con CC. En este trabajo no fue posible detectar a la proteína RIPOR2 en muestras de tumores o en lisados celulares, esto debido a que los anticuerpos comerciales utilizados presentaron una pobre inmunodetección.

Se ha reportado que la presencia de RIPOR2 en tumores se encuentra positivamente asociada con la infiltración de células T CD8+, macrófagos, neutrófilos y células dendríticas (Mei et al., 2020; Xu et al., 2022), mostrándose por lo tanto una mejor respuesta inmune en tumores con mayor expresión de RIPOR2. Además, los pacientes cuyos tumores expresaron RIPOR2 muestran también alta expresión de PD-1, PD-L1, PD-L2, y CTLA-4 (Mei et al., 2020). Concordando con estos datos, otro estudio reporta que los pacientes con RIPOR2 presentaron una mejor respuesta a la inmunoterapia con anticuerpos contra PD-1 solos o combinados con anticuerpos contra CTLA-4 (Xu et al., 2022). Tomando en cuenta estos hallazgos, el estudio de la expresión de RIPOR2 cuando el cáncer es diagnosticado, podría ayudar en la toma de decisiones en cuanto a la vigilancia y tratamiento de las pacientes, lo que indudablemente plantea una herramienta prometedora que mejore la calidad de vida

En general, podemos decir que las proteínas E6 y E7 modifican la expresión de genes que afectan la sobrevida global de las pacientes con cáncer cervical. Dentro de estos, nuestros hallazgos posicionan a RIPOR2 como un biomarcador pronóstico en CC y demuestran el efecto de las oncoproteínas virales en la disminución de las variantes transcripcionales de RIPOR2. Sin embargo, el estudio de los mecanismos específicos mediante los cuales E6 y E7 disminuyen la expresión de RIPOR2, así como su relación con el desarrollo y/o mantenimiento del cáncer es algo que merece más estudios.

RESUMEN DE RESULTADOS Y CONCLUSIÓN

- La expresión constitutiva de la proteína E6 del VPH-16 desregula la expresión de 2,689 genes en las células de cáncer cervical C-33 A. De los genes modulados, 1,520 fueron sobre expresados y 1,169 disminuidos.

- La expresión constitutiva de la proteína E7 del VPH-16 desregula la expresión de 2,018 genes en células C-33 A; 1,108 genes mostraron una expresión incrementada mientras la expresión de 910 genes disminuyó.

- De todos los genes cuya expresión fue desregulada por E6 y por E7, la expresión de 1130 genes se compartió por ambas oncoproteínas en las líneas celulares estables de cáncer cervical con expresión de las oncoproteínas.

- Los procesos y vías de señalización mayoritariamente desregulados por E616 en células C-33 A están relacionados con procesos de traducción y metabolismo.

- Los procesos y vías de señalización más desregulados por la proteína E7 en las células de cáncer cervical C-33 A se relacionan principalmente con adhesión, motilidad celular y transducción de señales en cáncer.

- La expresión de 6,667 genes está significativamente desregulada en células de cáncer cervical en una cohorte del TCGA.

- De los 1,130 genes desregulados por ambas oncoproteínas en C-33 A y los 6,667 genes que se observaron desregulados en cáncer cervical, 335 genes fueron se encontraron en ambos análisis.

- La baja expresión de RIPOR2, así como la alta expresión de PFKFB4 están asociadas con una disminución en la sobrevida global de las pacientes con cáncer cervical de una cohorte del TCGA.

- En células C-33 A se expresan 6 de las 7 variantes transcripcionales de RIPOR2. Las variantes 5 y 6 son las más abundantes, seguidas de la variante 3. Las variantes 1, 2 y 7 mostraron muy bajos niveles de expresión comparados con el total de los transcritos de RIPOR2. La variante 4 no se expresó en las células C-33 A.

- E6 y E7 disminuyen significativamente los niveles de las 6 variantes transcripcionales de RIPOR2 detectadas en células C-33 A.

- En una cohorte de pacientes mexicanas, la expresión de RIPOR2 es menor en lesiones intraepiteliales cervicales de alto grado y bajo grado, así como en muestras normales con infección del VPH cuando se comparan con la expresión de RIPOR2 en muestras normales sin infección viral.

En conclusión, las proteínas E6 y E7 del VPH-16 promueven la disminución de la expresión de las 6 variantes transcripcionales de RIPOR2 expresadas en células de cáncer cervical sin infección de VPH (C-33 A). Además de esto, RIPOR 2 tiene un efecto protector, ya que aquellas pacientes que expresaron niveles más bajos de RIPOR2 en una cohorte de pacientes con cáncer cervical, tuvieron una menor supervivencia global, posicionando a RIPOR 2 como un posible biomarcador pronóstico en CC, asociado con la actividad de las oncoproteínas virales. Estos hallazgos, comprueban la hipótesis planteada en este proyecto, pues se demostró que E6 y E7 de VPH-16 modificaron la expresión de genes relacionados con la sobrevida global de las pacientes con cáncer cervical.

PERSPECTIVAS

- Enriquecer la cohorte de pacientes con cáncer cervical para tener resultados más certeros en cuanto al efecto de los niveles de RIPOR2 en la supervivencia global de las pacientes mexicanas.

- Genotipificar los VPH presentes en las muestras y cuantificar los niveles de expresión de E6 y E7, esto para poder correlacionar dichos factores con la expresión de RIPOR2.

- Correlacionar los niveles proteicos de RIPOR2 con la infección viral y con el desenlace clínico.

- Investigar los mecanismos moleculares por los cuales las oncoproteínas E6 y E7 disminuyen la expresión de RIPOR2.

REFERENCIAS

1. Alfaro, A., Juárez-Torres, E., Medina-Martínez, I., Mateos-Guerrero, N., Bautista-Huerta, M., Román-Bassaure, E., Villegas-Sepúlveda, N. & Berumen, J. (2016). Different Association of Human Papillomavirus 16 Variants with Early and Late Presentation of Cervical Cancer. *PloS One*, *11*(12). https://doi.org/10.1371/JOURNAL.PONE.0169315
2. Arango-Bravo, E. A., Cetina-Pérez, L. del C., Cetina-Pérez, L. del C., Castro-Eguiluz, D., Gallardo-Rincón, D., Cruz-Bautista, I. & Duenas-Gonzalez, A. (2022). The health system and access to treatment in patients with cervical cancer in Mexico. *Frontiers in Oncology*, *12*.
3. Beyer, S., Wehrmann, M., Meister, S., Kolben, T. M., Trillsch, F., Burges, A., Czogalla, B., Schmoeckel, E., Mahner, S., Jeschke, U. & Kolben, T. (2022). Galectin-8 and -9 as prognostic factors for cervical cancer. *Archives of Gynecology and Obstetrics*, *306*(4). https://doi.org/10.1007/S00404-022-06449-9
4. Bhat, D. (2022). The “Why and How” of Cervical Cancers and Genital HPV Infection. *CytoJournal*, *19*. https://doi.org/10.25259/CMAS_03_03_2021
5. Bonab, F. R., Baghbanzadeh, A., Ghaseminia, M., Bolandi, N., Mokhtarzadeh, A., Amini, M., Dadashzadeh, K., Hajiasgharzadeh, K., Baradaran, B. & Baghi, H. B. (2021). Molecular pathways in the development of HPV-induced cervical cancer. *EXCLI Journal*, *20*, 320.
6. Burmeister, C. A., Khan, S. F., Schäfer, G., Mbatani, N., Adams, T., Moodley, J. & Prince, S. (2022). Cervical cancer therapies: Current challenges and future perspectives. *Tumour Virus Research*, *13*. https://doi.org/10.1016/J.TVR.2022.200238
7. Cai, Hu, C., Yu, S., Liu, L., Yu, X., Chen, J., Liu, X., Lin, F., Zhang, C., Li, W. & Yan, X. (2020). Identification and validation of a six-gene signature associated with glycolysis to predict the prognosis of patients with cervical cancer. *BMC Cancer*, *20*(1).
8. Cai, Y. C., Yang, H., Shan, H. B., Su, H. F., Jiang, W. Q. & Shi, Y. X. (2021).

PFKFB4 Overexpression Facilitates Proliferation by Promoting the G1/S Transition and Is Associated with a Poor Prognosis in Triple-Negative Breast Cancer. *Disease Markers*, *2021*. https://doi.org/10.1155/2021/8824589

9. Campos-Parra, A. D., Pérez-Quintanilla, M., Martínez-Gutierrez, A. D., Pérez-Montiel, D., Coronel-Martínez, J., Millan-Catalan, O., De León, D. C. & Pérez-Plasencia, C. (2022). Molecular Differences between Squamous Cell Carcinoma and Adenocarcinoma Cervical Cancer Subtypes: Potential Prognostic Biomarkers. *Current Oncology (Toronto, Ont.)*, *29*(7), 4689–4702. https://doi.org/10.3390/CURRONCOL29070372
10. Carbon, S., Douglass, E., Good, B. M., Unni, D. R., Harris, N. L., Howe, D. G., Toro, S., Cooper, L. & Elser, J. (2021). The Gene Ontology resource: enriching a GOld mine. *Nucleic Acids Research*, *49*(D1), D325–D334.
11. Chang, A., Shi, Y., Wang, P. & Ren, J. (2022). LINC00963 May Be Associated with a Poor Prognosis in Patients with Cervical Cancer. *Medical Science Monitor : International Medical Journal of Experimental and Clinical Research*, *28*. https://doi.org/10.12659/MSM.935070
12. Charette, S. T. & McCance, D. J. (2007). The E7 protein from human papillomavirus type 16 enhances keratinocyte migration in an Akt-dependent manner. *Oncogene*, *26*(52), 7386–7390. https://doi.org/10.1038/SJ.ONC.1210541
13. Chay, D. B., Han, G. H., Nam, S., Cho, H., Chung, J. Y. & Hewitt, S. M. (2019). Forkhead box protein O1 (FOXO1) and paired box gene 3 (PAX3) overexpression is associated with poor prognosis in patients with cervical cancer. *International Journal of Clinical Oncology*, *24*(11), 1429–1439. https://doi.org/10.1007/S10147-019-01507-W
14. Chen, M., Wang, H., Liang, Y. & Li, L. (2020). Establishment of multifactor predictive models for the occurrence and progression of cervical intraepithelial neoplasia. *BMC Cancer*, *20*(1).
15. *Clustal Omega*. (2023). http://www.clustal.org/omega/
16. Colaprico, A., Silva, T. C., Olsen, C., Garofano, L., Cava, C., Garolini, D., Sabedot, T. S., Malta, Tathiane Pagnotta, S. M., Castiglioni, I., Ceccarelli, M.,

Bontempi, G. & Noushmehr, H. (2016). TCGAbiolinks: an R/Bioconductor package for integrative analysis of TCGA data. *Nucleic Acids Research*, *44*(8).

17. Coquillard, G., Palao, B. & Patterson, B. K. (2011). Quantification of intracellular HPV E6/E7 mRNA expression increases the specificity and positive predictive value of cervical cancer screening compared to HPV DNA. *Gynecologic Oncology*, *120*(1), 89–93. https://doi.org/10.1016/J.YGYNO.2010.09.013
18. Cosper, P. F., Bradley, S., Luo, L. & Kimple, R. J. (2021). Biology of HPV Mediated Carcinogenesis and Tumor Progression. *Seminars in Radiation Oncology*, *31*(4), 265–273. https://doi.org/10.1016/J.SEMRADONC.2021.02.006
19. Cui, H., Ma, R., Hu, T., Xiao, G. G. & Wu, C. (2022). Bioinformatics Analysis Highlights Five Differentially Expressed Genes as Prognostic Biomarkers of Cervical Cancer and Novel Option for Anticancer Treatment. *Frontiers in Cellular and Infection Microbiology*, *12*. https://doi.org/10.3389/FCIMB.2022.926348
20. Dakour, J., Li, H. & Morrish, D. W. (1997). PL48: a novel gene associated with cytotrophoblast and lineage-specific HL-60 cell differentiation. *Gene*, *185*(2), 153–157. https://doi.org/10.1016/S0378-1119(96)00587-2
21. Dasari, S. & Bernard Tchounwou, P. (2014). Cisplatin in cancer therapy: molecular mechanisms of action. *European Journal of Pharmacology*, *740*, 364–378.
22. Dastsooz, H., Alizadeh, A., Habibzadeh, P., Nariman, A., Hosseini, A., Mansoori, Y. & Haghi-Aminjan, H. (n.d.). LncRNA-miRNA-mRNA Networks of Gastrointestinal Cancers Representing Common and Specific LncRNAs and mRNAs. *Frontiers in Genetics*, *12*.
23. de Martel, C., Georges, D., Bray, F., Ferlay, J. & Clifford, G. M. (2020). Global burden of cancer attributable to infections in 2018: a worldwide incidence analysis. *The Lancet. Global Health*, *8*(2), e180–e190. https://doi.org/10.1016/S2214-109X(19)30488-7

24. Dong, A., Xu, B., Wang, Z. & Miao, X. (2022). Survival-related DLEU1 is associated with HPV infection status and serves as a biomarker in HPV-infected cervical cancer. *Molecular Medicine Reports*, *25*(3). https://doi.org/10.3892/MMR.2022.12593
25. Dong, Z., Chang, X., Xie, L., Wang, Y. & Hou, Y. (2022). Increased expression of SRPK1 (serine/arginine-rich protein-specific kinase 1) is associated with progression and unfavorable prognosis in cervical squamous cell carcinoma. *Bioengineered*, *13*(3), 6100–6112. https://doi.org/10.1080/21655979.2022.2034705
26. Dürst, M., Hoyer, H., Altgassen, C., Greinke, C., Häfner, N., Fishta, A., Gajda, M., Mahnert, U., Hillemanns, P., Dimpfl, T., Lenhard, M., Ulrich Petry, K., Runnebaum, I. B. & Schneider, A. (2015). Prognostic value of HPV-mRNA in sentinel lymph nodes of cervical cancer patients with pN0-status. *Oncotarget*, *6*(26), 23015–23025. https://doi.org/10.18632/ONCOTARGET.4132
27. *EPD The Eukaryotic Promoter Database*. (2023). https://epd.epfl.ch/search_EPDnew.php?query=ripor2&db=human
28. *FANTOM. Functional Annotation of the Mammalian Genome*. (2014). https://fantom.gsc.riken.jp/5/
29. Ferlay, J., Ervik, M., Lam, F., Colombet, M., Mery, L., Piñeros, M., Znaor, A., Soerjomataram, I. & Bray, F. (2020). *IARC: Cancer Today*. Global Cancer Observatory: Cancer Today. Lyon, France: International Agency for Research on Cancer. https://gco.iarc.fr/today/home
30. FIGO Committee on Gynecologic Oncology. (2014). FIGO staging for carcinoma of the vulva, cervix, and corpus uteri. *International Journal of Gynaecology and Obstetrics: The Official Organ of the International Federation of Gynaecology and Obstetrics*, *125*(2), 97–98. https://doi.org/10.1016/J.IJGO.2014.02.003
31. Froehlich, J., Versapuech, M., Megrelis, L., Largeteau, Q., Meunier, S., Tanchot, C., Bismuth, G., Delon, J. & Mangeney, M. (2016). FAM65B controls the proliferation of transformed and primary T cells. *Oncotarget*, *7*(16), 63215–66325.

32. *Gene Ontology Resource*. (1999). http://geneontology.org/
33. Gupta, S. M., Warke, H., Chaudhari, H., Mavani, P., Katke, R. D., Kerkar, S. C. & Mania-Pramanik, J. (2022). Human Papillomavirus E6/E7 oncogene transcripts as biomarkers for the early detection of cervical cancer. *Journal of Medical Virology*, *94*(7), 3368–3375. https://doi.org/10.1002/JMV.27700
34. Hampson, L., Li, C., Oliver, anthony W., Kitchener, H. C. & Hampson, I. N. (2004). The PDZ protein Tip-1 is a gain of function target of the HPV16 E6 oncoprotein. International Journal of Oncology | 10.3892/ijo.25.5.1249. *INTERNATIONAL JOURNAL OF ONCOLOGY*, *25*, 1249–1256.
35. Ho, C. M., Lee, B. H., Chang, S. F., Chien, T. Y., Huang, S. H., Yan, C. C. & Cheng, W. F. (2010). Type-specific human papillomavirus oncogene messenger RNA levels correlate with the severity of cervical neoplasia. *International Journal of Cancer*, *127*(3), 622–632. https://doi.org/10.1002/IJC.25078
36. Hsin, M. C., Hsieh, Y. H., Hsiao, Y. H., Chen, P. N., Wang, P. H. & Yang, S. F. (2021). Carbonic Anhydrase IX Promotes Human Cervical Cancer Cell Motility by Regulating PFKFB4 Expression. *Cancers*, *13*(5), 1–13. https://doi.org/10.3390/CANCERS13051174
37. Hua, C., Zheng, Q., Zhu, J., Chen, S., Song, Y., Van Der Veen, S. & Cheng, H. (2022). Human Papillomavirus Type 16 Early Protein E7 Activates Autophagy through Inhibition of Dual-Specificity Phosphatase 5. *Oxidative Medicine and Cellular Longevity*, *2022*.
38. Huh, K., Zhou, X., Hayakawa, H., Cho, J.-Y., Libermann, T. A., Jin, J., Wade Harper, J. & Munger, K. (2007). Human papillomavirus type 16 E7 oncoprotein associates with the cullin 2 ubiquitin ligase complex, which contributes to degradation of the retinoblastoma tumor suppressor. *Journal of Virology*, *81*(18), 9737–9747. https://doi.org/10.1128/JVI.00881-07
39. Isla-Ortiz, D., Palomares-Castillo, E., Mille-Loera, J. E., Ramírez-Calderón, N., Mohar-Betancourt, A., Meneses-García, A. A. & Reynoso-Noverón, N. (2020). Cervical Cancer in Young Women: Do They Have a Worse Prognosis? A Retrospective Cohort Analysis in a Population of Mexico. *The*

Oncologist, *25*(9), e1363–e1371. https://doi.org/10.1634/THEONCOLOGIST.2019-0902

40. *KEGG: Kyoto Encyclopedia of Genes and Genomes*. (1995). https://www.genome.jp/kegg/
41. Li, N., Franceschi, S., Howell-Jones, R., Snijders, P. J. F. & Clifford, G. M. (2011). Human papillomavirus type distribution in 30,848 invasive cervical cancers worldwide: Variation by geographical region, histological type and year of publication. *International Journal of Cancer*, *128*(4), 927–935. https://doi.org/10.1002/IJC.25396
42. Ling, K., Yang, L., Yang, N., Chen, M., Wang, Y., Liang, S., Li, Y., Jiang, L., Yan, P. & Liang, Z. (2020). Gene Targeting of HPV18 E6 and E7 Synchronously by Nonviral Transfection of CRISPR/Cas9 System in Cervical Cancer. *Human Gene Therapy*, *31*(5–6), 297–308. https://doi.org/10.1089/HUM.2019.246
43. Liu, Z., Teng, L., Gao, L., Wang, H., Su, Y. & Li, J. (2018). The role of eukaryotic translation initiation factor 5A-1 (eIF5A-1) gene in HPV 16 E6 induces cell growth in human cervical squamous carcinoma cells. *Biochemical and Biophysical Research Communications*, *505*(1), 6–12.
44. Lizio, M., Abugessaisa, I., Noguchi, S., Kondo, A., Hasegawa, A., Hon, C. C., De Hoon, M., Severin, J., Oki, S., Hayashizaki, Y., Carninci, P., Kasukawa, T. & Kawaji, H. (2019). Update of the FANTOM web resource: expansion to provide additional transcriptome atlases. *Nucleic Acids Research*, *47*(D1), D752–D758.
45. Lizio, M., Harshbarger, J., Shimoji, H., Severin, J., Kasukawa, T., Sahin, S., Diehl, Alexander D.Abugessaisa, I., Fukuda, S., Hori, F., Ishikawa-Kato, S., Mungall, C. J., Arner, E., Baillie, J. K., Bertin, N., Bono, H., de Hoon, M., Diehl, A. D., Dimont, E., Freeman, T. C., … Kawaji, H. (2015). Gateways to the FANTOM5 promoter level mammalian expression atlas. *Genome Biology*, *16*(1).
46. Love, M. I., Huber, W. & Anders, S. (2014). Moderated estimation of fold change and dispersion for RNA-seq data with DESeq2. *Genome Biology*,

15(12).

47. Lu, H., Chen, S., You, Z., Xie, C., Huang, S. & Hu, X. (2020). PFKFB4 negatively regulated the expression of histone acetyltransferase GCN5 to mediate the tumorigenesis of thyroid cancer. *Development, Growth & Differentiation*, *62*(2), 129–138. https://doi.org/10.1111/DGD.12645
48. Lv, Z., Ding, Y., Cao, W., Wang, S. & Gao, K. (2022). Role of RHO family interacting cell polarization regulators (RIPORs) in health and disease: Recent advances and prospects. *International Journal of Biological Sciences*, *18*(2), 800–808. https://doi.org/10.7150/IJBS.65457
49. Martinez-Zapien, D., Ruiz, F. X., Poirson, J., Mitschler, A., Ramirez, J., Forster, A., Cousido-Siah, A., Masson, M., Pol, S. Vande, Podjarny, A., Travé, G. & Zanier, K. (2016). Structure of the E6/E6AP/p53 complex required for HPV-mediated degradation of p53. *Nature*, *529*(7587), 541–545. https://doi.org/10.1038/nature16481
50. McBride, A. A. & Warburton, A. (2017). The role of integration in oncogenic progression of HPV-associated cancers. *PLoS Pathogens*, *13*(4).
51. Mei, J., Xing, Y., Lv, J., Gu, D., Pan, J., Zhang, Y. & Liu, J. (2020). Construction of an immune-related gene signature for prediction of prognosis in patients with cervical cancer. *International Immunopharmacology*, *88*. https://doi.org/10.1016/J.INTIMP.2020.106882
52. Mincheva, A., Gissmann, L. & Zur Hausen, H. (1987). Chromosomal integration sites of human papillomavirus DNA in three cervical cancer cell lines mapped by in situ hybridization. Medical Microbiology and Immunology, 176(5) | 10.1007/bf00190531. *Microbiology and Immunology*, *176*(5), 245–256.
53. Mitra, S., Mazumder-Indra, D., Mondal, R. K., Basu, P. S., Roy, A., Roychoudhury, S. & Panda, C. K. (2012). Inactivation of SLIT2-ROBO1/2 pathway in premalignant lesions of uterine cervix: clinical and prognostic significances. *PloS One*, *7*(6). https://doi.org/10.1371/JOURNAL.PONE.0038342
54. Morrish, D. W., Linetsky, E., Bhardwaj, D., Li, H., Dakour, J., Marsh, R. G.,

Paterson, M. C. & Godbout, R. (1996). Identification by subtractive hybridization of a spectrum of novel and unexpected genes associated with in vitro differentiation of human cytotrophoblast cells. *Placenta*, *17*(7), 431–441. https://doi.org/10.1016/S0143-4004(96)90025-9

55. Münger, K., Phelps, W. C., Bubb, V., Howley, P. M. & Schlegel, R. (1989). The E6 and E7 genes of the human papillomavirus type 16 together are necessary and sufficient for transformation of primary human keratinocytes. *Journal of Virology*, *63*(10), 4417–4421. https://doi.org/10.1128/JVI.63.10.4417-4421.1989
56. Nahand, J. S., Taghizadeh-boroujeni, S., Karimzadeh, M., Borran, S., Pourhanifeh, M. H., Moghoofei, M., Bokharaei-Salim, F., Karampoor, S., Jafari, A., Asemi, Z., Tbibzadeh, A., Namdar, A. & Mirzaei, H. (2019). microRNAs: New prognostic, diagnostic, and therapeutic biomarkers in cervical cancer. *Journal of Cellular Physiology*, *234*(10), 17064–17099. https://doi.org/10.1002/JCP.28457
57. Narayan, G., Goparaju, C., Arias-Pulido, H., Kaufmann, A. M., Schneider, A., Dürst, M., Mansukhani, M., Pothuri, B. & Murty, V. V. (2006). Promoter hypermethylation-mediated inactivation of multiple Slit-Robo pathway genes in cervical cancer progression. *Molecular Cancer*, *5*. https://doi.org/10.1186/1476-4598-5-16
58. *NCBI. Gene RIPOR2*. (2023). https://www.ncbi.nlm.nih.gov/gene/9750
59. Olmedo-Nieva, L., Muñoz-Bello, J. O., Martínez-Ramírez, I., Martínez-Gutiérrez, A. D., Ortiz-Pedraza, Y., González-Espinosa, C., Madrid-Marina, V., Torres-Poveda, K., Bahena-Roman, M. & Lizano, M. (2022). RIPOR2 Expression Decreased by HPV-16 E6 and E7 Oncoproteins: An Opportunity in the Search for Prognostic Biomarkers in Cervical Cancer. *Cells*, *11*(23). https://doi.org/10.3390/CELLS11233942
60. Paik, E. S., Chang, C. S., Chae, Y. L., Oh, S. Y., Byeon, S. J., Kim, C. J., Lee, Y. Y., Kim, T. J., Lee, J. W., Kim, B. G. & Choi, C. H. (2021). Prognostic Relevance of BRCA1 Expression in Survival of Patients With Cervical Cancer. *Frontiers in Oncology*, *11*. https://doi.org/10.3389/FONC.2021.770103

61. Pal, A. & Kundu, R. (2020). Human Papillomavirus E6 and E7: The Cervical Cancer Hallmarks and Targets for Therapy. *Frontiers in Microbiology*, *10*. https://doi.org/10.3389/FMICB.2019.03116
62. Patel, K. A., Patel, B. M., Thobias, A. R., Gokani, R. A., Chhikara, A. B., Desai, A. D. & Patel, P. S. (2020). Overexpression of VEGF165 is associated with poor prognosis of cervical cancer. *The Journal of Obstetrics and Gynaecology Research*, *46*(11), 2397–2406. https://doi.org/10.1111/JOG.14483
63. *PaVE: The Papillomavirus Episteme*. (2022). https://pave.niaid.nih.gov/
64. Piri, R., Ghaffari, A., Gholami, N., Azami-Aghdash, S., PourAli-Akbar, Y., Saleh, P. & Naghavi-Behzad, M. (2015). Ki-67/MIB-1 as a Prognostic Marker in Cervical Cancer - a Systematic Review with Meta-Analysis. *Asian Pacific Journal of Cancer Prevention : APJCP*, *16*(16), 6997–7002. https://doi.org/10.7314/APJCP.2015.16.16.6997
65. Plummer, M., de Martel, C., Vignat, J., Ferlay, J., Bray, F. & Franceschi, S. (2016). Global burden of cancers attributable to infections in 2012: a synthetic analysis. *The Lancet. Global Health*, *4*(9), e609–e616. https://doi.org/10.1016/S2214-109X(16)30143-7
66. *Reactome Pathway Database*. (2023). https://reactome.org/
67. Rose, B. R., Thompson, C. H., Jiang, X. M., Tattersall, M. H. N., Elliott, P. M., Dalrymple, C. & Cossart, Y. E. (1994). Detection of human papillomavirus type 16 E6/E7 transcripts in histologically cancer-free pelvic lymph nodes of patients with cervical carcinoma. *Gynecologic Oncology*, *52*(2), 212–217. https://doi.org/10.1006/GYNO.1994.1033
68. Rosenberger, S., Arce, J. D. C., Langbein, L., Steenbergenc, R. D. M. & Rösla, F. (2010). Alternative splicing of human papillomavirus type-16 E6/E6* early mRNA is coupled to EGF signaling via Erk1/2 activation. *Proceedings of the National Academy of Sciences of the United States of America*, *107*(15), 7006–7011. https://doi.org/10.1073/PNAS.1002620107
69. Rossi, N. M., Dai, J., Xie, Y., Wangsa, D., Heselmeyer-Haddad, K., Lou, H., Boland, J. F., Yeager, M., Orozco, R., Alvirez Freites, E., Mirabello, L., Gharzouzi, E. & Dean, M. (2023). Extrachromosomal Amplification of Human

Papillomavirus Episomes is a Mechanism of Cervical Carcinogenesis. *Cancer Research*.

70. Rougerie, P., Largeteau, Q., Megrelis, L., Carrette, F., Lejeune, T., Toffali, L., Rossi, B., Zeghouf, M., Cherfils, J., Constantin, G., Laudanna, C., Bismuth, G., Mangeney, M. & Delon, J. (2013). Fam65b is a new transcriptional target of FOXO1 that regulates RhoA signaling for T lymphocyte migration. *Journal of Immunology (Baltimore, Md.: 1950)*, *190*(2), 748–755. https://doi.org/10.4049/JIMMUNOL.1201174
71. Ruiz, F. J., Inkman, M., Rashmi, R., Muhammad, N., Gabriel, N., Miller, C. A., McLellan, M. D., Goldstein, M., Markovina, S., Grigsby, P. W., Zhang, J. & Schwarz, J. K. (2021). HPV transcript expression affects cervical cancer response to chemoradiation. *JCI Insight*, *6*(16). https://doi.org/10.1172/JCI.INSIGHT.138734
72. Sasagawa, T., Takagi, H. & Makinoda, S. (2012). Immune responses against human papillomavirus (HPV) infection and evasion of host defense in cervical cancer. *Journal of Infection and Chemotherapy : Official Journal of the Japan Society of Chemotherapy*, *18*(6), 807–815. https://doi.org/10.1007/S10156-012-0485-5
73. Scheffner, M., Huibregtse, J. M., Vierstra, R. D. & Howley, P. M. (1993). The HPV-16 E6 and E6-AP complex functions as a ubiquitin-protein ligase in the ubiquitination of p53. *Cell*, *75*(3), 495–505. https://doi.org/10.1016/0092-8674(93)90384-3
74. Sen, P., Ganguly, P. & Ganguly, N. (2018). Modulation of DNA methylation by human papillomavirus E6 and E7 oncoproteins in cervical cancer. *Oncology Letters*, *15*(1), 11–22. https://doi.org/10.3892/OL.2017.7292
75. Singh, G., Azuine, R. & Siahpush, M. (2012). Global Inequalities in Cervical Cancer Incidence and Mortality are Linked to Deprivation, Low Socioeconomic Status, and Human Development. *International Journal of MCH and AIDS*, *1*(1). https://doi.org/10.21106/IJMA.12
76. Sun, J. & Jin, R. (2022). PFKFB4 modulated by miR-195-5p can boost the malignant progression of cervical cancer cells. *Bioorganic & Medicinal*

Chemistry Letters, *73*. https://doi.org/10.1016/J.BMCL.2022.128916

77. Sung, H., Ferlay, J., Siegel, R. L., Laversanne, M., Soerjomataram, I., Jemal, A. & Bray, F. (2021). Global Cancer Statistics 2020: GLOBOCAN Estimates of Incidence and Mortality Worldwide for 36 Cancers in 185 Countries. *CA: A Cancer Journal for Clinicians*, *71*(3), 209–249. https://doi.org/10.3322/CAAC.21660
78. Szymonowicz, K. A. & Chen, J. (2020). Biological and clinical aspects of HPV-related cancers. *Cancer Biology & Medicine*, *17*(4), 864–878. https://doi.org/10.20892/J.ISSN.2095-3941.2020.0370
79. Tong, M., Jun, T., Nie, Y., Hao, J. & Fan, D. (2019). The Role of the Slit/Robo Signaling Pathway. *Journal of Cancer*, *10*(12), 2694.
80. Torreglosa-Hernández, S., Grisales-Romero, H., Morales-Carmona, E., Hernández-Ávila, J. E., Huerta-Gutiérrez, R., Barquet-Muñoz, S. A. & Palacio-Mejía, L. S. (2022). Supervivencia y factores asociados en pacientes con cáncer cervicouterino atendidas por el Seguro Popular en México. *Salud Publica de Mexico*, *64*(1), 76–86. https://doi.org/10.21149/13119
81. Trojan, S. E., Piwowar, M., Ostrowska, B., Laidler, P. & Kocemba-Pilarczyk, K. A. (2018). Analysis of Malignant Melanoma Cell Lines Exposed to Hypoxia Reveals the Importance of PFKFB4 Overexpression for Disease Progression. *Anticancer Research*, *38*(12), 6745–6752. https://doi.org/10.21873/ANTICANRES.13044
82. Tulake, W., Yuemaier, R., Sheng, L., Ru, M., Lidifu, D. & Abudula, A. (2018). Upregulation of stem cell markers ALDH1A1 and OCT4 as potential biomarkers for the early detection of cervical carcinoma. *Oncology Letters*, *16*(5), 5525–5534.
83. Uc, P. Y., Miranda, J., Sandino, A. R., Alarcón, L., Roldán, M. L., Delgado, R. O., Malagón, E. M. C., Munguía, B., Ramírez, G., Asomoza, R. C., Shoshani, L., Gariglio, P. & Mariscal, L. G. (2020). E7 oncoprotein from human papillomavirus 16 alters claudins expression and the sealing of epithelial tight junctions. *International Journal of Oncology*, *57*(4), 905–924.
84. Van Doorslaer, K., Li, Z., Xirasagar, S., Maes, P., Kaminsky, D., Liou, D., Sun,

Q., Kaur, R., Huyen, Y. & McBride, A. A. (2017). The Papillomavirus Episteme: a major update to the papillomavirus sequence database. *Nucleic Acids Research*, *45*(D1), D499–D506. https://doi.org/10.1093/NAR/GKW879

85. Volkova, L. V., Pashov, A. I. & Omelchuk, N. N. (2021). Cervical Carcinoma: Oncobiology and Biomarkers. *International Journal of Molecular Sciences*, *22*(22). https://doi.org/10.3390/IJMS222212571
86. Wang, F., Wu, X., Li, Y., Cao, X., Zhang, C. & Gao, Y. (2021). PFKFB4 as a promising biomarker to predict a poor prognosis in patients with gastric cancer. *Oncology Letters*, *21*(4). https://doi.org/10.3892/OL.2021.12557
87. Wei, Y., Zhao, Z. & Ma, X. (2022). Description of CRISPR-Cas9 development and its prospects in human papillomavirus-driven cancer treatment. *Frontiers in Immunology*, *13*.
88. World Health Organization. (2020). World Cancer Report: Cancer Research for Cancer Prevention. In C. P. Wild, E. Weiderpass & B. W. Stewart (Eds.), *Cancer Control* (Vol. 199). International Agency for Research on Cancer.
89. Wu, Y., Zhang, L., Bao, Y., Wan, B., Shu, D., Luo, T. & He, Z. (2022). Loss of PFKFB4 induces cell cycle arrest and glucose metabolism inhibition by inactivating MEK/ERK/c-Myc pathway in cervical cancer cells. *Journal of Obstetrics and Gynaecology : The Journal of the Institute of Obstetrics and Gynaecology*, *42*(6), 2399–2405. https://doi.org/10.1080/01443615.2022.2062225
90. Xiong, J., Li, G., Mei, X., Ding, J., Shen, H., Zhu, D. & Wang, H. (2022). Co-Delivery of p53 Restored and E7 Targeted Nucleic Acids by Poly (Beta-Amino Ester) Complex Nanoparticles for the Treatment of HPV Related Cervical Lesions. *Frontiers in Pharmacology*, *13*. https://doi.org/10.3389/FPHAR.2022.826771
91. Xu, F., Zou, C., Gao, Y., Shen, J., Liu, T., He, Q., Li, S. & Xu, S. (2022). Comprehensive analyses identify RIPOR2 as a genomic instability-associated immune prognostic biomarker in cervical cancer. *Frontiers in Immunology*, *13*. https://doi.org/10.3389/FIMMU.2022.930488
92. Yalcin, A., Telang, S., Clem, B. & Chesney, J. (2009). Regulation of glucose

metabolism by 6-phosphofructo-2-kinase/fructose-2,6-bisphosphatases in cancer. *Experimental and Molecular Pathology*, *86*(3), 174–179. https://doi.org/10.1016/J.YEXMP.2009.01.003

93. Yoon, S., Molloy, M. J., Wu, M. P., Cowan, D. B. & Gussoni, E. (2007). C6ORF32 is upregulated during muscle cell differentiation and induces the formation of cellular filopodia. *Developmental Biology*, *301*(1), 70–81. https://doi.org/10.1016/J.YDBIO.2006.11.002
94. Yu, L., Majerciak, V. & Zheng, Z. M. (2022). HPV16 and HPV18 Genome Structure, Expression, and Post-Transcriptional Regulation. *International Journal of Molecular Sciences*, *23*(9). https://doi.org/10.3390/IJMS23094943
95. Zhang, G., Zhang, R., Bai, P., Li, S., Zuo, J., Zhang, Y., Liu, M. & Wu, L. (2022). Down-regulated expression of miR-99a is associated with lymph node metastasis and predicts poor outcome in stage IB cervical squamous cell carcinoma: a case-control study. *Annals of Translational Medicine*, *10*(12), 663–663. https://doi.org/10.21037/ATM-22-2483
96. Zhang, Gui, L. S., Zhao, X. L., Zhu, L. L. & Li, Q. W. (2015). FOXO1 is a tumor suppressor in cervical cancer. *Genetics and Molecular Research : GMR*, *14*(2), 6605–6616. https://doi.org/10.4238/2015.JUNE.18.3
97. Zhang, K. & Waxman, D. J. (2010). PC3 prostate tumor-initiating cells with molecular profile FAM65Bhigh/MFI2low/LEF1low increase tumor angiogenesis. *Molecular Cancer*, *9*. https://doi.org/10.1186/1476-4598-9-319
98. Zhao, L., Wang, L., Zhang, C., Liu, Z., Piao, Y., Yan, J., Xiang, R., Yao, Y. & Shi, Y. (2019). E6-induced selective translation of WNT4 and JIP2 promotes the progression of cervical cancer via a noncanonical WNT signaling pathway. *Signal Transduction and Targeted Therapy*, *4*(1).
99. Zhen, S., Liu, Y., Lu, J., Tuo, X., Yang, X., Chen, H., Chen, W. & Li, X. (2020). Human Papillomavirus Oncogene Manipulation Using Clustered Regularly Interspersed Short Palindromic Repeats/Cas9 Delivered by pH-Sensitive Cationic Liposomes. *Human Gene Therapy*, *31*(5–6), 309–324. https://doi.org/10.1089/HUM.2019.312
100. Zhou, Y., Fan, Y., Qiu, B., Lou, M., Liu, X., Yuan, K. & Tong, J. (2022).

Effect of PFKFB4 on the Prognosis and Immune Regulation of NSCLC and Its Mechanism. *International Journal of General Medicine*, *15*, 6341–6353. https://doi.org/10.2147/IJGM.S369126

101. Zhu, K., Deng, C., Du, P., Liu, T., Piao, J., Piao, Y., Yang, M. & Chen, L. (2022). G6PC indicated poor prognosis in cervical cancer and promoted cervical carcinogenesis in vitro and in vivo. *Reproductive Biology and Endocrinology : RB&E*, *20*(1). https://doi.org/10.1186/S12958-022-00921-6

cells

MDPI

Article

RIPOR2 Expression Decreased by HPV-16 E6 and E7 Oncoproteins: An Opportunity in the Search for Prognostic Biomarkers in Cervical Cancer

Leslie Olmedo-Nieva [1], J. Omar Muñoz-Bello [1], Imelda Martínez-Ramírez [1], Antonio Daniel Martínez-Gutiérrez [2], Yunuen Ortiz-Pedraza [1], Claudia González-Espinosa [3], Vicente Madrid-Marina [4], Kirvis Torres-Poveda [4], Margarita Bahena-Roman [4] and Marcela Lizano [1,5,*]

[1] Unidad de Investigación Biomédica en Cáncer, Instituto Nacional de Cancerología, Avenida San Fernando 22, Sección XVI, Tlalpan, Mexico City 14080, Mexico
[2] Laboratorio de Genómica, Instituto Nacional de Cancerología, Tlalpan, Mexico City 14080, Mexico
[3] Departamento de Farmacobiología, Centro de Investigación y de Estudios Avanzados, Unidad Sede Sur, Calzada de los Tenorios 235, Granjas Coapa, Tlalpan, Mexico City 14330, Mexico
[4] Centro de Investigación en Enfermedades Infecciosas, Instituto Nacional de Salud Pública, Cuernavaca, Morelos 62100, Mexico
[5] Departamento de Medicina Genómica y Toxicología Ambiental, Instituto de Investigaciones Biomédicas, Universidad Nacional Autónoma de México, Circuito Exterior S/N, Ciudad Universitaria, Mexico City 04510, Mexico
* Correspondence: lizanosoberon@gmail.com

Abstract: High-risk human papillomavirus (HPV) infection is the main risk factor for cervical cancer (CC) development, where the continuous expression of E6 and E7 oncoproteins maintain the malignant phenotype. In Mexico, around 70% of CC cases are diagnosed in advanced stages, impacting the survival of patients. The aim of this work was to identify biomarkers affected by HPV-16 E6 and E7 oncoproteins that impact the prognosis of CC patients. Expression profiles dependent on E6 and E7 oncoproteins, as well as their relationship with biological processes and cellular signaling pathways, were analyzed in CC cells. A comparison among expression profiles of E6- and E7-expressing cells and that from a CC cohort obtained from The Cancer Genome Atlas (TCGA) demonstrated that the expression of 13 genes impacts the overall survival (OS). A multivariate analysis revealed that the downregulated expression of RIPOR2 was strongly associated with a worse OS. RIPOR2, including its transcriptional variants, were overwhelmingly depleted in E6- and E7-expressing cells. Finally, in a Mexican cohort, it was found that in premalignant cervical lesions, RIPOR2 expression decreases as the lesions progress; meanwhile, decreased RIPOR2 expression was also associated with a worse OS in CC patients.

Keywords: RIPOR2; prognostic biomarker; HPV; cervical cancer; HPV-16 E6 and E7

Citation: Olmedo-Nieva, L.; Muñoz-Bello, J.O.; Martínez-Ramírez, I.; Martínez-Gutiérrez, A.D.; Ortiz-Pedraza, Y.; González-Espinosa, C.; Madrid-Marina, V.; Torres-Poveda, K.; Bahena-Roman, M.; Lizano, M. RIPOR2 Expression Decreased by HPV-16 E6 and E7 Oncoproteins: An Opportunity in the Search for Prognostic Biomarkers in Cervical Cancer. *Cells* **2022**, *11*, 3942. https://doi.org/10.3390/cells11233942

Academic Editors: Adriana Aguilar-Lemarroy and Luis Felipe Jave-Suárez

Received: 5 October 2022
Accepted: 30 November 2022
Published: 6 December 2022

1. Introduction

Cervical cancer (CC) ranks fourth in cancer mortality in women worldwide, while, in Mexico, it ranks second. This neoplasia continues to be a public health problem, since, in the last decade, there has been a considerable increase from 3357 cervical cancer deaths estimated in 2012 to 4335 cases in 2020 [1]. The main risk factor attributed to the development of CC is a persistent infection with high-risk (HR) human papillomaviruses (HPV), whose genome has been found in most of the cervical cancer cases (up to 90%) [2]. The most prevalent viral type in cervical cancer is HPV-16, which is found in 50% of all cases [3].

The oncogenicity of HPV lies mainly in the continuous expression of E6 and E7 oncogenes, whose protein products interact with different cellular proteins that promote cancer-associated processes such as proliferation, migration, invasion, the inhibition of apoptosis, and the evasion of the immune response, among others [4]. One of the most

studied functions of viral oncoproteins is the degradation of tumor suppressor proteins. E6 interacts with p53 and with the ubiquitin ligase E6AP, promoting the degradation of p53 through the proteasome, and this event allows the inhibition of apoptosis, the promotion of genomic instability, and the accumulation of mutations [5,6]. The E7 protein interacts with pRb and with the ubiquitin ligase Cullin2, favoring pRb proteasomal degradation. This event promotes the translocation of the E2F transcriptional factor to the nucleus and the transcription of genes related to G1-to-S-phase transition, promoting the continuity of the cell cycle [7].

In developing countries, such as Mexico, a high proportion of CC cases are diagnosed in advanced clinical stages, resulting in lower survival and a high mortality rate [8], which is largely due to the lack of effective cervical cancer screening programs. In Mexico, more than 70% of cervical cancer patients are detected in locally advanced or advanced stages [9], while the overall survival (OS) worsens as the clinical stage progresses [10]. Disease characteristics related to clinical stages, such as tumor size, lymph node infiltration, and distant metastasis, are related to patient survival; however, not all patients with the same clinical stage have the same outcome. Therefore, some studies have focused on searching for molecules that can predict patient survival. In this regard, some proteins have been proposed as prognostic biomarkers for CC, including the increased of Ki-67/MIB-1 protein levels [11], glucose-6-phosphatase catalytic subunit (G6PC) [12], and serine/arginine-rich protein-specific kinase 1 (SRPK1) [13], which are related with worse survival, while the high levels of Galectin 9 [14] correlate with a better prognosis in CC patients. Moreover, through the analysis of transcriptional profiles derived from genomic databases of CC patients, genes related to OS have been identified [15,16]. For instance, the high expression of BRCA1 [17] is associated with better OS, while high levels of VEGF165 transcript have been associated with worse disease-free survival [18] in CC patients. Alterations of non-coding RNAs have also been proposed as prognostic biomarkers in CC [19–21].

Since viral oncoproteins are responsible for maintaining the malignant phenotype, strategies aimed at finding new HPV-dependent biomarkers have been explored. The detection of HPV DNA and mRNA has been used for determining the risk of progression to cancer and as prognostic biomarkers. E6 and E7 transcripts have been shown to have higher specificity compared to HPV DNA positivity [22,23] and a higher positive predictive value of progressing to high cervical squamous intraepithelial lesions (HSIL) or cancer. Furthermore, it has been demonstrated that the presence and levels of E6 transcripts increase the risk of progression to cancer [24]. In cervical cancer, high expression of E6 oncogene and its isoform E6* are associated with poor overall survival [25]. Furthermore, the use of HPV mRNA as a molecular marker for cervical cancer metastatic spread tumor has been proposed [26,27]. In the sentinel node (SLN) of patients free of lymph node metastases, it was demonstrated that the presence of HPV mRNA has a prognostic value independent of tumor size, where recurrence-free survival was significantly longer for patients whose SLN was negative for HPV mRNA [27]. Genetic expression profiles dependent on viral oncogenes in CC offer a novel alternative in the search for biomarkers with prognostic value. A more precise classification of CC cases according to molecular profiles, considering viral oncogene expression would be useful to identify patients with more aggressive tumors. In addition, this information may identify targetable molecules as novel therapeutic potential options for patients with cervical cancer. The aim of this study was to identify molecules with potential as prognostic biomarkers, deregulated by HPV-16 E6 and E7 oncogenes that may impact the clinical outcome of patients with cervical cancer. Results showed that several transcripts were found to be altered by the E6 and E7 oncoproteins both in a cell model and in cervical cancer, where the decreased expression of RIPOR2 (RHO 2 family-interacting cell polarization regulators) was associated with poor OS, regardless of clinical stage. These findings position RIPOR2 as a potential prognostic biomarker in cervical cancer.

2. Materials and Methods

2.1. Cell Lines and Culture

Cervical cancer cell lines C-33 A, SiHa. and Ca Ski were purchased from ATCC (Manassas, VA, USA) and maintained at 37 °C with 5% CO_2. SiHa and C-33 A cells were grown in Dulbecco's modified Eagle's medium (DMEM) and Ca Ski cells in Roswell Park Memorial Institute (RPMI) medium, all supplemented with 10% of fetal bovine serum (FBS). C-33 A cells were stably transfected with the indicated plasmids using Lipofectamine reagent (Invitrogen, Waltham, MA, USA) according to the manufacturer's instructions, and selection was performed with 2 g/L of G418 (ChemCruz Bio, Dallas, TX, USA). The isolated C33-EV, C33-E616, and C33-E716 clones were used for specified experiments.

2.2. Plasmids

HPV-16 E6 and E7 Open Reading Frames (ORFs) were amplified from Ca Ski DNA using Polymerase Chain Reaction (PCR). Viral sequences, including an HA tag sequence, were amplified with specific primers (Supplementary Table S1) and cloned into the p3x-FLAG CMV.10 expression vector (Sigma, Burlington, MA, USA). Constructions were verified by DNA-sequencing. Finally, the plasmids named as empty vector p3x-FLAG (EV), p3x-FLAG-HA-E616 (E616), and p3x-FLAG-HA-E716 (E716) were used for the transfections of C-33 A cells to obtain stably transfected cells C33-EV, C33-E616, and C33-E716.

2.3. Western Blotting

C33-EV, C33-E616, and C33-E716 cells were cultured in 60 mm dishes and after 24 h lysed using 300 µL of RIPA buffer (100 mM Tris pH 8.0, 50 mM NaCl2, 0.5% Nonidet P-40, and protease inhibitor cocktail (Roche, Basel, CH)). A total of 20 µg of cell protein extracts were analyzed by SDS-PAGE gels (10–12%) and blotted onto a 0.22 µm nitrocellulose membrane (Bio-Rad, Hercules, CA, USA). Membranes were blocked with 10% skimmed milk in TBS-0.1% Tween 20 for 1 h at room temperature, followed by incubation with anti-HA (Cell Signaling, Danvers, MA, USA) and anti-H4 (Cell Signaling, Danvers, MA, USA) primary antibodies diluted 1:1000 and 1:20,000, respectively. After washing three times with TBS-0.1% Tween 20, membranes were incubated with HRP-conjugated secondary anti-mouse antibody (Santa Cruz, Bio., Dallas, TX, USA) in a dilution 1:10,000. Proteins were visualized utilizing the Clarity™ Western ECL Substrate (Bio-Rad, Hercules, CA, USA), according to the manufacturer's instructions. Then, membranes were visualized and analyzed in the iBright FL1500 imagining system (Invitrogen, Waltham, MA, USA).

2.4. Immunofluorescence Staining

Stable C-33 A cells were seeded over cover slides in 6-well plates. After 24 h, cells were fixed using 3.7% paraformaldehyde/PBS for 10 min and permeabilized with PBS-0.1% Triton-X100. Then, cells were blocked with a 0.3% BSA solution and incubated overnight at 4 °C with anti-HA antibody (Cell Signaling, Danvers, MA, USA) diluted 1:50. Cells were extensively washed with PBS and later incubated with anti-rabbit antibody conjugated to Alexa-488 (Invitrogen, Waltham, MA, USA) diluted 1:700. Slides were washed and mounted with Vectashield antifade mounting medium with DAPI (Vector laboratories, Burlingame, CA, USA). Cells were analyzed with EVOS FL fluorescence Microscope (Invitrogen, Waltham, MA, USA).

2.5. RNA Sequencing and Data Analysis

Total RNA was extracted from C33-EV, C33-E616, and C33-E716 cells using the RNeasy mini kit (Qiagen, Hilden, DE), according to the manufacturer's instructions. Three independent experiments of each condition were performed to ensure reproducibility. RNA integrity was verified through the Bioanalyzer 2100 system (Agilent, Santa Clara, CA, USA). RNA library preparation and sequencing was carried out by Novogene Bioinformatics Technology Co., Ltd. (Sacramento, CA, USA). Sequencing results were mapped zwith the reference human genome GRCh38, and the differential expression analysis was obtained

comparing groups C33-EV vs. C33-E616 and C33-EV vs. C33-E716 using the DESeq2 R package (1.16.1). Genes with adjusted p-value < 0.05 were considered as differentially expressed. Enrichment analysis of differentially expressed genes was implemented by the clusterProfiler R package for Gene Ontology (GO) [28] Encyclopedia of Genes and Genomes (KEGG) pathways [29] and Reactome [30]. Terms with corrected p value < 0.05 were considered significantly enriched by differentially expressed genes.

2.6. TCGA Analysis

Data from 309 cervical samples from the TCGA project were downloaded using the Bioconductor package TCGABiolinks [31]. Differential expression analysis was performed between normal tissue and tumoral samples using the DESeq2 package [32] and considering those transcripts with an p-adj < 0.05 as statistically significant.

2.7. Real-Time Quantitative PCR

Cells were seeded in 60 mm culture dishes, and 24 h after, total RNA extraction was performed using the RNeasy mini kit (Qiagen, Hilden, DE). The isolated RNA was treated with the DNase-Free DNA removal kit (Ambion, Austin, TX, USA), and 1000 µg of RNA was reverse-transcribed with random hexamers utilizing the GeneAmp RNA PCR Core Kit (Applied Biosystems, Waltham, MA, USA). The primers used for amplification of the different targets analyzed are contained in Supplementary Table S1. Maxima SYBR green/ROX qPCR Master Mix (2×) (Thermo Scientific, Waltham, MA, USA) was used for qPCR reaction. The results are presented as relative quantification using the ΔΔCt method.

2.8. Cervical Samples

A cohort of samples from Mexican patients with normal and premalignant lesions of the uterine cervix was tested for RIPOR2 expression, formed by 17 normal HPV-negative cervical samples, 7 normal HPV-positive cervical samples, 20 low-grade, and 15 high-grade cervical premalignant lesions, kindly provided by the Instituto Nacional de Salud Pública (INSP). In addition, 19 cervical cancer samples from the Tumor BioBank from the Instituto Nacional de Cancerología of Mexico City (INCan) were included. The protocol was revised and accepted on February 2017, by the Scientific and Ethical committees of INCan Ref. (017/007/IBI)(CEI/1144/17). All patients whose samples were utilized in this study agreed and signed the informed consent.

2.9. Statistical Analysis

Data showing the effects of HPV-16 E6 and E7 proteins on RIPOR2 transcript levels are presented as the mean ± SD. Analyses were performed using GraphPad Prism 5 software; p-value was calculated by Student's t-test and significant differences were accepted when $p < 0.05$, as indicated. To assess RIPOR2 expression in premalignant lesions compared to normal cervical samples, the statistical analysis was performed using Mann–Whitney U statistical test. For the survival analysis, clinical and follow-up data from the 309 cervical samples from the TCGA was obtained with the TCGABiolinks package. For each gene, patients were divided into two groups depending on the median expression as high or low. The overall survival of patients depending on analyzed gene was calculated using the Kaplan–Meier estimator. Comparison of the survival curves for both groups was performed using the log–rank test. Next, we performed Univariate and Multivariate Cox proportional hazard regressions using the R survival package. We considered a p-value < 0.05 as significant.

3. Results

3.1. HPV-16 E6 and E7 Oncoproteins Differentially Modify Transcriptome of Cervical Cancer Cells

To analyze the effect of HPV-16 E6 and E7 oncoproteins on cell gene expression profiles, a model of C-33 A cells stably transfected with vectors expressing E616 or E716 oncoproteins was generated, while cells harboring empty vector (EV) were used as a negative control.

The expression of the E6 and E7 transcripts was assessed by RT-PCR in the three cell lines (Figure 1A). As expected, the expression of full-length E6 and its small isoforms E6*I and E6*II were detected in the C33-E616 cell line, as it has been reported in HPV-positive cells [33,34]. On the other hand, E716-containing cells (C33-E716) only expressed E7 transcripts. The presence of the oncoproteins was also evaluated by immunoblot (Figure 1B). It is worth noting that protein levels of E6 full-length were hardly perceptible, even with long immunodetection exposure (data not shown), while the small isoform E6* is highly abundant. Meanwhile, the E7 protein was clearly detected in stably transfected cells. The immunofluorescence analysis showed that E6 and E7 were localized mainly at the nucleus and were present in all transfected cells, confirming that the model with a stable expression of the oncoproteins was successful (Figure 1C).

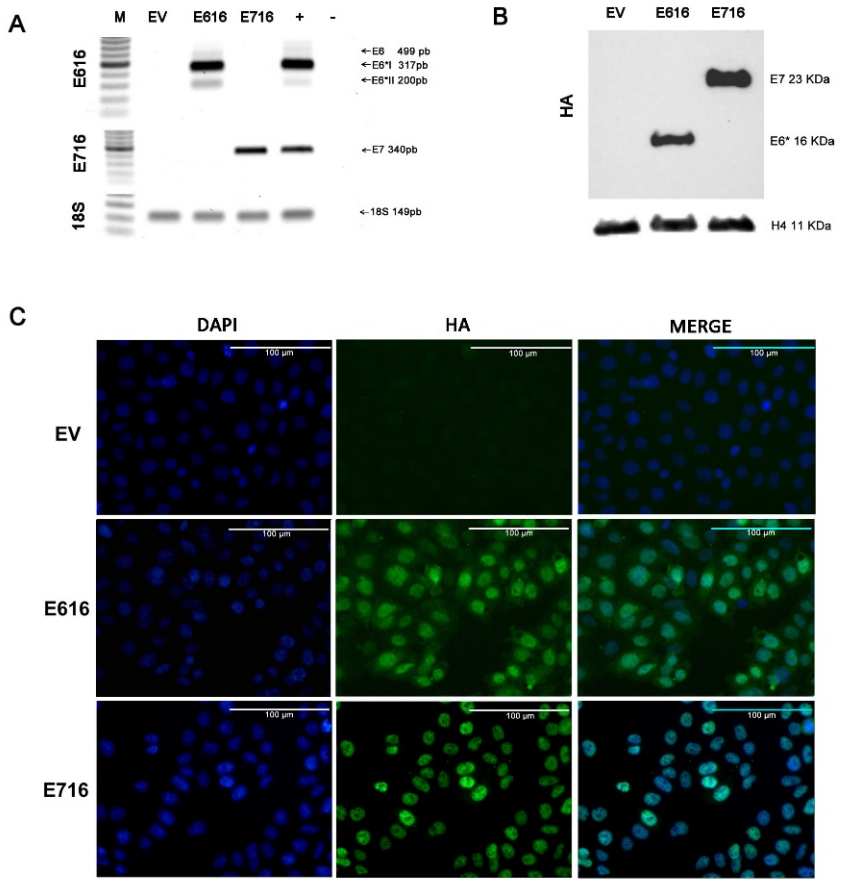

Figure 1. Stable expression of E616 and E716 in C-33 A cells: (**A**) RT-PCR showing the expression of E6, E6*I, and E6*II mRNA in C33-E616 cells, as well as the E7 mRNA in C33-E716 cells. 18S rRNA expression was used as a control. (**B**) Detection of HA-tagged E6 and E7 proteins by WB in stable C-33 A cell lines using HA antibody. H4 protein was used as the loading control; (**C**) Immunofluorescence staining using DAPI nuclear detection (blue) and anti-HA primary antibody to detect E6 and E7 oncoproteins (green). A representative image of each experiment is shown. Scale bar represents 100 µm long.

To identify gene expression profiles associated with the expression of E6 and E7 oncogenes, a mRNA massive sequencing analysis was performed in C-33 A stably transfected cells (E616, E716, or EV). Evident differential expression patterns were exhibited in E6- and E7-expressing cells when compared to the control group, as depicted in the heatmap of Figure 2. Differentially expressed genes are shown in Supplementary Tables S2 and S3.

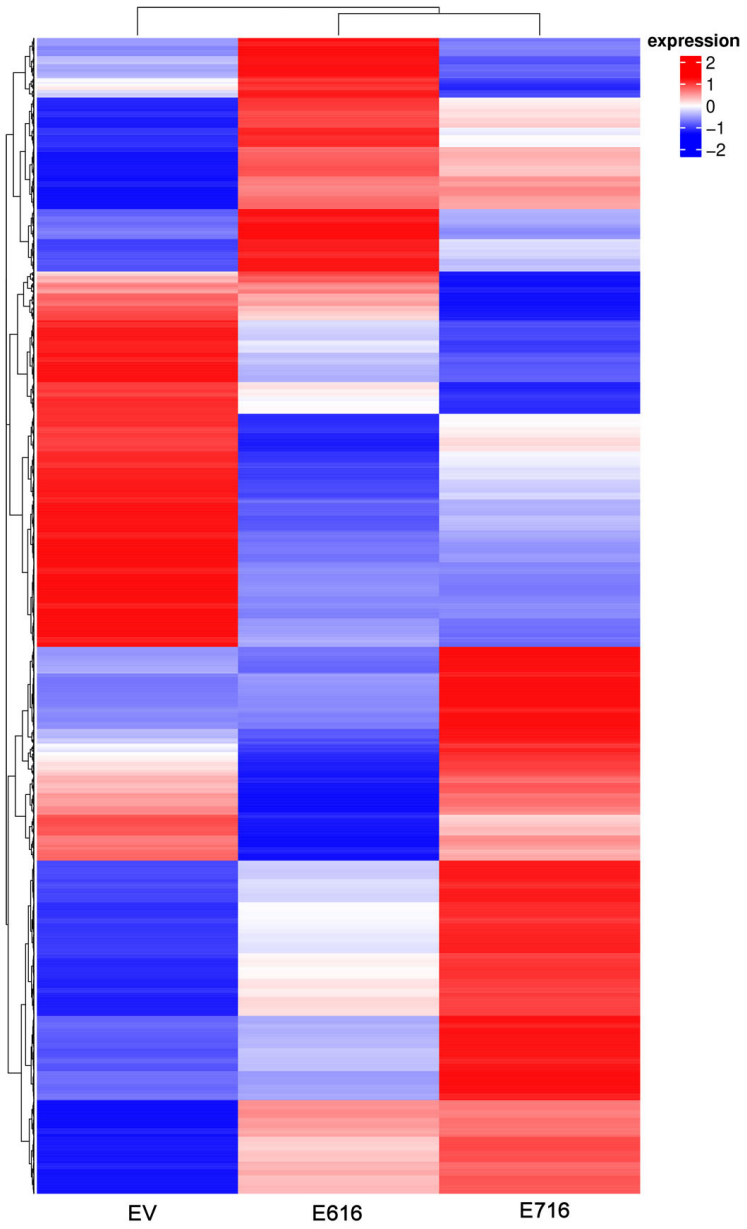

Figure 2. Gene expression patterns exhibited by C33EV, -E616, and -E716 cells. Heatmap showing the differential gene expression in Log2(FPKM+1) in the three cell groups in the columns (EV, E616, and E716). Each row represents the expression of a gene. Red color indicates increased expression levels and blue, decreased expression, while white means no significant change or the absence of data. Hierarchical clustering is shown at the top of the figure according to the transcriptional patterns of the groups (EV, E616, and E716), revealing that cells expressing the oncoproteins are closer than those with the empty vector. At the left, the clustering for differential gene expression is depicted.

A differential gene expression analysis was performed by comparing the gene expression levels (Log2 FC) in C33-E616 and C33-E716 cells in relation to C33-EV (Tables S2 and S3). A total of 2689 genes were found significantly differentially expressed (p-adj < 0.05) in the presence of E6. From those genes, 1520 were upregulated, while 1169 were downregulated (Figure 3A). Similarly, when comparing C33-E716 cells with C33-EV, 2018 genes were significantly deregulated (p-adj < 0.05), of which 1108 were upregulated and 910 were downregulated (Figure 3B).

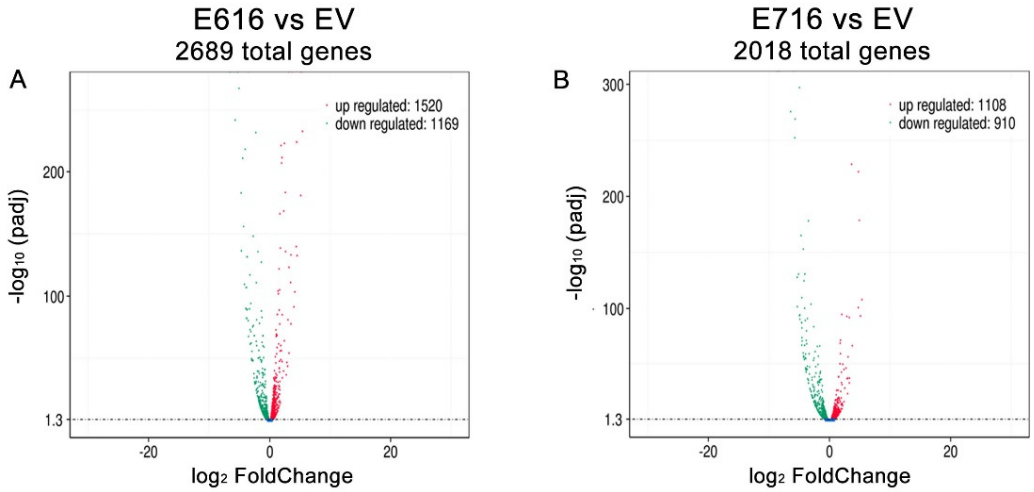

Figure 3. E616 and E716 differentially affected gene expression in C-33 A cells. Volcano plot illustrating the genes that were significantly (p-adj < 0.05) deregulated in: (**A**) C33-E616 cells and (**B**) C33-E716 cells, compared with the EV control. The upregulated genes are depicted in red color and the downregulated ones in green.

3.2. Cellular Processes and Signaling Pathways Modified by E6 and E7

An enrichment analysis was performed to identify pathways and biological functions significantly affected by E616 and E716. For this purpose, information from three different databases, including Gene Ontology (GO), Kyoto Encyclopedia of Genes and Genomes (KEGG), and Reactome database, was used.

When evaluating the sets of genes deregulated by E616, the GO enrichment analysis demonstrated that processes of nucleobase-containing compounds of catabolism, ribosomes, and translation were mostly affected (Figure 4A). Furthermore, a KEGG analysis showed that the top deregulated pathways included ribosomes, carbon metabolism, and glycolysis/gluconeogenesis (Figure 4C), and the Reactome analysis showed that processes related with ROBO proteins and translation are also deregulated by E616 (Figure 4E).

Regarding those processes altered by E716, the GO analysis demonstrated that the positive regulation of locomotion, adherens junctions, protein serine/threonine kinase activity, and actin binding are among the most deregulated processes (Figure 4B). Meanwhile, the KEGG analysis showed that E716 deregulated genes involved in the pathways in cancer, including MAPK, PI3K/Akt, NF-kB, and Ras signaling, among others (Figure 4D). Furthermore, the most significant processes revealed by the Reactome analysis were those related to syndecan interactions and non-integrin membrane–extracellular matrix interactions (Figure 4F).

3.3. E616 and E716 Regulated Genes Involved in Overall Survival of Cervical Cancer Patients

To determine genes affected by both oncoproteins, a Venn diagram was constructed (Figure 5). The results indicated that 1130 genes were deregulated by both E616 and E716 in C-33 A stable cell lines. Since E6 and E7 are constitutively overexpressed in CC, the aim of this study was to analyze those genes that were affected by both oncoproteins. Bioinformatic analyses derived from a TCGA cohort revealed differentially expressed genes in CC compared with normal tissue in data obtained from 309 cervical cancer patients. The results demonstrated that 6667 genes were significantly ($p < 0.05$) deregulated in CC. From those, 335 genes that were deregulated in CC patient samples, as well as in C33-E616 and C33-E716 cells.

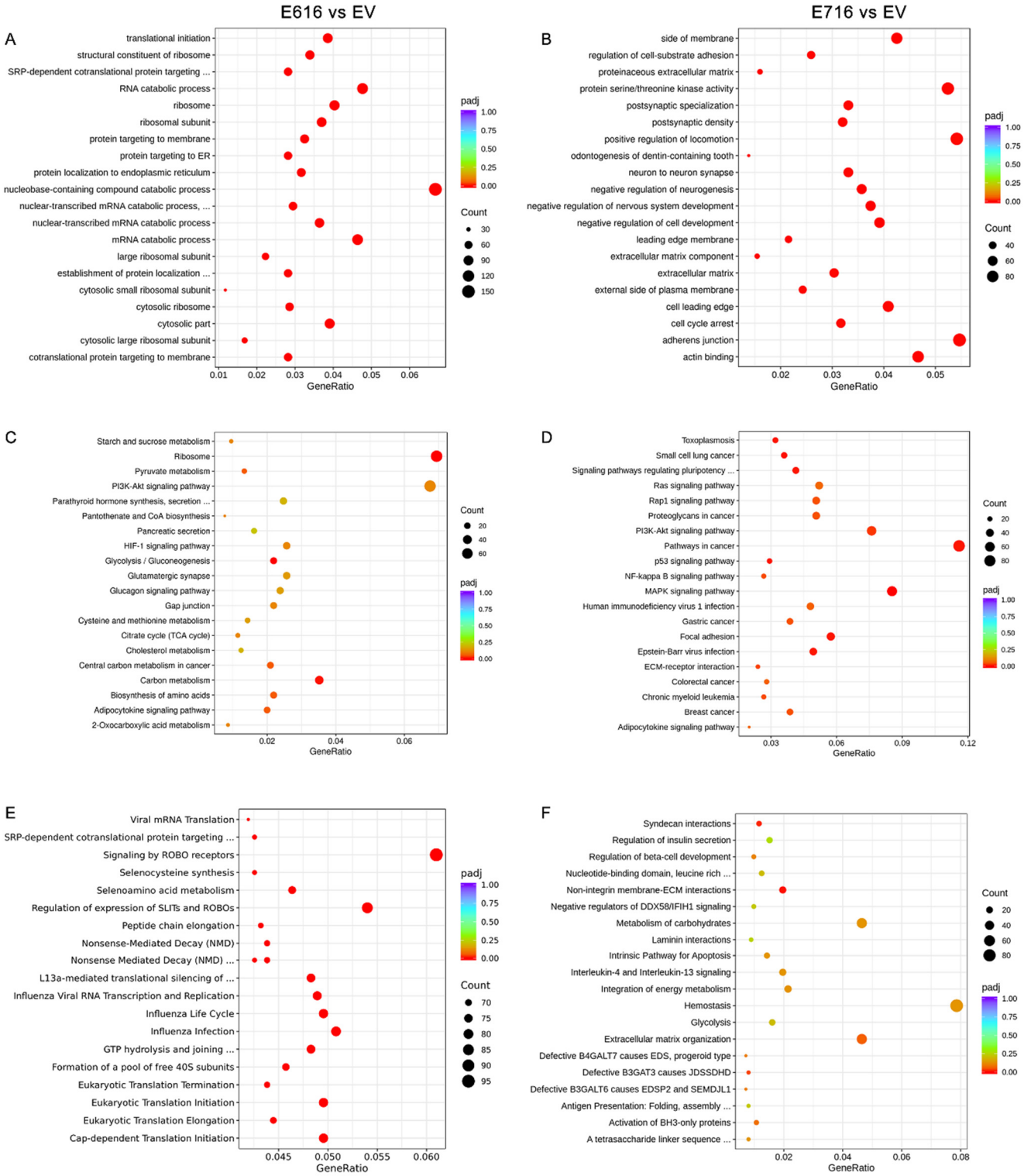

Figure 4. Enrichment analysis of differentially expressed genes (DEGs) in cells containing E616 and E716 oncoproteins. Dot plots of the 20 biological functions or pathways more significantly related with the DEGs modulated by E616 and E716 are depicted. Enrichment analysis was performed using data from GO for (**A**) E6- and (**B**) E7-expressing cells; while KEGG analysis exhibited cellular pathways affected in (**C**) E6- and (**D**) E7-containing cells. Reactome analysis showed processes associated with (**E**) E6 and (**F**) E7 expression. Significantly deregulated processes (p-adj < 0.05) were depicted in red color. Count means the number of genes assigned to a term. GeneRatio refers to the number of observed genes (DEGs) divided by the number of expected genes related to each category.

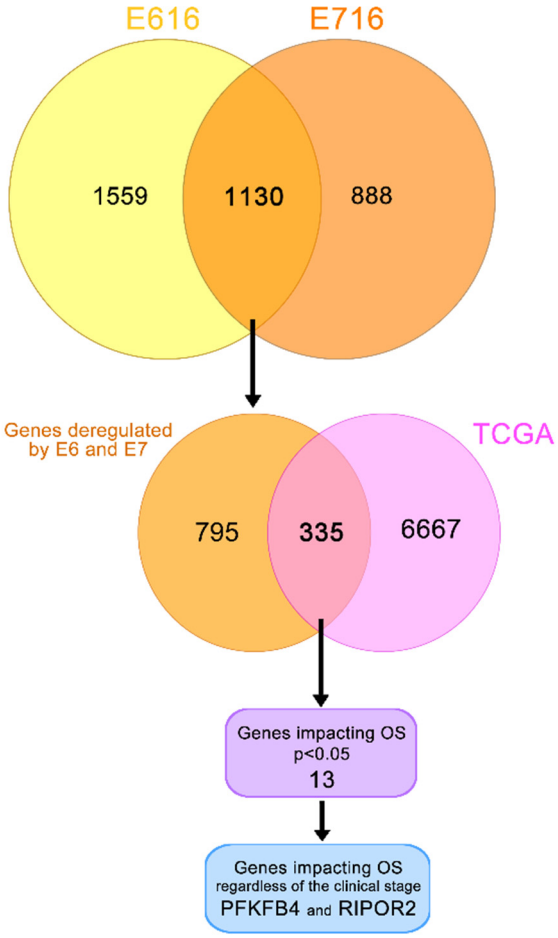

Figure 5. Genes deregulated in cervical cancer and in E6- and E7-expressing cells. Yellow/orange Venn diagram shows the genes deregulated by E616 and E716 in C-33 A stably transfected cells; the intersection of this diagram refers to the 1130 genes significantly modulated by both viral oncoproteins. Orange/pink Venn diagram intersects 335 genes modulated in CC according to the data obtained from TCGA and by the E6 and E7 viral oncoproteins. From these data, a univariate analysis showed 13 genes significantly affecting the OS ($p < 0.05$). A multivariate analysis demonstrated that PFKFB4 and RIPOR2 genes affected the OS independently of the clinical stage ($p < 0.05$).

A univariate Cox regression analysis exposed that 13 of these 335 genes significantly ($p < 0.05$) affected the OS in CC patients, as shown in Table 1. Since the OS is also affected by the clinical stage, the independence of the clinical stage was analyzed through a multivariate analysis, which demonstrated that the expression of two genes act as independent predictors of the OS; interestingly, a high RIPOR2 expression increases the OS (HR = 1.8, CI 1.00–3.25, $p = 0.048$), while a high expression of PFKFB4 decreases the OS (HR = 0.50, CI 0.27–0.93, $p = 0.029$) (Table 1).

The survival analysis and Kaplan–Meyer curves were performed taking into consideration the high or low expression of PFKFB4 and RIPOR2, according to the median expression levels, in TCGA cervical cancer samples. As depicted in Figure 6A, a high expression of PFKFB4 was found associated with unfavorable OS ($p = 0.0075$), evidenced by the decrease in the median survival from 8.48 years in patients with a low expression of PFKFB4 to 5.57 years in patients with a high expression. Contrariwise, a high expression of RIPOR2 exhibited a protector effect ($p = 0.0011$) (Figure 6B), since patients with high expression showed a median survival of 8.48 years compared to 5.57 years in patients who expressed low levels of RIPOR2. The obtained results evidence that RIPOR2 and PFKFB4 are deregulated in CC patients and in C33-E616 and C33-E7 CC cell lines, suggesting that their modulation in this cancer type is partially mediated by E6 and E7 oncoproteins.

Table 1. Univariate and multivariate analyses of the genes affecting the overall survival.

		Univariate Analysis		Multivariate Analysis	
	Overall Survival	**HR (95% CI)**	***p*-Value**	**HR (95% CI)**	***p*-Value**
SLC4A11	High vs. low expression	2 (1.2–3.5)	**0.0081**	1.42 (0.79–2.55)	0.228
NUP188		2 (1.2–3.4)	**0.0097**	1.10 (0.54–2.23)	0.773
CREM		2 (1.2–3.3)	**0.013**	0.80 (0.40–1.62)	0.55
AP1B1		1.9 (1.1–3.1)	**0.016**	0.99 (0.52–1.88)	0.99
RIPOR2		2.4 (1.4–4.1)	**0.0016**	1.80 (1.00–3.25)	**0.048**
PFKFB4		0.5 (0.3–0.84)	**0.0085**	0.50 (0.27–0.93)	**0.029**
CC2D1A		1.9 (1.1–3.2)	**0.015**	1.14 (0.56–2.30)	0.704
BICDL1		1.9 (1.1–3.2)	**0.015**	1.16 (0.62–2.15)	0.629
RHOT2		2 (1.2–3.4)	**0.0073**	1.44 (0.74–2.79)	0.278
NBEAL2		1.9 (1.1–3.2)	**0.016**	1.27 (0.69–2.33)	0.436
CPNE7		2.2 (1.3–3.7)	**0.0033**	1.55 (0.83–2.90)	0.165
FARSA		1.9 (1.1–3.2)	**0.013**	1.15 (0.55–2.40)	0.692
SHTN1		2.2 (1.3–3.7)	**0.0033**	1.46 (0.73–2.91)	0.281
Clinical Stage		1.5 (1.2–1.9)	**0.0003**		

Bold denotes a significant *p* value.

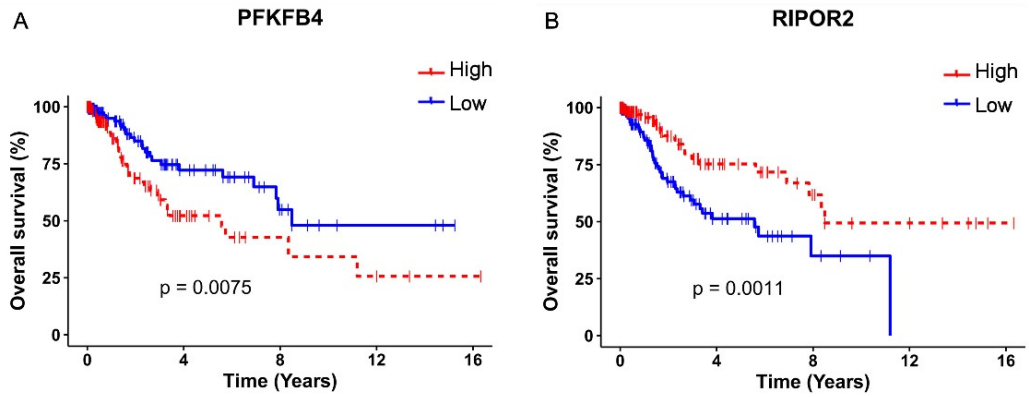

Figure 6. Kaplan–Meier OS analysis according to PFKFB4 and RIPOR2 expressions. Differences in OS of CC patients according to high or low expression of: (**A**) PFKFB4 ($p = 0.0075$) and (**B**) RIPOR2 ($p = 0.0011$). Low mRNA levels are represented with blue lines and high levels with red lines.

3.4. PFKFB4 and RIPOR2 Transcripts Are Affected by E6 and E7 in Cervical Cancer Cells

To validate the results obtained in the RNAseq analysis, transcript levels of PFKFB4 and RIPOR2 were analyzed in C-33 A E6- and E7-expressing cells in relation to EV cells through RT-qPCR. Surprisingly, as shown in Figure 7A, a trend for increased expression of PFKFB4 was observed in E6- and E7-expressing cells, although no statistical changes were obtained. In contrast, RIPOR2 levels were overwhelmingly ablated by E616 and E716 ($p < 0.0001$) (Figure 7B). These results were comparable with those obtained for RIPOR2 in the RNAseq analysis, where its expression levels were Log2FC–2.622 ($p = 7.16–39$) and Log2FC–3.839 ($p = 4.32–44$) for cells expressing E616 and E716, respectively. Those data corroborate the effect of both oncoproteins in the decrease of RIPOR2 mRNA levels in the CC cell line C-33 A. Furthermore, the expression of RIPOR2 was analyzed in CC cell lines harboring HPV-16 sequences. As shown in Figure 7C, SiHa cells did not exhibit significant differences in RIPOR2 expression levels in relation to C-33 A cells. In contrast, Ca Ski cells practically did not express RIPOR2. These results may be partially explained by the differences in HPV copy number which may influence the RIPOR2 expression levels, since Ca Ski cells harbor 500 HPV viral copies and SiHa cells contain 1–2 copies [35].

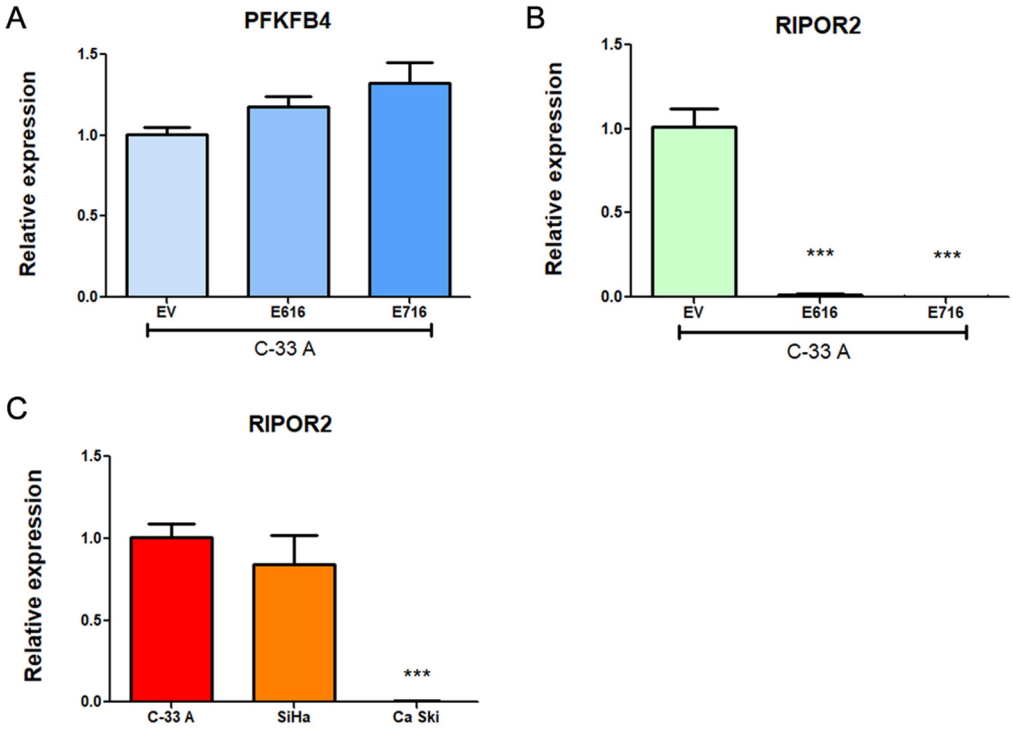

Figure 7. Expression of PFKFB4 and RIPOR2 in CC cell lines. Results obtained by RT-qPCR in C33-E616 and C33-E716 compared to C33-EV for: (**A**) PFKFB4 mRNA levels; (**B**) RIPOR2 mRNA levels; and (**C**) RIPOR2 mRNA levels in CC cell lines C-33 A, SiHa, and Ca Ski. Each graph is a representative experiment from three independently performed. Statistics was performed using GraphPad prism, mean ± SD, Student's *t*-test, *** $p < 0.0001$.

3.5. HPV-16 E6 and E7 Oncoproteins Decrease the Levels of Six Transcriptional Variants of RIPOR2 in C-33 A Cells

According to the National Center for Biotechnology Information (NCBI) [36], there are at least seven RIPOR2 transcriptional variants, which code for six different RIPOR2 protein isoforms (Table 2). Therefore, we became interested in investigating the impact of HPV oncoproteins on the amount of each of the RIPOR2 transcriptional variants.

Table 2. Transcripts and proteins coded by the RIPOR2 gene.

Transcript	Length (nt)	Transcript Type	Protein Isoform	Length (aa)
1	5553	protein coding	1	1068
2	2372	protein coding	2	591
3	5295	protein coding	3	1047
4	3546	protein coding	4	647
5	3548	protein coding	5	613
6	5403	protein coding	6	1018
7	5359	protein coding	6	1018

Since few information is available about transcriptional variants of RIPOR2 [37,38], and the primers first used for quantification of RIPOR2 detected all the transcriptional variants (Figure 8), we designed primers to detect the 7 RIPOR2 transcriptional variants (Supplementary Table S1). Due to the similarity among some of the RIPOR2 variants sequences, it was only possible to use specific primers for variants 1, 2, 3, 4, and 7. There are no unique sequences within the exons or in exon–exon junctions distinguishing variants 5 and 6; nevertheless, new primers able to detect variant 5 (and also to detect variant 4), as well as primers detecting variant 6 (and also variant 1) were used. Figure 8 depicts this strategy.

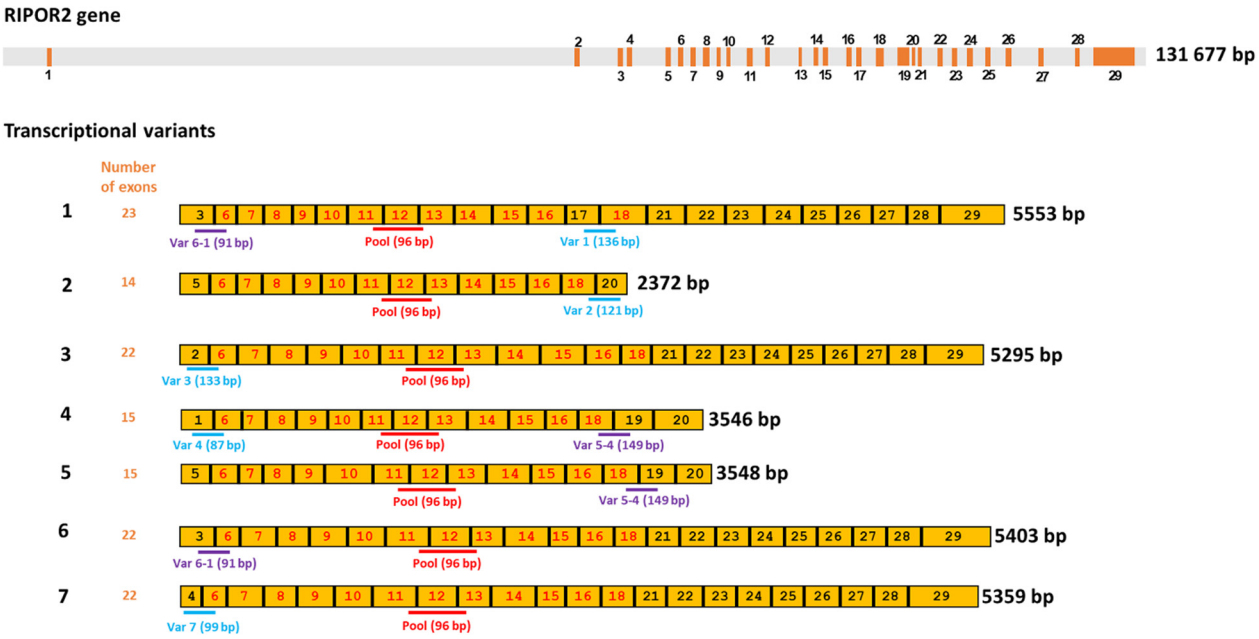

Figure 8. Human RIPOR2 gene and its transcriptional variants. Upper grey bar shows the position of introns in RIPOR2 gene, whereas the enumerated orange boxes, the exons of the gene. Seven transcriptional variants are enlisted under the gene in yellow color, showing the enumeration of the exons that comprise each transcript (1–7). Exons with numbers in red color are those shared by all the transcripts. Below the representation of each the transcriptional variant, the position of the specific primers and the size of the expected amplicon is shown. The pool primers amplify a fragment (shown in red) within a common region. Exons with the numbers in black color are only shared by some transcripts; therefore, primers for specific variants were designed within these areas. Amplicons shown in blue are those that allow the detection of a given specific variant, whereas amplicons in purple are shared by two variants (i.e., variants 1 and 6; variants 4 and 5).

To determine the basal gene expression levels of the seven transcriptional variants of RIPOR2 in C-33 A cells, RT-qPCRs were performed. Figure 9A,B show the expression of each transcriptional variant compared to the levels of total RIPOR2 transcripts detected by RIPOR2-pool primers. Variants 5 and 6 were the most abundant in relation to the other variants, which were reduced in 2.84- and 2.68-fold respectively, followed by variant 3 with a reduction of 4.95-fold, compared with the pool primers. Otherwise, variants 1, 2, and 7 exhibited the lowest levels in this cell line, being decreased 200-, 43.47-, and 76.9-fold, respectively. Interestingly, we could not detect variant 4 in C-33 A cells; nevertheless, we did detect it in human leukocytes (Figure 9C), demonstrating that the primers correctly amplify the variant 4 fragment.

Further, we investigated the effect of E6 and E7 proteins on mRNA levels of the seven RIPOR2 variants in C-33 A stable transfected cells (Figure 10). When analyzing the expression of all the RIPOR2 transcripts detected with the pool primers, a dramatic decrease in RIPOR2 expression in the presence of E6 and E7 of 50- and 250-fold, respectively, was observed in relation to the EV control. An evident effect of both oncoproteins in the decreased levels of variants 1, 2, 3, 5, 6, and 7 was observed even when the basal expression of some of these variants was low in comparison with the value observed in EV cells. Notably, those variants with the highest expression, such as variants 5 and 6, reduced 20- and 29.4-fold, respectively, in E6-expressing cells, while, in those cells with E7, in 76.9- and 500-fold, respectively. While variant 3 was completely ablated by the viral oncoproteins. As expected, the expression of variant 4 was not detected in all tested groups.

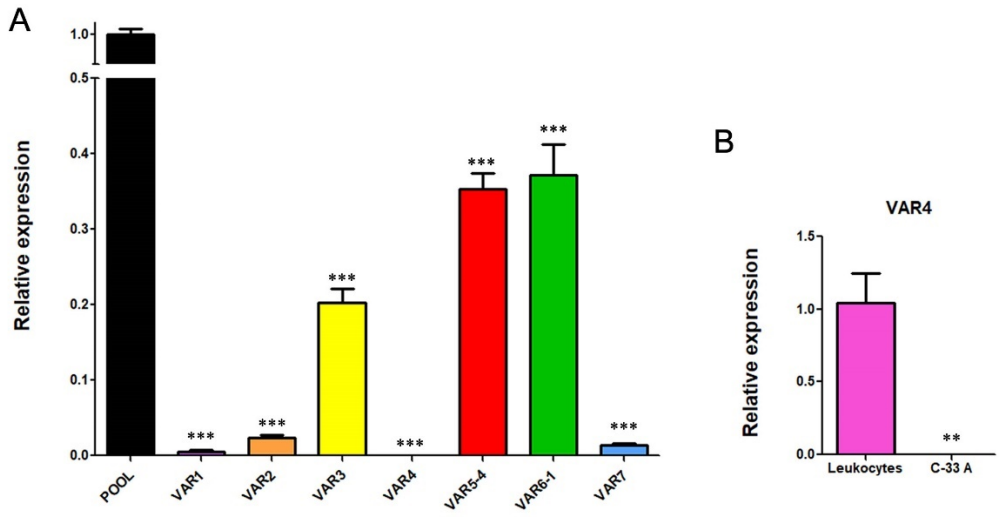

Figure 9. RIPOR2 variants expressed in C-33 A cells. (**A**) RT-qPCR showing the basal levels of the transcriptional variants, compared to RIPOR2-pool levels. (**B**) Expression of variant 4 in lymphocytes compared to C-33 A cells. *** $p < 0.0001$, ** $p = 0.0066$.

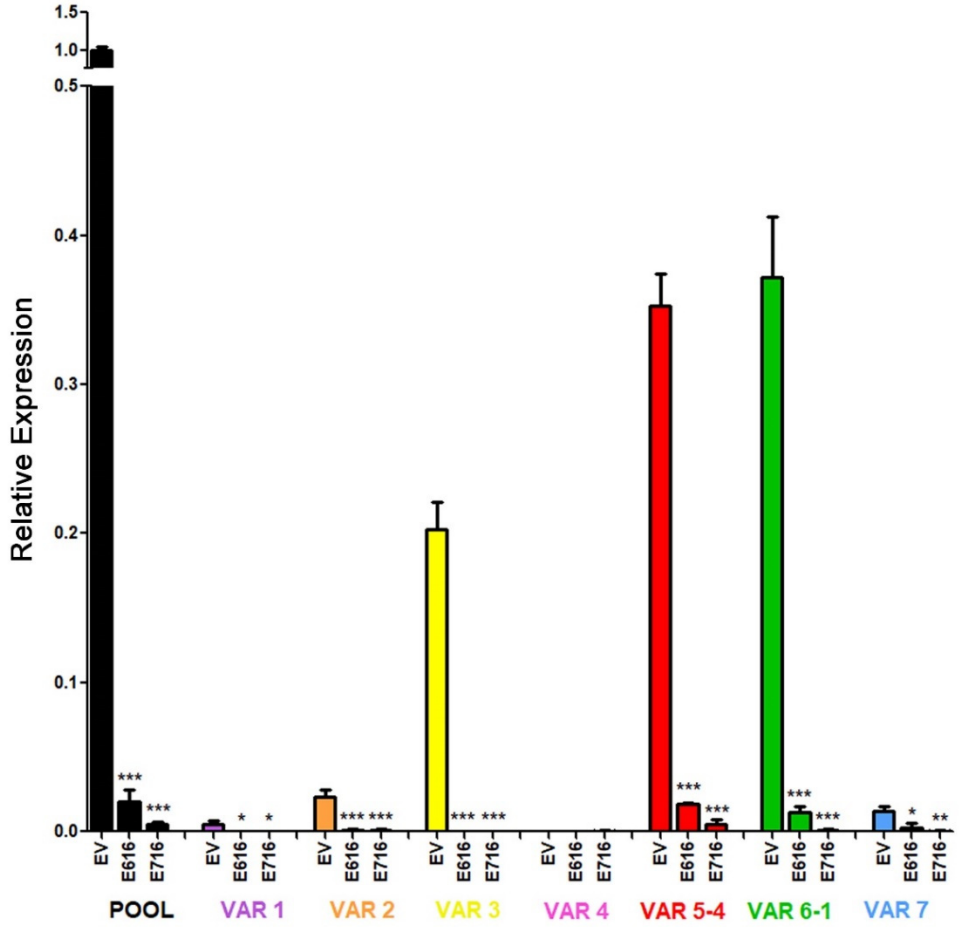

Figure 10. Effect of E616 and E716 oncoproteins on the amount of RIPOR2 transcriptional variants. Expression levels of the 1–7 transcriptional variants were assessed in C33-EV, C33-E616, and C33-E716 cells by RT-qPCR using RIPOR2 pool or specific variant primers. Statistical differences are expressed as *** $p \leq 0.0009$, ** $p = 0.0029$, and * $p \leq 0.0166$ when comparing EV vs. E616 or E716 groups.

Expression data obtained from C-33 A, SiHa, and Ca Ski cells regarding the seven transcriptional variants analyzed are shown in Figure 11. Interestingly, Variants 5 and 6, the most abundant previously observed in C-33 A (Figure 9) were also the most enriched in SiHa cells. Other variants, such as 2 and 7, were poorly expressed in SiHa cells, while 1, 3, and 4 were absent. Moreover, no expression of any variant was observed in the Ca Ski cell line, correlating with the absence of RIPOR2 pool transcripts observed in Ca Ski cells (Figure 7C).

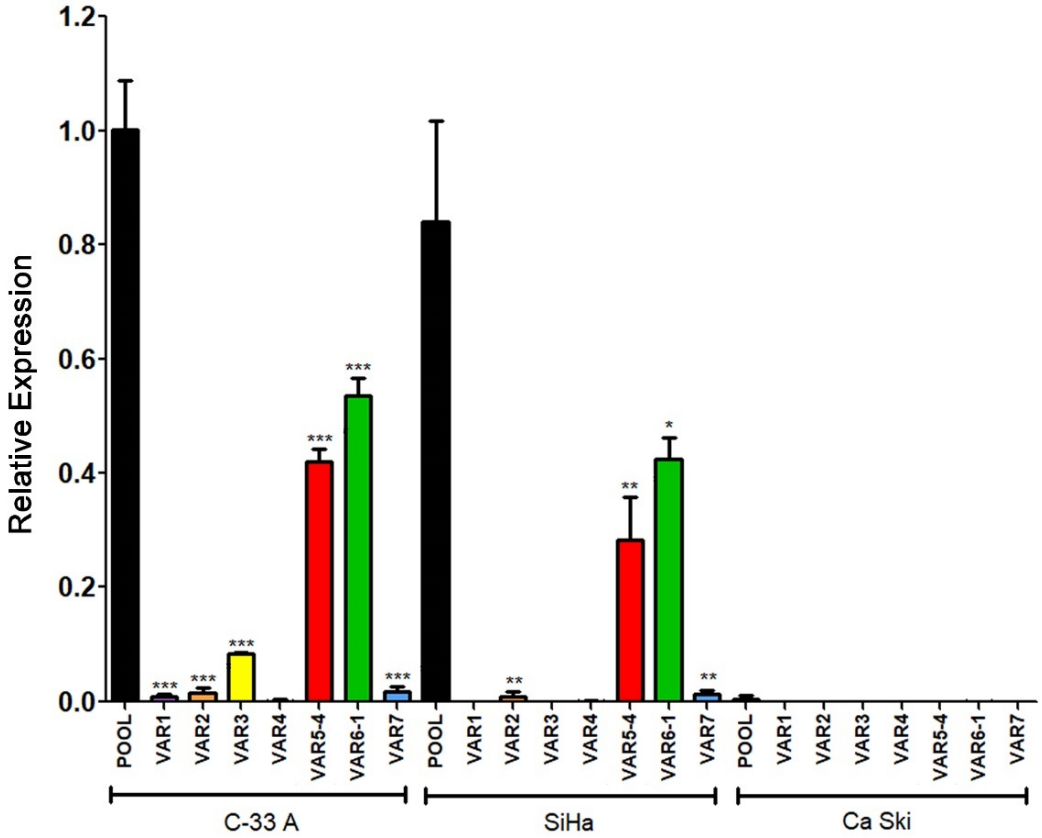

Figure 11. Expression of RIPOR2 transcriptional variants in cervical cancer cell lines. The levels of the 7 transcriptional variants were evaluated in C-33 A, SiHa, and Ca Ski cell lines by RT-qPCR. Fold change data were calculated compared with RIPOR2 pool levels within each cell line, and statistical analyses were performed using GraphPad prism and expressed in mean ± SD, significance is represented as *** $p \leq 0.009$, ** $p \leq 0.0072$, and * $p = 0.0159$.

3.6. RIPOR2 Expression Is Downregulated in Premalignant Lesions and Lower Levels of RIPOR2 Are Associated with Worse Prognosis of Cervical Cancer

RT-qPCR analysis was performed to determine whether the expression of RIPOR2 was altered in premalignant lesions of the cervix comprising low and high grade squamous intraepithelial lesions (LSIL and HSIL) and normal samples with HPV infection, compared to normal HPV negative samples. As shown in Figure 12A, the expression of RIPOR2 significantly decrease as the cervical lesion progresses. In addition, the evaluation of RIPOR2 expression in cervical cancer cases (n = 19) showed that the low expression of RIPOR2 was associated with a worse OS, although no significant results were obtained, probably due to the lack of an adequate number of samples available; therefore, a larger cohort of CC samples is required to ascertain this association (Figure 12B).

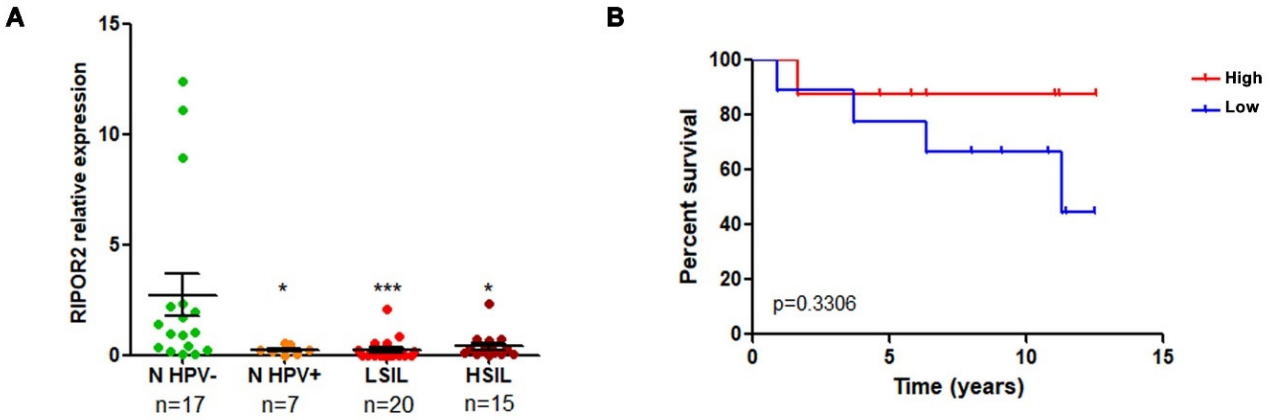

Figure 12. RIPOR2 expression in cervical premalignant lesions and cervical cancer. (**A**) RIPOR2 mRNA levels were analyzed by RT-qPCR using RIPOR2 pool primers in normal (*n*) HPV positive and negative samples, as well as LSIL and HSIL * $p \leq 0.0222$; *** $p = 0.0001$. (**B**) Overall survival analysis comparing RIPOR2 low (blue line) vs. high (red line) expression in cervical cancer patients ($p = 0.3306$).

Taken together, these results suggest that RIPOR2 expression is downregulated by HPV-16 E6 and E7 oncoproteins, and it is probably affected from the onset of infection; moreover, our data indicate that decreased expression of RIPOR2 is associated with unfavorable clinical outcome of patients.

4. Discussion

In Mexico, cervical cancer continues to be an important health problem, where a vast majority of cases are diagnosed in advanced stages [9]. For those patients, conventional treatments may not be as effective, so targeted strategies could give better results. In this sense, the search for prognostic markers becomes an area of interest, to identify patients who may benefit from specific therapies, in addition to identifying possible therapeutic targets.

The continuous expression of HPV E6 and E7 oncoproteins promotes and maintains the malignant phenotype in CC. It has been demonstrated that reducing the expression of E6 and E7 oncogenes of HPV-16 reverses the malignant phenotype. In this regard, an in vivo study revealed that a xenograft HPV positive tumor mice model that was locally injected with liposomes containing a CRISPR-Cas9 knocking-down system for E6/E7 from HPV-18 and -16, recovered the expression of p53 and p21 tumor suppressors, followed by a reduction in tumor growth [39,40]. Additionally, it was recently demonstrated that restoration of p53 expression and inhibition of HPV-16 E7 by CRISPR-Cas9 system delivered in nanoparticles in xenograft mice tumors induces a reduction of tumor growth and it is worth mentioning that such treatment exhibits a low toxicity and high transfection efficiency [41]. However, the use of CRISPR/Cas vectors specifically targeting E6 or E7 in tumor cells is still limited since such vectors have demonstrated low safety and are restricted to a specific HPV viral type. This prompts the study of not only the viral oncoproteins but also their molecular targets that could be used as prognostic biomarkers and/or as pharmacological targets to improve the quality of life of patients with cervical cancer.

Previous efforts have been made to identify molecules that allow predicting the clinical outcome of CC patients, based on deregulated molecules in cancer [42], or on the presence and expression of viral oncogenes [43]. Although little information is available about those cellular elements deregulated by viral oncoproteins that could be used as biomarkers associated with clinical outcome in CC. The study of molecules based on RNAs, identified by massive RNA sequencing, provides extensive information on those molecules altered in cervical cancer [16], in addition to those altered by viral oncogenes that could eventually serve as prognostic biomarkers, as is proposed in this study. With this in mind, we analyzed the transcriptome of cervical cancer C-33 A cells stably transfected with HPV E6 or E7 oncogenes, to further identify potential prognostic biomarkers in CC. This work led to

the identification of genes deregulated by both viral oncoproteins that also were found to be altered in CC and associated with overall survival. As a result, we show for the first time that E6 and E7 oncoproteins suppress the expression of RIPOR2 and increases the expression of PFKFB4, which in turn was associated with poor survival in CC patients.

PFKFB4 (Phosphofructo-2-kinase/fructose-2,6-bisphosphatase 4) is one of four isoenzymes of PFKFB [44], which generate fructose-2,6-bisphosphate, an allosteric activator of 6-phosphofructo-1- kinase, which is a rate-limiting enzyme in glycolysis and regulate the pentose phosphate pathway. Recent studies have demonstrated that the high expression of PFKFB4 predicts a poor prognosis in various types of cancer, including breast [45], gastric [46]; lung [47]; melanoma [48]; and thyroid cancer [49]. In this work, the RNAseq analysis revealed that PFKFB4 is overexpressed in the presence of E6 and E7, and the data obtained by qPCR showed a trend towards increased expression of this gene, although not significant; probably because PFBKB4 expression could be highly sensitive to regulation by other cancer-associated processes such as hypoxia [50], which warrants further study.

The family of RIPOR (RHO family interacting cell polarization regulators) proteins comprises 3 isoforms termed RIPOR1, RIPOR2 and RIPOR3, encoded by the FAM65A, FAM65B and FAM65C genes, respectively. RIPOR proteins bind directly to RHO GTPases (A, B, and C) through their RHO-binding motif, thereby inhibiting RHO activity and negatively influencing cellular functions regulated by these GTPases, such as receptor trafficking, cell migration, growth and polarization [51].

There is little information on the involvement of RIPOR2 in cancer. Dakour et al., in 1997 [37], described the lack of expression of RIPOR2 in a wide variety of proliferating cancer cell lines. Tumors derived from prostate cancer cell line PC3, exhibited low expression of RIPOR2, even though a stem-like subpopulation derived from such cell line showed the opposite phenotype [52]. A bioinformatic study revealed that a signature comprising four genes (RIPOR2, DAAM2, SORBS1, CXCL8) was found to be associated with survival in cervical cancer patients [53]. Moreover, those tumors with this signature where RIPOR2 was downexpressed had a worse prognosis. Furthermore, the presence of RIPOR2 in tumors is positively associated with the infiltration of CD8 + cells T cells, macrophages, neutrophils, and dendritic cells. Furthermore, those patients whose tumors express RIPOR2 in the signature exhibit high expression of PD-1, PD-L1, PD-L2, and CTLA-4, making them potential candidates for immune checkpoint inhibitors.

In agreement, a recent study identified a four gene antitumor signature related to the tumor microenvironment, which included RIPOR2, CCL22, PAMR1, and FBN1 genes [54]. Authors found that tumors with high expression of RIPOR2, had a lower mutation burden, and higher levels of CD8 + T cells. Interestingly, patients with those tumors presented a better response to immunotherapy with antibodies against PD-1 alone or combined with CTLA4. Concordantly with the results obtained in the present work, the authors found that CC patients with higher RIPOR2 expression had a longer overall survival, concluding that RIPOR2 is a protective factor in CC. Moreover, when RIPOR2 was overexpressed in SiHa and HeLa CC cell lines, cell viability and migration capacity significantly diminished, suggesting that RIPOR2 is a tumor suppressor gene in cervical cancer. In this sense, our work provides valuable information on the participation of E6 and E7 viral oncoproteins in the regulation of RIPOR2 and its association with clinical evolution in CC, regardless of the tumor microenvironment.

It is known that the expression of RIPOR2, which negatively regulates the activation of RhoA GTPase, is promoted by transcriptional factors such as FOXO1 [55]. Previous studies have shown that FOXO1 expression is ablated in cervical tumors compared to normal tissue, and that FOXO1 expression decreases as precancerous lesions progress [56]. However, other studies evidence a controversy on the possible role of FOXO1 in cervical cancer, since its overexpression has been associated with a poor prognosis [57]. Moreover, it has been shown that the inhibition of the expression of E6 and E7 in Ca Ski cells recovers the expression of FOXO1, leading to apoptosis and to a reduction in the proliferation of cancer cells [58]. Interestingly, our RNAseq data showed a decrease in FOXO1 expression of -0.49 and -0.41

log2FC in cells with E6 and E7, respectively (Tables S2 and S3). On the other hand, it has been described that the overexpression of GTPase RhoA in cervical cancer is associated with distant metastasis after concomitant treatment with chemotherapy and radiotherapy [59]; concordantly, it is known that E6 and E7 oncoproteins regulate the activation of the GTPase RhoA [60,61]. This suggests the existence of a FOXO1/RIPOR2/RhoA axis mediated by HPV oncoproteins which is affected in cervical cancer and related to an unfavorable clinical outcome.

Over time, different names have been used for RIPOR2 (PL48, C6orf32, FAM65B) and it has also been reported with different nucleotide numbers or protein sizes. The first RIPOR2 variants identified in the differentiating cytotrophoblast included three mRNAs (2.8, 3.5 and 4.8 kb) [37,62]. Subsequently, multiple isoforms of the RIPOR2 protein were detected by immunoblot, and those described as isoforms 1 and 2, which were composed of 1018 and 591 amino acids, respectively [38], correspond to isoforms 6 and 2 of the protein according to most recent NCBI data [36] (Table 2). Furthermore, PL48 was described as a short isoform of C6orf32 composed of 536 amino acids [38], which could be the current variant 2. Therefore, the specific roles of each RIPOR2 isoform in physiological and cancer-related are not yet known.

Our results show a significant decrease in the expression of the transcriptional variants of RIPOR2 by the E6 and E7 oncoproteins, which suggests that their modulation is at the transcriptional level. It is not ruled out that the low expression of RIPOR2 in cells harboring HPV-16 E6 and E7 oncoproteins could involve epigenetic changes in the RIPOR2 promoter, since E6 and E7 oncoproteins have been shown to promote the hypermethylation of various tumor suppressor genes, which is associated with increased cell proliferation [63].

Interestingly, according to the Eukaryotic Promoter Database (EPD) [64], four promoters mediating the transcription of RIPOR2 are described. Besides, data derived from the FAMTOM5 project [65], show that expression of the RIPOR2 transcripts from promoters 1, 2 and 4 is decreased in CC cell lines naturally infected with HPV-16, -18 or -68, compared to normal cervical epithelium. Functional analysis of the promoters that regulate the expression of the RIPOR2 transcriptional variants is necessary to elucidate the specific processes involved and the factors participating in these regulations.

In addition to showing the possible use of RIPOR2 as a prognostic biomarker deregulated by both viral oncoproteins, our study provides information on the molecular mechanisms involved in the establishment and maintenance of tumors with papillomavirus infection and on molecules that could eventually be useful as therapeutic targets. It is important to mention, that also the deregulated molecules identified as dependent on the clinical stage in the multivariate analysis (Table 1), could provide valuable information for therapeutics, even when they do not offer an advantage in prognosis.

Although the present work focuses on the genes that were altered by both oncoproteins, all the genes that were found to be significantly upregulated or downregulated by each of the oncoproteins independently, are of interest to be studied both at the molecular level, as well as for their association with cancer and with the clinical outcome of patients either in TCGA databases or in other cohorts.

It is worth noting that enrichment analysis of Differentially Expressed Genes (DEG) demonstrated that E6 and E7, affect biological functions or pathways related to cancer. For instance, E6 alters glycolysis, translation initiation, carbon metabolism and ROBO-Slit signaling, among others; while E7 affects extra cellular matrix organization, MAPK signaling pathway and focal adhesion pathways, among others. It is known that alterations in such processes drive to increased proliferation, migration, or invasion, which are key elements for cancer development. Those processes have been shown to be affected in other types of cancer. For example, disturbed glucose metabolism has been reported in lung cancer cells [66]; aberrant expression of translation initiation factors is a common feature in gastrointestinal, lung, colorectal, breast, and prostate cancers [67]; moreover, alterations in the Slit/ROBO signaling induce malignant transformation in colorectal cancer [68].

The study of the expression of RIPOR2 when cancer is diagnosed could have a potential utility as a prognostic biomarker that allows the appropriate decision on surveillance and therapeutic intervention in patients with low risk of survival. Undoubtedly, the analysis of RIPOR2 offers a promising tool that would help improve the quality of life of patients. A limitation of this study is that the number of patients from the analyzed Mexican cohorts were restricted to the available samples, being mandatory the validation of RIPOR2 expression as a potential biomarker in a larger cohort of premalignant lesions and cervical cancer samples in a representative proportion of the studied population. On the other hand, we could not detect the RIPOR2 protein in tumor samples nor in cell lysates since the available commercial antibodies had poor immunodetection by western blot and immunohistochemistry; therefore, the obtention of more specific antibodies for the detection of RIPOR2 variants would be valuable to evaluate its association with poor OS in cervical cancer patients.

Our findings firmly position RIPOR2 as a promising prognostic biomarker in cervical cancer and demonstrate the effect of viral oncoproteins in downregulating RIPOR2 transcriptional variants. However, the specific mechanisms by which E6 and E7 downregulate RIPOR2 and their relationship with the development and/or maintenance of cancer is something that deserves further study.

Supplementary Materials: The following supporting information can be downloaded at: https://www.mdpi.com/article/10.3390/cells11233942/s1, Table S1: Primers used in this work; Table S2: Gene expression profiles of E616 expressing cells; Table S3: Gene expression profiles of E716 expressing cells.

Author Contributions: Conceptualization, M.L., J.O.M.-B., and L.O.-N.; methodology, J.O.M.-B., I.M.-R., Y.O.-P., and L.O.-N.; software, A.D.M.-G.; validation, J.O.M.-B., I.M.-R., and L.O.-N.; formal analysis, M.L., J.O.M.-B., and L.O.-N.; investigation, M.L., J.O.M.-B., and L.O.-N.; resources, M.L., C.G.-E., V.M.-M., K.T.-P., and M.B.-R.; data curation, A.D.M.-G.; writing—original draft preparation, M.L., J.O.M.-B., and L.O.-N.; writing—review and editing, M.L., J.O.M.-B., I.M.-R., C.G.-E., and L.O.-N.; supervision, M.L.; and funding acquisition, M.L., J.O.M.-B., and C.G.-E. All authors have read and agreed to the published version of the manuscript.

Funding: This research was partially supported by the Programa de Apoyo en Proyectos de Investigación e Innovación Tecnológica, Universidad Nacional Autónoma de México PAPIIT-UNAM (IN200219); Instituto Nacional de Cancerología (017/007/IBI)(CEI/1144/17); PRONAII-7-Virus y Cáncer #303044 and Paradigmas y Controversias de la Ciencia #320812; and CF-2019-51488 from Consejo Nacional de Ciencia y Tecnología (CONACyT), México.

Institutional Review Board Statement: The study was conducted in accordance with the Declaration of Helsinki and approved by the Scientific and Ethical Institutional Review Boards of Instituto Nacional de Cancerología (017/007/IBI)(CEI/1144/17).

Informed Consent Statement: Informed consent was obtained from all subjects involved in the study.

Data Availability Statement: Data is contained within the article and supplementary material.

Acknowledgments: L.O.-N. is a doctoral student from the Programa de Doctorado en Ciencias Bioquímicas, Universidad Nacional Autónoma de México (UNAM) who received support from the Programa de Apoyo a los Estudios del Posgrado (PAEP), a fellowship from PAPIIT-UNAM (IN200219) and CONACyT (404293). J.O.M.-B. received a postdoctoral fellowship from CONACyT (741222). We thank Virginia Enriquez-Carcamo, María Alexandra Rodríguez-Sastre and Patricia de la Torre for technical support, and the Tumor Bank Department of the Instituto Nacional de Cancerología for providing biological samples.

Conflicts of Interest: The authors declare no conflict of interest.

References

1. Ferlay, J.; Ervik, M.; Lam, F.; Colombet, M.; Mery, L.; Piñeros, M.; Znaor, A.; Soerjomataram, I.B.F. IARC: Cancer Today. Available online: https://gco.iarc.fr/today/home (accessed on 29 June 2022).
2. Li, N.; Franceschi, S.; Howell-Jones, R.; Snijders, P.J.F.; Clifford, G.M. Human Papillomavirus Type Distribution in 30,848 Invasive Cervical Cancers Worldwide: Variation by Geographical Region, Histological Type and Year of Publication. *Int. J. cancer* **2011**, *128*, 927–935. [CrossRef]
3. Alfaro, A.; Juárez-Torres, E.; Medina-Martínez, I.; Mateos-Guerrero, N.; Bautista-Huerta, M.; Román-Bassaure, E.; Villegas-Sepúlveda, N.; Berumen, J. Different Association of Human Papillomavirus 16 Variants with Early and Late Presentation of Cervical Cancer. *PLoS ONE* **2016**, *11*, e0169315. [CrossRef]
4. Pal, A.; Kundu, R. Human Papillomavirus E6 and E7: The Cervical Cancer Hallmarks and Targets for Therapy. *Front. Microbiol.* **2020**, *10*, 3116. [CrossRef] [PubMed]
5. Martinez-Zapien, D.; Ruiz, F.X.; Poirson, J.; Mitschler, A.; Ramirez, J.; Forster, A.; Cousido-Siah, A.; Masson, M.; Pol, S.V.; Podjarny, A.; et al. Structure of the E6/E6AP/P53 Complex Required for HPV-Mediated Degradation of P53. *Nature* **2016**, *529*, 541–545. [CrossRef] [PubMed]
6. Scheffner, M.; Huibregtse, J.M.; Vierstra, R.D.; Howley, P.M. The HPV-16 E6 and E6-AP Complex Functions as a Ubiquitin-Protein Ligase in the Ubiquitination of P53. *Cell* **1993**, *75*, 495–505. [CrossRef] [PubMed]
7. Huh, K.; Zhou, X.; Hayakawa, H.; Cho, J.-Y.; Libermann, T.A.; Jin, J.; Wade Harper, J.; Munger, K. Human Papillomavirus Type 16 E7 Oncoprotein Associates with the Cullin 2 Ubiquitin Ligase Complex, Which Contributes to Degradation of the Retinoblastoma Tumor Suppressor. *J. Virol.* **2007**, *81*, 9737–9747. [CrossRef]
8. Singh, G.K.; Azuine, R.E.; Siahpush, M. Global Inequalities in Cervical Cancer Incidence and Mortality Are Linked to Deprivation, Low Socioeconomic Status, and Human Development. *Int. J. MCH AIDS* **2012**, *1*, 17–30. [CrossRef] [PubMed]
9. Isla-Ortiz, D.; Palomares-Castillo, E.; Mille-Loera, J.E.; Ramírez-Calderón, N.; Mohar-Betancourt, A.; Meneses-García, A.A.; Reynoso-Noverón, N. Cervical Cancer in Young Women: Do They Have a Worse Prognosis? A Retrospective Cohort Analysis in a Population of Mexico. *Oncologist* **2020**, *25*, e1363–e1371. [CrossRef]
10. Torreglosa-Hernández, S.; Grisales-Romero, H.; Morales-Carmona, E.; Hernández-Ávila, J.E.; Huerta-Gutiérrez, R.; Barquet-Muñoz, S.A.; Palacio-Mejía, L.S. Supervivencia y Factores Asociados En Pacientes Con Cáncer Cervicouterino Atendidas Por El Seguro Popular En México. *Salud Publica Mex.* **2022**, *64*, 76–86. [CrossRef]
11. Piri, R.; Ghaffari, A.; Gholami, N.; Azami-Aghdash, S.; PourAli-Akbar, Y.; Saleh, P.; Naghavi-Behzad, M. Ki-67/MIB-1 as a Prognostic Marker in Cervical Cancer—A Systematic Review with Meta-Analysis. *Asian Pac. J. Cancer Prev.* **2015**, *16*, 6997–7002. [CrossRef]
12. Zhu, K.; Deng, C.; Du, P.; Liu, T.; Piao, J.; Piao, Y.; Yang, M.; Chen, L. G6PC Indicated Poor Prognosis in Cervical Cancer and Promoted Cervical Carcinogenesis in Vitro and in Vivo. *Reprod. Biol. Endocrinol.* **2022**, *20*, 50. [CrossRef]
13. Dong, Z.; Chang, X.; Xie, L.; Wang, Y.; Hou, Y. Increased Expression of SRPK1 (Serine/Arginine-Rich Protein-Specific Kinase 1) Is Associated with Progression and Unfavorable Prognosis in Cervical Squamous Cell Carcinoma. *Bioengineered* **2022**, *13*, 6100–6112. [CrossRef] [PubMed]
14. Beyer, S.; Wehrmann, M.; Meister, S.; Kolben, T.M.; Trillsch, F.; Burges, A.; Czogalla, B.; Schmoeckel, E.; Mahner, S.; Jeschke, U.; et al. Galectin-8 and -9 as Prognostic Factors for Cervical Cancer. *Arch. Gynecol. Obstet.* **2022**, *306*, 105. [CrossRef] [PubMed]
15. Cui, H.; Ma, R.; Hu, T.; Xiao, G.G.; Wu, C. Bioinformatics Analysis Highlights Five Differentially Expressed Genes as Prognostic Biomarkers of Cervical Cancer and Novel Option for Anticancer Treatment. *Front. Cell. Infect. Microbiol.* **2022**, *12*, 926348. [CrossRef]
16. Campos-Parra, A.D.; Pérez-Quintanilla, M.; Martínez-Gutierrez, A.D.; Pérez-Montiel, D.; Coronel-Martínez, J.; Millan-Catalan, O.; De León, D.C.; Pérez-Plasencia, C. Molecular Differences between Squamous Cell Carcinoma and Adenocarcinoma Cervical Cancer Subtypes: Potential Prognostic Biomarkers. *Curr. Oncol.* **2022**, *29*, 4689–4702. [CrossRef] [PubMed]
17. Paik, E.S.; Chang, C.S.; Chae, Y.L.; Oh, S.Y.; Byeon, S.J.; Kim, C.J.; Lee, Y.Y.; Kim, T.J.; Lee, J.W.; Kim, B.G.; et al. Prognostic Relevance of BRCA1 Expression in Survival of Patients With Cervical Cancer. *Front. Oncol.* **2021**, *11*, 770103. [CrossRef] [PubMed]
18. Patel, K.A.; Patel, B.M.; Thobias, A.R.; Gokani, R.A.; Chhikara, A.B.; Desai, A.D.; Patel, P.S. Overexpression of VEGF165 Is Associated with Poor Prognosis of Cervical Cancer. *J. Obstet. Gynaecol. Res.* **2020**, *46*, 2397–2406. [CrossRef]
19. Nahand, J.S.; Taghizadeh-boroujeni, S.; Karimzadeh, M.; Borran, S.; Pourhanifeh, M.H.; Moghoofei, M.; Bokharaei-Salim, F.; Karampoor, S.; Jafari, A.; Asemi, Z.; et al. MicroRNAs: New Prognostic, Diagnostic, and Therapeutic Biomarkers in Cervical Cancer. *J. Cell. Physiol.* **2019**, *234*, 17064–17099. [CrossRef]
20. Zhang, G.; Zhang, R.; Bai, P.; Li, S.; Zuo, J.; Zhang, Y.; Liu, M.; Wu, L. Down-Regulated Expression of MiR-99a Is Associated with Lymph Node Metastasis and Predicts Poor Outcome in Stage IB Cervical Squamous Cell Carcinoma: A Case-Control Study. *Ann. Transl. Med.* **2022**, *10*, 663. [CrossRef]
21. Chang, A.; Shi, Y.; Wang, P.; Ren, J. LINC00963 May Be Associated with a Poor Prognosis in Patients with Cervical Cancer. *Med. Sci. Monit.* **2022**, *28*, e935070. [CrossRef]
22. Coquillard, G.; Palao, B.; Patterson, B.K. Quantification of Intracellular HPV E6/E7 MRNA Expression Increases the Specificity and Positive Predictive Value of Cervical Cancer Screening Compared to HPV DNA. *Gynecol. Oncol.* **2011**, *120*, 89–93. [CrossRef] [PubMed]

23. Gupta, S.M.; Warke, H.; Chaudhari, H.; Mavani, P.; Katke, R.D.; Kerkar, S.C.; Mania-Pramanik, J. Human Papillomavirus E6/E7 Oncogene Transcripts as Biomarkers for the Early Detection of Cervical Cancer. *J. Med. Virol.* **2022**, *94*, 3368–3375. [CrossRef]
24. Ho, C.M.; Lee, B.H.; Chang, S.F.; Chien, T.Y.; Huang, S.H.; Yan, C.C.; Cheng, W.F. Type-Specific Human Papillomavirus Oncogene Messenger RNA Levels Correlate with the Severity of Cervical Neoplasia. *Int. J. cancer* **2010**, *127*, 622–632. [CrossRef] [PubMed]
25. Ruiz, F.J.; Inkman, M.; Rashmi, R.; Muhammad, N.; Gabriel, N.; Miller, C.A.; McLellan, M.D.; Goldstein, M.; Markovina, S.; Grigsby, P.W.; et al. HPV Transcript Expression Affects Cervical Cancer Response to Chemoradiation. *JCI insight* **2021**, *6*, e138734. [CrossRef]
26. Rose, B.R.; Thompson, C.H.; Jiang, X.M.; Tattersall, M.H.N.; Elliott, P.M.; Dalrymple, C.; Cossart, Y.E. Detection of Human Papillomavirus Type 16 E6/E7 Transcripts in Histologically Cancer-Free Pelvic Lymph Nodes of Patients with Cervical Carcinoma. *Gynecol. Oncol.* **1994**, *52*, 212–217. [CrossRef] [PubMed]
27. Dürst, M.; Hoyer, H.; Altgassen, C.; Greinke, C.; Häfner, N.; Fishta, A.; Gajda, M.; Mahnert, U.; Hillemanns, P.; Dimpfl, T.; et al. Prognostic Value of HPV-mRNA in Sentinel Lymph Nodes of Cervical Cancer Patients with pN0-Status. *Oncotarget* **2015**, *6*, 23015–23025. [CrossRef] [PubMed]
28. Gene Ontology Resource. Available online: http://geneontology.org/ (accessed on 5 October 2022).
29. KEGG: Kyoto Encyclopedia of Genes and Genomes. Available online: https://www.genome.jp/kegg/ (accessed on 5 October 2022).
30. Home—Reactome Pathway Database. Available online: https://reactome.org/ (accessed on 5 October 2022).
31. TCGAbiolinks: An R/Bioconductor Package for Integrative Analysis of TCGA Data | Nucleic Acids Research | Oxford Academic. Available online: https://academic.oup.com/nar/article/44/8/e71/2465925 (accessed on 5 October 2022).
32. Moderated Estimation of Fold Change and Dispersion for RNA-Seq Data with DESeq2 | Genome Biology | Full Text. Available online: https://genomebiology.biomedcentral.com/articles/10.1186/s13059-014-0550-8 (accessed on 5 October 2022).
33. Yu, L.; Zheng, Z.M. Human Papillomavirus Type 16 Circular RNA Is Barely Detectable for the Claimed Biological Activity. *MBio* **2022**, *13*, e0359421. [CrossRef] [PubMed]
34. Paget-Bailly, P.; Meznad, K.; Bruyère, D.; Perrard, J.; Herfs, M.; Jung, A.C.; Mougin, C.; Prétet, J.L.; Baguet, A. Comparative RNA Sequencing Reveals That HPV16 E6 Abrogates the Effect of E6*I on ROS Metabolism. *Sci. Rep.* **2019**, *9*, 5938. [CrossRef] [PubMed]
35. Mincheva, A.; Gissmann, L.; Hausen, H.Z. Chromosomal integration sites of human papillomavirus DNA in three cervical cancer cell lines mapped by in situ hybridization. *Med. Microbiol. Immunol.* **1987**, *176*, 245–256.
36. NCBI. RIPOR2 RHO Family Interacting Cell Polarization Regulator 2 [Homo Sapiens (Human)]-Gene-NCBI. Available online: https://www.ncbi.nlm.nih.gov/gene/9750 (accessed on 5 October 2022).
37. Dakour, J.; Li, H.; Morrish, D.W. PL48: A Novel Gene Associated with Cytotrophoblast and Lineage-Specific HL-60 Cell Differentiation. *Gene* **1997**, *185*, 153–157. [CrossRef]
38. Yoon, S.; Molloy, M.J.; Wu, M.P.; Cowan, D.B.; Gussoni, E. C6ORF32 Is Upregulated during Muscle Cell Differentiation and Induces the Formation of Cellular Filopodia. *Dev. Biol.* **2007**, *301*, 70–81. [CrossRef]
39. Ling, K.; Yang, L.; Yang, N.; Chen, M.; Wang, Y.; Liang, S.; Li, Y.; Jiang, L.; Yan, P.; Liang, Z. Gene Targeting of HPV18 E6 and E7 Synchronously by Nonviral Transfection of CRISPR/Cas9 System in Cervical Cancer. *Hum. Gene Ther.* **2020**, *31*, 297–308. [CrossRef]
40. Zhen, S.; Liu, Y.; Lu, J.; Tuo, X.; Yang, X.; Chen, H.; Chen, W.; Li, X. Human Papillomavirus Oncogene Manipulation Using Clustered Regularly Interspersed Short Palindromic Repeats/Cas9 Delivered by PH-Sensitive Cationic Liposomes. *Hum. Gene Ther.* **2020**, *31*, 309–324. [CrossRef] [PubMed]
41. Xiong, J.; Li, G.; Mei, X.; Ding, J.; Shen, H.; Zhu, D.; Wang, H. Co-Delivery of P53 Restored and E7 Targeted Nucleic Acids by Poly (Beta-Amino Ester) Complex Nanoparticles for the Treatment of HPV Related Cervical Lesions. *Front. Pharmacol.* **2022**, *13*, 826771. [CrossRef]
42. Volkova, L.V.; Pashov, A.I.; Omelchuk, N.N. Cervical Carcinoma: Oncobiology and Biomarkers. *Int. J. Mol. Sci.* **2021**, *22*, 12571. [CrossRef] [PubMed]
43. Dong, A.; Xu, B.; Wang, Z.; Miao, X. Survival-related DLEU1 Is Associated with HPV Infection Status and Serves as a Biomarker in HPV-infected Cervical Cancer. *Mol. Med. Rep.* **2022**, *25*, 77. [CrossRef] [PubMed]
44. Yalcin, A.; Telang, S.; Clem, B.; Chesney, J. Regulation of Glucose Metabolism by 6-Phosphofructo-2-Kinase/Fructose-2,6-Bisphosphatases in Cancer. *Exp. Mol. Pathol.* **2009**, *86*, 174–179. [CrossRef]
45. Cai, Y.C.; Yang, H.; Shan, H.B.; Su, H.F.; Jiang, W.Q.; Shi, Y.X. PFKFB4 Overexpression Facilitates Proliferation by Promoting the G1/S Transition and Is Associated with a Poor Prognosis in Triple-Negative Breast Cancer. *Dis. Markers* **2021**, *2021*, 8824589. [CrossRef] [PubMed]
46. Wang, F.; Wu, X.; Li, Y.; Cao, X.; Zhang, C.; Gao, Y. PFKFB4 as a Promising Biomarker to Predict a Poor Prognosis in Patients with Gastric Cancer. *Oncol. Lett.* **2021**, *21*, 296. [CrossRef] [PubMed]
47. Zhou, Y.; Fan, Y.; Qiu, B.; Lou, M.; Liu, X.; Yuan, K.; Tong, J. Effect of PFKFB4 on the Prognosis and Immune Regulation of NSCLC and Its Mechanism. *Int. J. Gen. Med.* **2022**, *15*, 6341–6353. [CrossRef]
48. Trojan, S.E.; Piwowar, M.; Ostrowska, B.; Laidler, P.; Kocemba-Pilarczyk, K.A. Analysis of Malignant Melanoma Cell Lines Exposed to Hypoxia Reveals the Importance of PFKFB4 Overexpression for Disease Progression. *Anticancer Res.* **2018**, *38*, 6745–6752. [CrossRef] [PubMed]

49. Lu, H.; Chen, S.; You, Z.; Xie, C.; Huang, S.; Hu, X. PFKFB4 Negatively Regulated the Expression of Histone Acetyltransferase GCN5 to Mediate the Tumorigenesis of Thyroid Cancer. *Dev. Growth Differ.* **2020**, *62*, 129–138. [CrossRef]
50. Zhang, H.; Lu, C.; Fang, M.; Yan, W.; Chen, M.; Ji, Y.; He, S.; Liu, T.; Chen, T.; Xiao, J. HIF-1α Activates Hypoxia-Induced PFKFB4 Expression in Human Bladder Cancer Cells. *Biochem. Biophys. Res. Commun.* **2016**, *476*, 146–152. [CrossRef]
51. Lv, Z.; Ding, Y.; Cao, W.; Wang, S.; Gao, K. Role of RHO Family Interacting Cell Polarization Regulators (RIPORs) in Health and Disease: Recent Advances and Prospects. *Int. J. Biol. Sci.* **2022**, *18*, 800–808. [CrossRef]
52. Zhang, K.; Waxman, D.J. PC3 Prostate Tumor-Initiating Cells with Molecular Profile FAM65Bhigh/MFI2low/LEF1low Increase Tumor Angiogenesis. *Mol. Cancer* **2010**, *9*, 319. [CrossRef]
53. Mei, J.; Xing, Y.; Lv, J.; Gu, D.; Pan, J.; Zhang, Y.; Liu, J. Construction of an Immune-Related Gene Signature for Prediction of Prognosis in Patients with Cervical Cancer. *Int. Immunopharmacol.* **2020**, *88*, 106882. [CrossRef] [PubMed]
54. Xu, F.; Zou, C.; Gao, Y.; Shen, J.; Liu, T.; He, Q.; Li, S.; Xu, S. Comprehensive Analyses Identify RIPOR2 as a Genomic Instability-Associated Immune Prognostic Biomarker in Cervical Cancer. *Front. Immunol.* **2022**, *13*, 930488. [CrossRef] [PubMed]
55. Rougerie, P.; Largeteau, Q.; Megrelis, L.; Carrette, F.; Lejeune, T.; Toffali, L.; Rossi, B.; Zeghouf, M.; Cherfils, J.; Constantin, G.; et al. Fam65b Is a New Transcriptional Target of FOXO1 That Regulates RhoA Signaling for T Lymphocyte Migration. *J. Immunol.* **2013**, *190*, 748–755. [CrossRef]
56. Zhang, B.; Gui, L.S.; Zhao, X.L.; Zhu, L.L.; Li, Q.W. FOXO1 Is a Tumor Suppressor in Cervical Cancer. *Genet. Mol. Res.* **2015**, *14*, 6605–6616. [CrossRef] [PubMed]
57. Chay, D.B.; Han, G.H.; Nam, S.; Cho, H.; Chung, J.Y.; Hewitt, S.M. Forkhead Box Protein O1 (FOXO1) and Paired Box Gene 3 (PAX3) Overexpression Is Associated with Poor Prognosis in Patients with Cervical Cancer. *Int. J. Clin. Oncol.* **2019**, *24*, 1429–1439. [CrossRef] [PubMed]
58. Javadi, H.; Lotfi, A.S.; Hosseinkhani, S.; Mehrani, H.; Amani, J.; Soheili, Z.S.; Hojati, Z.; Kamali, M. The Combinational Effect of E6/E7 SiRNA and Anti-MiR-182 on Apoptosis Induction in HPV16-Positive Cervical Cells. *Artif. Cells Nanomed. Biotechnol.* **2018**, *46*, 727–736. [CrossRef]
59. Tanaka, K.; Matsumoto, Y.; Ishikawa, H.; Fukumitsu, N.; Numajiri, H.; Murofushi, K.; Oshiro, Y.; Okumura, T.; Satoh, T.; Sakurai, H. Impact of RhoA Overexpression on Clinical Outcomes in Cervical Squamous Cell Carcinoma Treated with Concurrent Chemoradiotherapy. *J. Radiat. Res.* **2020**, *61*, 221–230. [CrossRef]
60. Hampson, L.; Li, C.; Oliver, A.W.; Kitchener, H.C.; Hampson, I.N. The PDZ Protein Tip-1 Is a Gain of Function Target of the HPV16 E6 Oncoprotein. *Int. J. Oncol.* **2004**, *25*, 1249–1256. [PubMed]
61. Charette, S.T.; McCance, D.J. The E7 Protein from Human Papillomavirus Type 16 Enhances Keratinocyte Migration in an Akt-Dependent Manner. *Oncogene* **2007**, *26*, 7386–7390. [CrossRef] [PubMed]
62. Morrish, D.W.; Linetsky, E.; Bhardwaj, D.; Li, H.; Dakour, J.; Marsh, R.G.; Paterson, M.C.; Godbout, R. Identification by Subtractive Hybridization of a Spectrum of Novel and Unexpected Genes Associated with in Vitro Differentiation of Human Cytotrophoblast Cells. *Placenta* **1996**, *17*, 431–441. [CrossRef]
63. Sen, P.; Ganguly, P.; Ganguly, N. Modulation of DNA Methylation by Human Papillomavirus E6 and E7 Oncoproteins in Cervical Cancer. *Oncol. Lett.* **2018**, *15*, 11–22. [CrossRef] [PubMed]
64. EPD The Eukaryotic Promoter Database. Available online: https://epd.epfl.ch/search_EPDnew.php?query=ripor2&db=human (accessed on 30 September 2022).
65. FANTOM. Available online: https://fantom.gsc.riken.jp/ (accessed on 5 October 2022).
66. Vanhove, K.; Graulus, G.J.; Mesotten, L.; Thomeer, M.; Derveaux, E.; Noben, J.P.; Guedens, W.; Adriaensens, P. The Metabolic Landscape of Lung Cancer: New Insights in a Disturbed Glucose Metabolism. *Front. Oncol.* **2019**, *9*, 1215. [CrossRef] [PubMed]
67. Hao, P.; Yu, J.; Ward, R.; Liu, Y.; Hao, Q.; An, S.; Xu, T. Eukaryotic Translation Initiation Factors as Promising Targets in Cancer Therapy. *Cell Commun. Signal.* **2020**, *18*, 175. [CrossRef]
68. Zhou, W.J.; Geng, Z.H.; Chi, S.; Zhang, W.; Niu, X.F.; Lan, S.J.; Ma, L.; Yang, X.; Wang, L.J.; Ding, Y.Q.; et al. Slit-Robo Signaling Induces Malignant Transformation through Hakai-Mediated E-Cadherin Degradation during Colorectal Epithelial Cell Carcinogenesis. *Cell Res.* **2011**, *21*, 609–626. [CrossRef]

viruses

MDPI

Review

The Role of E6 Spliced Isoforms (E6*) in Human Papillomavirus-Induced Carcinogenesis

Leslie Olmedo-Nieva [1], J. Omar Muñoz-Bello [1], Adriana Contreras-Paredes [1] and Marcela Lizano [1,2,*]

[1] Unidad de Investigación Biomédica en Cáncer, Instituto Nacional de Cancerología, México/Instituto de Investigaciones Biomédicas, Universidad Nacional Autónoma de México, Av. San Fernando No. 22, Col. Sección XVI, Tlalpan, 14080 Mexico City, Mexico; leslie_azul25@hotmail.com (L.O.-N.); omarmube@gmail.com (J.O.M.-B.); adrycont@yahoo.com.mx (A.C.-P.)

[2] Departamento de Medicina Genómica y Toxicología Ambiental, Instituto de Investigaciones Biomédicas, Universidad Nacional Autónoma de México, 04510 Mexico City, Mexico

* Correspondence: lizanosoberon@gmail.com; Tel.: +52-555-628-0400 (ext. 31035)

Received: 22 December 2017; Accepted: 15 January 2018; Published: 18 January 2018

Abstract: Persistent infections with High Risk Human Papillomaviruses (HR-HPVs) are the main cause of cervical cancer development. The E6 and E7 oncoproteins of HR-HPVs are derived from a polycistronic pre-mRNA transcribed from an HPV early promoter. Through alternative splicing, this pre-mRNA produces a variety of E6 spliced transcripts termed E6*. In pre-malignant lesions and HPV-related cancers, different E6/E6* transcriptional patterns have been found, although they have not been clearly associated to cancer development. Moreover, there is a controversy about the participation of E6* proteins in cancer progression. This review addresses the regulation of E6 splicing and the different functions that have been found for E6* proteins, as well as their possible role in HPV-induced carcinogenesis.

Keywords: HPV; E6; splicing; E6*; spliceosome

1. Introduction

Cervical cancer continues to be a major public health problem, being the fourth cause of cancer mortality among women worldwide [1]. The persistent infection with High-Risk Human Papillomavirus (HR-HPV) is the main risk factor associated with cervical cancer development [2]. HPV sequences have been detected in almost 99% of the analyzed cervical cancer biopsies [3,4]. Moreover, HPV has also been linked to other anogenital [5,6] and oropharyngeal cancers [7].

Hitherto, more than 200 HPV types have been identified [8,9], which differ in more than 10% of nucleotide sequences within the L1 gene [10]. Commonly, HPVs infect basal layer cells of epithelia and are classified as cutaneous or mucosal types, being the infections with mucosal HPVs the most frequent sexually transmitted diseases worldwide [11]. From approximately 40 HPV types that infect the anogenital mucosal epithelium, 15 types are the most commonly found in cancer biopsies and thus, have been classified as HR-HPVs: HPV16, 18, 31, 33, 35, 39, 45, 51, 52, 56, 58, 59, 68, 73 and 82. Low-Risk HPV (LR-HPV) types are mainly related to mild dysplasia or genital warts [12]. HR-HPV16 and 18 are the most prevalent HR types, found in close to 60% and 15% of cervical cancer cases, respectively. LR-HPV6 and 11 are the most frequent types found in warts [13].

Human Papillomaviruses are small non-enveloped viruses of 55 nm, containing a circular double-stranded DNA of approximately 8 kb in length. The HPV genome is divided into three regions: the long control region (LCR) that regulates transcription and replication, the early region harboring nucleotide sequences of six common genes (E6, E7, E1, E2, E4 and E5) expressed in a primary

infection [14] and the late region that contains open reading frames (ORFs) encoding the L1 and L2 structural proteins involved in viral encapsidation [15].

The main viral oncoproteins E6 and E7 regulate cell cycle progression by promoting the degradation of the tumor suppressor proteins p53 and pRb, respectively. These and other interactions affect cellular pathways leading to malignant transformation [16,17].

Multiple HPV genes are expressed in a polycistronic pre-mRNA from a single strand. Depending on the state of differentiation of the epithelial layers, early or late promoters are activated leading the transcription of the early and late regions as polycistronic mRNAs. These transcripts are polyadenylated at sequences termed early and late polyadenylation sites, which are located downstream of each polycistronic mRNA [18,19].

Several transcripts are produced throughout an HPV infection by alternative splicing, which generates different mRNA expression patterns [20]. Alternative splicing within E6-E7 ORFs is a common feature of HR-HPVs, while no splicing in this region has been detected among LR-HPVs [21]. Full-length E6 from HR-HPV types is expressed from mRNAs with no splicing within E6 ORF, while E7 can be transcribed from different mRNAs including those with splicing in E6 [22,23]. The splicing process produces several transcripts containing E6 truncated mRNAs named E6*, which are derived from a donor splicing site within the E6 ORF and one of the different acceptor sites located in the early mRNA [24]. The most abundant E6 truncated mRNA is termed E6*I, which is a poorly studied protein. E6*I shares approximately the first 44 aa with the E6 full-length protein (E6) and the intron removal promotes a change in the E6 ORF adding approximately 13 aa that are only contained in E6*I isoform and generating a new stop codon [25].

This review focusses on the transcription patterns of E6/E6* and their regulation in different models, as well as the controversial roles of E6* proteins that affect cellular processes. The evidences and controversies represent an opportunity for the study of E6* proteins in order to establish their participation in the HPV life cycle and/or in the initiation or progression of cancer.

2. HPV Life Cycle

The HPV life cycle depends on differentiation and replication of the host-infected cells and is characterized by having two phases: latent infection, where the episome is replicated and maintained and productive infection, where the late proteins are produced and virions are formed [26].

Depending on HPV type, multiple entry pathways have been suggested. Generally, HPVs infect the undifferentiated basal cells of the epithelium through a micro-wound. Additionally, the accessibility of cells that are close to the squamo-columnar junction increases the possibility of HPV infection of this single cell layer [27]. The precise mechanism and receptors used by HPV to infect the epithelial cells are poorly known. The most accepted models for HPV16 suggest that the HPV L1 capsid protein attaches to heparan sulfate proteoglycans (HSPGs) [28] inducing conformational changes in the capsid and transferring the viral particle to a secondary non-HSPG entry receptor [29]. This transfer is facilitated through cleavage of the L2 protein by the convertase furin [30]. In contrast to the use of pseudovirus models, some analyses with native viruses have shown that the heparan sulfate receptor and furin cleavage activity are not required for all HPV types [31–33].

Several secondary L1-specific receptors have been proposed to mediate the infection, such as α-6 integrin [34], keratinocyte growth factor receptor (KGFR), epidermal growth factor receptor (EGFR) [35] and tetraspanins [36]. Finally, an L2-specific receptor, the S100A10 subunit of the annexin A2 heterotetramer, is thought to be involved in promoting viral entry [37].

After viral attachment to the host cell, the endocytic uptake of HPV implies a non-canonical internalization pathway related to micropinocytosis dependent on actin dynamics [38]; however, the precise cellular components mediating HPV uptake into host cells remain unknown.

Following virus entry, the viral capsid binds to Sortin nexin 17 at the endosomal compartments, which seems to help the L2-DNA complex to escape from the lysosome [39] and finally travel to the nucleus via dynein-mediated transport along microtubules [40].

In the latent phase, low levels of E1, E2, E6 and E7 are expressed in undifferentiated basal cells, where normal differentiation is retarded. During this phase, low replication rate occurs generating approximately 50–100 viral genomes per cell [41]. Further, in the proliferative phase, E6 and E7 are highly expressed from the middle to the upper layers of the differentiating epithelium [42]. The E2 protein recruits E1, a viral DNA helicase, to its binding site in the viral origin of replication, facilitating viral DNA replication and leading to the production of thousands of viral genome copies per cell in differentiated keratinocytes [26,43]. E4 stabilizes E2 and facilitates nuclear localization of E1, increasing E1/E2 dependent viral genome amplification [44]. Moreover, E2 acts as transcriptional factor controlling the expression of viral genes, through the recruitment of cellular factors to the LCR, promoting the activation or repression of viral transcription [43].

Finally, the viral life cycle is completed by the synthesis of L1 and L2 proteins in the uppermost layer of the epithelium, allowing the encapsidation of newly replicated genomes and the release of mature virions [27].

Most of the HPV infections are transient and cleared by the immune system in less than two years. Furthermore, when clinical lesions are generated, the majority undergo spontaneous regression [45]. It has been proposed that a determinant key to neoplastic progression is the persistent infection by HR-HPVs, which after a long time could lead to genomic instability and to viral genome integration into the host genome, at this stage, no viral progeny is produced [46]. As an episome, viral early gene expression is controlled by E2 but when integration occurs, E2 gene expression is commonly disrupted, leading to an increase in the expression of E6 and E7. The formation and maintenance of tumors needs the constant expression of E6 and E7 oncoproteins [47].

In cervical cancer biopsies, the HR-HPV genome is commonly found integrated, although in a small proportion of the cases HPV-DNA remains as an episome but at a high copy number [48]. It has been proposed that in HPV episomes, E2 binding sites contained in the LCR can be methylated preventing the E2 transcriptional repression and allowing the overexpression of E6 and E7 oncoproteins [49]. This indicates that HPV integration in some cases may not be a requirement for cellular transformation.

3. The Splicing Process

The splicing process is an essential mechanism that regulates gene expression and contributes to cell proteomic diversity. During transcription, RNA polymerase II generates a pre-mRNA that harbors exonic and intronic *cis* regulatory elements, able to recruit the spliceosome complex. The spliceosome regulates the exon-exon junction, generated when the intronic sequences are released, which is a crucial step in the maturation of the pre-mRNA [50,51]. The spliceosome is formed by a variety of small nuclear RNAs (U1, U2, U4/U6 and U5) organized in small nuclear ribonucleoproteins (snRPNs), complexed to several regulatory proteins [52,53]. The spliceosome complex assembly is directed by consensus sequences that flank exon-intron joints at the 5′ donor site ((C/A)AGGU(A/G)AGU) and 3′ acceptor site ((C/U)AG) of the pre-mRNA, in addition to intronic sequences termed branch points ((C/U)NC/U)U(A/G)A(C/U)) and a polypyrimidine tract [54]. Moreover, the pre-mRNA harbors auxiliary *cis*-acting elements termed exonic/intronic splicing enhancers (ESEs and ISEs, respectively) and exonic/intronic splicing silencers (ESSs and ISSs, respectively) that regulate splicing through the binding with regulatory proteins that stimulate or repress the spliceosome complex assembly [54].

Briefly, the U1 small nuclear ribonucleoprotein (snRNP) binds to the 5′ splice site, allowing the binding of the splicing factor 1/mammalian branch point binding protein (SF1/mBBP) to the branch point and the interaction of the U2 Auxiliary Factor (U2AF) with the polypyrimidine tract, forming the E complex which approaches the 5′ and 3′ splicing sites. Then, the U2 snRNP associates with the branch point and induces the displacement of SF1/mBBP, leading to the formation of the A complex. Later, the pre-assembled complex, U4/U6/U5 tri-snRNP, is recruited, generating the pre-catalytic B complex. In this step, all snRNPs are catalytically inactive and require other rearrangements to induce the first splicing reaction. Afterwards, U1 and U4 are removed from the B complex while U2, U5 and

U6 are rearranged, forming the active B complex. This complex is then catalytically activated by the DEAH (Asp-Glu-Ala-His)-box RNA helicase Prp2 (catalytically activated B complex). In this step, the phosphodiester bond at the 5′ splice site (exon-intron joint) is attacked and broken by the 2′-OH of the adenosine at the branch point, which creates a new bond between the 5′ side of the intron and the adenosine, forming the lariat structure. At this point the C complex is formed, which induces the catalysis of the second bond between the 3′-OH of the first exon and the 5′ acceptor site of the second exon (exon-exon joint). Finally, the intronic sequences are discarded, the exons come together and the spliceosome is disassembled [20,54,55] (Figure 1).

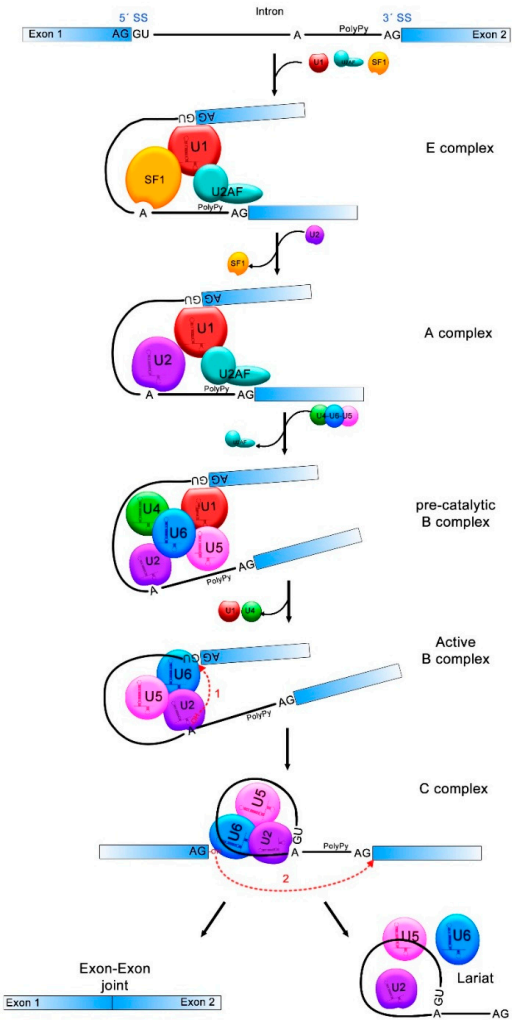

Figure 1. pre-mRNA splicing process. Donor and acceptor splicing sites (5′SS and 3′SS) in the exon-intron junctions, the branch point (A) and the polypyrimidine tract (PolyPy) are contained in the pre-mRNA. In the E complex, the U1 small nuclear ribonucleoprotein (snRNP) binds to the 5′SS, the splicing factor 1 (SF1) to the branch point and the U2 Auxiliary Factor (U2AF) to the PolyPy, approaching the 5′SS and 3′SS. In the A complex, U2 associates to the branch point and SF1 is disassembled. U4/U6/U5 complex binds and U2AF is released from the spliceosome in the pre-catalytic B complex. The active B complex is formed when U1 and U4 exit from the spliceosome and structure rearrangements induce the first splicing reaction where the phosphodiester bond at the 5′SS is attacked by the 2′-OH of the A forming a lariat structure. In the C complex, the second reaction forms a bond between the 3′-OH of the first exon and the 5′-P of the second exon. The intronic sequences are discarded and exons 1 and 2 come together. The transitions between one and other splicing complex are indicated with black solid arrows and the two splicing reactions are indicated with red dotted arrows.

Since the consensus sequences in splicing sites are not well conserved, the nucleotide combinations increase the possibility of multiple choices of splice sites within the pre-mRNAs, which leads to selective intron and exon removal, allowing the expression of a great variety of isoforms derived from a single pre-mRNA. This process is termed alternative splicing [20].

In addition, exonic and intronic splicing enhancers (ESEs and ISEs) and/or silencers (ESSs and ISSs) are required to regulate the splicing process: negatively, by the interaction with the heterogeneous ribonucleoproteins (hnRNPs) and positively, with serine/arginine-rich protein (SR). The hnRNPs (i.e., hnRNPA1 and hnRNPA2) bind mainly to the silencer elements, blocking the recognition of the exon-intron junctions by elements of the spliceosome. In contrast, the SR proteins (SRF1-12) usually bind to the enhancer sequences, acting as general activators of exon definition. The contribution of the SR and hnRNP proteins defines the overall recognition potential of an exon and/or the affinity for the spliceosome [20,52,56,57] (Figure 2A).

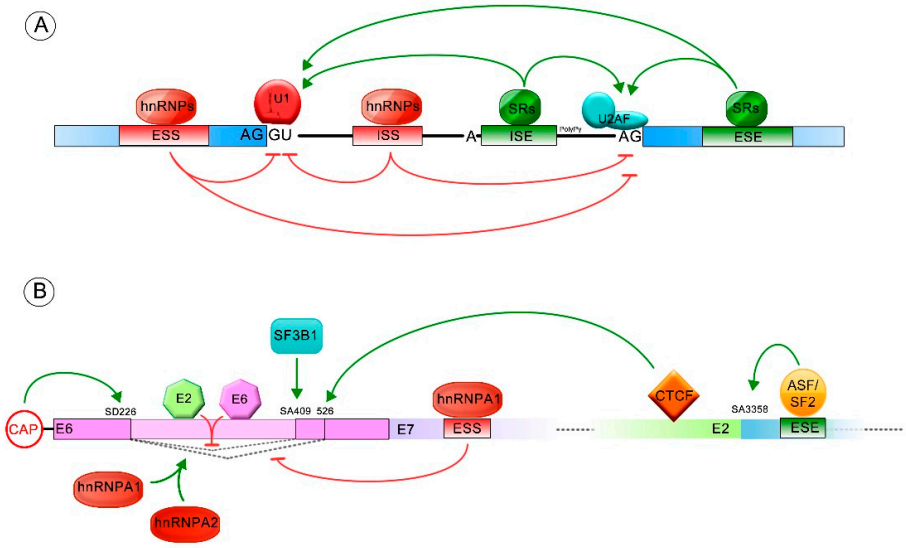

Figure 2. Splicing regulation. Green arrows indicate positive splicing regulation, while red arrows represent negative splicing regulation. (**A**) General regulation mediated by *cis* and/or *trans* elements is shown. The exonic and intronic splicing enhancers (ESE and ISE) frequently stimulate the splicing process by binding to serine/arginine-rich proteins (SR proteins). The exonic and intronic splicing silencers (ESS and ISS) commonly repress the splicing process, through binding with heterogeneous ribonucleoproteins (hnRNP) regulatory proteins; (**B**) Splicing regulated by *cis* and *trans* acting elements, allowing formation of different E6/E6* transcript patterns. The ESS and ESE sequences (exonic splicing silencer and enhancer, respectively) and the splicing donor (SD) and acceptor (SA) sites involved in E6 splicing regulation are also shown.

4. Splicing within HR-HPV E6

The LCR contains cellular and viral transcription factor binding sites, as well as transcriptional enhancers, a replication origin, a late polyadenylation site and late regulatory elements [19,27]. The early promoter is located upstream of the E6 ORF (p105 for HPV18 and p97 for HPV16) and is responsible for early gene transcription. The late promoter that resides inside of the E7 ORF, drives E4, L1 and L2 gene expression. Other sequences that could act as possible promoters have been described but their functions are not clearly understood.

In low-risk HPVs the E6 and E7 genes are transcribed from two independent promoters, while in high-risk HPVs those genes are transcribed as a single polycistronic pre-mRNA from the early promoters. A common feature of high-risk HPVs is that the E6/E7 polycistronic mRNA contains at least one donor and one acceptor splicing site that can trigger the alternative splicing process, inducing

the expression of a variety of E6 spliced transcripts termed E6* [18,58]. In contrast, low-risk HPVs and beta-papillomavirus types do not undergo splicing in this region [21].

Depending on the HR-HPV type, different transcripts are derived from one of the donor splicing sites contained in the E6 ORF and one of the acceptor splicing sites located within E7, E2 or E4 ORFs. The splicing pattern of HPV type 16 has been thoroughly studied and the following spliced transcripts have been identified: E6*I, E6*II, E6*III, E6^E7, E6^E7*I, E6^E7*II, E6*IV, E6*V and E6*VI [18,59–62]. Conversely, the described transcripts for HPV18 are: E6*I, E6*II, E6*III, E6^E7 [60,63,64]. Less is known about transcripts resulting from splicing in the E6 pre-mRNA of other HR-HPV types, such as HPV31 having E6*I and E6^E4; HPV33 with E6*I, E6*II and E6*III; and HPV58 with E6*I and E6*II [65–68]. For other HPV types only the E6*I transcript has been detected, although the existence of other E6 spliced transcripts cannot be discarded [21,69]. Donor and acceptor sites for the identified different transcripts are depicted in Table 1.

Table 1. Transcripts derived from alternative splicing within the E6 open reading frame (ORF). The table summarizes the E6* isoforms for 23 HPV types where alternative splicing has been observed. The detailed donor and acceptor splicing sites for each E6 truncated transcript are enlisted below.

HPV Type	E6* Transcripts	Donor-Acceptor Splicing Sites (Nucleotide Position)	References
16	E6*I	226–409	[59]
	E6*II	226–526	[70]
	E6*III	226–3358	[59]
	E6*IV	226–2709	[71]
	E6*V	221–409	[61]
	E6*VI	191–409	[61]
	E6^E7 (E6*X)	226–742	[60]
	E6^E7*I	174–718	[62]
	E6^E7*II	221–850	[62]
18	E6*I	233–416	[63,64]
	E6*II	233–3434	[63,64]
	E6*III	233–2779	[64]
	E6^E7	233–791	[60,64]
26	E6*I	173–406	[21]
30	E6*I	229–420	[21]
31	E6*I	210–413	[65,68]
	E6^E4 (E6*III)	210–3295	[65]
33	E6*I	231–509	[66]
	E6*II	231–785	[66]
	E6*III	231–3351	[66]
34	E6*I	223–414	[21]
35	E6*I	228–419	[21]
39	E6*I	231–420	[21]
45	E6*I	230–413	[69]
51	E6*I	173–406	[21]
52	E6*I	224–502	[69]
53	E6*I	236–419	[69]
56	E6*I	157–420	[21]
58	E6*I	232–510	[67]
	E6*II	232–3355	[67]
59	E6*I	183–582	[69]
66	E6*I	157–420	[21]
67	E6*I	224–502	[69]
68b	E6*I	232–415	[69]
69	E6*I	178–411	[21]
70	E6*I	231–422	[21]
73	E6*I	227–410	[69]
82	E6*I	178–411	[21]

Interestingly, it has been proposed that E6 nucleotides 226 and 409 (donor and acceptor sites, respectively) from HPV16 are preferentially selected among other splicing sites, leading to the release of intron I, generating E6*I [61]. A suboptimal branch point sequence was previously identified within intron I of HPV16 (AGUGAGU) which contains the 328G instead of the typical adenosine [72]. An optimal branch point was further discovered within the same intron (AACAAAC), proposed to be the preferred branch point sequence, where 385A allows the selection of E6*I and expression of E7 [61].

5. E6/E6* Transcription Patterns

Many studies have described the E6/E6* patterns found in cervical cancer cell lines with endogenous expression of HPV or in cells with ectopic expression of HPV sequences. These patterns have also been identified in HPV infected biopsies with normal or altered cytology and in HPV-related cancers. Most of those studies are focused on the expression patterns of HPV16 and HVP18; although, information is available for other HR-HPV types such as, 31, 33 and 58 (Figure 3) [65–67].

The donor and acceptor splicing sites necessary to generate E6*I were described for the first time in the HPV16 positive CaSki cell line [73]; however, this isoform was first named E6* in a study performed using the HPV18 positive HeLa cell line [74].

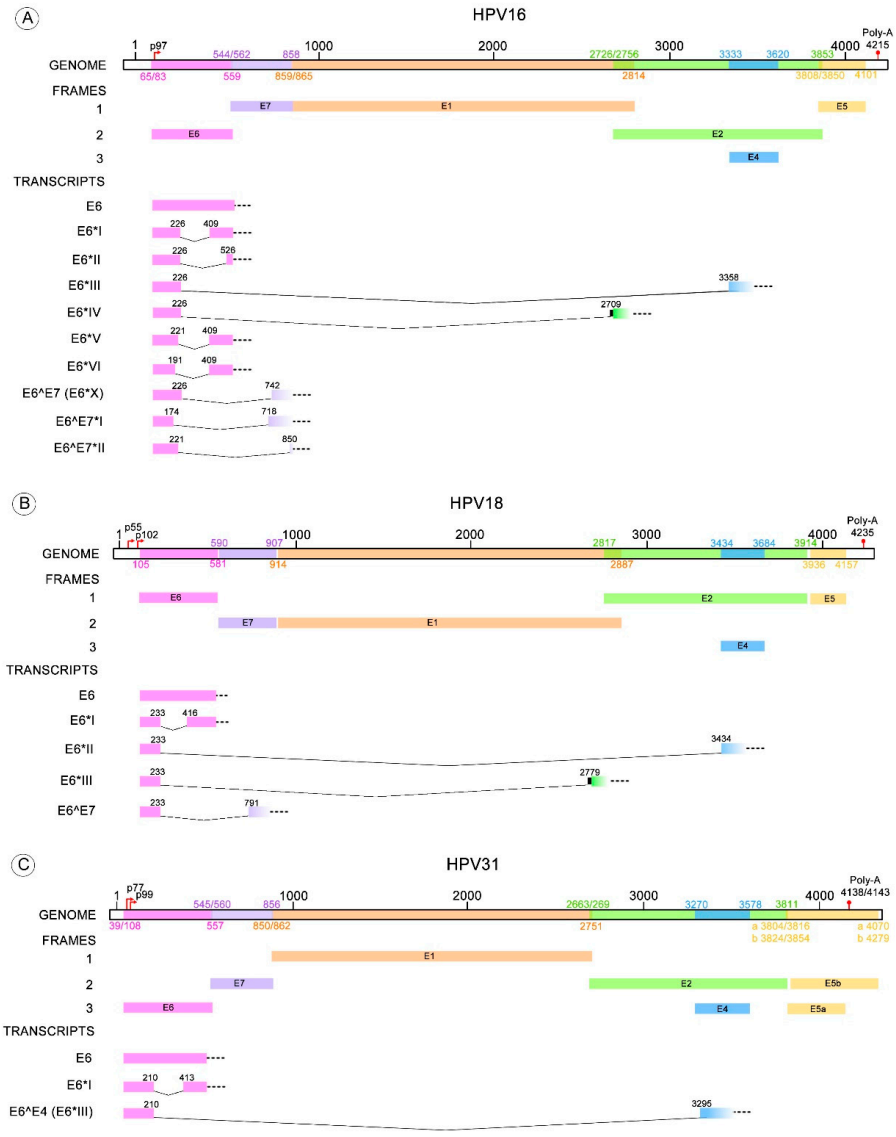

Figure 3. *Cont.*

Viruses **2018**, *10*, 45 8 of 20

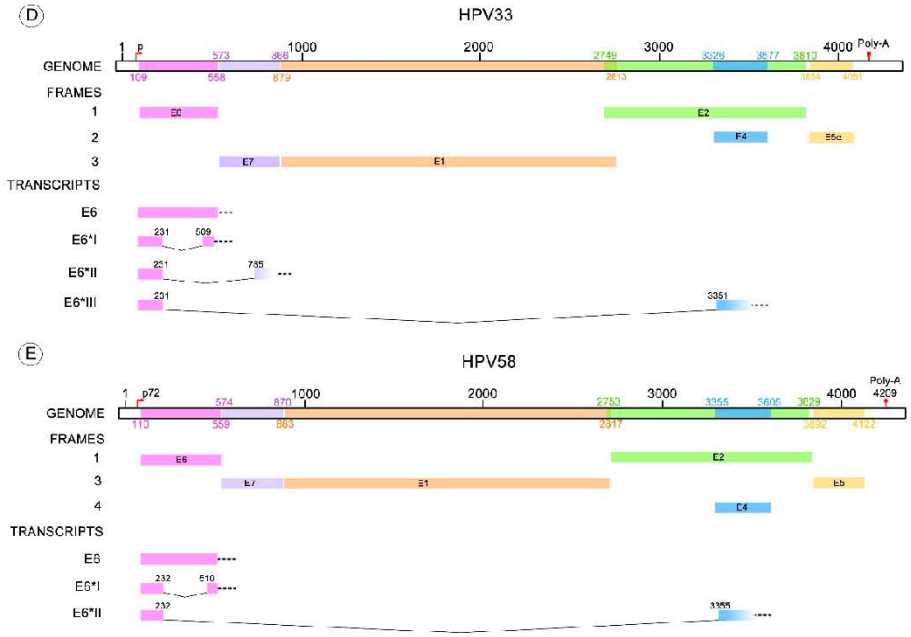

Figure 3. HR-HPV E6 alternative RNA splicing. The donor and acceptor splicing sites for the E6 truncated transcripts of different HPV types that possess more than one variant of E6* mRNA. (**A**) The E6* transcripts identified in HPV16 are E6*I to VI, E6^E7, E6^E7*I and E6^E7*II; (**B**) Four E6* transcripts have been described for HPV18 termed E6*I to III and E6^E7; (**C**) E6*I and E6^E4 transcripts are known for HPV31; (**D**) E6*I to III for HPV33; (**E**) E6*I and II transcripts for HPV58. All these transcript variants contain a donor splicing site within the E6 open reading frame (ORF), while the acceptor site is contained downstream in the unique E1 or E2 ORF(s). The nucleotide positions of early promoters (p) and early polyadenylation (Poly-A) sequences, as well as the positions of early genes, were obtained from Papillomavirus episteme [8]. The early promoter of HPV58 was obtained from Li Y. et al. 2013 [67]. All the donor and acceptor splicing sites are listed in Table 1.

E6/E7 splicing patterns have been recognized by different methods in a variety of HR-HPV containing cell lines and those studies consistently reveal the presence of higher amounts of E6*I mRNA compared to the E6 transcript [74–77]. In addition, the E6*II transcript is usually present in higher amounts than E6 but at lower levels than E6*I [75].

It has been demonstrated that E6*I is highly expressed in a model of HPV primary infection, where the replication cycle of HPV 18 is efficient [63], suggesting that the expression of E6*I could have an important role in the first stages of viral infection.

Moreover, studies in W12—cells derived from a low grade cervical lesion with episomal HPV16—showed that while E6 mRNA was not detected, E6*I and E6*III were expressed [59]. In further studies, different subclones were isolated from the W12 cell line, generating a W12-derived model of cervical tumor progression. Such clones contain different physical states of the HPV 16 genome (episomal or integrated), exhibiting different biological outcomes: differentiated non-tumorigenic, less differentiated non-tumorigenic, tumorigenic and invasive cells. Interestingly all of these cell lines express E6, E6*I and E6*II transcripts but the carcinogenic clones showed a significant increase in the expression of all E6 transcripts, in addition to the expression of the E6*X [70]. These findings suggest that the E6/E6* expression patterns could be independent of the physical state of the HPV genome but dependent on the lesion grade.

The E6/E6*I transcription patterns were evaluated in 12 oncogenic and 11 possibly-oncogenic HPVs, where E6/E6*I were found to be expressed in the majority of those HPV types, although with different patterns. In contrast to several studies, this report shows that E6*I transcript from HPV16 and 18 were present in lower amounts than E6 [21]. It was previously demonstrated that the distance

between the 5′ Cap site and the intron is rate limiting for E6 RNA splicing [78]. Therefore, changes in the proportion of E6/E6* observed in different studies could be partially explained by the 5′ added nucleotide sequences in the E6 expressing vectors, which increase the distance between the E6 intron and the 5′ Cap in the pre-mRNA.

E6 and E6-spliced mRNAs have been investigated in patient samples, aiming to find a correlation with different stages during transformation. Many studies show that premalignant or malignant cervical and oropharyngeal lesions positive for HPV16 genomes, exhibit higher amounts of E6*I than E6, similar to the results described in cell lines [77,79,80]. Other studies detected E6*I and E6*III transcripts in cervical cancer, as well as in low and high-grade lesions, where no E6 mRNA was identified, maybe due to the different sensitivities of the technical approaches used [81]. In HPV16 positive cervical cancer biopsies, the proportion of E6, E6*I, E6*II and E6ˆE7 transcripts varies but E6ˆE7 is consistently present at lower levels, while the expression of E6*I is the highest [60]. Furthermore, the levels of HPV16 E6, E6*I and E6*II mRNAs are higher in cervical cancer samples compared to those in oropharyngeal cancer [82], suggesting that cellular contexts could be involved in the expression of HPV sequences.

Through RNA-seq quantitative sequencing, the proportion of HPV transcripts in cervical samples has been determined. In Cervical Intraepithelial Neoplasia grade 3 (CIN3) and Squamous Cervical Cancer (SCC), low levels of E6 transcripts were found, representing less than 5% of all HPV transcripts in each sample; conversely, E6*I represented close to 5%, 40% and 50% of all HPV mRNAs in Cervical Intraepithelial Neoplasia grade 2 (CIN2), CIN3 and SCC samples, respectively [24].

Controversial results about the association between the expression of E6*I/E6*II and the grade of cervical lesions have been reported. A positive association between higher concentrations of E6*I and E6*II transcripts and high-grade cervical lesions, as well as cervical cancer, was found, being E6*I the most abundant of these mRNAs [82,83]. In contrast, another study did not reveal differences in E6*I levels in the different lesion grades but a significant decrease of E6*II was observed in high-grade lesions [84]. Moreover, some studies have proposed E6*II expression as an indicator of cervical neoplasia severity [85]. These results show that the association between E6*I/E6*II patterns and lesion grade cannot be confirmed at this moment.

E6* expression has also been studied in uncommon HPV-related cancers. In squamous cell scrotal cancer samples, HPV16 E6*I transcripts were found [86]. Additionally, in breast tumor samples infected with HPV16, E6*I, E6*II, E6ˆE7 (E6*X), E6ˆE7*I and E6ˆE7*II transcripts were detected [62]. These results suggest that HPV is transcriptionally active in those tumor samples.

It is worth mentioning that variations in 2 to 5% of genomic sequences within the same HPV type are defined as intra-type variants, which have been associated with distinct biological outcomes of HPV infections [87]. It has been reported that nucleotide changes within HPV18 E6 variant genes (Asian-Amerindian, European and African phylogenetic branches) result in different E6/E6*I splicing patterns in MCF-7 cells and cervical tumor biopsies. Interestingly, the cells and tumors harboring the Asian-Amerindian variant of E6 expressed higher levels of E6 than E6*I, while those with the African variant exhibited a higher proportion of E6*I [88,89]. Furthermore, European variants of HPV16 do not exhibit differences in E6/E6* splicing patterns [90].

In conclusion, even when E6/E6* patterns differ in pre-malignant lesions and cancer, E6*I is the transcript present in higher amounts. Moreover, it seems that all transcript levels increase as the lesions progress to cancer. This effect could be related to an increase in HPV transcription and/or replication rates, which might allow the detection of those spliced transcripts found at low levels. However, further studies are needed to confirm this statement.

6. Regulation of E6/E6* Patterns

Alternative splicing of HPV transcripts increases the complexity of viral gene expression. The E6/E6* patterns change through the cell cycle, being the E6*I transcript more abundant than E6 during G2/M phase [91]. Several regulators have been identified that control transcription, splicing

and polyadenylation of early and late mRNAs. However, few *cis* and *trans* acting regulators have been found to modulate E6/E6* splicing patterns (Figure 2B) [19,20,92,93].

The serine/arginine-rich splicing factor 1, 2 and 3 (SRSF1, 2 and 3) are augmented in HPV16 positive cervical cancer cell lines compared with HPV16 positive non-tumorigenic cells. These proteins increase E6/E7 mRNA stability and protect E6 transcript from decay. Interestingly, E6/E6* splicing is not affected by the SRSF overexpression [70].

Using a raft culture model, it has been shown that CCCTC-Binding Factor (CTCF) can bind to E2 ORF of HR-HPV types and induce an increase of E6*II mRNA without affecting other E6 spliced transcripts [94].

The ASF/SF2 splicing factor interacts with an HPV16 splicing enhancer located downstream of the SA3358 site, promoting splicing particularly at this acceptor site. SA3358 site allows the production of E6*III if the SD226 site is selected but can also produce other E6* mRNAs with the SD880, promoting an increase in all of the E6 spliced transcripts [95,96].

The SF3B1 splicing factor has also been reported to increase HPV16 E6 mRNA splicing, favoring the E6*I isoform [97]. Head and neck cancer cells positive for HPV16 were treated with meayamycin B, a potent inhibitor of SF3B1, showing a decrease in the levels of E6*I mRNA with an increase of the full-length E6 transcript. When SF3B1 was knocked down, similar effects were observed, demonstrating that the biogenesis of E6*I is influenced by SF3B.

The splicing at the SD226 site is favored when E6/E7 mRNAs are capped through the interaction with Cap binding factors. When the distance from 5′mRNA Cap to the SD226 is increased, the levels of E6 are higher, while a distance less than 307 nucleotides seems to be optimal to promote the splicing at SD226, facilitating E6*I expression [78].

Together, hnRNPA1 and hnRNPA2 promote splicing of E6 HPV16 mRNA. In contrast to hnRNPA1 only, that in the presence of Epidermal Growth Factor (EGF) induces an increase in un-spliced E6 mRNA [98]. This evidence could be associated to the exonic splicing silencer (ESS) within the E7 ORF, which contains an hnRNPA1 binding motif that reduces 233ˆ416 splicing (E6*I) and induces E6 expression in HPV18-transfected or -infected cells [64].

Upon activation of EGFR and Erk1/2 MAPK by EGF, E6/E7 splicing is reduced. Although the exact mechanism has not yet been described, it is proposed that this effect could be mediated through regulators controlled by growth factor pathways, such as Brm and Sam68, which increase the levels of E6/E7 mRNA in the presence of EGF [98].

Interestingly, HPV proteins also modulate E6/E7 mRNA splicing by acting as RNA binding proteins. E2 and E6 proteins bind to intron 226–409 and might interfere with the cellular splicing machinery, decreasing the levels of E6*I transcript in HPV16 infected cells. This reduction could be carried out by SR proteins through their interaction with E2 and E6 viral proteins [99]. Therefore, expression of E6, E6* and E7 can be affected by the different splicing regulatory proteins, depending on their availability during cellular differentiation or cancer progression.

7. E6* Related Functions

One of the most characterized E6* transcript functions is to facilitate translation of the E7 oncoprotein by increasing the space in the mRNA between the E6 stop codon and the E7 start codon, allowing better ribosome assembly [23,78,100]. However, other studies demonstrate that intron exclusion has a minimal or no effect on E7 translation, since the E7 protein is mainly translated from E6 non-spliced mRNA [22,101]. Moreover, other functions have been attributed to E6* proteins, mainly to E6*I, independent of E6 and E7 expression (Figure 4).

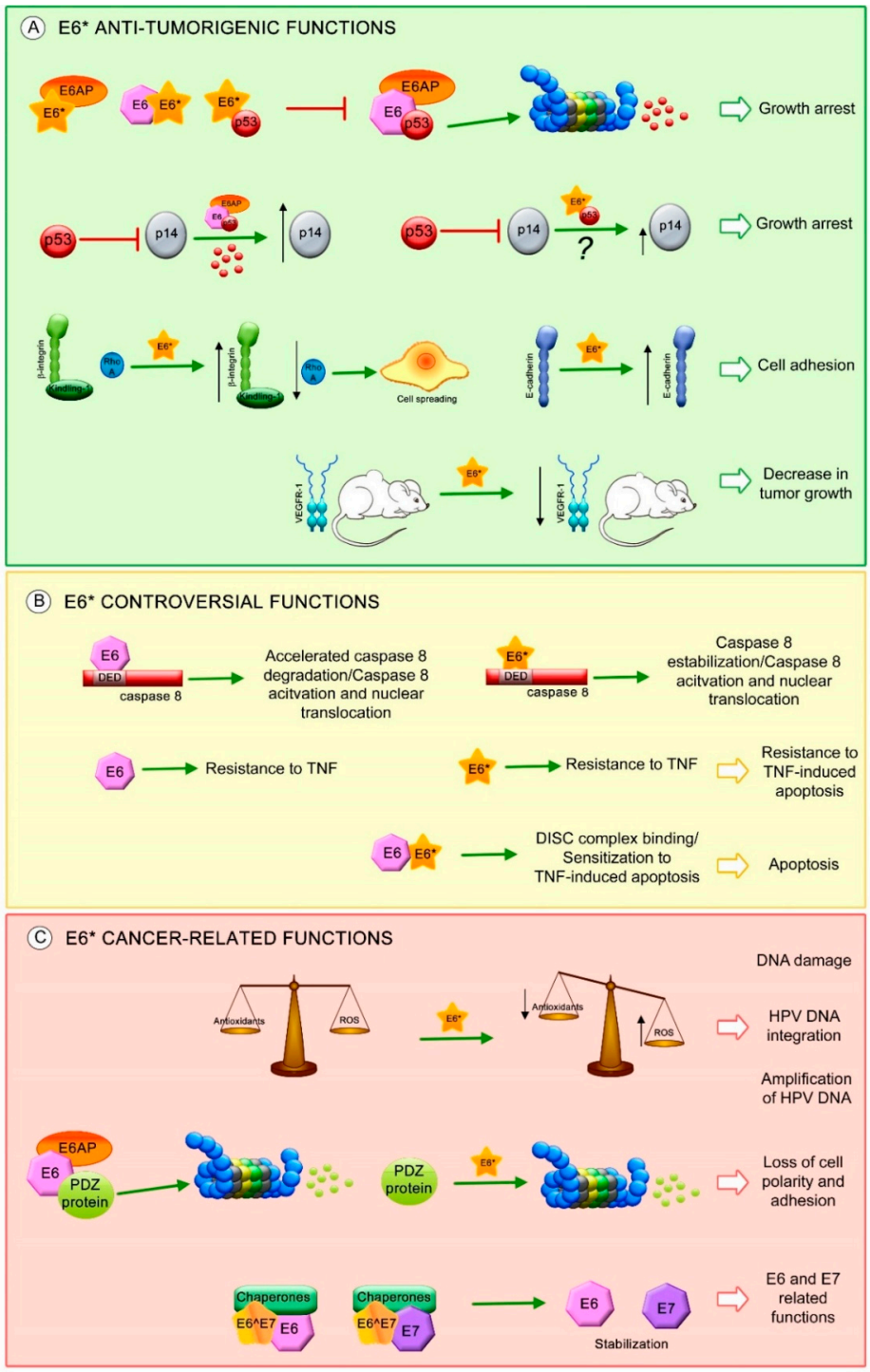

Figure 4. E6* isoform-related functions. Proposed E6* functions involved in (**A**) anti-tumorigenic effects, such as: increase in growth arrest through inhibition of E6-mediated p53 degradation and increase in p14 protein levels possibly through E6*/p53 interaction (?), increase in cell adhesion by the activation of β-integrin signaling and overexpression of E-cadherin, decrease in tumor growth associated with a reduction in VEGFR-1; (**B**) Controversial effects of E6* in apoptosis regulation; and (**C**) Carcinogenic characteristics, such as: promotion of DNA damage by ROS, which may allow HPV DNA amplification and integration into the host genome, degradation of postsynaptic density-95/discs large/zonula occludens-1 domain (PDZ) containing proteins involved in cell polarity and adhesion and stabilization of E6 and E7 oncoproteins. The red T-bars indicate inhibition, the green arrows show induction of the related process, the black arrows depict an increment or a reduction in protein levels.

E6*I protein was detected for the first time in 1987 in CaSki cells [102] and like E6*II, displays both nuclear and cytoplasmic localization; conversely, E6 is mostly found in the cell nucleus [91,103,104].

E6*I HPV18 is a polypeptide of 57 aa that shares the first 44 aa of its N-terminal domain with E6 and contains 13 aa derived from the change in the E6 open reading frame after the splicing sites [25]. Due to different donor and acceptor splicing sites contained in HR-HPVs, the predicted E6*I proteins differ from E6, in size, by approximately 50 to 55 aa for HPV16, 18, 30, 33, 34, 36, 35, 39, 68 and 70; and 29 to 36 aa for HPV26, 31, 51, 56, 66, 69 and 82 [21].

The specific structure of E6*I has not been well characterized due to the difficulty in acquiring a compact monomeric fold in such a small polypeptide. However, α-helix or β-sheet conformations, depending on experimental conditions, have been suggested [105]. E6*I conserves only half of the N-terminal zinc binding motif present in E6. Moreover, most of the HR-HPV E6*I, excepting HPV56 and 66, contain a hydrophobic motif (L/M/I)XX(L/I/V)X(L/V/I) which is associated to E6 and E6AP binding [106].

It has been widely demonstrated that the HR-HPV E6 proteins promote p53 degradation through binding with the E3 ubiquitin ligase E6AP [107,108]. Furthermore, E6*I protein interferes with E6-mediated degradation of p53 by its binding to E6AP, E6 and to p53, although with lower affinity [21,91,109,110].

Furthermore, it has been shown that HPV18 E6 increases the levels of p14ARF through p53 degradation, while HPV18 E6*I over-expression only induces a moderate increase of the p14ARF [88]. This result shows that E6*I may have a direct effect over p14ARF, independent of E6, possibly through E6*I and p53 interaction, preventing p14ARF regulation by p53. However, more evidence is still needed.

Additionally, it has been demonstrated that HPV16 E6*I does not increase keratinocyte immortalization and proliferation [100]. HPV18 E6*I decreases cell proliferation in HPV16 positive cancer cells, while HPV18 E6*I overexpression in p53 null cancer cells does not exhibit this anti-proliferative effect, indicating that this effect could be attributed to protection of p53 by E6*I [110].

Anti-tumorigenic features have been associated with E6*I expression. The β-integrin pathway that regulates cytoskeleton rearrangements, cellular shape and mobility was evaluated in SiHa cells. The levels of β-integrin and its co-stimulatory molecule kindling-1, increased in the presence of E6*I, while a reduction in RhoA levels was observed, promoting cell morphological changes related to cell spreading. Moreover, this study found a decrease in Alkaline phosphatase activity in those cells transfected with HPV16 E6*I, which is related to loss of both pluripotency and undifferentiated cell phenotype [111].

Furthermore, in a study performed in SiHa cells, HPV16 E6*I promoted the overexpression of E-cadherin protein, a biological marker related to cell adhesion and epithelial phenotype. However, in C33A cells, this effect was not observed. Interestingly, a xenograft mouse model using SiHa and C33A cells transfected with HPV16 E6*I, showed an evident decrease in tumor size with a decrease in VEGFR-1 levels, a biological marker for angiogenesis [112].

Since E6*I does not induce immortalization and cell proliferation, it has been postulated that it could be regulating pathways involved in cell death, such as apoptosis. Different studies showed that both E6 and E6*I of HPV16 and HPV18 bind to the dead effector domain (DED) of procaspase 8 via different sites [113–115]; however, only HPV16 E6 can bind to Fas-associated protein with death domain (FADD) DED [116]. One of the studies showed that HPV16 E6*I stabilizes procaspase 8 while E6 has the opposite effect [114]; however, a further study demonstrates that neither HPV18 E6 nor E6*I induces procaspase 8 stabilization. Nevertheless, these viral proteins increase the levels of active caspase 8 and induce its nuclear translocation without inducing apoptosis [113].

Additionally, it has been shown that HPV16 E6 and E6*I exert different effects in apoptosis either together or alone. Both viral proteins independently expressed, promote resistance to TNF-induced apoptosis; in contrast, when they are expressed together they promote TNF-dependent apoptosis [109]. Furthermore, it has been demonstrated that overexpression of HPV16 E6*I but not E6*II, sensitizes oropharyngeal squamous cell carcinoma cell lines to radiation, promoting cell death [117]. Recent

studies suggest that this effect could be dependent on cellular context, since it is not observed in non-head and neck cancer cell lines. Together, these facts indicate that the regulation of apoptosis by E6*I and E6 is a complicated mechanism and that the E6/E6* expression patterns and cellular contexts could play an important role.

A proteomic analysis comparing HPV16 positive and negative cell lines revealed that HPV16 E6*I modifies the expression of cellular proteins involved in a variety of cellular signaling pathways such as: integrin-linked kinase (ILK), oxidative phosphorylation and mitochondrial dysfunction. HPV16 E6*I promotes an increase in mitochondrial dysfunction in HPV positive and negative cells, which then induces a decrease in the levels of the antioxidant molecule GSH and subsequent DNA damage [111]. These data correlate with results observed in HPV16 positive cells, where HPV16 E6*I protein but not E6, decreases the levels of the antioxidant enzymes SOD2 and Gpx, leading to the accumulation of reactive oxygen species (ROS) and an increase in DNA damage [118]. Even when the DNA damage promoted by E6*I could eventually culminate in apoptosis, some data support the idea that the induction of DNA damage by ROS could be related to the amplification of HPV DNA, which would require different regulators of the homologous recombination DNA repair system [119] or to HPV genome integration [120], suggesting that E6*I could be participating in the HPV viral cycle, as well as in cancer establishment.

It is well known that E6 targets PDZ (postsynaptic density-95/discs large/zonula occludens-1 domain) containing proteins, inducing their degradation. Moreover, HPV18 E6*I protein, as well as E6, induces the degradation of PDZ containing proteins such as Dlg (Drosophila disc-large), MAGI-1 and h-Scrib. The ability to promote Dlg degradation is conserved among HPV31, 16 and 81 E6*I proteins; however, E6*I cannot bind to this protein. Currently, there is only one PDZ containing protein shown to interact with E6*I, allowing its degradation. This protein, termed PATJ can interact with E6*I in a PDZ binding motif (PBM)-independent manner or through other cell proteins that allow this interaction. In addition, this study demonstrated that HPV18 E6*I induces the degradation of Akt, in contrast to E6, which is not able to decrease Akt levels. This suggests that E6*I of HPV18 could be regulating processes involved in survival and cell growth [25,121].

Very little is known about the functions of other E6 spliced isoforms. HPV16 E6^E7 is a predominantly cytoplasmic protein that contains 41 aa of E6 in its N-terminal half and 38 aa of E7 in its C-terminal half. It has been shown that E6^E7 binds to the cellular chaperones HSP90α, HSP90β and Glucose-regulated protein 78 (GRP78) but only HSP90β and GRP78 induce E6^E7, E6 and E6*I stabilization. In addition, E6, E7 and E6*I proteins are stabilized by E6^E7, in a manner dependent on the endogenous chaperones [60].

8. Conclusions

The sustained higher proportion of E6*I compared to E6 mRNA observed in different lesions and tumors, suggests that the generation of E6* isoforms has an important role in cancer development.

Alternative splicing within the E6 ORF could be mediated by donor and acceptor splicing site sequences and surrounding fragments, which regulate the most efficient recruitment of the spliceosome elements. Discrepancies found in E6 splice patterns in diverse study models could be due to the presence of specific regulatory factors depending of the cell context or to differences in the physical state of the HPV genome during the progression of an HPV infection to cancer. The loss of E2 protein due to viral genome integration [122] could also affect the splicing process, since E2 is a mRNA binding protein which regulates E6 splicing [99]. Moreover, since HPV genome integration occurs at distinct sites in the host genome [75], it cannot be discarded that in some cases host genes involved in splicing regulation could be disrupted and therefore change the splicing patterns. Until now, little is known about the specific mechanisms regarding the modulation of E6 splicing patterns but all the evidence suggests that the presence of E6 spliced transcripts is a common event in cervical carcinogenesis.

It is worth mentioning that comparing the E6 splicing patterns among biological models analyzed with different methodological tools is a difficult task. The variations in results among different studies may be due to the choice of different techniques.

In studies using RT-PCR, the selection of primers commonly leads to the amplification of splice variants just within the E6/E7 ORFs, excluding some of the spliced transcripts involving the early HPV mRNA. In contrast, studies using deep sequencing techniques describe the splice forms extensively, allowing a robust analysis of the transcripts. Although this technology gives us a better approach to the diversity and quantity of E6 transcripts, more information is still needed to associate these transcripts with cancer progression. Moreover, it is difficult to achieve an adequate comparison between observations obtained through diverse methods that present different sensitivity. Nevertheless, the quality of the studies has increased over the time, permitting the detection of transcripts that are present in very low concentrations, such as E6^E7 (E6*X).

Some authors argue that while E6* transcripts can be abundant in some models, E6* proteins cannot be detected [59,101,123]. Nevertheless, other researchers have clearly identified E6* proteins, supporting that E6* transcripts can produce at least one E6* protein [91,109,114,118,124]. Anti-oncogenic effects have been attributed to E6* proteins [112], although other effects, such as promotion of DNA damage [118,120], degradation of PDZ containing proteins related to cellular polarity [25] and stabilization of E6 and E7 oncogenic proteins [60] are effects involved in cancer development, clearly demonstrated for E6* proteins . In addition, E6* proteins could have different effects depending on the cellular context where different E6* protein conformations could be generated [105], promoting distinct interactions with cellular binding partners.

The different splicing patterns for E6/E6* observed among tumors or during the different stages in cancer progression could provide a wide variety of E6 isoforms with an impact on biological processes. Nevertheless, oncogenic and/or non-oncogenic functions reported for E6* proteins, make it difficult to sort them out as tumor suppressor or oncoproteins in HPV-related tumors. Currently, the possibility that E6* proteins contribute to the HPV transformation process has gained attention and much data has been generated that has opened a window of opportunities in the study of these proteins regarding their participation in the HPV life cycle and/or in cancer establishment.

Acknowledgments: This manuscript was partially supported by Instituto Nacional de Cancerología, México Ref. (017/007/IBI) (CEI/1144/17). Leslie Olmedo-Nieva and J. Omar Muñoz-Bello are students from the following programs: "Doctorado en Ciencias Bioquímicas" and "Doctorado en Ciencias Biomédicas", respectively, at the Universidad Nacional Autónoma de México and are recipients of scholarships from CONACyT, México (289892 and 444223, respectively). We thank Elizabeth Langley for performing English editing.

Author Contributions: Leslie Olmedo-Nieva, J. Omar Muñoz-Bello, Adriana Contreras-Paredes and Marcela Lizano performed the bibliographic review and wrote the manuscript; Marcela Lizano directed the manuscript.

Conflicts of Interest: The authors declare no conflict of interest.

References

1. GLOBOCAN. 2012. Available online: http://globocan.iarc.fr (accessed on 21 December 2017).
2. Radley, D.; Saah, A.; Stanley, M. Persistent infection with human papillomavirus 16 or 18 is strongly linked with high-grade cervical disease. *Hum. Vaccines Immunother.* **2016**, *12*, 768–772. [CrossRef] [PubMed]
3. Walboomers, J.M.; Jacobs, M.V.; Manos, M.M.; Bosch, F.X.; Kummer, J.A.; Shah, K.V.; Snijders, P.J.; Peto, J.; Meijer, C.J.; Muñoz, N. Human papillomavirus is a necessary cause of invasive cervical cancer worldwide. *J. Pathol.* **1999**, *189*, 12–19. [CrossRef]
4. Clifford, G.M.; Smith, J.S.; Aguado, T.; Franceschi, S. Comparison of HPV type distribution in high-grade cervical lesions and cervical cancer: A meta-analysis. *Br. J. Cancer* **2003**, *89*, 101–105. [CrossRef] [PubMed]
5. Benevolo, M.; Donà, M.G.; Ravenda, P.S.; Chiocca, S. Anal human papillomavirus infection: Prevalence, diagnosis and treatment of related lesions. *Expert Rev. Anti-Infect. Ther.* **2016**, *14*, 465–477. [CrossRef] [PubMed]
6. Lee, L.J.; Howitt, B.; Catalano, P.; Tanaka, C.; Murphy, R.; Cimbak, N.; DeMaria, R.; Bu, P.; Crum, C.; Horowitz, N.; et al. Prognostic importance of human papillomavirus (HPV) and p16 positivity in squamous cell carcinoma of the vulva treated with radiotherapy. *Gynecol. Oncol.* **2016**, *142*, 293–298. [CrossRef] [PubMed]

7. Chaturvedi, A.K.; Engels, E.A.; Pfeiffer, R.M.; Hernandez, B.Y.; Xiao, W.; Kim, E.; Jiang, B.; Goodman, M.T.; Sibug-Saber, M.; Cozen, W.; et al. Human papillomavirus and rising oropharyngeal cancer incidence in the United States. *J. Clin. Oncol.* **2011**, *29*, 4294–4301. [CrossRef] [PubMed]
8. Papillomavirus Episteme. Available online: https://pave.niaid.nih.gov/ (accessed on 21 December 2017).
9. International Human Papillomavirus Reference Center. Available online: http://www.hpvcenter.se (accessed 12 on January 2018).
10. De Villiers, E.-M. Cross-roads in the classification of papillomaviruses. *Virology* **2013**, *445*, 2–10. [CrossRef] [PubMed]
11. Burd, E.M. Human papillomavirus and cervical cancer. *Clin. Microbiol. Rev.* **2003**, *16*, 1–17. [CrossRef] [PubMed]
12. Muñoz, N.; Bosch, F.X.; de Sanjosé, S.; Herrero, R.; Castellsagué, X.; Shah, K.V.; Snijders, P.J.F.; Meijer, C.J.L.M. Epidemiologic classification of human papillomavirus types associated with cervical cancer. *N. Engl. J. Med.* **2003**, *348*, 518–527. [CrossRef] [PubMed]
13. Clifford, G.M.; Rana, R.K.; Franceschi, S.; Smith, J.S.; Gough, G.; Pimenta, J.M. Human papillomavirus genotype distribution in low-grade cervical lesions: Comparison by geographic region and with cervical cancer. *Cancer Epidemiol. Biomark. Prev.* **2005**, *14*, 1157–1164. [CrossRef] [PubMed]
14. Thierry, F.; Heard, J.M.; Dartmann, K.; Yaniv, M. Characterization of a transcriptional promoter of human papillomavirus 18 and modulation of its expression by simian virus 40 and adenovirus early antigens. *J. Virol.* **1987**, *61*, 134–142. [PubMed]
15. Egawa, N.; Egawa, K.; Griffin, H.; Doorbar, J. Human Papillomaviruses; Epithelial Tropisms, and the Development of Neoplasia. *Viruses* **2015**, *7*, 3863–3890. [CrossRef] [PubMed]
16. Vande Pol, S.B.; Klingelhutz, A.J. Papillomavirus E6 oncoproteins. *Virology* **2013**, *445*, 115–137. [CrossRef] [PubMed]
17. Roman, A.; Munger, K. The papillomavirus E7 proteins. *Virology* **2013**, *445*, 138–168. [CrossRef] [PubMed]
18. Zheng, Z.-M.; Baker, C.C. Papillomavirus genome structure, expression, and post-transcriptional regulation. *Front. Biosci.* **2006**, *11*, 2286–2302. [CrossRef] [PubMed]
19. Graham, S.V. Keratinocyte Differentiation-Dependent Human Papillomavirus Gene Regulation. *Viruses* **2017**, *9*, 245. [CrossRef] [PubMed]
20. Graham, S.V.; Faizo, A.A.A. Control of human papillomavirus gene expression by alternative splicing. *Virus Res.* **2017**, *231*, 83–95. [CrossRef] [PubMed]
21. Mesplède, T.; Gagnon, D.; Bergeron-Labrecque, F.; Azar, I.; Sénéchal, H.; Coutlée, F.; Archambault, J. p53 degradation activity, expression, and subcellular localization of E6 proteins from 29 human papillomavirus genotypes. *J. Virol.* **2012**, *86*, 94–107. [CrossRef] [PubMed]
22. Del Moral-Hernández, O.; López-Urrutia, E.; Bonilla-Moreno, R.; Martínez-Salazar, M.; Arechaga-Ocampo, E.; Berumen, J.; Villegas-Sepúlveda, N. The HPV-16 E7 oncoprotein is expressed mainly from the unspliced E6/E7 transcript in cervical carcinoma C33-A cells. *Arch. Virol.* **2010**, *155*, 1959–1970. [CrossRef] [PubMed]
23. Tang, S.; Tao, M.; McCoy, J.P.; Zheng, Z.-M. The E7 oncoprotein is translated from spliced E6*I transcripts in high-risk human papillomavirus type 16- or type 18-positive cervical cancer cell lines via translation reinitiation. *J. Virol.* **2006**, *80*, 4249–4263. [CrossRef] [PubMed]
24. Chen, J.; Xue, Y.; Poidinger, M.; Lim, T.; Chew, S.H.; Pang, C.L.; Abastado, J.-P.; Thierry, F. Mapping of HPV transcripts in four human cervical lesions using RNAseq suggests quantitative rearrangements during carcinogenic progression. *Virology* **2014**, *462–463*, 14–24. [CrossRef] [PubMed]
25. Pim, D.; Tomaic, V.; Banks, L. The human papillomavirus (HPV) E6* proteins from high-risk, mucosal HPVs can direct degradation of cellular proteins in the absence of full-length E6 protein. *J. Virol.* **2009**, *83*, 9863–9874. [CrossRef] [PubMed]
26. Pinidis, P.; Tsikouras, P.; Iatrakis, G.; Zervoudis, S.; Koukouli, Z.; Bothou, A.; Galazios, G.; Vladareanu, S. Human Papilloma Virus' Life Cycle and Carcinogenesis. *Maedica* **2016**, *11*, 48–54. [PubMed]
27. Doorbar, J.; Quint, W.; Banks, L.; Bravo, I.G.; Stoler, M.; Broker, T.R.; Stanley, M.A. The biology and life-cycle of human papillomaviruses. *Vaccine* **2012**, *30*, F55–F70. [CrossRef] [PubMed]
28. Shafti-Keramat, S.; Handisurya, A.; Kriehuber, E.; Meneguzzi, G.; Slupetzky, K.; Kirnbauer, R. Different heparan sulfate proteoglycans serve as cellular receptors for human papillomaviruses. *J. Virol.* **2003**, *77*, 13125–13135. [CrossRef] [PubMed]

29. Cerqueira, C.; Samperio Ventayol, P.; Vogeley, C.; Schelhaas, M. Kallikrein-8 Proteolytically Processes Human Papillomaviruses in the Extracellular Space to Facilitate Entry into Host Cells. *J. Virol.* **2015**, *89*, 7038–7052. [CrossRef] [PubMed]
30. Day, P.M.; Lowy, D.R.; Schiller, J.T. Heparan sulfate-independent cell binding and infection with furin-precleaved papillomavirus capsids. *J. Virol.* **2008**, *82*, 12565–12568. [CrossRef] [PubMed]
31. Patterson, N.A.; Smith, J.L.; Ozbun, M.A. Human papillomavirus type 31b infection of human keratinocytes does not require heparan sulfate. *J. Virol.* **2005**, *79*, 6838–6847. [CrossRef] [PubMed]
32. Cruz, L.; Meyers, C. Differential dependence on host cell glycosaminoglycans for infection of epithelial cells by high-risk HPV types. *PLoS ONE* **2013**, *8*, e68379. [CrossRef] [PubMed]
33. Cruz, L.; Biryukov, J.; Conway, M.J.; Meyers, C. Cleavage of the HPV16 Minor Capsid Protein L2 during Virion Morphogenesis Ablates the Requirement for Cellular Furin during De Novo Infection. *Viruses* **2015**, *7*, 5813–5830. [CrossRef] [PubMed]
34. Evander, M.; Frazer, I.H.; Payne, E.; Qi, Y.M.; Hengst, K.; McMillan, N.A. Identification of the alpha6 integrin as a candidate receptor for papillomaviruses. *J. Virol.* **1997**, *71*, 2449–2456. [PubMed]
35. Surviladze, Z.; Dziduszko, A.; Ozbun, M.A. Essential roles for soluble virion-associated heparan sulfonated proteoglycans and growth factors in human papillomavirus infections. *PLoS Pathog.* **2012**, *8*, e1002519. [CrossRef] [PubMed]
36. Spoden, G.; Freitag, K.; Husmann, M.; Boller, K.; Sapp, M.; Lambert, C.; Florin, L. Clathrin- and caveolin-independent entry of human papillomavirus type 16—Involvement of tetraspanin-enriched microdomains (TEMs). *PLoS ONE* **2008**, *3*, e3313. [CrossRef] [PubMed]
37. Woodham, A.W.; Da Silva, D.M.; Skeate, J.G.; Raff, A.B.; Ambroso, M.R.; Brand, H.E.; Isas, J.M.; Langen, R.; Kast, W.M. The S100A10 subunit of the annexin A2 heterotetramer facilitates L2-mediated human papillomavirus infection. *PLoS ONE* **2012**, *7*, e43519. [CrossRef] [PubMed]
38. Schelhaas, M.; Shah, B.; Holzer, M.; Blattmann, P.; Kühling, L.; Day, P.M.; Schiller, J.T.; Helenius, A. Entry of human papillomavirus type 16 by actin-dependent, clathrin- and lipid raft-independent endocytosis. *PLoS Pathog.* **2012**, *8*, e1002657. [CrossRef] [PubMed]
39. Bergant, M.; Banks, L. SNX17 facilitates infection with diverse papillomavirus types. *J. Virol.* **2013**, *87*, 1270–1273. [CrossRef] [PubMed]
40. Schneider, M.A.; Spoden, G.A.; Florin, L.; Lambert, C. Identification of the dynein light chains required for human papillomavirus infection. *Cell. Microbiol.* **2011**, *13*, 32–46. [CrossRef] [PubMed]
41. Moody, C. Mechanisms by which HPV Induces a Replication Competent Environment in Differentiating Keratinocytes. *Viruses* **2017**, *9*, 261. [CrossRef] [PubMed]
42. Coupe, V.M.; González-Barreiro, L.; Gutiérrez-Berzal, J.; Melián-Bóveda, A.L.; López-Rodríguez, O.; Alba-Domínguez, J.; Alba-Losada, J. Transcriptional analysis of human papillomavirus type 16 in histological sections of cervical dysplasia by in situ hybridisation. *J. Clin. Pathol.* **2012**, *65*, 164–170. [CrossRef] [PubMed]
43. McBride, A.A. The papillomavirus E2 proteins. *Virology* **2013**, *445*, 57–79. [CrossRef] [PubMed]
44. Egawa, N.; Wang, Q.; Griffin, H.M.; Murakami, I.; Jackson, D.; Mahmood, R.; Doorbar, J. HPV16 and 18 genome amplification show different E4-dependence, with 16E4 enhancing E1 nuclear accumulation and replicative efficiency via its cell cycle arrest and kinase activation functions. *PLoS Pathog.* **2017**, *13*, e1006282. [CrossRef] [PubMed]
45. Ho, G.Y.F.; Einstein, M.H.; Romney, S.L.; Kadish, A.S.; Abadi, M.; Mikhail, M.; Basu, J.; Thysen, B.; Reimers, L.; Palan, P.R.; et al. Albert Einstein Cervix Dysplasia Clinical Consortium Risk factors for persistent cervical intraepithelial neoplasia grades 1 and 2: Managed by watchful waiting. *J. Low. Genit. Tract Dis.* **2011**, *15*, 268–275. [CrossRef] [PubMed]
46. Groves, I.J.; Coleman, N. Pathogenesis of human papillomavirus-associated mucosal disease. *J. Pathol.* **2015**, *235*, 527–538. [CrossRef] [PubMed]
47. Goodwin, E.C.; DiMaio, D. Repression of human papillomavirus oncogenes in HeLa cervical carcinoma cells causes the orderly reactivation of dormant tumor suppressor pathways. *Proc. Natl. Acad. Sci. USA* **2000**, *97*, 12513–12518. [CrossRef] [PubMed]
48. Vinokurova, S.; Wentzensen, N.; Kraus, I.; Klaes, R.; Driesch, C.; Melsheimer, P.; Kisseljov, F.; Durst, M.; Schneider, A.; von Knebel Doeberitz, M. Type-Dependent Integration Frequency of Human Papillomavirus Genomes in Cervical Lesions. *Cancer Res.* **2008**, *68*, 307–313. [CrossRef] [PubMed]

49. Chaiwongkot, A.; Vinokurova, S.; Pientong, C.; Ekalaksananan, T.; Kongyingyoes, B.; Kleebkaow, P.; Chumworathayi, B.; Patarapadungkit, N.; Reuschenbach, M.; von Knebel Doeberitz, M. Differential methylation of E2 binding sites in episomal and integrated HPV 16 genomes in preinvasive and invasive cervical lesions. *Int. J. Cancer* **2013**, *132*, 2087–2094. [CrossRef] [PubMed]
50. Wang, Z.; Burge, C.B. Splicing regulation: From a parts list of regulatory elements to an integrated splicing code. *RNA* **2008**, *14*, 802–813. [CrossRef] [PubMed]
51. Black, D.L. Mechanisms of alternative pre-messenger RNA splicing. *Annu. Rev. Biochem.* **2003**, *72*, 291–336. [CrossRef] [PubMed]
52. Baralle, M.; Baralle, F.E. The splicing code. *Biosystems* **2017**. [CrossRef] [PubMed]
53. Jurica, M.S.; Moore, M.J. Pre-mRNA splicing: Awash in a sea of proteins. *Mol. Cell* **2003**, *12*, 5–14. [CrossRef]
54. Will, C.L.; Lührmann, R. Spliceosome structure and function. *Cold Spring Harb. Perspect. Biol.* **2011**, *3*, a003707. [CrossRef] [PubMed]
55. Wahl, M.C.; Will, C.L.; Lührmann, R. The spliceosome: Design principles of a dynamic RNP machine. *Cell* **2009**, *136*, 701–718. [CrossRef] [PubMed]
56. Busch, A.; Hertel, K.J. Evolution of SR protein and hnRNP splicing regulatory factors. *Wiley Interdiscip. Rev. RNA* **2012**, *3*, 1–12. [CrossRef] [PubMed]
57. De Conti, L.; Baralle, M.; Buratti, E. Exon and intron definition in pre-mRNA splicing. *Wiley Interdiscip. Rev. RNA* **2013**, *4*, 49–60. [CrossRef] [PubMed]
58. Ajiro, M.; Zheng, Z.-M. Oncogenes and RNA splicing of human tumor viruses. *Emerg. Microbes Infect.* **2014**, *3*, e63. [CrossRef] [PubMed]
59. Doorbar, J.; Parton, A.; Hartley, K.; Banks, L.; Crook, T.; Stanley, M.; Crawford, L. Detection of novel splicing patterns in a HPV16-containing keratinocyte cell line. *Virology* **1990**, *178*, 254–262. [CrossRef]
60. Ajiro, M.; Zheng, Z.-M. E6^E7, a novel splice isoform protein of human papillomavirus 16, stabilizes viral E6 and E7 oncoproteins via HSP90 and GRP78. *mBio* **2015**, *6*, e02068-14. [CrossRef] [PubMed]
61. Ajiro, M.; Jia, R.; Zhang, L.; Liu, X.; Zheng, Z.-M. Intron definition and a branch site adenosine at nt 385 control RNA splicing of HPV16 E6*I and E7 expression. *PLoS ONE* **2012**, *7*, e46412. [CrossRef] [PubMed]
62. Islam, S.; Dasgupta, H.; Roychowdhury, A.; Bhattacharya, R.; Mukherjee, N.; Roy, A.; Mandal, G.K.; Alam, N.; Biswas, J.; Mandal, S.; et al. Study of association and molecular analysis of human papillomavirus in breast cancer of Indian patients: Clinical and prognostic implication. *PLoS ONE* **2017**, *12*, e0172760. [CrossRef] [PubMed]
63. Toots, M.; Männik, A.; Kivi, G.; Ustav, M.; Ustav, E.; Ustav, M. The transcription map of human papillomavirus type 18 during genome replication in U2OS cells. *PLoS ONE* **2014**, *9*, e116151. [CrossRef] [PubMed]
64. Ajiro, M.; Tang, S.; Doorbar, J.; Zheng, Z.-M. Serine/Arginine-Rich Splicing Factor 3 and Heterogeneous Nuclear Ribonucleoprotein A1 Regulate Alternative RNA Splicing and Gene Expression of Human Papillomavirus 18 through Two Functionally Distinguishable cis Elements. *J. Virol.* **2016**, *90*, 9138–9152. [CrossRef] [PubMed]
65. Ozbun, M.A. Human papillomavirus type 31b infection of human keratinocytes and the onset of early transcription. *J. Virol.* **2002**, *76*, 11291–11300. [CrossRef] [PubMed]
66. Snijders, P.J.; van den Brule, A.J.; Schrijnemakers, H.F.; Raaphorst, P.M.; Meijer, C.J.; Walboomers, J.M. Human papillomavirus type 33 in a tonsillar carcinoma generates its putative E7 mRNA via two E6* transcript species which are terminated at different early region poly(A) sites. *J. Virol.* **1992**, *66*, 3172–3178. [PubMed]
67. Li, Y.; Wang, X.; Ni, T.; Wang, F.; Lu, W.; Zhu, J.; Xie, X.; Zheng, Z.-M. Human papillomavirus type 58 genome variations and RNA expression in cervical lesions. *J. Virol.* **2013**, *87*, 9313–9322. [CrossRef] [PubMed]
68. Hummel, M.; Hudson, J.B.; Laimins, L.A. Differentiation-induced and constitutive transcription of human papillomavirus type 31b in cell lines containing viral episomes. *J. Virol.* **1992**, *66*, 6070–6080. [PubMed]
69. Halec, G.; Schmitt, M.; Dondog, B.; Sharkhuu, E.; Wentzensen, N.; Gheit, T.; Tommasino, M.; Kommoss, F.; Bosch, F.X.; Franceschi, S.; et al. Biological activity of probable/possible high-risk human papillomavirus types in cervical cancer. *Int. J. Cancer* **2013**, *132*, 63–71. [CrossRef] [PubMed]
70. McFarlane, M.; MacDonald, A.I.; Stevenson, A.; Graham, S.V. Human Papillomavirus 16 Oncoprotein Expression Is Controlled by the Cellular Splicing Factor SRSF2 (SC35). *J. Virol.* **2015**, *89*, 5276–5287. [CrossRef] [PubMed]
71. Schmitt, M.; Dalstein, V.; Waterboer, T.; Clavel, C.; Gissmann, L.; Pawlita, M. Diagnosing cervical cancer and high-grade precursors by HPV16 transcription patterns. *Cancer Res.* **2010**, *70*, 249–256. [CrossRef] [PubMed]

72. De la Rosa-Rios, M.A.; Martínez-Salazar, M.; Martínez-Garcia, M.; González-Bonilla, C.; Villegas-Sepúlveda, N. The intron 1 of HPV 16 has a suboptimal branch point at a guanosine. *Virus Res.* **2006**, *118*, 46–54. [CrossRef] [PubMed]
73. Smotkin, D.; Wettstein, F.O. Transcription of human papillomavirus type 16 early genes in a cervical cancer and a cancer-derived cell line and identification of the E7 protein. *Proc. Natl. Acad. Sci. USA* **1986**, *83*, 4680–4684. [CrossRef] [PubMed]
74. Schneider-Gädicke, A.; Schwarz, E. Different human cervical carcinoma cell lines show similar transcription patterns of human papillomavirus type 18 early genes. *EMBO J.* **1986**, *5*, 2285–2292. [PubMed]
75. Walline, H.M.; Goudsmit, C.M.; McHugh, J.B.; Tang, A.L.; Owen, J.H.; Teh, B.T.; McKean, E.; Glover, T.W.; Graham, M.P.; Prince, M.E.; et al. University of Michigan Head and Neck Specialized Program of Research Excellence (SPORE) Program Integration of high-risk human papillomavirus into cellular cancer-related genes in head and neck cancer cell lines. *Head Neck* **2017**, *39*, 840–852. [CrossRef] [PubMed]
76. Baker, C.C.; Phelps, W.C.; Lindgren, V.; Braun, M.J.; Gonda, M.A.; Howley, P.M. Structural and transcriptional analysis of human papillomavirus type 16 sequences in cervical carcinoma cell lines. *J. Virol.* **1987**, *61*, 962–971. [PubMed]
77. Smotkin, D.; Prokoph, H.; Wettstein, F.O. Oncogenic and nononcogenic human genital papillomaviruses generate the E7 mRNA by different mechanisms. *J. Virol.* **1989**, *63*, 1441–1447. [PubMed]
78. Zheng, Z.-M.; Tao, M.; Yamanegi, K.; Bodaghi, S.; Xiao, W. Splicing of a cap-proximal human Papillomavirus 16 E6E7 intron promotes E7 expression, but can be restrained by distance of the intron from its RNA 5′ cap. *J. Mol. Biol.* **2004**, *337*, 1091–1108. [CrossRef] [PubMed]
79. Cornelissen, M.T.; Smits, H.L.; Briët, M.A.; van den Tweel, J.G.; Struyk, A.P.; van der Noordaa, J.; ter Schegget, J. Uniformity of the splicing pattern of the E6/E7 transcripts in human papillomavirus type 16-transformed human fibroblasts, human cervical premalignant lesions and carcinomas. *J. Gen. Virol.* **1990**, *71*, 1243–1246. [CrossRef] [PubMed]
80. Walline, H.M.; Komarck, C.M.; McHugh, J.B.; Bellile, E.L.; Brenner, J.C.; Prince, M.E.; McKean, E.L.; Chepeha, D.B.; Wolf, G.T.; Worden, F.P.; et al. Genomic Integration of High-Risk HPV Alters Gene Expression in Oropharyngeal Squamous Cell Carcinoma. *Mol. Cancer Res.* **2016**, *14*, 941–952. [CrossRef] [PubMed]
81. Lin, K.; Lu, X.; Chen, J.; Zou, R.; Zhang, L.; Xue, X. E6-associated transcription patterns in human papilloma virus 16-positive cervical tissues. *Oncol. Lett.* **2015**, *9*, 478–482. [CrossRef] [PubMed]
82. Cerasuolo, A.; Annunziata, C.; Tortora, M.; Starita, N.; Stellato, G.; Greggi, S.; Maglione, M.G.; Ionna, F.; Losito, S.; Botti, G.; et al. Comparative analysis of HPV16 gene expression profiles in cervical and in oropharyngeal squamous cell carcinoma. *Oncotarget* **2017**, *8*, 34070–34081. [CrossRef] [PubMed]
83. Cricca, M.; Venturoli, S.; Leo, E.; Costa, S.; Musiani, M.; Zerbini, M. Molecular analysis of HPV 16 E6I/E6II spliced mRNAs and correlation with the viral physical state and the grade of the cervical lesion. *J. Med. Virol.* **2009**, *81*, 1276–1282. [CrossRef] [PubMed]
84. McNicol, P.; Guijon, F.; Wayne, S.; Hidajat, R.; Paraskevas, M. Expression of human papillomavirus type 16 E6-E7 open reading frame varies quantitatively in biopsy tissue from different grades of cervical intraepithelial neoplasia. *J. Clin. Microbiol.* **1995**, *33*, 1169–1173. [PubMed]
85. Pastuszak-Lewandoska, D.; Bartosińska-Dyc, A.; Migdalska-Sęk, M.; Czarnecka, K.H.; Nawrot, E.; Domańska, D.; Szyłło, K.; Brzeziańska, E. HPV16 E6*II gene expression in intraepithelial cervical lesions as an indicator of neoplastic grade: A pilot study. *Med. Oncol.* **2014**, *31*, 842. [CrossRef] [PubMed]
86. Guimerà, N.; Alemany, L.; Halec, G.; Pawlita, M.; Wain, G.V.; Vailén, J.S.S.; Azike, J.E.; Jenkins, D.; de Sanjosé, S.; Quint, W.; et al. Human papillomavirus 16 is an aetiological factor of scrotal cancer. *Br. J. Cancer* **2017**, *116*, 1218–1222. [CrossRef] [PubMed]
87. Lizano, M.; Berumen, J.; García-Carrancá, A. HPV-related carcinogenesis: Basic concepts, viral types and variants. *Arch. Med. Res.* **2009**, *40*, 428–434. [CrossRef] [PubMed]
88. Vazquez-Vega, S.; Sanchez-Suarez, L.P.; Andrade-Cruz, R.; Castellanos-Juarez, E.; Contreras-Paredes, A.; Lizano-Soberon, M.; Garcia-Carranca, A.; Benitez Bribiesca, L. Regulation of p14ARF expression by HPV-18 E6 variants. *J. Med. Virol.* **2013**, *85*, 1215–1221. [CrossRef] [PubMed]
89. De la Cruz-Hernández, E.; García-Carrancá, A.; Mohar-Betancourt, A.; Dueñas-González, A.; Contreras-Paredes, A.; Pérez-Cardenas, E.; Herrera-Goepfert, R.; Lizano-Soberón, M. Differential splicing of E6 within human papillomavirus type 18 variants and functional consequences. *J. Gen. Virol.* **2005**, *86*, 2459–2468. [CrossRef] [PubMed]

90. Zehbe, I.; Lichtig, H.; Westerback, A.; Lambert, P.F.; Tommasino, M.; Sherman, L. Rare human papillomavirus 16 E6 variants reveal significant oncogenic potential. *Mol. Cancer* **2011**, *10*, 77. [CrossRef] [PubMed]
91. Guccione, E.; Pim, D.; Banks, L. HPV-18 E6*I modulates HPV-18 full-length E6 functions in a cell cycle dependent manner. *Int. J. Cancer* **2004**, *110*, 928–933. [CrossRef] [PubMed]
92. Johansson, C.; Schwartz, S. Regulation of human papillomavirus gene expression by splicing and polyadenylation. *Nat. Rev. Microbiol.* **2013**, *11*, 239–251. [CrossRef] [PubMed]
93. Kajitani, N.; Schwartz, S. RNA Binding Proteins that Control Human Papillomavirus Gene Expression. *Biomolecules* **2015**, *5*, 758–774. [CrossRef] [PubMed]
94. Paris, C.; Pentland, I.; Groves, I.; Roberts, D.C.; Powis, S.J.; Coleman, N.; Roberts, S.; Parish, J.L. CCCTC-binding factor recruitment to the early region of the human papillomavirus 18 genome regulates viral oncogene expression. *J. Virol.* **2015**, *89*, 4770–4785. [CrossRef] [PubMed]
95. Somberg, M.; Schwartz, S. Multiple ASF/SF2 sites in the human papillomavirus type 16 (HPV-16) E4-coding region promote splicing to the most commonly used 3′-splice site on the HPV-16 genome. *J. Virol.* **2010**, *84*, 8219–8230. [CrossRef] [PubMed]
96. Li, X.; Johansson, C.; Cardoso Palacios, C.; Mossberg, A.; Dhanjal, S.; Bergvall, M.; Schwartz, S. Eight nucleotide substitutions inhibit splicing to HPV-16 3′-splice site SA3358 and reduce the efficiency by which HPV-16 increases the life span of primary human keratinocytes. *PLoS ONE* **2013**, *8*, e72776. [CrossRef] [PubMed]
97. Gao, Y.; Trivedi, S.; Ferris, R.L.; Koide, K. Regulation of HPV16 E6 and MCL1 by SF3B1 inhibitor in head and neck cancer cells. *Sci. Rep.* **2014**, *4*, 6098. [CrossRef] [PubMed]
98. Rosenberger, S.; de-Castro Arce, J.; Langbein, L.; Steenbergen, R.D.M.; Rösl, F. Alternative splicing of human papillomavirus type-16 E6/E6* early mRNA is coupled to EGF signaling via Erk1/2 activation. *Proc. Natl. Acad. Sci. USA* **2010**, *107*, 7006–7011. [CrossRef] [PubMed]
99. Bodaghi, S.; Jia, R.; Zheng, Z.-M. Human papillomavirus type 16 E2 and E6 are RNA-binding proteins and inhibit in vitro splicing of pre-mRNAs with suboptimal splice sites. *Virology* **2009**, *386*, 32–43. [CrossRef] [PubMed]
100. Sedman, S.A.; Barbosa, M.S.; Vass, W.C.; Hubbert, N.L.; Haas, J.A.; Lowy, D.R.; Schiller, J.T. The full-length E6 protein of human papillomavirus type 16 has transforming and trans-activating activities and cooperates with E7 to immortalize keratinocytes in culture. *J. Virol.* **1991**, *65*, 4860–4866. [PubMed]
101. Stacey, S.N.; Jordan, D.; Williamson, A.J.; Brown, M.; Coote, J.H.; Arrand, J.R. Leaky scanning is the predominant mechanism for translation of human papillomavirus type 16 E7 oncoprotein from E6/E7 bicistronic mRNA. *J. Virol.* **2000**, *74*, 7284–7297. [CrossRef] [PubMed]
102. Seedorf, K.; Oltersdorf, T.; Krämmer, G.; Röwekamp, W. Identification of early proteins of the human papilloma viruses type 16 (HPV 16) and type 18 (HPV 18) in cervical carcinoma cells. *EMBO J.* **1987**, *6*, 139–144. [PubMed]
103. Vaeteewoottacharn, K.; Chamutpong, S.; Ponglikitmongkol, M.; Angeletti, P.C. Differential localization of HPV16 E6 splice products with E6-associated protein. *Virol. J.* **2005**, *2*, 50. [CrossRef] [PubMed]
104. Tao, M.; Kruhlak, M.; Xia, S.; Androphy, E.; Zheng, Z.-M. Signals that dictate nuclear localization of human papillomavirus type 16 oncoprotein E6 in living cells. *J. Virol.* **2003**, *77*, 13232–13247. [CrossRef] [PubMed]
105. Heer, A.; Alonso, L.G.; de Prat-Gay, G. E6*, the 50 amino acid product of the most abundant spliced transcript of the e6 oncoprotein in high-risk human papillomavirus, is a promiscuous folder and binder. *Biochemistry* **2011**, *50*, 1376–1383. [CrossRef] [PubMed]
106. Pim, D.; Banks, L. HPV-18 E6*I protein modulates the E6-directed degradation of p53 by binding to full-length HPV-18 E6. *Oncogene* **1999**, *18*, 7403–7408. [CrossRef] [PubMed]
107. Scheffner, M.; Werness, B.A.; Huibregtse, J.M.; Levine, A.J.; Howley, P.M. The E6 oncoprotein encoded by human papillomavirus types 16 and 18 promotes the degradation of p53. *Cell* **1990**, *63*, 1129–1136. [CrossRef]
108. Talis, A.L.; Huibregtse, J.M.; Howley, P.M. The role of E6AP in the regulation of p53 protein levels in human papillomavirus (HPV)-positive and HPV-negative cells. *J. Biol. Chem.* **1998**, *273*, 6439–6445. [CrossRef] [PubMed]
109. Filippova, M.; Filippov, V.A.; Kagoda, M.; Garnett, T.; Fodor, N.; Duerksen-Hughes, P.J. Complexes of human papillomavirus type 16 E6 proteins form pseudo-death-inducing signaling complex structures during tumor necrosis factor-mediated apoptosis. *J. Virol.* **2009**, *83*, 210–227. [CrossRef] [PubMed]

110. Pim, D.; Massimi, P.; Banks, L. Alternatively spliced HPV-18 E6* protein inhibits E6 mediated degradation of p53 and suppresses transformed cell growth. *Oncogene* **1997**, *15*, 257–264. [CrossRef] [PubMed]
111. Evans, W.; Filippova, M.; Filippov, V.; Bashkirova, S.; Zhang, G.; Reeves, M.E.; Duerksen-Hughes, P. Overexpression of HPV16 E6* Alters β-Integrin and Mitochondrial Dysfunction Pathways in Cervical Cancer Cells. *Cancer Genom. Proteom.* **2016**, *13*, 259–273.
112. Filippova, M.; Evans, W.; Aragon, R.; Filippov, V.; Williams, V.M.; Hong, L.; Reeves, M.E.; Duerksen-Hughes, P. The small splice variant of HPV16 E6, E6, reduces tumor formation in cervical carcinoma xenografts. *Virology* **2014**, *450–451*, 153–164. [CrossRef] [PubMed]
113. Manzo-Merino, J.; Massimi, P.; Lizano, M.; Banks, L. The human papillomavirus (HPV) E6 oncoproteins promotes nuclear localization of active caspase 8. *Virology* **2014**, *450–451*, 146–152. [CrossRef] [PubMed]
114. Filippova, M.; Johnson, M.M.; Bautista, M.; Filippov, V.; Fodor, N.; Tungteakkhun, S.S.; Williams, K.; Duerksen-Hughes, P.J. The large and small isoforms of human papillomavirus type 16 E6 bind to and differentially affect procaspase 8 stability and activity. *J. Virol.* **2007**, *81*, 4116–4129. [CrossRef] [PubMed]
115. Tungteakkhun, S.S.; Filippova, M.; Fodor, N.; Duerksen-Hughes, P.J. The full-length isoform of human papillomavirus 16 E6 and its splice variant E6* bind to different sites on the procaspase 8 death effector domain. *J. Virol.* **2010**, *84*, 1453–1463. [CrossRef] [PubMed]
116. Filippova, M.; Parkhurst, L.; Duerksen-Hughes, P.J. The human papillomavirus 16 E6 protein binds to Fas-associated death domain and protects cells from Fas-triggered apoptosis. *J. Biol. Chem.* **2004**, *279*, 25729–25744. [CrossRef] [PubMed]
117. Pang, E.; Delic, N.C.; Hong, A.; Zhang, M.; Rose, B.R.; Lyons, J.G. Radiosensitization of oropharyngeal squamous cell carcinoma cells by human papillomavirus 16 oncoprotein E6∗I. *Int. J. Radiat. Oncol. Biol. Phys.* **2011**, *79*, 860–865. [CrossRef] [PubMed]
118. Williams, V.M.; Filippova, M.; Filippov, V.; Payne, K.J.; Duerksen-Hughes, P. Human papillomavirus type 16 E6* induces oxidative stress and DNA damage. *J. Virol.* **2014**, *88*, 6751–6761. [CrossRef] [PubMed]
119. Gillespie, K.A.; Mehta, K.P.; Laimins, L.A.; Moody, C.A. Human papillomaviruses recruit cellular DNA repair and homologous recombination factors to viral replication centers. *J. Virol.* **2012**, *86*, 9520–9526. [CrossRef] [PubMed]
120. Chen Wongworawat, Y.; Filippova, M.; Williams, V.M.; Filippov, V.; Duerksen-Hughes, P.J. Chronic oxidative stress increases the integration frequency of foreign DNA and human papillomavirus 16 in human keratinocytes. *Am. J. Cancer Res.* **2016**, *6*, 764–780. [PubMed]
121. Storrs, C.H.; Silverstein, S.J. PATJ, a tight junction-associated PDZ protein, is a novel degradation target of high-risk human papillomavirus E6 and the alternatively spliced isoform 18 E6. *J. Virol.* **2007**, *81*, 4080–4090. [CrossRef] [PubMed]
122. Gonzalez-Losa, M.D.R.; Puerto-Solís, M.; Ayora-Talavera, G.; Gómez-Carvallo, J.; Euán-López, A.; Cisneros-Cutz, J.I.; Rosado-López, A.; Echeverría Salazar, J.; Conde-Ferráez, L. Prevalence of anal infection due to high-risk human papillomavirus and analysis of E2 gene integrity among women with cervical abnormalities. *Enferm. Infecc. Microbiol. Clin.* **2017**. [CrossRef] [PubMed]
123. Roggenbuck, B.; Larsen, P.M.; Fey, S.J.; Bartsch, D.; Gissmann, L.; Schwarz, E. Human papillomavirus type 18 E6*, E6, and E7 protein synthesis in cell-free translation systems and comparison of E6 and E7 in vitro translation products to proteins immunoprecipitated from human epithelial cells. *J. Virol.* **1991**, *65*, 5068–5072. [PubMed]
124. Poirson, J.; Biquand, E.; Straub, M.-L.; Cassonnet, P.; Nominé, Y.; Jones, L.; van der Werf, S.; Travé, G.; Zanier, K.; Jacob, Y.; et al. Mapping the interactome of HPV E6 and E7 oncoproteins with the ubiquitin-proteasome system. *FEBS J.* **2017**, *284*, 3171–3201. [CrossRef] [PubMed]

viruses

MDPI

Article

HPV16 E6 and E7 Oncoproteins Stimulate the Glutamine Pathway Maintaining Cell Proliferation in a SNAT1-Dependent Fashion

Yunuen Ortiz-Pedraza [1,2], J. Omar Muñoz-Bello [1], Lucio Antonio Ramos-Chávez [3], Imelda Martínez-Ramírez [1], Leslie Olmedo-Nieva [1], Joaquín Manzo-Merino [1,4], Alejandro López-Saavedra [1], Verónica Pérez-de la Cruz [5] and Marcela Lizano [1,6,*]

1 Unidad de Investigación Biomédica en Cáncer, Instituto Nacional de Cancerología, Mexico City 14080, Mexico
2 Posgrado en Biología Experimental, DCBS, Universidad Autónoma Metropolitana-Iztapalapa, Mexico City 09340, Mexico
3 Departamento de Neuromorfología Funcional, Dirección de Investigaciones en Neurociencias, Instituto Nacional de Psiquiatría Ramón de la Fuente Muñiz, Mexico City 14370, Mexico
4 Cátedras CONACyT- Instituto Nacional de Cancerología, Mexico City 14080, Mexico
5 Laboratorio de Neurobioquímica y Conducta, Departamento de Neuroquímica, Instituto Nacional de Neurología y Neurocirugía Manuel Velasco Suárez, Mexico City 14269, Mexico
6 Departamento de Medicina Genómica y Toxicologóa Ambiental, Instituto de Investigaciones Biomédicas, Universidad Nacional Autónoma de Meóxico, Ciudad Universitaria, Mexico City 04510, Mexico
* Correspondence: lizanosoberon@gmail.com

Abstract: Persistent high-risk human papillomavirus infection is the main risk factor for cervical cancer establishment, where the viral oncogenes E6 and E7 promote a cancerous phenotype. Metabolic reprogramming in cancer involves alterations in glutamine metabolism, also named glutaminolysis, to provide energy for supporting cancer processes including migration, proliferation, and production of reactive oxygen species, among others. The aim of this work was to analyze the effect of HPV16 E6 and E7 oncoproteins on the regulation of glutaminolysis and its contribution to cell proliferation. We found that the E6 and E7 oncoproteins exacerbate cell proliferation in a glutamine-dependent manner. Both oncoproteins increased the levels of transporter SNAT1, as well as GLS2 and GS enzymes; E6 also increased LAT1 transporter protein levels, while E7 increased ASCT2 and xCT. Some of these alterations are also regulated at a transcriptional level. Consistently, the amount of SNAT1 protein decreased in Ca Ski cells when E6 and E7 expression was knocked down. In addition, we demonstrated that cell proliferation was partially dependent on SNAT1 in the presence of glutamine. Interestingly, SNAT1 expression was higher in cervical cancer compared with normal cervical cells. The high expression of SNAT1 was associated with poor overall survival of cervical cancer patients. Our results indicate that HPV oncoproteins exacerbate glutaminolysis supporting the malignant phenotype.

Keywords: HPV16 E6 and E7 oncoproteins; SNAT1 transporter; glutaminolysis

Citation: Ortiz-Pedraza, Y.; Muñoz-Bello, J.O.; Ramos-Chávez, L.A.; Martínez-Ramírez, I.; Olmedo-Nieva, L.; Manzo-Merino, J.; López-Saavedra, A.; Pérez-de la Cruz, V.; Lizano, M. HPV16 E6 and E7 Oncoproteins Stimulate the Glutamine Pathway Maintaining Cell Proliferation in a SNAT1-Dependent Fashion. *Viruses* **2023**, *15*, 324. https://doi.org/10.3390/v15020324

Academic Editor: Daniel DiMaio

Received: 20 December 2022
Revised: 17 January 2023
Accepted: 20 January 2023
Published: 24 January 2023

1. Introduction

Persistent high-risk *human papillomavirus* (HR-HPV) infection is the main risk factor for the development of different types of anogenital as well as head and neck cancers of which cervical cancer (CC) has the largest fraction attributable to HPV [1,2]. CC ranks fourth in mortality and incidence of neoplasms in women worldwide, particularly in developing countries [3,4].

The oncogenic potential of HPV is mainly attributed to the sustained expression of E6 and E7 oncoproteins, which affect a plethora of proteins involved in the acquisition of transforming characteristics that impact cell differentiation, inhibition of apoptosis, immortalization, metabolic reprogramming, and evasion of the immune response [5,6].

The most studied functions of the E6 and E7 oncoproteins lie in their ability to bind to and promote the degradation of p53 and pRb tumor suppressor proteins, respectively [7–9], leading to cell cycle dysregulation and resistance to apoptosis, which are key processes in carcinogenesis.

Cancer cells reprogram their metabolic pathways to support the increased energy demand necessary for cell proliferation, which in CC is achieved by the actions of both E6 and E7 oncoproteins [10]. In cancer cells, glycolysis is the most widely used pathway to produce energy and drive different metabolic activities [11]. Other metabolic pathways are also altered during carcinogenesis or cancer maintenance, such as the glutamine pathway or glutaminolysis [12,13]. Glutamine is a carbon and nitrogen source with an essential role in cancer cell growth [14,15]. Glutamine participates in the synthesis of purines and pyrimidines and other amino acids, and it is a precursor for the synthesis of reduced glutathione (GSH) in the regulation of oxidative stress [16–19]. Therefore, glutamine is an important player in cancer metabolism. Under normal conditions, glutamine enters the cell via members of various families of transporters such as SLC38A, SLC7A, and SLC1A; the most characterized being SNAT1, ASCT2, LAT1, and xCT. Accumulated evidence reveals that glutamine transporters are dysregulated in various types of cancer [20–24]. Once in the cell, glutamine is deaminated in the mitochondria by glutaminase 1 and 2 (GLS and GLS2) enzymes, generating glutamate and ammonia [25]. Afterwards, glutamate is converted to α-ketoglutarate and ammonia by glutamate dehydrogenase (GLUD) [26]. Furthermore, glutamic-oxaloacetic transaminase 1 (GOT1) catalyzes the formation of glutamate from α-ketoglutarate in the cytosol, which is the reverse activity of aspartate aminotransferase (AST or GOT2) within the mitochondria [25]. In addition, glutamine can also be obtained from glutamate through glutamine synthetase (GS) activity [26].

Little information is available on the involvement of HPV16 in glutamine metabolism. Previous reports show that the HPV16 E7 oncoprotein increased glutamine and pyruvate uptake in NIH 3T3 cells with high glycolytic index, compared with those cells with low glycolytic index [27,28]. In A2780 ovarian cancer cells, ectopically expressed E6 increased glucose and glutamine uptake, which also promoted lactate and alanine secretion [29]. Moreover, an RNAseq analysis revealed low expression of the xCT transporter in HPV-positive head and neck squamous cell carcinomas (HNSCC) compared with HPV-negative HNSCC [30]. However, the regulation of elements involved in glutaminolysis by HPV oncoproteins remains elusive. Therefore, the aim of this study was to evaluate the role of the HPV16 E6 and E7 oncoproteins in the glutamine pathway and their contribution in supporting cervical cancer cell proliferation.

We found that proliferation is preferentially dependent on glutamine in cells expressing E6 and E7. Interestingly, E6 and E7 increase the levels of the SNAT1 transporter, as well as the GLS2 and GS enzymes. Furthermore, E6 also increases LAT1 transporter levels, while E7 increases ASCT2 and xCT. In some cases, the modulation of these proteins was also associated with increased gene expression. Consistently, the SNAT1 transporter protein was decreased in Ca Ski cells when E6 and E7 expression was abrogated. Finally, SNAT1 expression was found to be significantly higher in cervical cancer samples compared with normal cervical cells and was also associated with poorer overall survival in cervical cancer patients.

2. Materials and Methods

2.1. Cell Culture

C-33 A stably transfected cells harboring HPV16 E6 and E7 coding sequences cloned into the pXFLAG-CMV™-10 expression vector (Sigma Aldrich, Tokyo, Japan) were used. For protein identification, E6 and E7 genes were fused to Flag and HA-tag sequences, as previously described [31]. Stably transfected cells were grown in Eagle's Minimum Essential Medium (EMEM) (ATCC) supplemented with 10% fetal bovine serum (FBS) and 2 g/L of Geneticin 418 (ChemCruz, Santa Cruz, CA, USA). Experimental groups of stably transfected cells were defined as EV (Empty Vector), E6 (HPV16 E6), or E7 (HPV16 E7).

HPV16-positive Ca Ski cells were maintained in Roswell Park Memorial Institute (RPMI) 1640 Medium (Gibco, Thermo Fisher, Waltham, MA, USA) supplemented with 10% FBS. Cell cultures were maintained in a humified incubator at 37 °C in a 5% CO_2 atmosphere.

2.2. Proliferation Assays

Stably transfected C-33 A cells were seeded in 60 mm dishes. After 24 h, cells were harvested and re-seeded in a 96-well plate and incubated with different treatments for 24 h, 48 h, and 72 h. Cells were grown with Dulbecco's Modified Eagle's Medium (DMEM) (Gibco, Thermo Fisher, Waltham, MA, USA) lacking D-glucose, L-glutamine, phenol red, and sodium pyruvate. Where indicated, the medium was supplemented with 4.5 g/L of glucose solution (Gibco, Thermo Fisher, Waltham, MA, USA) and/or 2 mM of L-glutamine solution (Gibco, Thermo Fisher, Waltham, MA, USA). Then, MTS (3-(4,5-dimethylthiazol-2-yl)-5-(3-carboxymethoxyphenyl)-2-(4-sulfophenyl)-2H-tetrazolium, inner salt) assay was performed using CellTiter 96 AQueous One Solution Cell Proliferation Assay Kit (Promega, Madison, WI, USA) according to the instructions indicated by the manufacturer.

For cell density evaluation, cells were fixed with PBS/formalin (10%) for 30 min at room temperature while shaking. Cells were then stained with crystal violet solution for 20 min. After several washes, the dye was eluted using PBS/acetic acid (10%) and absorbance was measured at 490 nm. Data were graphed to determine the percentage of cell proliferation for each tested condition.

2.3. Reverse Transcription Quantitative Polymerase Chain Reaction (RT-qPCR)

Cells were seeded in 60 mm culture dishes and total RNA extraction was performed using the RNeasy Mini kit (Qiagen, Hilden, Germany). Isolated RNA was treated with DNAse Free DNA removal kit (Thermo Fisher Scientific, Waltham, MA, USA) and then 1 µg of RNA was reverse transcribed with random hexamers utilizing the High-Capacity cDNA Reverse Transcription Kit (Applied Biosystems, Foster City, CA, USA). Primers used for the amplification of each transcript are shown in the Supplementary Materials, Table S1. SYBR select Master Mix (Applied Biosystems, Foster City, CA, USA) was utilized for qPCR reactions. The results are presented as relative quantification using the $^{\Delta\Delta}$Ct method.

2.4. Western Blotting

Cells were cultured in 60 mm dishes. After 24 h, cells were lysed using 100 µL of RIPA lysis buffer (50 mM Tris-HCl, pH 7.4, 150 mM NaCl, 1% NP-40, 0.25% Sodium Deoxycholate, 1% SDS and protease inhibitor cocktail (Roche, Basel, Switzerland)). Total cell protein extracts (20 µg) were analyzed by 10% and 12% SDS-PAGE gels and transferred onto a 0.22 µm nitrocellulose membrane (Bio-Rad, Hercules, CA, USA). A solution of 10% skimmed milk in TBS-0.1% Tween 20 was used to block membranes during 1 h at room temperature. Further, membranes were incubated overnight with the appropriate primary antibody diluted in 2.5% milk/0.1% Tween 20/PBS.

Primary antibodies included anti-GLS2 (Invitrogen, Waltham, MA, USA); anti-SLC7A5 (Invitrogen, Waltham, MA, USA); anti-xCT (Cell signaling); anti-ASCT2 (Cell signaling, Danvers, MA, USA); anti-GLS1 (Cell signaling); anti-SNAT1 (Cell signaling); anti-GS (Abcam, Cambridge, UK); anti-p53 (Santa Cruz Biotechnology, Santa Cruz, CA, USA); anti-Myc (Abcam), anti-HA-tag (Cell signaling); and anti-α-Tubulin (Cell signaling). Membranes were washed thrice with TBS-0.1% Tween 20 and incubated with HRP-conjugated secondary anti-mouse or anti-rabbit antibody in a dilution 1:10000 dilution (Santa Cruz Biotechnology). Proteins were visualized through film-based imaging utilizing the Clarity Western ECL (Bio-Rad). Western blots were performed at least thrice to ensure result reproducibility.

2.5. Metabolic Measurements

Stably transfected C-33 cells were seeded for 24 h in DMEM medium with 10% FBS. Later, cells were thoroughly washed with PBS to ensure removal of glutamine or other metabolites, excluding possible cross contaminations. Cells were then starved for two

hours in DMEM medium without glucose or glutamine. Afterward, 2 mM of glutamine was added to cell cultures for subsequent measurements by HPLC at different times (5 min, 15 min, and 30 min). The group of cells that were not treated with glutamine was considered as time 0. Glutamine and glutamate levels were determined by HPLC (high-performance liquid chromatography) using a fluorescence detector model S200 (PerkinElmer, Waltham, MA, USA) at excitation wavelength 232 nm and emission wavelength 455 nm. For such purposes, samples were previously lysed with 85% methanol, centrifuged at 12500 rpm for 15 min at 4 °C, and supernatant was obtained. Afterward, 10 µL of supernatant was treated with OPA reagent (containing 25 mg OPA + 625 µL methanol + 5.6 mL of 0.3 M borate buffer (pH 9.5) + 25 µL 2-mercaptoethanol) and eluted through a methanol gradient at a flow rate of 1.5 mL/min. The mobile phase containing 0.29% acetic acid (JT Baker, Gallade Chemical, Santa Ana, CA, USA) and 1.5% tetrahydrofuran (Mallinckrodt, Blanchardstown, Dublin, Ireland), pH 5.9, was added. The derivatives were separated through a PROTECOL C18G125 column of 5 µm particle size, 150 mm × 4.6 mm (Alltech, Nicholasville, KY, USA). The retention time for glutamate was ~3.6 min and for glutamine ~6.4 min. The results are presented as nmoles of glutamine/mg of protein and nmoles of glutamate/mg of protein.

2.6. HPV16 E6/E7 and SNAT1 siRNA Knock Down

Ca Ski cells were seeded in 60 mm dishes and transfected with small interfering RNAs targeting siE6/E7 (Dharmacon, Lafayette, CO, USA) or siSNAT1 (Santa Cruz, Bio, Santa Cruz, CA, USA). As the control, siLuc (Dharmacon, Lafayette, CO, USA) was used. Transfections were performed with 9 µL of Lipofectamine™ RNAiMAX (Invitrogen, Waltham, MA, USA) according to the manufacturer's instructions. After 72 h, cells were either fixed for fluorescence analyses or harvested to obtain protein extracts using RIPA buffer. Protein levels were evaluated by Western blot, the location of each protein was analyzed by immunofluorescence, and gene expression was evaluated by qRT-PCR, as indicated.

2.7. Immunofluorescence and Cell Imaging

Ca Ski cells were seeded on slides in 60 mm dishes and transfected with the indicated siRNA. After 72 h, cells were fixed with 3.7% paraformaldehyde in PBS for 15 min and permeabilized with 0.04% NP-40/PBS. Cells were incubated with 0.1M Glycine and 5% BSA solution for 1h at room temperature for blocking purposes. Then, cells were incubated overnight at 4 °C with anti-p53 (Santa Cruz Biotechnology) and anti-SNAT1 (Cell signaling) antibodies. After several washes with PBS 1×, cells were incubated with Alexa fluor 488 donkey anti-mouse (Invitrogen, Waltham, MA, USA) and Alexa fluor Rhodamine Red-X goat anti-rabbit (Invitrogen, Waltham, MA, USA), respectively, for 2 h at 4 °C. Slides were washed and mounted with Vectashield mounting medium containing DAPI (Vector Laboratories, Newark, CA, USA). Slides were visualized with a confocal microscope (Zeiss LSM 710 DUO, Oberkochen, Baden-Wurttemberg, Germany) with lasers giving excitation lines at 488 and 594 nm. Around twenty fields were observed for each treatment and representative images were acquired. Data of three independent experiments were collected with a 63X objective oil immersion lens. In addition, the same protocol was carried out to evaluate SNAT1 in C-33 A stably transfected cells.

2.8. Cervical Samples

A total of 23 cervical cancer samples were obtained from the Tumor Biobank of the Instituto Nacional de Cancerología of Mexico City (INCan) and 18 normal HPV-negative cervical samples were kindly provided by the Instituto Nacional de Salud Pública (INSP). Samples were subjected to RNA extraction for qPCR analysis to determine SNAT1 expression. The protocol was approved by the Institutional Scientific and Ethical committees of INCan, ref. (017/007/IBI) (CEI/1144/17). All patients whose samples were utilized in this study agreed to participate and signed the informed consent form.

2.9. Statistical Analysis

All experiments were performed three times and data were depicted as the mean ± standard error of the mean (SEM). To determine significant statistical changes in the experimental conditions compared with the control, we used a Student's *t*-test and a *p* value of <0.05 was considered statistically significant.

3. Results

3.1. HPV16 E6 and E7 Oncoproteins Promote Glutamine-Dependent Proliferation

C-33 A cells stably transfected with plasmids expressing HPV-16 E6 and E7 and Empty Vector (EV) were used as previously described [31]. As expected, detection of exogenous HA-tagged HPV16 E6 and E7 proteins was successfully achieved by immunofluorescence (Figure 1A) exhibiting mostly a nuclear localization; although, viral oncoproteins are also observed in the cytoplasm. Western blot assays (Figure 1B) show HA-tagged E6 and E7 proteins, where E6* is the most abundant isoform in E6-expressing cells.

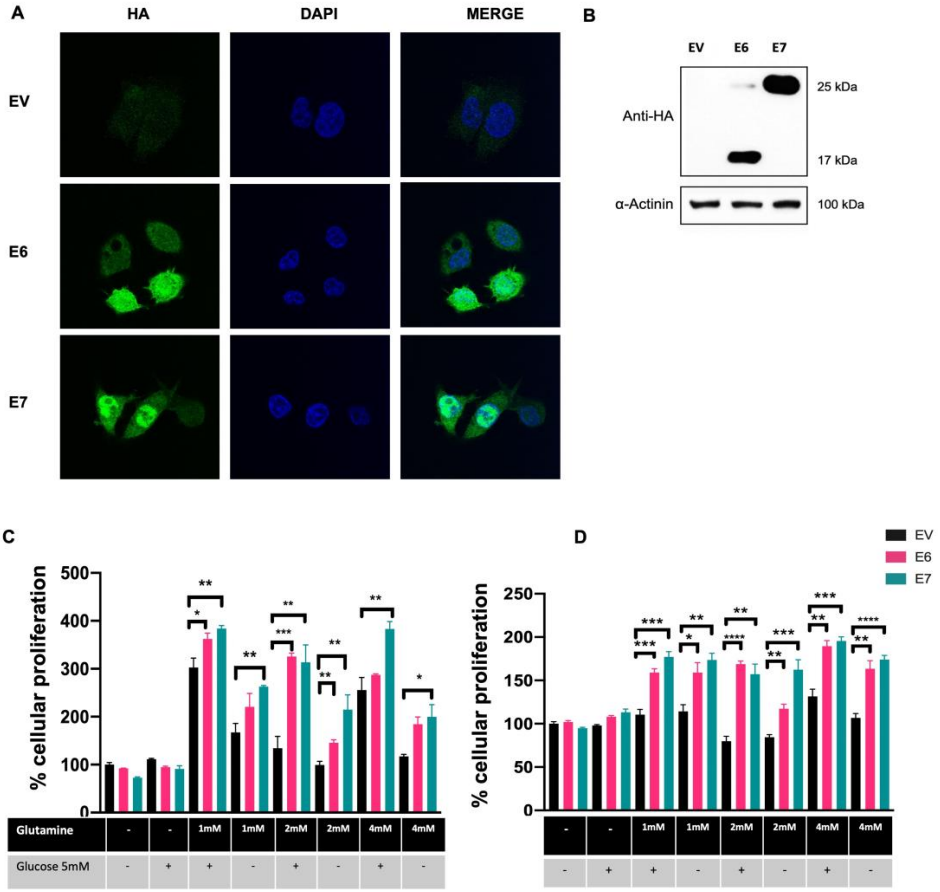

Figure 1. HPV16 E6 and E7 promote glutamine-dependent proliferation in C-33 A cells stably transfected with the HPV-16 E6 and E7 oncoproteins. (**A**) Detection of E6 and E7 HA-tagged oncoproteins in C-33 A cells (green) and DAPI-stained cell nuclei are shown in blue. (**B**) Immunodetection of E6 and E7 HA-tagged proteins in C-33 A cells. In E6-expressing C-33 A cells, the full length and the spliced E6* isoform are also detected. (**C**) MTS and (**D**) Crystal Violet assays were performed to assess glutamine-dependent cell proliferation. Cells were grown in media supplemented with different concentrations of glutamine (1 mM, 2 mM, and 4 mM) and glucose (5 mM) as indicated. Cells harboring E6 (pink bars), E7 (green bars), or the control EV (black bars) are depicted. Graphs show the data as the mean and ± SEM of three independent experiments. Statistical analysis was performed using Student's *t*-test to analyze significant values when comparing E6 and E7 with EV within each group, as indicated. * $p < 0.05$, ** $p < 0.01$ and *** $p < 0.001$ and **** $p < 0.0001$.

To demonstrate glutamine-dependent proliferation in cells expressing E6 and E7 oncoproteins, cells were supplemented with different concentrations of glutamine (0 mM, 1 mM, 2 mM, and 4 mM) in the presence or absence of 5 mM of glucose. Cell proliferation was assessed 72 h after glutamine exposure using MTS or Crystal Violet assays. As shown in Figure 1C, the MTS assay revealed no differences in cell proliferation in cells expressing E6 and E7 compared with those with EV, when glutamine and glucose were absent. Surprisingly, the same effect was observed even when the growth medium was supplemented with 5 mM glucose alone. After glutamine addition, increased proliferation was observed in all tested groups when evaluated in MTS assays, being significantly higher in cells expressing E6 and E7. Importantly, cells expressing E7 treated with 1 mM, 2 mM, or 4 mM glutamine alone had a significant increase in proliferation, relative to the control group with the same treatment (1.56-, 2.16-, 1.70-fold change, respectively). Similarly, E6-expressing cells treated with 1 mM, 2 mM, or 4mM glutamine alone presented an increase in proliferation, relative to the control group with the same treatment (1.31-, 1.46-, 1.57-fold change, respectively), however, only 2 mM glutamine treatment showed significance. Interestingly, when cells were incubated with 5 mM glucose plus glutamine, proliferation was increased when compared with cells without glutamine/glucose treatment or glucose alone. Particularly, in the group treated with 2 mM glutamine plus glucose, a significant difference was observed in cells expressing E6 and E7 compared with EV (2.42- and 2.33-fold change, respectively).

The crystal violet assay depicted in Figure 1D shows similar behavior to that obtained using the MTS assay, where cells with E6 and E7 increased proliferation in the presence of glutamine alone at 1 mM (1.39- and 1.52-fold change, respectively); 2 mM (1.39- and 1.92-fold change, respectively); and 4 mM (1.53- and 1.62-fold change, respectively). However, no additional advantage in this effect was identified by adding glucose. According to the results obtained with the MTS assays, no changes were observed in the absence of glutamine and glucose, nor in cells treated with glucose alone. These results strongly suggest that E6 and E7 oncoproteins promote the use of the glutamine pathway as the primary energy source to support cell proliferation.

3.2. Intracellular Glutamine and Glutamate Increase in the Presence of HPV16 E6 Oncoprotein

To characterize the glutaminolysis profile of C-33A cells expressing EV, E6, or E7, intracellular glutamine and glutamate metabolites were measured through HPLC assay. Cells were fasted for two hours in medium deprived of glutamine and glucose. Subsequently, EV, E6, and E7 groups were exposed to 2 mM glutamine at different times (0 min, 5 min, 15 min, and 30 min) and HPLC assays were performed. The group of cells that were not treated with glutamine was considered as time 0.

Figure 2A shows that after 5 min of treating the cells with glutamine, a significant increase in intracellular glutamine concentrations was achieved in cells expressing the E6 oncoprotein, compared with with those harboring EV (4.91-fold increase), and an increase was also observed compared with E6 expressing cells at time 0 (2.85-fold change). At 15 min and 30 min, intracellular glutamine values in cells expressing E6 return to levels similar to those detected for EV in each group. These results suggest that the HPV16 E6 oncoprotein increases intracellular glutamine immediately after exposure to glutamine. Meanwhile, in cells with E7 expression, an increase in intracellular glutamine was observed after 15 min of glutamine treatment (1.63-fold increase), which was related to the EV condition and to cells expressing E7 at time 0 (1.58-fold); however, even when an increasing trend was observed, the results were not significant.

When evaluating the intracellular glutamate concentrations upon exposure to glutamine (Figure 2B), it was observed that cells expressing E6 or E7 had lower glutamate levels than those with EV at time 0. This could be partly explained if cells with the viral oncoproteins have accelerated glutamate consumption which deserves further study. Upon addition of glutamine, E6-expressing cells showed a significant increase in the intracellular glutamate concentration after 30 min (4-fold change, relative to time 0). Furthermore, glutamate levels in EV cells remained similar in all tested conditions. Interestingly, cells

expressing E7 showed an increase in intracellular glutamate levels after 5 min, 15 min, and 30 min (1.64-, 2.13-, and 1.71-fold change, respectively), compared with E7-expressing cells at time 0, although not significant. These results suggest that in E6- and E7-containing cells, glutamate is derived from the deamination of glutamine along glutaminolysis.

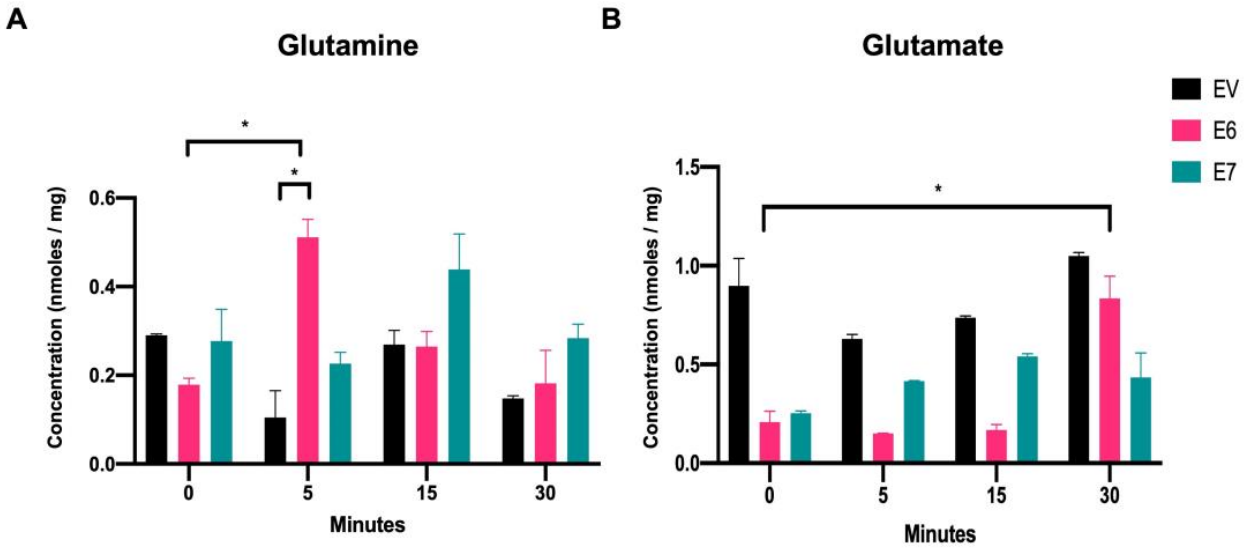

Figure 2. Intracellular glutamine and glutamate increase in the presence of the HPV16 E6 and E7 oncoproteins. HPLC analysis of (**A**) intracellular glutamine and (**B**) intracellular glutamate in C-33 A cells stably transfected with EV (black bars), E6 (pink bars), or E7 (green bars). The data were evaluated at 0 min, 5 min, 15 min, and 30 min after adding glutamine to the media. Statistical analysis using Student's *t*-test was performed to obtain significant values when comparing cells harboring E6 and E7 with the EV group, as indicated. * $p < 0.05$ is considered to be significant.

3.3. SNAT1 Glutamine Transporter Expression and Protein Levels Increase in the Presence of HPV16 E6 and E7 Oncoproteins

To determine whether E6 and E7 oncoproteins affect the expression and protein content of glutamine-related transporters, Western blot, qPCR, and immunofluorescence assays were performed. As shown in Figure 3A and B, a remarkable increase in the protein levels of SNAT1 and LAT1 transporters was observed in the presence of E6, relative to the EV control group (7.97- and 2.04-fold change, respectively). Meanwhile, E7 significantly increased the levels of the ASCT2 and xCT transporter proteins (1.70- and 1.68-fold, respectively).

Furthermore, qPCR assays (Figure 3C) revealed that E6 and E7 induced the expression of the SLC38A1 gene (SNAT1) (2.07- and 2.11-fold change, respectively). Moreover, E7 significantly upregulated gene expression of SLC1A5 (ASTC2) (1.57-fold change) and SLC7A11 (xCT) (1.74-fold change). Interestingly, immunofluorescence assays shown in Figure 3D and E confirm overexpression of SNAT1 in E6- and E7-expressing cells, compared with the EV control. Taken together, these results indicate that E6 and E7 oncoproteins preferentially regulate SNAT1 as a key glutamine transporter.

To support these results, we evaluated another stably transfected clone of C-33 A cells expressing E6 or E7 (E6-Clone 2 and E7-Clone 2) and found increased SNAT1 protein in relation to the control (EV-Clone 2) (1.72-, 2.31-fold change, respectively) (Supplementary Materials, Figure S1).

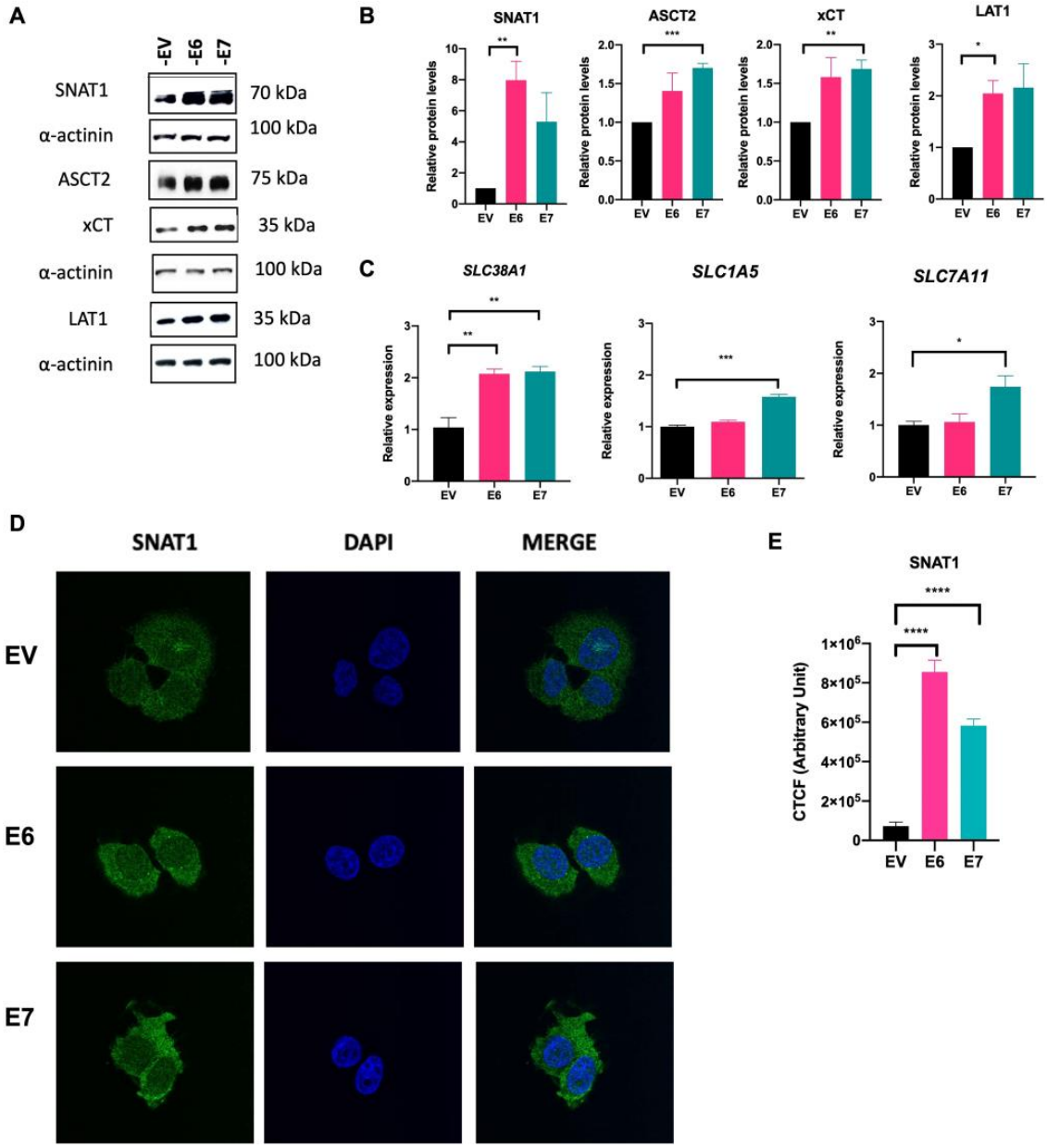

Figure 3. SNAT1 transporter is increased in the presence of HPV16 E6 and E7 oncoproteins. Protein levels and gene expression of the glutamine transporters were analyzed by Western blot and qPCR assays, respectively, in C-33 A cells harboring EV (black bars), E6 (pink bars), and E7 (green bars). (**A**) Representative immunoblots of SNAT1, ASCT2, xCT, and LAT1 are depicted. As loading control α-actinin was used. (**B**) Relative protein levels were obtained from densitometric analysis of immunoblots. (**C**) Relative expression analysis of SLC38A1, SLC1A5, and SLC7A11 genes was assessed by qPCR. (**D**) Stably transfected C-33 A cells were immunostained with anti-SNAT1 antibody (green) and DAPI for nuclear visualization (blue). (**E**) Corrected total cell fluorescence (CTCF) was obtained for SNAT1. Images were visualized with a 63x objective oil immersion lens. Data from three independent experiments were collected and plotted showing the mean and ±SEM. Student's *t*-test was performed to obtain statistical differences between the E7 and E6 groups compared with empty vector values (EV). * $p < 0.05$, ** $p < 0.01$, *** $p < 0.001$, and **** $p < 0.0001$ values are represented as indicated.

3.4. HPV16 E6 and E7 Modify Glutaminolysis-Related Components

As we previously demonstrated that the HPV16 E6 and E7 oncoproteins promote upregulation of transporters that mediate glutamine uptake, we evaluated key components of the glutamine pathway. GLS, GLS2, and GS protein levels were assessed by Western blot. In Figure 4A,B, GLS protein levels do not change in cells expressing E6 and E7, compared with EV cells. Surprisingly, when evaluating GLS2 and GS, protein levels increased in the presence of E6 (4.76- and 1.97-fold change, respectively) and E7 (3.83- and 1.94-fold change, respectively). We also evaluated p53 and c-Myc proteins since they are known to be transcriptional regulators of glutaminolysis. As expected, p53 protein is virtually eliminated in the presence of E6, while an increase in this protein was observed in cells containing E7, which is consistent with previously reported data [32]. In addition, there is a significant increase in c-Myc protein levels in cells expressing E6 (1.52-fold change) or E7 (2.36-fold change).

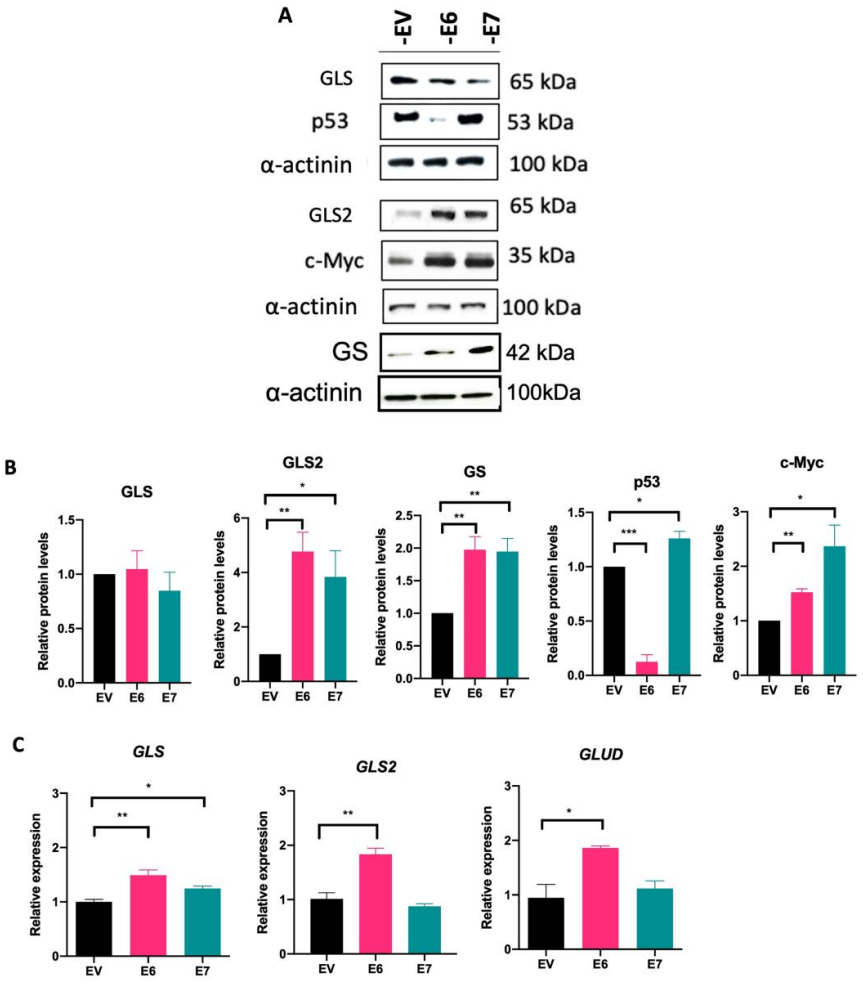

Figure 4. HPV16 E6 and E7 oncoproteins alter components of the glutamine pathway. (**A**) Immunodetection of GLS, GLS2, GS, p53, and c-Myc proteins in cells expressing E6 and E7 and (**B**) densitometric analysis. (**C**) Transcript levels of GLS, GLS2, and GLUD analyzed by qPCR. Data from three independent experiments were collected and plotted showing the mean and ±SEM. Statistical analysis was performed using Student's *t*-test to decipher significant values * $p < 0.05$, ** $p < 0.01$, and *** $p < 0.001$ vs the values of the empty vector. As a loading control, α-actinin was used in the Western blot assay and 18S was used for normalization in the qPCR assays.

The transcript levels of GLS, GLS2, and GLUD were analyzed by qPCR (Figure 4C). The E6 and E7 oncoproteins promote a significant increase in GLS expression compared with EV (1.37- and 1.26-fold change, respectively), while GLS2 and GLUD expression only

augmented in the presence of E6 (1.88- and 1.86-fold change, respectively). Taken together, our results demonstrate that both viral oncoproteins regulate the glutamine pathway by enhancing amino acid transporters and downstream components involved in this pathway.

3.5. SNAT1 Transporter Expression and Protein Levels Are Reduced in Ca Ski E6/E7-Silenced Cells

Since ectopically expressed E6 and E7 oncoproteins increased SNAT1, we were interested in evaluating the consequences of silencing E6 and E7 in Ca Ski cells, which endogenously contain HPV16 sequences and continuously express those oncoproteins. Ca Ski cells were transfected with small interfering RNAs (siRNA) targeting E6 mRNA (siE6), E7 mRNA (siE7), and E6/E7 mRNA bicistron (siE6/E7). An unspecific siRNA (siLuc) was used as a control. Figure 5E and F show that silencing of E6 and E7 expression was efficiently achieved. After 72 h, cell protein lysates were collected or fixed for immunodetection analysis by Western blot and immunofluorescence assays, respectively. As expected, when E6/E7 were knocked down in Ca Ski cells, a recovery in p53 protein levels was observed by Western blot (Figure 5A,B) and immunofluorescence (green) (Figure 5J,L). Interestingly, when evaluating the SNAT1 transporter by immunoblot as shown in Figure 5C,D and immunofluorescence (red) (Figure 5J,K), SNAT1 levels were significantly decreased when E6/E7 expression was ablated. In addition, a significant decrease in the expression of SLC38A1 (SNAT1), SLC15A (ASCT2), and GLS2 was observed in cells where E6 or E7 expression was knocked down (Figure 5G–I, respectively). These data confirm that E6 and E7 alter elements of glutaminolysis, particularly the SNAT1 transporter, which may have an impact on the glutamine metabolism.

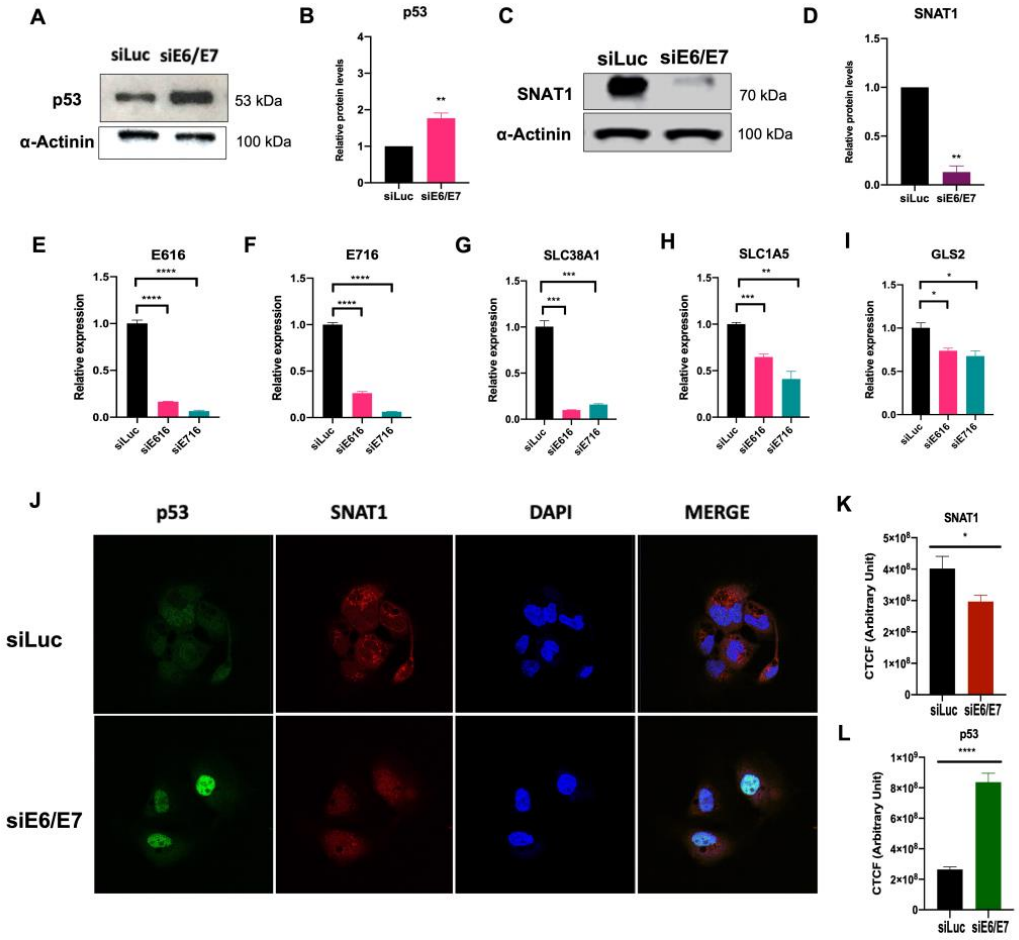

Figure 5. SNAT1 transporter is affected by the silencing of E6 and E7 expression in HPV-positive Ca Ski cells. Ca Ski cells were transfected with siLuc (control), siRNAE6/E7, siE6, or siE7. After 72 h of

treatment, proteins were analyzed through Western blot. (**A**,**B**) Protein levels of p53 were restored in the absence of E6 and E7. (**C**,**D**) SNAT1 protein transporter levels decreased after ablation of E6/E7, as loading control α-actinin was used in Western blot. (**E**) Gene expression of HPV16 E6 and (**F**) E7, (**G**) SLC38A1 (SNAT1), (**H**) SLC1A5 (ASCT2), and (**I**) GLS2 decreased after ablation of E6 or E7. The 18S gene was used for normalization in qPCR assays. (**J**) SNAT1 and p53 levels were analyzed through immunofluorescence. Restoration of p53 (shown in green) and a decrease in SNAT1 protein levels (shown in red) were observed in E6/E7-silenced cells. Images were collected with a 63× objective oil immersion lens. (**K**) CTCF arbitrary fluorescence units were obtained for quantification of SNAT1 and (**L**) p53 protein levels. Data from three independent experiments were collected and plotted showing the mean and ±SEM. Statistical analysis was carried out using Student's *t*-test to obtain significant values. * $p < 0.05$, ** $p < 0.01$, and **** $p < 0.0001$ vs. siLuc.

3.6. SNAT1 Transporter Partially Contributes to Ca Ski Cell Proliferation

To determine whether glutamine supports Ca Ski cell proliferation, MTS assays were performed in cells supplemented with low concentrations of glucose (1 mM) in the presence or absence of 2 mM glutamine, and assays were performed 72 h after treatments. As shown in Figure 6A, when Ca Ski cells were treated with low glucose plus 2 mM glutamine, a significant 2-fold increase in cell viability was observed compared with Ca Ski cells exposed to low glucose alone. It is worth mentioning that when Ca Ski cells are treated with 2 mM glutamine in the absence of glucose at 72 h, proliferation is also increased compared with the absence of glutamine (data not shown), evidencing the glutamine requirement for successful growth.

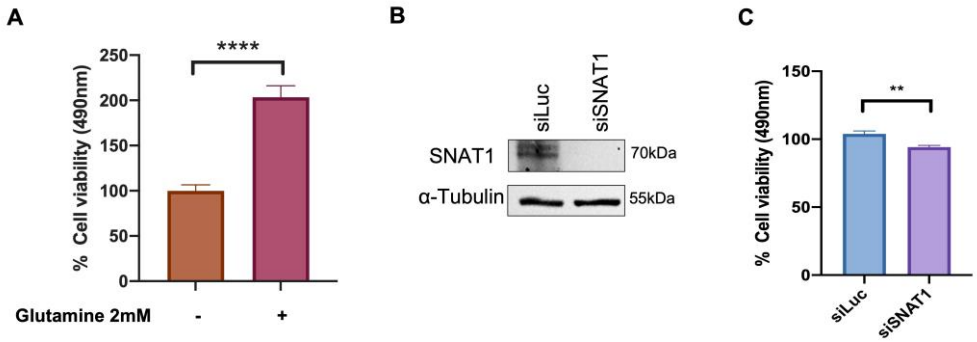

Figure 6. Ca Ski cell proliferation is increased in the presence of glutamine which is partially attributed to the SNAT1 transporter. (**A**) Ca Ski cells were grown in DMEM medium supplemented with 1 mM glucose and in the presence or absence of 2 mM glutamine as indicated. MTS proliferation assay was performed after 72 h. (**B**) SNAT1 silencing was evaluated through immunoblot in cells transfected with siLuc or siSNAT1; α-tubulin was used as loading control. (**C**) Proliferation was measured by MTS assay in Ca Ski cells doubly transfected with siSNAT1 and siLuc was used as the control. Graphs show data as the mean and ± SEM of three independent experiments. Statistical analysis was performed using Student's *t*-test to analyze the significant values when comparing with the indicated groups, significance is represented as ** $p < 0.01$ and **** $p < 0.0001$.

Furthermore, to elucidate the specific involvement of the SNAT1 transporter in Ca Ski cell proliferation, cells were transfected with siRNA targeting SNAT1 and siLuc (as control). As previously reported by Liu X. et al. 2020 [33], a double knockdown of SNAT1 was performed. Ca Ski cells were transfected again 72 h after the first transfection. Then, 24 h after the second transfection, Ca SKi cell proliferation was assessed using the MTS assay. SNAT1 protein levels were evaluated after 72 h of silencing and virtually no SNAT1 protein was detected (Figure 6B). A significant 8% reduction in proliferation was observed when SNAT1 was abolished, compared with the control (siLuc) (Figure 6C). These results support the idea that SNAT1 partially sustains cell proliferation of Ca Ski cells.

3.7. SNAT1 Expression Is Increased in Cervical Cancer Samples and Its High Expression Is Associated with a Poorer Prognosis in Cervical Cancer Patients

Our results suggest that HPV16 E6 and E7 induce the proliferation of cervical cancer cells partially dependent on the SNAT1 transporter. We wondered whether SNAT1 expression could be affected in cervical cancer and if it was also associated with patient clinical outcome. To assess differences in SNAT1 expression in cervical cancer samples compared with normal samples, RT-qPCR assays were performed. As shown in Figure 7A, SNAT1 expression was significantly increased in cervical cancer tissues compared with normal samples. Interestingly, as shown in Figure 7B, based on median expression, high SNAT1 expression in cervical cancer samples tends to be associated with poor overall survival (OS) although not significant ($p = 0.544$). These interesting results are consistent with those described in the Human Protein Atlas portal [34], where high SNAT1 expression exhibits low OS in patients with cervical cancer. However, a more robust study including a larger number of patient samples is needed to confirm such observations.

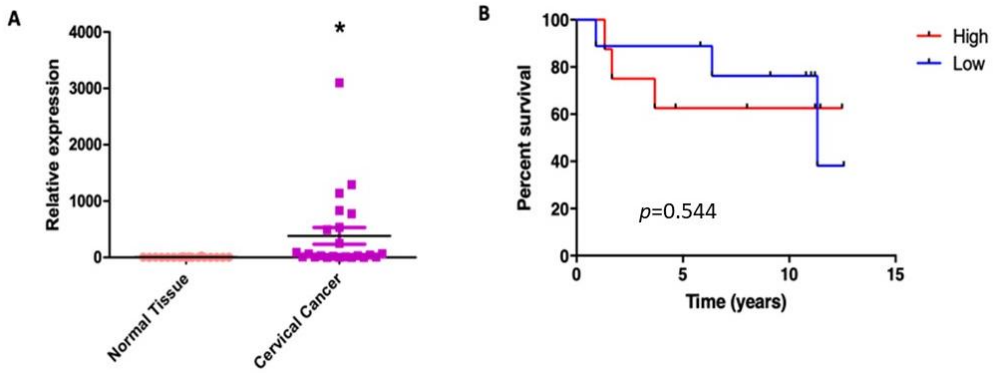

Figure 7. SNAT1 expression is increased in cervical cancer and its high expression is associated with worse prognosis. (**A**) SNAT1 expression was increased in cervical cancer samples ($n = 23$) compared with normal cervical samples ($n = 18$); * $p < 0.05$ represents significant differences in both groups. (**B**) Differences in the overall survival analysis according to the median expression of SNAT1, as high ($n = 10$) or low expression ($n = 9$) ($p = 0.544$). Low mRNA levels are represented by blue lines and high levels by red lines.

4. Discussion

An emerging feature of cancer cells is energetic metabolic reprogramming [35], which rewires metabolic pathways for different nutritional requirements to provide energy and building blocks to support several cellular processes associated with carcinogenesis, such as cell survival and exacerbated growth, among others [36–38].

Metabolic reprogramming of the glutamine pathway has been reported to promote pleiotropic functions in cells, including the synthesis of fatty acids, purines, and pyrimidines as well as redox homeostasis, which are also essential for the maintenance of cancer cell functions. Glutaminolysis has been found to be increased in different types of cancer including liver [39], glioma [40], lung [41], breast [42], and ovarian [43], among others. Therefore, the study of the elements involved in the glutamine pathway is of interest to understand the molecular mechanisms that underlie the cancerous process, in addition to exploring the potential use of these elements as therapeutic targets. However, little is known about the alterations that occur in glutamine metabolism in cervical cancer and the involvement of the HPV16 E6 and E7 oncoproteins in this process to maintain the malignant phenotype.

Previously, E6 and E7 oncoproteins were reported to induce metabolic reprogramming by affecting other metabolic pathways such as glycolysis, Krebs cycle, nucleotide synthesis, fatty acid synthesis, mitochondrial respiration, and autophagy [10,44]. In this study, we focused on elucidating the participation of HPV16 E6 and E7 oncoproteins in the regulation of the glutamine pathway in a cellular model of cervical cancer. We show that C-33 A cells,

exogenously expressing HPV-E6 and -E7 oncoproteins, exhibit exacerbated proliferation in a glutamine-dependent manner and, surprisingly, no effect was observed when cells were exposed to glucose alone. These data consistently support the idea that HPV oncoproteins induce cell proliferation in a glutamine-dependent manner, being essential for maintaining oncogenic processes in HPV-related cancers. Similarly, Ca Ski cells, which contain HPV16 sequences, also showed increased proliferation in the presence of glutamine. It is worth mentioning that other amino acids, such as leucine and cysteine, enhance glutaminolysis [45,46]; therefore, their involvement in cell proliferation in HPV-related cancers cannot be ruled out and warrants further studies.

Comparably, it has been reported that in glutamine-deprived ovarian cancer cell lines (HEY, SKOV3, and IGROV-1) the addition of glutamine augments cell proliferation in a dose-dependent manner [43]. Moreover, it has been demonstrated that cancer aggressiveness correlates with glutamine-dependent proliferation. In breast cancer cell lines, it was observed that when cells were deprived of glutamine for 96 h, metastatic cells (MCF7 and MDA-MB231) substantially reduced their proliferation, while non-metastatic cells were not affected (MCF-10A and BT-20) [47].

Furthermore, by evaluating the participation of E6 and E7 in the glutamine/glutamate flux, we have shown that after exposing cells to 2 mM glutamine, E6 proteins increased intracellular glutamine concentrations after 5 min. Meanwhile, a trend towards increased intracellular glutamine in cells expressing E7 was observed at 15 min and 30 min. Likewise, E6 promotes accumulation of glutamate at 30 min, while an ascending behavior was detected in those cells with E7 expression at 5 to 30 min, although not significant.

Consistent with our results, in a cell model of ovarian cancer, E6 expression increased glutamine consumption in A2780 cells [29]. In addition, HPV-16 E7 oncoprotein was reported to enhance glutamine uptake in two strains of NIH 3T3 cells with different metabolic characteristics, high- (hg-NIH) and low- (lg-NIH) glycolytic rate, where lg-NIH cells with E7 exhibited the highest consumption of glutamine and lower intracellular glutamate concentration [27]. It should be noted that these cells were treated with DMEM medium supplemented with 2 mM glutamine, which are similar conditions to those used in this work, where the culture medium lacked glucose. These results suggest that E6 and E7 oncoproteins can mediate glutamine/glutamate flux though alterations in glutamine transporters, facilitating intracellular glutamine access.

Several amino acid transporters that mediate glutamine uptake have been shown to be overexpressed in different types of cancer, including colon, breast, liver, lung, and osteosarcoma, among others [22,48–52]. This fact suggests that tumors strongly require glutamine intake to support cell survival and tumor growth. Since we found an increase in intracellular glutamine in cells expressing E6 and E7, we focused on evaluating the best-known glutamine transporters involved in glutamine uptake. Interestingly, we found that both E6 and E7 increased SNAT1 protein and transcript levels compared with EV cells (Figure 3).

Furthermore, effects individually exerted by each oncoprotein were observed, where E6 increased LAT1 protein levels and E7 increased ASCT2 and xCT proteins and transcripts. To demonstrate the specific involvement of E6 and E7 oncoproteins in glutamine regulation in an HPV-positive cancer cell line, we knocked down the expression of E6 and E7 in Ca Ski cells. As expected, recovery of p53 in the nucleus was observed after E6/E7 ablation, compared with control cells. Interestingly, in Western blot and immunofluorescence assays (Figure 5), SNAT1 was significantly decreased when E6/E7 was knocked down. Furthermore, the expression of SNAT1, ASCT2, and GLS2 genes was also reduced. Taken together, these results suggest that E6 and E7 oncoproteins converge in modulating SNAT1, which may play a key role in glutamine uptake in cervical cancer, although other transporters, including ASCT2 and xCT, are also involved.

Additionally, by evaluating downstream components of the glutamine pathway, E7 and E6 were found to increase GLS2 and GS protein content, demonstrating that there is a balance in glutamine and glutamate metabolic flux. It should be noted that both

oncoproteins may favor the use of the GLS2 enzyme over GLS. Previous studies indicate that both isoforms may play oncogenic and anti-oncogenic roles depending on the type of cancer [53]. For example, in breast cancer, GLS2 amplification or overexpression is associated with acquisition of a malignant phenotype and poor prognosis [54,55]. Moreover, GLS2 is known to be transcriptionally regulated by p53 [56,57], promoting glutamate synthesis and glutathione homeostasis [58]. As expected, in C-33 A cells expressing E6, p53 levels are overwhelmingly decreased, and despite this, GLS2 levels are increased. This could be explained if GLS2 expression could also take place in a p53-independent context, for example, being regulated by p63 [59]. Moreover, c-Myc has been shown to promote GLS expression in different cancer cell lines [60]. We demonstrated a significant increase in c-Myc protein in E6 and E7 expressing cells, which correlates with increased GLS expression, suggesting that viral oncoproteins upregulate c-Myc, affecting GLS transcription. However, no differences in GLS protein content were observed, possibly due to other GLS regulation mechanisms not explored in this work.

As we demonstrated that HPV-16 E6 and E7 oncoproteins consistently increase SNAT1 protein levels, our research focused on elucidating the specific involvement of SNAT1 in glutamine-dependent proliferation in Ca Ski cells. Interestingly, a slight but significant reduction in cellular proliferation (Figure 6C) was observed when Ca Ski cells were knocked down for SNAT1, even in the presence of 2 mM glutamine, suggesting that proliferation induced by E6 and E7 is partially attributable to SNAT1 in Ca Ski cells. Nevertheless, it is possible that other glutamine or glutamate transporters help to compensate for the absence of SNAT1 in the presence of glutamine. As we show in this study, both E6 and E7 oncoproteins upregulate other glutamine transporters such as ASCT2, LAT1, and xCT. Future studies are required to elucidate the joint participation of the different glutamine transporters affected by E6 and E7 in glutamine-dependent proliferation.

In accordance with these data, ablation of SNAT1 was reported to decrease cell proliferation and migration in melanoma and gastric cancer cell models, evidencing that SNAT1 might play an important role in the maintenance of the malignant phenotype [61,62].

Several studies have reported that SNAT1 is a critical glutamine transporter for cancer cells, the overexpression of which is associated with a poor prognosis [51,62,63]. Our results (Figure 7) demonstrate that SNAT1 is increased in tumors compared with normal tissues, and furthermore, that high SNAT1 expression is associated with poorer overall survival of cervical cancer patients. Similarly, the data from the Human Protein Atlas portal confirm this statement since an increase in the expression of SNAT1 also exhibited a worse prognosis for patients with cervical cancer. Other studies demonstrated that high SNAT1 expression is strongly related to pulmonary metastasis and reduced survival in patients with osteosarcoma [51]. Furthermore, Jing X. et al., demonstrated that high levels of SNAT1 protein are related to invasion, metastasis, and progression of gastric carcinomas and are associated with poor survival of patients with gastric cancer [62].

Finally, our results demonstrate that the E6 and E7 oncoproteins promote glutamine uptake and glutamine-dependent cell proliferation, partially attributed to the SNAT1 transporter, although the involvement of other transporters in such events should not be ruled out, as summarized in Figure 8. In addition, we demonstrate that SNAT1 is increased in cervical cancer in relation to the normal cervix and its high expression could be associated with a poor prognosis in patients with cervical cancer. Therefore, understanding the biological mechanisms by which HPV induces an increase in the activity of metabolic pathways, such as glutaminolysis, will eventually allow the development of therapeutic strategies, as well as the identification of biomarkers in HPV-associated cancers.

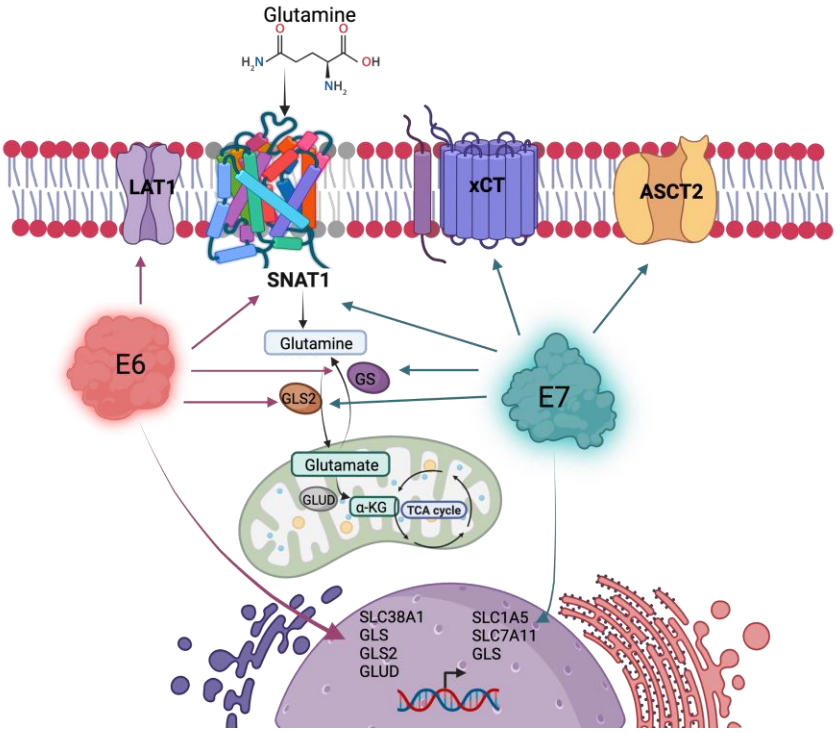

Figure 8. HPV16 E6 and E7 oncoproteins alter the glutamine pathway. Both viral oncoproteins upregulate the protein levels of the SNAT1 transporter, GLS2, and GS. Independently, E6 upregulates LAT1 protein levels and gene expression of SLC38A1, GLS, GLS2, and GLUD; while E7 upregulates ASCT2 and xCT protein levels and gene expression of SLC1A5, SLC7A11, and GLS. Figure created with BioRender.com.

Supplementary Materials: The following supporting information can be downloaded at: https://www.mdpi.com/article/10.3390/v15020324/s1, Figure S1: The SNAT1 transporter is increased in presence of the HPV16 E6 and E7 oncoproteins; Table S1: Primers used for the amplification of genes analyzed by RT-qPCR.

Author Contributions: All the authors listed made substantial contributions to the manuscript and qualify for authorship, and no authors have been omitted. Y.O.-P.: methodology, validation, formal analysis, investigation, visualization, writing—original draft preparation, and writing—review and editing. J.O.M.-B.: methodology, validation, formal analysis, investigation, visualization, writing—original draft preparation, writing—review and editing, and funding acquisition. L.A.R.-C.: methodology and validation. I.M.-R.: methodology. L.O.-N.: methodology. J.M.-M.: writing—review and editing. A.L.-S.: methodology. V.P.-d.l.C.: methodology. M.L.: conceptualization, visualization, formal analysis, resources, writing—original draft preparation, writing—review and editing, supervision, project administration, and funding acquisition. All authors have read and agreed to the published version of the manuscript.

Funding: This research was partially funded by CONACyT PRONAII-7-Virus y Cáncer 303044, Paradigmas y Controversias de la Ciencia #320812 and Instituto Nacional de Cancerología, Mexico City (017/007/IBI) (CEI/1144/17).

Institutional Review Board Statement: The study was conducted in accordance with the Declaration of Helsinki and approved by the Scientific and Ethical Institutional Review Boards of Instituto Nacional de Cancerología (017/007/IBI)(CEI/1144/17).

Informed Consent Statement: Informed consent was obtained from all subjects involved in the study.

Data Availability Statement: Data are contained within the article and Supplementary Materials.

Acknowledgments: Yunuen Ismerai Ortiz-Pedraza is a student from the Doctorado en Biología Experimental at the Universidad Autónoma Metropolitana Iztapalapa, Mexico City, and is the recipient of a scholarship from CONACyT, México (458510) CVU 792176. We acknowledge the Instituto Nacional de Cancerología - INCan Mexico, RAI, UNAM - Advanced Microscopy Applications Unit (ADMiRA), RRID:SCR_022788. We thank Virginia Enriquez-Carcamo, María Alexandra Rodríguez-Sastre, and Patricia de la Torre for technical support, and the Tumor Bank Department of the Instituto Nacional de Cancerología, México, for providing biological samples.

Conflicts of Interest: The authors declare no conflict of interest.

References

1. HPV Information Centre. Available online: https://hpvcentre.net/ (accessed on 19 December 2022).
2. Sabatini, M.E.; Chiocca, S. Human Papillomavirus as a Driver of Head and Neck Cancers. *Br. J. Cancer* **2020**, *122*, 306–314. [CrossRef] [PubMed]
3. Bray, F.; Ferlay, J.; Soerjomataram, I.; Siegel, R.L.; Torre, L.A.; Jemal, A. Global Cancer Statistics 2018: GLOBOCAN Estimates of Incidence and Mortality Worldwide for 36 Cancers in 185 Countries. *CA Cancer J. Clin.* **2018**, *68*, 394–424. [CrossRef]
4. Arbyn, M.; Weiderpass, E.; Bruni, L.; de Sanjosé, S.; Saraiya, M.; Ferlay, J.; Bray, F. Estimates of Incidence and Mortality of Cervical Cancer in 2018: A Worldwide Analysis. *Lancet Glob. Health* **2020**, *8*, e191–e203. [CrossRef] [PubMed]
5. Mittal, S.; Banks, L. Molecular Mechanisms Underlying Human Papillomavirus E6 and E7 Oncoprotein-Induced Cell Transformation. *Mutat. Res. Rev. Mutat. Res.* **2017**, *772*, 23–35. [CrossRef]
6. Gupta, S.; Kumar, P.; Das, B.C. HPV: Molecular Pathways and Targets. *Curr. Probl. Cancer* **2018**, *42*, 161–174. [CrossRef]
7. Thomas, M.; David, P.; Banks, L. The Role of the E6-P53 Interaction in the Molecular Pathogenesis of HPV. *Oncogene* **1999**, *18*, 7690–7700. [CrossRef]
8. Boyer, S.N.; Wazer, D.E.; Band2, V. E7 Protein of Human Papilloma Virus-16 Induces Degradation of Retinoblastoma Protein through the Ubiquitin-Proteasome Pathway'. *Cancer* **1996**, *56*, 4620–4624.
9. Vats, A.; Trejo-Cerro, O.; Thomas, M.; Banks, L. Human Papillomavirus E6 and E7: What Remains? *Tumour Virus Res.* **2021**, *11*, 200213. [CrossRef]
10. Martínez-Ramírez, I.; Carrillo-García, A.; Contreras-Paredes, A.; Ortiz-Sánchez, E.; Cruz-Gregorio, A.; Lizano, M. Regulation of Cellular Metabolism by High-Risk Human Papillomaviruses. *Int. J. Mol. Sci.* **2018**, *19*, 1839. [CrossRef] [PubMed]
11. Abbaszadeh, Z.; Çeşmeli, S.; Biray Avcı, Ç. Crucial Players in Glycolysis: Cancer Progress. *Gene* **2020**, *726*, 144158. [CrossRef]
12. Yang, L.; Venneti, S.; Nagrath, D. Glutaminolysis: A Hallmark of Cancer Metabolism. *Annu. Rev. Biomed. Eng.* **2017**, *19*, 163–194. [CrossRef]
13. Zou, J.; Du, K.; Li, S.; Lu, L.; Mei, J.; Lin, W.; Deng, M.; Wei, W.; Guo, R. Glutamine Metabolism Regulators Associated with Cancer Development and the Tumor Microenvironment: A Pan-Cancer Multi-Omics Analysis. *Genes* **2021**, *12*, 1305. [CrossRef]
14. Deberardinis, R.J.; Cheng, T. Q's next: The Diverse Functions of Glutamine in Metabolism, Cell Biology and Cancer. *Oncogene* **2010**, *29*, 313–324. [CrossRef]
15. Kodama, M.; Oshikawa, K.; Shimizu, H.; Yoshioka, S.; Takahashi, M.; Izumi, Y.; Bamba, T.; Tateishi, C.; Tomonaga, T.; Matsumoto, M.; et al. A Shift in Glutamine Nitrogen Metabolism Contributes to the Malignant Progression of Cancer. *Nat Commun.* **2020**, *11*, 1320. [CrossRef]
16. Bott, A.J.; Maimouni, S.; Zong, W.X. The Pleiotropic Effects of Glutamine Metabolism in Cancer. *Cancers* **2019**, *11*, 770. [CrossRef] [PubMed]
17. Erickson, J.W.; Cerione, R.A. Glutaminase: A Hot Spot for Regulation of Cancer Cell Metabolism? *Oncotarget* **2010**, *1*, 734–740. [CrossRef]
18. Kim, M.H.; Kim, H. Oncogenes and Tumor Suppressors Regulate Glutamine Metabolism in Cancer Cells. *J. Cancer Prev.* **2013**, *18*, 221–226. [CrossRef]
19. Yoo, H.C.; Yu, Y.C.; Sung, Y.; Han, J.M. Glutamine Reliance in Cell Metabolism. *Exp. Mol. Med.* **2020**, *52*, 1496–1516. [CrossRef]
20. Bröer, A.; Gauthier-Coles, G.; Rahimi, F.; van Geldermalsen, M.; Dorsch, D.; Wegener, A.; Holst, J.; Bröer, S. Ablation of the ASCT2 (SLC1A5) Gene Encoding a Neutral Amino Acid Transporter Reveals Transporter Plasticity and Redundancy in Cancer Cells. *J. Biol. Chem.* **2019**, *294*, 4012–4026. [CrossRef]
21. Park, Y.Y.; Sohn, B.H.; Johnson, R.L.; Kang, M.H.; Kim, S.B.; Shim, J.J.; Mangala, L.S.; Kim, J.H.; Yoo, J.E.; Rodriguez-Aguayo, C.; et al. Yes-Associated Protein 1 and Transcriptional Coactivator with PDZ-Binding Motif Activate the Mammalian Target of Rapamycin Complex 1 Pathway by Regulating Amino Acid Transporters in Hepatocellular Carcinoma. *Hepatology* **2016**, *63*, 159–172. [CrossRef] [PubMed]
22. Cormerais, Y.; Massard, P.A.; Vucetic, M.; Giuliano, S.; Tambutté, E.; Durivault, J.; Vial, V.; Endou, H.; Wempe, M.F.; Parks, S.K.; et al. The Glutamine Transporter ASCT2 (SLC1A5) Promotes Tumor Growth Independently of the Amino Acid Transporter LAT1 (SLC7A5). *J. Biol. Chem.* **2018**, *293*, 2877–2887. [CrossRef] [PubMed]
23. Leke, R.; Schousboe, A. The Glutamine Transporters and Their Role in the Glutamate/GABA-Glutamine Cycle. *Adv. Neurobiol.* **2016**, *13*, 223–257. [CrossRef] [PubMed]

24. Bhutia, Y.D.; Ganapathy, V. Glutamine Transporters in Mammalian Cells and Their Functions in Physiology and Cancer. *Biochim. Biophys. Acta* **2016**, *1863*, 2531–2539. [CrossRef]
25. López de la Oliva, A.R.; Campos-Sandoval, J.A.; Gómez-García, M.C.; Cardona, C.; Martín-Rufián, M.; Sialana, F.J.; Castilla, L.; Bae, N.; Lobo, C.; Peñalver, A.; et al. Nuclear Translocation of Glutaminase GLS2 in Human Cancer Cells Associates with Proliferation Arrest and Differentiation. *Sci. Rep.* **2020**, *10*, 2259. [CrossRef] [PubMed]
26. Ortiz-Pedraza, Y.; Muñoz-Bello, J.O.; Olmedo-Nieva, L.; Contreras-Paredes, A.; Martínez-Ramírez, I.; Langley, E.; Lizano, M. Non-Coding RNAs as Key Regulators of Glutaminolysis in Cancer. *Int. J. Mol. Sci.* **2020**, *21*, 2872. [CrossRef]
27. Mazurek, S.; Zwerschke, W.; Jansen-Dürr, P.; Eigenbrodt, E. Effects of the Human Papilloma Virus HPV-16 E7 Oncoprotein on Glycolysis and Glutaminolysis: Role of Pyruvate Kinase Type M2 and the Glycolytic-Enzyme Complex. *Biochem. J.* **2001**, *356*, 247–256. [CrossRef]
28. Zwerschke, W.; Mazurek, S.; Massimi, P.; Banks, L.; Eigenbrodt, E.; Jansen-Dürr, P. Modulation of Type M2 Pyruvate Kinase Activity by the Human Papillomavirus Type 16 E7 Oncoprotein. *Proc. Natl. Acad. Sci. USA* **1999**, *96*, 1291–1296. [CrossRef]
29. Chung, Y.L.; Nagy, E.; Zietkowski, D.; Payne, G.S.; Phillips, D.H.; DeSouza, N.M. Molecular and Metabolic Consequences Following E6 Transfection in an Isogenic Ovarian Cell Line (A2780) Pair. *Cell Physiol. Biochem.* **2013**, *32*, 1460–1472. [CrossRef]
30. Hémon, A.; Louandre, C.; Lailler, C.; Godin, C.; Bottelin, M.; Morel, V.; François, C.; Galmiche, A.; Saidak, Z. SLC7A11 as a Biomarker and Therapeutic Target in HPV-Positive Head and Neck Squamous Cell Carcinoma. *Biochem. Biophys. Res. Commun.* **2020**, *533*, 1083–1087. [CrossRef]
31. Olmedo-Nieva, L.; Muñoz-Bello, J.O.; Martínez-Ramírez, I.; Martínez-Gutiérrez, A.D.; Ortiz-Pedraza, Y.; González-Espinosa, C.; Madrid-Marina, V.; Torres-Poveda, K.; Bahena-Roman, M.; Lizano, M. RIPOR2 Expression Decreased by HPV-16 E6 and E7 Oncoproteins: An Opportunity in the Search for Prognostic Biomarkers in Cervical Cancer. *Cells* **2022**, *11*, 3942. [CrossRef]
32. Seavey, S.E.; Holubar, M.; Saucedo, L.J.; Perry, M.E. The E7 Oncoprotein of Human Papillomavirus Type 16 Stabilizes P53 through a Mechanism Independent of P19(ARF). *J. Virol.* **1999**, *73*, 7590–7598. [CrossRef]
33. Liu, X.; Liu, P.; Chernock, R.D.; Kuhs, K.A.L.; Lewis, J.S.; Luo, J.; Gay, H.A.; Thorstad, W.L.; Wang, X. A Prognostic Gene Expression Signature for Oropharyngeal Squamous Cell Carcinoma. *EBioMedicine* **2020**, *61*, 102805. [CrossRef]
34. The Human Protein Atlas. Available online: https://www.proteinatlas.org/ (accessed on 18 December 2022).
35. Ma, G.; Zhang, Z.; Li, P.; Zhang, Z.; Zeng, M.; Liang, Z.; Li, D.; Wang, L.; Chen, Y.; Liang, Y.; et al. Reprogramming of Glutamine Metabolism and Its Impact on Immune Response in the Tumor Microenvironment. *Cell Commun. Signal* **2022**, *20*, 14. [CrossRef] [PubMed]
36. Ahmad, F.; Cherukuri, M.K.; Choyke, P.L. Metabolic Reprogramming in Prostate Cancer. *Br. J. Cancer* **2021**, *125*, 1185–1196. [CrossRef]
37. Pavlova, N.N.; Thompson, C.B. The Emerging Hallmarks of Cancer Metabolism. *Cell Metab.* **2016**, *23*, 27–47. [CrossRef] [PubMed]
38. Sun, T.; Liu, Z.; Yang, Q. The Role of Ubiquitination and Deubiquitination in Cancer Metabolism. *Mol. Cancer* **2020**, *19*, 146. [CrossRef]
39. Jin, H.; Wang, S.; Zaal, E.A.; Wang, C.; Wu, H.; Bosma, A.; Jochems, F.; Isima, N.; Jin, G.; Lieftink, C.; et al. A Powerful Drug Combination Strategy Targeting Glutamine Addiction for the Treatment of Human Liver Cancer. *Elife* **2020**, *9*, e56749. [CrossRef]
40. Ekici, S.; Risk, B.B.; Neill, S.G.; Shu, H.K.; Fleischer, C.C. Characterization of Dysregulated Glutamine Metabolism in Human Glioma Tissue with 1H NMR. *Sci. Rep.* **2020**, *10*, 20435. [CrossRef]
41. Vanhove, K.; Derveaux, E.; Graulus, G.J.; Mesotten, L.; Thomeer, M.; Noben, J.P.; Guedens, W.; Adriaensens, P. Glutamine Addiction and Therapeutic Strategies in Lung Cancer. *Int. J. Mol. Sci.* **2019**, *20*, 252. [CrossRef]
42. Demas, D.M.; Demo, S.; Fallah, Y.; Clarke, R.; Nephew, K.P.; Althouse, S.; Sandusky, G.; He, W.; Shajahan-Haq, A.N. Glutamine Metabolism Drives Growth in Advanced Hormone Receptor Positive Breast Cancer. *Front Oncol.* **2019**, *9*, 686. [CrossRef]
43. Yuan, L.; Sheng, X.; Willson, A.K.; Roque, D.R.; Stine, J.E.; Guo, H.; Jones, H.M.; Zhou, C.; Bae-Jump, V.L. Glutamine Promotes Ovarian Cancer Cell Proliferation through the MTOR/S6 Pathway. *Endocr. Relat. Cancer* **2015**, *22*, 577–591. [CrossRef] [PubMed]
44. Arizmendi-Izazaga, A.; Navarro-Tito, N.; Jiménez-Wences, H.; Mendoza-Catalán, M.A.; Martínez-Carrillo, D.N.; Zacapala-Gómez, A.E.; Olea-Flores, M.; Dircio-Maldonado, R.; Torres-Rojas, F.I.; Soto-Flores, D.G.; et al. Metabolic Reprogramming in Cancer: Role of HPV 16 Variants. *Pathogens* **2021**, *10*, 347. [CrossRef]
45. Durán, R.V.; Oppliger, W.; Robitaille, A.M.; Heiserich, L.; Skendaj, R.; Gottlieb, E.; Hall, M.N. Glutaminolysis Activates Rag-MTORC1 Signaling. *Mol. Cell* **2012**, *47*, 349–358. [CrossRef] [PubMed]
46. Yoshida, G.J. The Harmonious Interplay of Amino Acid and Monocarboxylate Transporters Induces the Robustness of Cancer Cells. *Metabolites* **2021**, *11*, 27. [CrossRef] [PubMed]
47. Gwangwa, M.V.; Joubert, A.M.; Visagie, M.H. Effects of Glutamine Deprivation on Oxidative Stress and Cell Survival in Breast Cell Lines. *Biol. Res.* **2019**, *52*, 15. [CrossRef] [PubMed]
48. Janpipatkul, K.; Suksen, K.; Borwornpinyo, S.; Jearawiriyapaisarn, N.; Hongeng, S.; Piyachaturawat, P.; Chairoungdua, A. Downregulation of LAT1 Expression Suppresses Cholangiocarcinoma Cell Invasion and Migration. *Cell Signal* **2014**, *26*, 1668–1679. [CrossRef] [PubMed]
49. Guo, W.; Zhao, Y.; Zhang, Z.; Tan, N.; Zhao, F.; Ge, C.; Liang, L.; Jia, D.; Chen, T.; Yao, M.; et al. Disruption of XCT Inhibits Cell Growth via the ROS/Autophagy Pathway in Hepatocellular Carcinoma. *Cancer Lett.* **2011**, *312*, 55–61. [CrossRef] [PubMed]

50. Bothwell, P.J.; Kron, C.D.; Wittke, E.F.; Czerniak, B.N.; Bode, B.P. Targeted Suppression and Knockout of ASCT2 or LAT1 in Epithelial and Mesenchymal Human Liver Cancer Cells Fail to Inhibit Growth. *Int. J. Mol. Sci.* **2018**, *19*, 2093. [CrossRef] [PubMed]
51. Wang, M.; Liu, Y.; Fang, W.; Liu, K.; Jiao, X.; Wang, Z.; Wang, J.; Zang, Y.S. Increased SNAT1 Is a Marker of Human Osteosarcoma and Potential Therapeutic Target. *Oncotarget* **2017**, *8*, 78930–78939. [CrossRef] [PubMed]
52. Bröer, A.; Rahimi, F.; Bröer, S. Deletion of Amino Acid Transporter ASCT2 (SLC1A5) Reveals an Essential Role for Transporters SNAT1 (SLC38A1) and SNAT2 (SLC38A2) to Sustain Glutaminolysis in Cancer Cells. *J. Biol. Chem.* **2016**, *291*, 13194–13205. [CrossRef]
53. Saha, S.K.; Riazul Islam, S.M.; Abdullah-Al-Wadud, M.; Islam, S.; Ali, F.; Park, K.S. Multiomics Analysis Reveals That GLS and GLS2 Differentially Modulate the Clinical Outcomes of Cancer. *J. Clin. Med.* **2019**, *8*, 355. [CrossRef] [PubMed]
54. Dias, M.M.; Adamoski, D.; dos Reis, L.M.; Ascenção, C.F.R.; de Oliveira, K.R.S.; Mafra, A.C.P.; da Silva Bastos, A.C.; Quintero, M.; Cassago, C.D.G.; Ferreira, I.M.; et al. GLS2 Is Protumorigenic in Breast Cancers. *Oncogene* **2020**, *39*, 690–702. [CrossRef] [PubMed]
55. Lukey, M.J.; Cluntun, A.A.; Katt, W.P.; Lin, M.; Chong, J.; Druso, J.E.; Ramachandran, S.; Erickson, J.W.; Le, H.H.; Wang, Z.E.; et al. Liver-Type Glutaminase GLS2 Is a Druggable Metabolic Node in Luminal-Subtype Breast Cancer. *Cell Rep.* **2019**, *29*, 76–88. [CrossRef] [PubMed]
56. Hu, W.; Zhang, C.; Wu, R.; Sun, Y.; Levine, A.; Feng, Z. Glutaminase 2, a Novel P53 Target Gene Regulating Energy Metabolism and Antioxidant Function. *Proc. Natl. Acad. Sci. USA* **2010**, *107*, 7455–7460. [CrossRef] [PubMed]
57. Zhang, C.; Liu, J.; Zhao, Y.; Yue, X.; Zhu, Y.; Wang, X.; Wu, H.; Blanco, F.; Li, S.; Bhanot, G.; et al. Glutaminase 2 Is a Novel Negative Regulator of Small GTPase Rac1 and Mediates P53 Function in Suppressing Metastasis. *Elife* **2016**, *5*, e10727. [CrossRef]
58. Suzuki, S.; Tanaka, T.; Poyurovsky, M.V.; Nagano, H.; Mayama, T.; Ohkubo, S.; Lokshin, M.; Hosokawa, H.; Nakayama, T.; Suzuki, Y.; et al. Phosphate-Activated Glutaminase (GLS2), a P53-Inducible Regulator of Glutamine Metabolism and Reactive Oxygen Species. *Proc. Natl. Acad. Sci. USA* **2010**, *107*, 7461–7466. [CrossRef] [PubMed]
59. Giacobbe, A.; Bongiorno-Borbone, L.; Bernassola, F.; Terrinoni, A.; Markert, E.K.; Levine, A.J.; Feng, Z.; Agostini, M.; Zolla, L.; Agrò, A.F.; et al. P63 Regulates Glutaminase 2 Expression. *Cell Cycle* **2013**, *12*, 1395–1405. [CrossRef]
60. Wang, T.; Cai, B.; Ding, M.; Su, Z.; Liu, Y.; Shen, L. C-Myc Overexpression Promotes Oral Cancer Cell Proliferation and Migration by Enhancing Glutaminase and Glutamine Synthetase Activity. *Am. J. Med. Sci.* **2019**, *358*, 235–242. [CrossRef]
61. Böhme-Schäfer, I.; Lörentz, S.; Bosserhoff, A.K. Role of Amino Acid Transporter SNAT1/SLC38A1 in Human Melanoma. *Cancers* **2022**, *14*, 2151. [CrossRef]
62. Xie, J.; Li, P.; Gao, H.F.; Qian, J.X.; Yuan, L.Y.; Wang, J.J. Overexpression of SLC38A1 Is Associated with Poorer Prognosis in Chinese Patients with Gastric Cancer. *BMC Gastroenterol.* **2014**, *14*, 70. [CrossRef]
63. Wang, K.; Cao, F.; Fang, W.; Hu, Y.; Chen, Y.; Ding, H.; Yu, G. Activation of SNAT1/SLC38A1 in Human Breast Cancer: Correlation with p-Akt Overexpression. *BMC Cancer* **2013**, *13*, 343. [CrossRef] [PubMed]

pathogens

MDPI

Article

HPV Prevalence and Predictive Biomarkers for Oropharyngeal Squamous Cell Carcinoma in Mexican Patients

Diego Octavio Reyes-Hernández [1], Adriana Morán-Torres [1], Roberto Jimenez-Lima [1], Ana María Cano-Valdez [1], Carlo César Cortés-González [1], Leonardo Josué Castro-Muñoz [1,2], Leslie Olmedo-Nieva [1], Silvia Maldonado-Frías [3], Nidia Gary Pazos-Salazar [4], José de Jesús Marín-Aquíno [5], Alejandro García-Carrancá [1,6], Adela Carrillo-García [1], J. Omar Muñoz-Bello [1], Marcela Lizano [1,6,*] and Joaquín Manzo-Merino [1,7,*]

1 Unidad de Investigación Biomédica en Cáncer, Instituto Nacional de Cancerología, Mexico City 14080, Mexico
2 The Wistar Institute, Philadelphia, PA 19104, USA
3 División de Estudios de Posgrado e Investigación, Facultad de Odontología, Universidad Nacional Autónoma de México, Mexico City 04360, Mexico
4 Facultad de Ciencias Químicas, Benemérita Universidad Autónoma de Puebla, Puebla City 72570, Mexico
5 Departamento de Patología, Hospital Dr. Manuel Gea González, Mexico City 14080, Mexico
6 Departamento de Medicina Genómica y Toxicología Ambiental, Instituto de Investigaciones Biomédicas, Universidad Nacional Autónoma de México, Mexico City 04510, Mexico
7 Cátedras CONACyT-Instituto Nacional de Cancerología, Mexico City 14080, Mexico
* Correspondence: lizanosoberon@gmail.com (M.L.); jmanzomerino@gmail.com (J.M.-M.)

Citation: Reyes-Hernández, D.O.; Morán-Torres, A.; Jimenez-Lima, R.; Cano-Valdez, A.M.; Cortés-González, C.C.; Castro-Muñoz, L.J.; Olmedo-Nieva, L.; Maldonado-Frías, S.; Pazos-Salazar, N.G.; de Jesús Marín-Aquíno, J.; et al. HPV Prevalence and Predictive Biomarkers for Oropharyngeal Squamous Cell Carcinoma in Mexican Patients. *Pathogens* **2022**, *11*, 1527. https://doi.org/10.3390/pathogens11121527

Academic Editor: Yao-Min Hung

Received: 22 October 2022
Accepted: 7 December 2022
Published: 13 December 2022

Abstract: Background: Worldwide prevalence of Oropharyngeal Squamous Cell Carcinoma (OPSCC) has increased, affecting mostly young males. OPSCC associated with Human Papillomavirus (HPV) infection exhibits particular characteristics in terms of response to treatment, hence HPV has been proposed as a prognostic factor. The impact of HPV positivity and associated biomarkers on OPSCC in the Mexican population has not been addressed. Therefore, the analysis of OPSCC prognostic markers in the Mexican population is necessary. Methods: Retrolective study in Mexican OPSCC patients, where HPV prevalence, p16 and EGFR levels were assessed using INNO-LiPA and immunohistochemistry. Results: We found an HPV prevalence of 57.6% in OPSCC cases treated at a reference center in Mexico. HPV and p16 positivity, as well as EGFR, associate with better outcomes in OPSCC patients, and they also promote reduced death risk. Notably, HPV presence and p16 positivity showed a significant association with disease-free survival (DFS), with a HR of 0.15 ($p = 0.006$) and a HR of 0.17 ($p = 0.012$), respectively, indicating a possible role as predictive biomarkers in Mexican OPSCC patients. Conclusions: Our results reflect the clinical utility of p16 analysis to improve overall survival (OS) and to predict recurrence in oropharyngeal cancer. These results position p16 and HPV as predictive biomarkers for OPSCC.

Keywords: HPV; OPSCC; p16; biomarker; Mexican population

1. Introduction

Head and neck cancer (HNC) is a public health threat, representing the seventh most common neoplasia with approximately 562,328 annual cases [1]. HNC has been associated with alcohol and tobacco consumption traditionally. Nonetheless, Human Papillomavirus (HPV) infection has been recognized as an important etiological factor for HNC development in the past years, mainly affecting the oropharyngeal region [2]. Particularly, oropharyngeal squamous cell carcinoma (OPSCC) has gained attention in past decades due to the alarming increase in numbers, especially in HPV-associated cases [3,4]. HPV-positive HNC is associated with the practice of oral sex, mainly affecting young men. The presence of HPV confers better prognosis after a radiotherapy treatment and a better overall survival (OS) [5].

An improvement in OS has been described for HPV-positive cancers, as determined by detecting HPV DNA or by analysis of subrogate marker, p16, expression by immunohistochemistry (IHC) [6]. Recently, the RTOG-0234 group presented the results of a retrospective analysis of clinical trials 0129 and 0522, where the utility of p16 as a predictive factor was found, indicating that positivity to this biomarker not only predicts OS, but also recurrence-free survival (RFS), thus promoting the value of p16 identification in patients with HNC [7]. Although the evidence indicates that p16 could be a good prognostic factor in HNC, its potential utility, together with the presence of HPV, has yielded controversial results, indicating that these markers should be further explored in different populations [8–10].

Moreover, several proteins are associated with improved survival in HNC. For instance, the epidermal growth factor receptor (EGFR) is found to be overexpressed in head and neck squamous cell carcinomas (HNSCC) [11], mostly in HPV-negative cases [12–14]. In the majority of these tumors, this receptor is overexpressed or harbors mutations [15], representing a drug target that provides therapeutic opportunities for these patients [16]. However, the search for additional biomarkers for HNC is still underway.

The prevalence of HPV in HNC in Mexico and biomarker application studies are currently limited. In a retrospective case series of HNC of Mexican patients, the prevalence of HPV ranged from 22.3 to 42%. Specifically, for the oral cavity, 17.2–18.75% has been reported, while in oropharyngeal cancer, the prevalence ranges from 40.5–68.75%, and a low proportion has been identified for the larynx, ranging between 6.25 to 18.2% [17–19]. However, the potential clinical application of the presence of HPV or the expression of additional subrogate biomarkers, particularly for OPSCC, has been poorly explored in the Mexican population, considering the possible increase in this neoplasm in the coming years. Thus, we aimed to describe the prevalence of HPV, as well as the clinical features of OPSCC patients in a national reference institution in Mexico, and to determine the potential utility of HPV presence and p16 positivity as prognostic biomarkers in the Mexican population.

2. Materials and Methods

2.1. Clinical Specimens and Patient Characteristics

This retrospective study analyzed biopsies from OPSCC patients treated at the National Cancer Institute of Mexico. We obtained data from patients who received treatment between 2000 to 2017, and their respective clinical and sociodemographic characteristics were collected. The study protocol was approved by the Ethics (CEI/998/15) and Scientific (015/039/IBI) Institutional review boards and followed the guidelines of the Declaration of Helsinki.

The present cohort study comprised 66 cases, selected for meeting the following criteria: existence of formalin-fixed paraffin-embedded (FFPE) primary tumor material prior to treatment with curative intent, histologically proven squamous cell carcinoma (SCC) originated from the tonsillar portion, and different stages were included according to the 7th TNM edition for oropharyngeal cancer (I, II, III, IV and IVa). Medical records were used to collect demographic and clinical features. Cases treated for metastatic and palliative treatment were excluded, as well as those lacking complete data.

2.2. Histological Evaluation

FFPE tumor blocks were obtained from the institutional pathology bank. Subsequently, 2 µm-thick tissue sections were obtained. To verify the diagnosis of SCC and demarcate the malignant cells, evaluation of H&E tissue slides was performed by a pathologist specializing in head and neck cancer

2.3. Immunohistochemistry

Tissue sections from 66 patients were used for the IHC staining, using the p16 mouse monoclonal antibody (ROCHE®) (Roche Holding AG, Basel, Swiss). The Ventana Benchmark LT automated immunostainer (ROCHE®) was used following the standard protocol for p16 [20]. Appropriate tissue staining controls were used routinely. A p16 IHC was

considered positive if the tumor section had strong and diffuse nuclear and cytoplasmatic staining in >70% of malignant cells [21]. EGFR IHC was performed with anti-EGFR antibody (Abcam®) (Abcam Biotechnology company, Cambridge, UK) using the Mouse/Rabbit Polydetector DAB HRP Brown System (Bio SB®) (Bio SB, Inc., Goleta, CA, UEA), according to the manufacturer's instructions. The level of expression was assessed by an expert pathologist, and data were categorized into high or low expression.

2.4. DNA Extraction and HPV Genotyping

Ten µm-thick tissue sections were obtained from the FFPE blocks and then employed for DNA purification using the DNeasy Blood & Tissue Kit (QIAGEN®) (QIAGEN, Hilden, Germany) according to manufacturer's instructions. DNA samples were quantified in a full spectrum Nanodrop™ spectrophotometer (ThermoScientific®) (Thermo Fisher Scientific, Waltham, MA, UEA) and further utilized for HPV identification using the INNO-LiPA® HPV Genotyping Extra II (Fujirebio®) (Fujirebio, Tokyo, Japan) assay. This test is based on reverse hybridization after highly sensitive PCR amplification with SPF10 primers that allow the detection of 32 HPV genotypes simultaneously [22]. For each test, internal routine controls were used.

2.5. Statistical Analysis

Data were collected and descriptive statistics were used to summarize the demographic and clinical features. The OS and disease-free survival (DFS) estimations were made using the Kaplan–Meier method according to positiveness or protein levels. Additionally, the Log-Rank test was employed to make comparisons between tests. Hazard Ratios (HR) were calculated for each group if statistical significance was achieved. $p \leq 0.05$ was considered as statistically significant. All statistical analyses were carried out using SPSS® V.21 (IBM Corp., Armonk, NY, USA).

3. Results

3.1. Population Description and HPV Prevalence

A total of 66 cases of OPSCC that met the inclusion criteria were included. The demographic and pathological characteristics are described in Table 1. Most of the study population were men (78.7%) with a median age of 60.67 years; 43.9% had only elementary school education. Alcohol and tobacco consumption were present in 66.7% and 71.2% of the patients, respectively. Advanced stages (IVA, IVB) represented 39.4% of the cohort.

Table 1. Population description.

Variable.	n = 66 (100%)
Age median (±SD)	
Both sexes	60.67 * (±11.78)
Men	59.48 * (±11.20)
Women	65.07 ** (±13.25)
Sex	
Men	52 (78.7%)
Education &	
Illiterate	17 (25.8%)
Elementary school	29 (43.9%)
High school	11 (16.7%)
Superior school	7 (10.6%)
Undetermined	2 (3%)
Comorbidities	
No	48 (72.7%)
Yes	14 (21.2%)
Undetermined	4 (6.1%)

Table 1. *Cont.*

Variable.	n = 66 (100%)
History of alcoholism	
Yes	44 (66.7%)
No	21 (31.8%)
Undeterminate	1 (1.5%)
History of smoking	
Yes	47 (71.2%)
No	18 (27.3%)
Undetermined	1 (1.5%)
Clinical stage	
II	3 (4.5%)
III	7 (10.6%)
IV A	17 (25.8%)
IV B	9 (13.6%)
Indeterminate	30 (45.5%)
Therapeutic regimen	
Surgery	10 (15.2%)
Chemotherapy	4 (6.1%)
Chemo-radiotherapy	27 (40.9%)
Radiotherapy	6 (9.1%)
Undetermined	19 (28.8%)
Clinical response	
Complete	23 (34.8%)
Partial	8 (12.1%)
Stable disease	5 (7.6%)
Progression	3 (4.5%)
Undetermined	5 (7.6%)
No data	22 (33.3%)
Recurrence (Only complete response)	n = 23 (100%)
No	12 (52.18%)
Yes	11 (47.82%)
HPV	n = 66 (100%)
Positive	38 (57.6%)
Negative	26 (39.4%)
Undetermined	2 (3.0%)
p16	n = 66 (100%)
Positive	27 (40.9%)
Negative	38 (57.6%)
Indeterminate	1 (1.5%)
EGFR (Intensity)	n = 29 (100%)
High	12 (41.4%)
Low	13 (44.8%)
Undetermined	4 (13.8%)

* Kolmogorov–Smirnov normality test; Global: $p = 0.041$; Men: $p = 0.015$; ** Shapiro–Wilk normality test: Women: $p = 0.816$; & Elementary: 6–12 yo; High school: 12–18 yo; Superior school: 18 yo and on.

Chemoradiation was the most common therapy regimen (40.9% of cases), and 23 cases (34.8%) presented complete clinical response, among which 11 cases presented disease recurrence.

57.6% of the cases were positive for HPV, with HPV16 the most prevalent genotype in 28 cases (73.68%). In addition, the presence of other HPV types, including HPV 6, 11, 18, 53 and 59, were detected as coinfections with HPV16, and 3 cases were positive for both HPV11 and 16. The median age of HPV-positive cases was 60.64 years, while HPV-negative cases exhibited a median age of 60.67 years.

3.2. Protein Expression and HPV Association

The expression patterns of p16 and EGFR proteins were evaluated by immunohistochemistry. Each antibody was validated on positive tissues prior to evaluating OPSCC cases. Protein levels were classified as positive or negative for p16 and high or low for EGFR, based on expression. A total of 27 cases were classified as p16 positive (40.9%), while 12 cases were EGFR high (41.4%).

In addition, association tests were performed to determine whether viral presence influenced the expression of the analyzed proteins. We determined that there was no statistically significant association between the presence of HPV and EGFR (data not shown). However, the presence of HPV is significantly associated with p16 expression ($p = 0.008$), as previously shown [23].

3.3. Association of Viral Presence, EGFR and p16 Levels with OS in Mexican Patients

We proceeded to analyze the impact of EGFR and p16 protein levels, as well as viral presence, on OS. First, the OS time in the analyzed cohort was calculated, resulting in a median of 8.31 months (95% CI: 2.38–14.24) (Figure 1A). Subsequently, the impact of the presence of HPV on OS was determined, resulting in viral presence significantly associated with an increase in OS ($p = 0.008$), where positive cases exhibit a median survival of 10.44 months (95% CI: 0.0–21.40), compared to HPV-negative cases with only 4.66 months (95% CI: 0.0–9.91) (Figure 1B). Furthermore, when performing Cox regression analysis, viral presence provides a 53% risk reduction for death with a HR (Hazard ratio) of 0.47 (95% CI: 0.26–0.83) ($p = 0.010$).

When analyzing OS with respect to p16 and EGFR levels, both proteins were found to have an impact on patient OS. High EGFR expression had a significant impact on OS ($p = 0.024$), predicting an unfavorable outcome, with the high expression group showing a median of only 4.66 months (95% CI: 0.0–10.68), while patients with low EGFR expression had a median of 61.89 months (95% CI: 0.0–127.63) (Figure 1C). The estimated median survival for p16-negative patients was 4.66 months (95% CI: 0.0–9.75), while for those who were positive for p16, it was 46.75 months (95% CI: 0.0–111.05). A statistically significant difference was found ($p \leq 0.0001$) when performing the Cox proportional hazards analysis for p16 levels, with a HR of 0.31 (95% CI: 0.26–0.83). In other words, there is a 69% reduction in the risk of death with positive p16 staining (Figure 1D).

3.4. Viral Presence and p16 Positivity Are Associated with DFS in OPSCC Mexican Patients

A total of 23 cases had a complete response to treatment. Nevertheless, 11 of these cases presented recurrence of the disease (47.82%) during the first 9 months after clinical response. A median of 8.47 months for DFS was calculated for the population examined (Figure 2A). To assess the usefulness of p16 and the presence of HPV as predictive biomarkers, their association with DFS was tested.

The association between viral presence and DFS was analyzed, showing a median of 6.01 months for HPV-negative cases (95% CI: 0.0–12.31). While positive HPV cases did not reach the median, a fraction of 40% was free of disease after 60 months. A statistically significant difference (* $p = 0.002$) was found for viral presence and DFS (Figure 2B). This result strongly indicates that HPV positivity establishes a late appearance of recurrence. Cox proportional hazards analysis indicated a statistically significant difference ($p = 0.006$), obtaining a HR of 0.15 (95% CI: 0.03–0.57), which indicates that the presence of HPV reduces the risk of recurrence by 85%. Furthermore, when analyzing the performance of p16 for DFS, p16-negative cases exhibited a median DFS of 9.13 months (95% CI: 2.28–15.98), while positive cases did not reach a median; however, 60% of the patients were disease-free after 60 months. Importantly, we found p16 levels were statistically associated with DFS ($p = 0.005$), indicating that p16 positivity predicts late-onset recurrence (Figure 2C). Cox proportional hazards analysis indicated a statistically significant difference ($p = 0.012$) with a HR of 0.17 (95% CI: 0.04–0.68), showing that p16 positivity reduces the risk of recurrence by 83%.

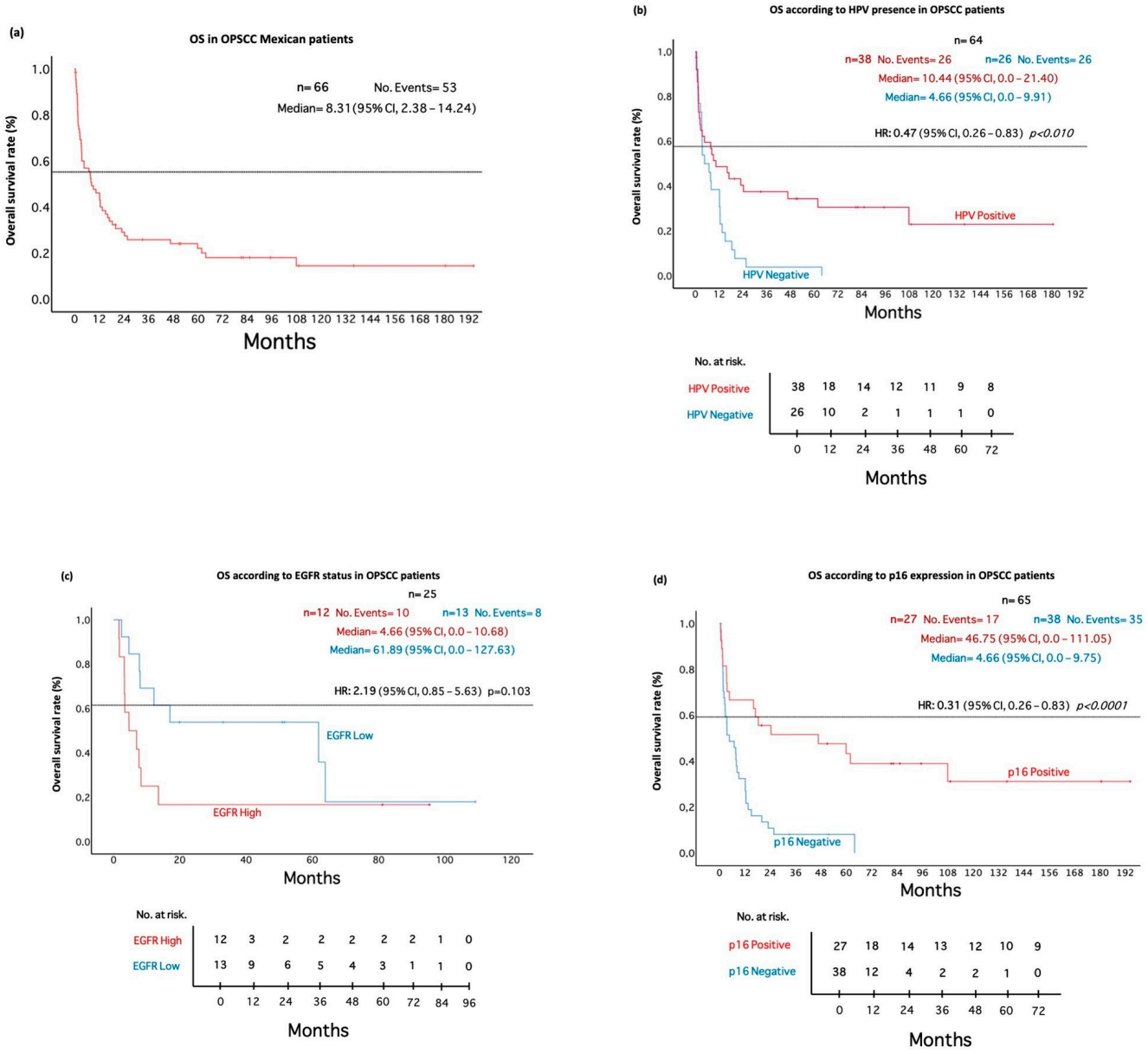

Figure 1. Overall survival in OPSCC patients according to HPV, p16 and EGFR. (**a**) Overall survival of the analyzed cohort. (**b**) HPV presence improves OS in OPSCC Mexican patients. (**c**) p16 impacts OS in OPSCC patients. (**d**) High EGFR levels are associated with poor OS in OPSCC Mexican patients.

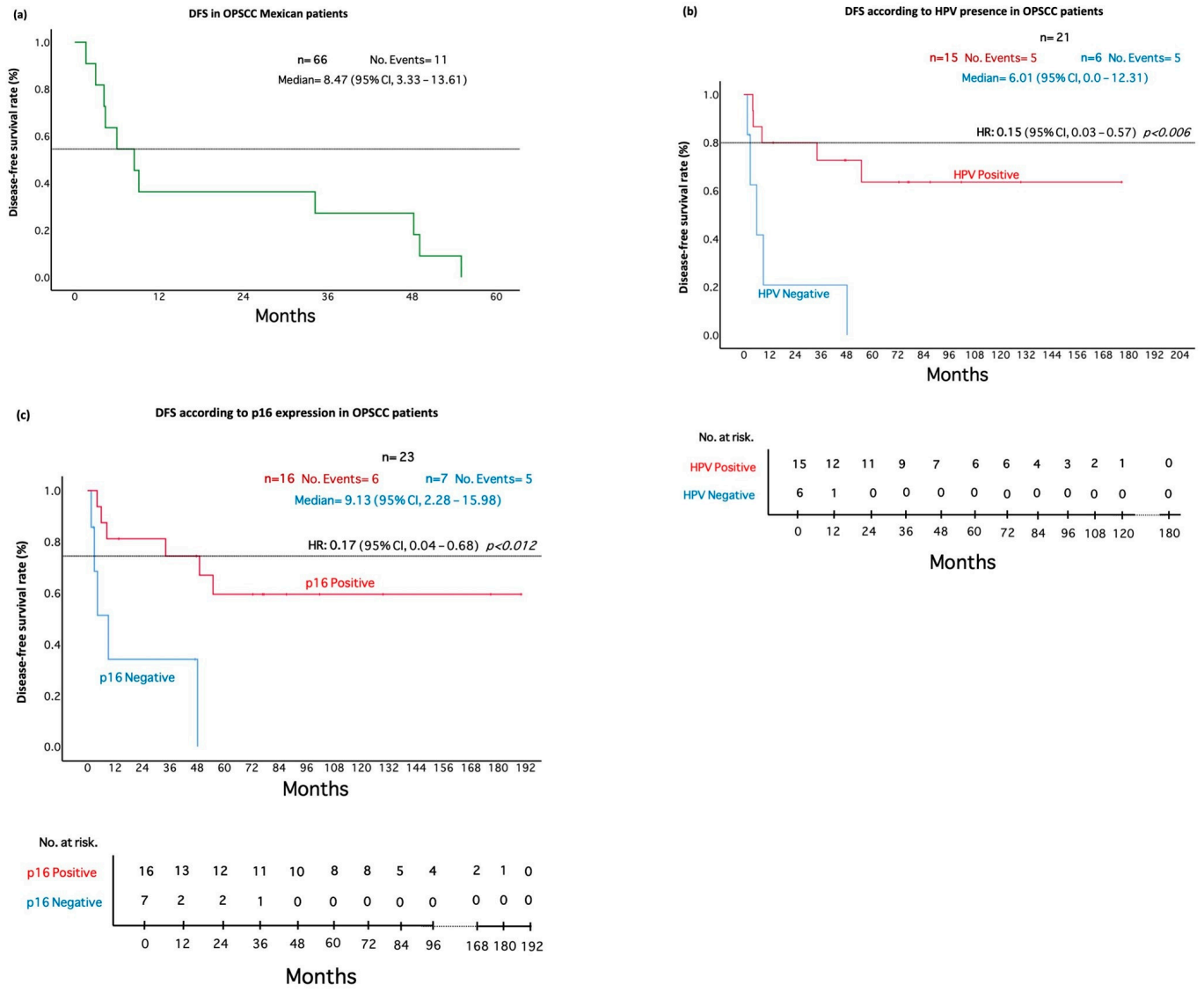

Figure 2. Disease-free survival in OPSCC patients according to HPV and p16 positivity. (**a**) Disease-free survival of the analyzed cohort. (**b**) HPV presence is associated with better DFS in OPSCC Mexican patients. (**c**) p16 predicts improved DFS in OPSCC Mexican patients.

4. Discussion

In recent years, OPSCC has shown an increase in incidence, especially in young men [5,24,25]. According to various reports, OPSCC has shown a greater increase than cervical cancer in the United States [3,4,26,27]. Although, this scenario has not yet been documented in Mexico, this possibility cannot be ruled out in the future because GLOBOCAN predictions estimate an increase of 100% in the coming years [28]. Thus, we aimed to analyze OPSCC cases in a Mexican population, determining HPV and potential biomarkers to support clinical management of patients and to improve therapeutic options with the ultimate goal of increasing therapeutic success.

We found a high prevalence of HPV in OPSCC (57.6%); in particular, HPV16 was detected in 73.68% of the positive cases. It has been stated that HPV-positive cases are associated with better prognosis [6], but the role of HPV in this phenomenon remains unclear. Although HPV positivity improves OS, its role in recurrence has only been explored in a couple of studies. In addition, there are cases of OPSCC that do not present an optimal response to treatment; therefore, we took on the task of exploring potential predictive biomarkers that could be useful in clinical practice.

In the present cohort, we found that men are the most affected by OPSCC (78.7%), which is consistent with other reports that associate this phenomenon with alcohol and tobacco consumption [5,29,30], a fact that was repeated in our cohort. Conversely, when analyzing the age at diagnosis, it was found that our patients had a median age of 60.91 years, including both HPV positive and HPV negative. Age over 60 is associated with HPV-negative cases, while HPV-positive cases exhibit a younger age at presentation [5,31]. Our results support the hypothesis that our population does not yet present the epidemiological transition towards young individuals. However, according to epidemiological predictions, an increase in the number of OPSCC cases is expected for our country, which could mean an increase in HPV-positive cases in the young population. In this regard, a recent work by our research group showed that young individuals exhibit a high prevalence of HPV infection (about 50%) in the oral cavity and oropharynx, presenting constant reinfections [32]. This fact may represent an important stimulus in cancer induction for future OPSCC cases.

One of the markers associated with the presence of HPV is the p16 protein, which acts as a surrogate marker for the effects of the E7 viral oncoprotein on pRb [33]. In the present work, p16 was found to be a potential prognostic and predictive biomarker, with a protective factor similar to that reported by Sturgis EM et al. and Harari et al. [34,35], although with lower median OS, probably because most of our cases were diagnosed in advanced clinical stages (IVA and IVB).

One of the factors associated with lower OS is the presence of disease recurrence after a successful treatment [36,37]. In our cohort, half of the patients with complete response were found to develop recurrence at a median of 54.99 months. Notably, only two reports have explored prognostic markers that help to predict recurrence events, thus our study lays the groundwork for using p16 as a marker capable of predicting the delayed onset of OPSCC recurrence in our population. To our knowledge, only Harari et al. (2014) and recently Bigelow et al. (2022) have reported similar results in randomized clinical trials (RTOG-0234) [7,35]. Particularly, these studies used combined therapy based on chemoradiotherapy (Cisplatin or Docetaxel) plus Cetuximab, and their results indicate that p16 positivity confers a longer DFS time [7,35]. In this study, we propose that p16 could function as a recurrence marker, regardless of the treatment regimen. Although only one of the patients in our cohort received anti-EGFR therapy, the finding that high EGFR levels are associated with lower OS highlights the need to classify patients based on EGFR status, as they might be candidates for anti-EGFR therapies, which represents an opportunity to increase OS and DFS in patients with OPSCC in Mexico.

Our study presents some limitations regarding the number of cases included and the late stages at diagnosis. Nonetheless, we present solid data regarding HPV prevalence in the OPSCC Mexican population that could help to identify patients with better prognoses. Future studies are required to postulate additional biomarkers to improve OS, DFS and quality of life in Mexican patients.

5. Conclusions

We identified p16 expression as a biomarker for recurrence and OS in OPSCC Mexican patients. These results pose p16 as a predictive biomarker when HPV detection is not possible. Moreover, it was verified that HPV positivity has an impact on the OS of patients with OPSCC, whose pattern of protein expression could help in the improvement of therapies.

Author Contributions: Conceptualization, J.M.-M. and M.L.; methodology, D.O.R.-H., R.J.-L., A.M.-T., A.M.C.-V., C.C.C.-G., L.J.C.-M., L.O.-N., S.M.-F., N.G.P.-S., J.d.J.M.-A., A.G.-C., A.C.-G. and J.O.M.-B.; writing—original draft preparation, J.M.-M., D.O.R.-H. and M.L.; writing—review and editing, S.M.-F., N.G.P.-S., A.G.-C. and J.O.M.-B.; visualization, D.O.R.-H., R.J.-L., L.O.-N., A.M.C.-V. and C.C.C.-G.; supervision, J.M.-M. and M.L.; funding acquisition, J.M.-M. and M.L. All authors have read and agreed to the published version of the manuscript.

Funding: This work was partially supported CONACyT PRONAII-7-VIRUS Y CÁNCER Ref: 303044 and by Instituto Nacional de Cancerología, Mexico, Ref: (015/039/IBI)(CEI/998/15) and (018/037/IBI)(CEI/1284/18).

Institutional Review Board Statement: The study was approved by the Institutional Ethics and Scientific Boards of Instituto Nacional de Cancerología (015/039/IBI)(CEI/998/15).

Informed Consent Statement: Patient consent was waived by the Institutional Ethics Board due to the retrospective nature of this project.

Data Availability Statement: The data that support the findings of this study are available from the corresponding author upon reasonable request.

Acknowledgments: We are very grateful to Miriam C. Guido-Jiménez and María Alexandra Rodriguez Sastre from Instituto de Investigaciones Biomédicas, UNAM for technical assistance. We are also very grateful to Elizabeth Langley from the National Cancer Institute of Mexico for critical reading and language revision of the manuscript.

Conflicts of Interest: The authors declare no conflict of interest.

References

1. Mody, M.D.; Rocco, J.W.; Yom, S.S.; Haddad, R.I.; Saba, N.F. Head and Neck Cancer. *Lancet* **2021**, *398*, 2289–2299. [CrossRef] [PubMed]
2. Castellsagué, X.; Alemany, L.; Quer, M.; Halec, G.; Quirós, B.; Tous, S.; Clavero, O.; Alòs, L.; Biegner, T.; Szafarowski, T.; et al. HPV Involvement in Head and Neck Cancers: Comprehensive Assessment of Biomarkers in 3680 Patients. *J. Natl. Cancer Inst.* **2016**, *108*, djv403. [CrossRef] [PubMed]
3. Chaturvedi, A.K.; Engels, E.A.; Pfeiffer, R.M.; Hernandez, B.Y.; Xiao, W.; Kim, E.; Jiang, B.; Goodman, M.T.; Sibug-Saber, M.; Cozen, W.; et al. Human Papillomavirus and Rising Oropharyngeal Cancer Incidence in the United States. *J. Clin. Oncol.* **2011**, *29*, 4294–4301. [CrossRef]
4. Gillison, M.L.; Castellsagué, X.; Chaturvedi, A.; Goodman, M.T.; Snijders, P.; Tommasino, M.; Arbyn, M.; Franceschi, S. Eurogin Roadmap: Comparative Epidemiology of HPV Infection and Associated Cancers of the Head and Neck and Cervix. *Int. J. Cancer* **2014**, *134*, 497–507. [CrossRef] [PubMed]
5. Taberna, M.; Mena, M.; Pavón, M.A.; Alemany, L.; Gillison, M.L.; Mesía, R. Human Papillomavirus-Related Oropharyngeal Cancer. *Ann. Oncol.* **2017**, *28*, 2386–2398. [CrossRef]
6. Ang, K.K.; Harris, J.; Wheeler, R.; Weber, R.; Rosenthal, D.I.; Nguyen-Tân, P.F.; Westra, W.H.; Chung, C.H.; Jordan, R.C.; Lu, C.; et al. Human Papillomavirus and Survival of Patients with Oropharyngeal Cancer. *N. Engl. J. Med.* **2010**, *363*, 24–35. [CrossRef]
7. Bigelow, E.O.; Harris, J.; Fakhry, C.; Gillison, M.L.; Nguyen-Tân, P.F.; Rosenthal, D.I.; Frank, S.J.; Nair, S.G.; Bahig, H.; Ridge, J.A.; et al. Risk Stratification after Recurrence of Human Papillomavirus (HPV)-Related and Non-HPV-Related Oropharyngeal Cancer: Secondary Analysis of NRG Oncology RTOG 0129 and 0522. *Head Neck* **2022**, *44*, 158–167. [CrossRef]
8. Golusiński, P.; Pazdrowski, J.; Szewczyk, M.; Misiołek, M.; Pietruszewska, W.; Klatka, J.; Okła, S.; Kaźmierczak, H.; Marszałek, A.; Filas, V.; et al. Is Immunohistochemical Evaluation of P16 in Oropharyngeal Cancer Enough to Predict the HPV Positivity? *Rep. Pract. Oncol. Radiother.* **2017**, *22*, 237–242. [CrossRef]
9. Liang, C.; Marsit, C.J.; McClean, M.D.; Nelson, H.H.; Christensen, B.C.; Haddad, R.I.; Clark, J.R.; Wein, R.O.; Grillone, G.A.; Houseman, E.A.; et al. Biomarkers of HPV in Head and Neck Squamous Cell Carcinoma. *Cancer Res.* **2012**, *72*, 5004–5013. [CrossRef]
10. Wilde, D.C.; Castro, P.D.; Bera, K.; Lai, S.; Madabhushi, A.; Corredor, G.; Koyuncu, C.; Lewis, J.S.J.; Lu, C.; Frederick, M.J.; et al. Oropharyngeal Cancer Outcomes Correlate with P16 Status, Multinucleation and Immune Infiltration. *Mod. Pathol.* **2022**, *35*, 1045–1054. [CrossRef]
11. The Cancer Genome Atlas Network. Comprehensive Genomic Characterization of Head and Neck Squamous Cell Carcinomas. *Nature* **2015**, *517*, 576–582. [CrossRef] [PubMed]
12. Taberna, M.; Torres, M.; Alejo, M.; Mena, M.; Tous, S.; Marquez, S.; Pavón, M.A.; León, X.; García, J.; Guix, M.; et al. The Use of HPV16-E5, EGFR, and PEGFR as Prognostic Biomarkers for Oropharyngeal Cancer Patients. *Front. Oncol.* **2018**, *8*, 589. [CrossRef] [PubMed]
13. Aggarwal, N.; Yadav, J.; Thakur, K.; Bibban, R.; Chhokar, A.; Tripathi, T.; Bhat, A.; Singh, T.; Jadli, M.; Singh, U.; et al. Human Papillomavirus Infection in Head and Neck Squamous Cell Carcinomas: Transcriptional Triggers and Changed Disease Patterns. *Front. Cell. Infect. Microbiol.* **2020**, *10*, 537650. [CrossRef] [PubMed]
14. Janecka-Widła, A.; Majchrzyk, K.; Mucha-Małecka, A.; Biesaga, B. EGFR/PI3K/Akt/MTOR Pathway in Head and Neck Squamous Cell Carcinoma Patients with Different HPV Status. *Pol. J. Pathol.* **2021**, *72*, 296–314. [CrossRef] [PubMed]
15. Nair, S.; Bonner, J.A.; Bredel, M. EGFR Mutations in Head and Neck Squamous Cell Carcinoma. *Int. J. Mol. Sci.* **2022**, *23*, 3818. [CrossRef] [PubMed]

16. Astsaturov, I.; Cohen, R.B.; Harari, P. EGFR-Targeting Monoclonal Antibodies in Head and Neck Cancer. *Curr. Cancer Drug Targets* **2007**, *7*, 650–665. [CrossRef]
17. Ibieta-Zarco, B.R.; Carrillo-García, A.; Ponce-De-León-Rosales, S.; Flores-Miranda, M.M.; Mohar, A.; Lizano, M. Frequency and Genotype Distribution of Multiple Human Papillomavirus Infections in Cancer of the Head and Neck in a Mexican Population. *Oral Surg. Oral Med. Oral Pathol. Oral Radiol.* **2012**, *114*, 350–357. [CrossRef]
18. Ibieta, B.R.; Lizano, M.; Fras-Mendivil, M.; Barrera, J.L.; Carrillo, A.; Ma Ruz-Godoy, L.; Mohar, A. Human Papilloma Virus in Oral Squamous Cell Carcinoma in a Mexican Population. *Oral Surg. Oral Med. Oral Pathol. Oral Radiol. Endod.* **2005**, *99*, 311–315. [CrossRef]
19. Méndez-Matías, G.; Velázquez-Velázquez, C.; Castro-Oropeza, R.; Mantilla-Morales, A.; Ocampo-Sandoval, D.; Burgos-González, A.; Heredia-Gutiérrez, C.; Alvarado-Cabrero, I.; Sánchez-Sandoval, R.; Barco-Bazán, A.; et al. Prevalence of HPV in Mexican Patients with Head and Neck Squamous Carcinoma and Identification of Potential Prognostic Biomarkers. *Cancers* **2021**, *13*, 5602. [CrossRef]
20. Jordan, R.C.; Lingen, M.W.; Perez-Ordonez, B.; He, X.; Pickard, R.; Koluder, M.; Jiang, B.; Wakely, P.; Xiao, W.; Gillison, M.L. Validation of Methods for Oropharyngeal Cancer HPV Status Determination in US Cooperative Group Trials. *Am. J. Surg. Pathol.* **2012**, *36*, 945–954. [CrossRef]
21. Atkins, D.; Reiffen, K.-A.; Tegtmeier, C.L.; Winther, H.; Bonato, M.S.; Störkel, S. Immunohistochemical Detection of EGFR in Paraffin-Embedded Tumor Tissues: Variation in Staining Intensity Due to Choice of Fixative and Storage Time of Tissue Sections. *J. Histochem. Cytochem.* **2004**, *52*, 893–901. [CrossRef] [PubMed]
22. Kleter, B.; van Doorn, L.J.; Schrauwen, L.; Molijn, A.; Sastrowijoto, S.; ter Schegget, J.; Lindeman, J.; ter Harmsel, B.; Burger, M.; Quint, W. Development and Clinical Evaluation of a Highly Sensitive PCR-Reverse Hybridization Line Probe Assay for Detection and Identification of Anogenital Human Papillomavirus. *J. Clin. Microbiol.* **1999**, *37*, 2508–2517. [CrossRef] [PubMed]
23. Saito, Y.; Yoshida, M.; Omura, G.; Kobayashi, K.; Fujimoto, C.; Ando, M.; Sakamoto, T.; Asakage, T.; Yamasoba, T. Prognostic Value of P16 Expression Irrespective of Human Papillomavirus Status in Patients with Oropharyngeal Carcinoma. *Jpn. J. Clin. Oncol.* **2015**, *45*, 828–836. [CrossRef] [PubMed]
24. Chaturvedi, A.K.; Anderson, W.F.; Lortet-Tieulent, J.; Paula Curado, M.; Ferlay, J.; Franceschi, S.; Rosenberg, P.S.; Bray, F.; Gillison, M.L. Worldwide Trends in Incidence Rates for Oral Cavity and Oropharyngeal Cancers. *J. Clin. Oncol.* **2013**, *31*, 4550–4559. [CrossRef] [PubMed]
25. Young, D.; Xiao, C.C.; Murphy, B.; Moore, M.; Fakhry, C.; Day, T.A. Increase in Head and Neck Cancer in Younger Patients Due to Human Papillomavirus (HPV). *Oral Oncol.* **2015**, *51*, 727–730. [CrossRef]
26. Organizacion Mundial de la Salud. *Human Papillomavirus and Related Diseases Report WORLD*; ICO/IARC HPV Information Centre. Available online: www.hpvcentre.net (accessed on 23 November 2022).
27. Chaturvedi, A.K.; Graubard, B.I.; Broutian, T.; Xiao, W.; Pickard, R.K.L.; Kahle, L.; Gillison, M.L. Prevalence of Oral HPV Infection in Unvaccinated Men and Women in the United States, 2009-2016. *JAMA* **2019**, *322*, 977–979. [CrossRef]
28. Bray, F.; Ferlay, J.; Soerjomataram, I. Global Cancer Statistics 2018: GLOBOCAN Estimates of Incidence and Mortality Worldwide for 36 Cancers in 185 Countries. *CA Cancer J. Clin.* **2018**, *68*, 394–424. [CrossRef]
29. Santos Carvalho, R.; Scapulatempo-Neto, C.; Curado, M.P.; de Castro Capuzzo, R.; Marsico Teixeira, F.; Cardoso Pires, R.; Cirino, M.T.; Cambrea Joaquim Martins, J.; Almeida Oliveira da Silva, I.; Oliveira, M.A.; et al. HPV-Induced Oropharyngeal Squamous Cell Carcinomas in Brazil: Prevalence, Trend, Clinical, and Epidemiologic Characterization. *Cancer Epidemiol. Biomark. Prev.* **2021**, *30*, 1697–1707. [CrossRef]
30. Jiarpinitnun, C.; Larbcharoensub, N.; Pattaranutaporn, P.; Chureemas, T.; Juengsamarn, J.; Trachu, N.; Lukerak, S.; Chansriwong, P.; Ngamphaiboon, N. Characteristics and Impact of HPV-Associated P16 Expression on Head and Neck Squamous Cell Carcinoma in Thai Patients. *Asian Pac. J. Cancer Prev.* **2020**, *21*, 1679–1687. [CrossRef]
31. Marur, S.; D'Souza, G.; Westra, W.H.; Forastiere, A.A. HPV-Associated Head and Neck Cancer: A Virus-Related Cancer Epidemic. *Lancet Oncol.* **2010**, *11*, 781–789. [CrossRef]
32. Morán-Torres, A.; Pazos-Salazar, N.G.; Téllez-Lorenzo, S.; Jiménez-Lima, R.; Lizano, M.; Reyes-Hernández, D.O.; Marin-Aquino, J.d.J.; Manzo-Merino, J. HPV Oral and Oropharynx Infection Dynamics in Young Population. *Braz. J. Microbiol.* **2021**, *52*, 1991–2000. [CrossRef] [PubMed]
33. Moody, C.A.; Laimins, L.A. Human Papillomavirus Oncoproteins: Pathways to Transformation. *Nat. Rev. Cancer* **2010**, *10*, 550–560. [CrossRef] [PubMed]
34. Sturgis, E.M.; Ang, K.K. The Epidemic of HPV-Associated Oropharyngeal Cancer Is Here: Is It Time to Change Our Treatment Paradigms? *J. Natl. Compr. Cancer Netw.* **2011**, *9*, 665–673. [CrossRef] [PubMed]
35. Harari, P.M.; Harris, J.; Kies, M.S.; Myers, J.N.; Jordan, R.C.; Gillison, M.L.; Foote, R.L.; Machtay, M.; Rotman, M.; Khuntia, D.; et al. Postoperative Chemoradiotherapy and Cetuximab for High-Risk Squamous Cell Carcinoma of the Head and Neck: Radiation Therapy Oncology Group RTOG-0234. *J. Clin. Oncol.* **2014**, *32*, 2486–2495. [CrossRef] [PubMed]
36. Yin, L.X.; D'Souza, G.; Westra, W.H.; Wang, S.J.; van Zante, A.; Zhang, Y.; Rettig, E.M.; Ryan, W.R.; Ha, P.K.; Wentz, A.; et al. Prognostic Factors for Human Papillomavirus-Positive and Negative Oropharyngeal Carcinomas. *Laryngoscope* **2018**, *128*, E287–E295. [CrossRef] [PubMed]
37. Kourelis, K.; Tsue, T.; Girod, D.; Tawfik, O.; Sykes, K.; Shnayder, Y. Negative Prognostic Factors for Head and Neck Cancer in the Young. *J. BUON* **2013**, *18*, 459–464.

Cellular Signalling 76 (2020) 109815

Contents lists available at ScienceDirect

Cellular Signalling

journal homepage: www.elsevier.com/locate/cellsig

Review

New insights in Hippo signalling alteration in human papillomavirus-related cancers

Leslie Olmedo-Nieva [a,b], J. Omar Muñoz-Bello [a,c], Joaquín Manzo-Merino [a,d], Marcela Lizano [a,e,*]

[a] Unidad de Investigación Biomédica en Cáncer, Instituto Nacional de Cancerología-Instituto de Investigaciones Biomédicas, Universidad Nacional Autónoma de México, Mexico City 14080, Mexico
[b] Programa de Doctorado en Ciencias Bioquímicas, Universidad Nacional Autónoma de México, Ciudad Universitaria, Mexico City 04510, Mexico
[c] Departamento de Farmacobiología, Centro de Investigación y Estudios Avanzados del Instituto Politécnico Nacional, Sede sur, Mexico City 14330, Mexico
[d] Cátedras CONACyT-Instituto Nacional de Cancerología, Mexico City, Mexico
[e] Departamento de Medicina Genómica y Toxicología Ambiental, Instituto de Investigaciones Biomédicas, Universidad Nacional Autónoma de México, Ciudad Universitaria, Mexico City 04510, Mexico

ARTICLE INFO

Keywords:
Cancer
Hippo signalling
YAP/TAZ
TEAD
HPV
E6/E7 oncoproteins

ABSTRACT

The persistent infection with high-risk human papillomavirus (HPV) is an etiologic factor for the development of different types of cancers, mainly attributed to the continuous expression of E6 and E7 HPV oncoproteins, which regulate several cell signalling pathways including the Hippo pathway. It has been demonstrated that E6 proteins promote the increase of the Hippo elements YAP, TAZ and TEAD, at protein level, as well as their transcriptional targets. Also, E6 and E7 oncoproteins promote nuclear YAP localization and a decrease in YAP negative regulators such as MST1, PTPN14 or SOCS6. Interestingly, Hippo signalling components modulate HPV activity, such as TEAD1 and the transcriptional co-factor VGLL1, induce the activation of HPV early and late promoters, while hyperactivation of YAP in specific cells facilitates virus infection by increasing putative HPV receptors and by evading innate immunity. Additionally, alterations in Hippo signalling elements have been found in HPV-related cancers and particularly, the involvement of HPV oncoproteins on the regulation of some of these Hippo components has been also proposed, although the precise mechanisms remain unclear. The present review addresses the recent findings describing the interplay between HPV and Hippo signalling in HPV-related cancers, a fact that highlights the importance of developing more in-depth studies in this field to establish key therapeutic targets.

1. Introduction

Human papillomaviruses (HPVs) are non enveloped double-stranded DNA viruses of about 60 nm in diameter that infect epithelial cells of the skin and mucosa. HPVs belong to the *Papillomaviridae* family, comprising more than 200 HPV types based on L1 viral gene sequence identity. Accordingly, HPVs are classified into five genera: Alpha-, Beta-, Gamma-, Mu- and Nu-papillomavirus (α, β, γ, μ, and ν) [1,2]. Alpha-papillomavirus is the group containing more HPV types, which mainly infects mucosal epithelia [3], followed in size by the β group associated with cutaneous epithelia infections [4].

HPVs commonly cause benign lesions, although the persistent infection with high-risk types (HR-HPV) is the main etiologic factor for developing different types of cancer; commonly associated with the αHPV group. It is estimated that HPVs are responsible of 5% of all human cancers worldwide [5], including cervical cancer (CC) (up to>94%) [6], anal cancer (88%), vulvar (25%), vaginal (78%), penile (50%), oropharyngeal (31%) and oral cancers (2.2%) [7,8]. Importantly, HPV16 is the most prevalent type in HPV-related cancers, followed by HPV18, which constitute an important health issue in both females and males [6,9,10].

Although a correlation between βHPVs and skin cancer remains unclear, βHPVs have demonstrated to be the cause of a proportion of cutaneous squamous cell carcinoma in immunocompromised individuals [11]. Unlike αHPV-related cancers, it appears that βHPVs play a role in cancer onset and are no longer necessary for tumour maintenance [12].

Viral particles from the different HPV genus share the same genomic

* Corresponding author at: Instituto Nacional de Cancerología, Mexico City 14080, Mexico.
E-mail address: lizanosoberon@gmail.com (M. Lizano).

https://doi.org/10.1016/j.cellsig.2020.109815
Received 31 July 2020; Received in revised form 20 October 2020; Accepted 20 October 2020
Available online 22 October 2020

structure and organization, consisting of a double-stranded circular genome of approximately 8000 base pairs (bp) with three genomic regions. The early region (E) encodes for proteins required for the viral life cycle (E1, E2, E4, E5, E6 and E7), although the E5 open reading frame (ORF) is not present in βHPV types [4]. The late region (L), encodes for L1 and L2 capsid proteins; and the long control region (LCR), a non-coding region containing the origin of replication and the early promoter that regulates the expression of early genes [13,14]. Late genes are expressed from promoters localized within the early coding regions [15].

The early genes produce a variety of viral proteins necessary for genome maintenance, the E1 protein is an ATP-dependent helicase involved in viral DNA replication [16], along with E2 protein, which also regulates viral transcription [17], controlling the expression of E6 and E7 genes. In transforming HPV types, E6 and E7 proteins exert an oncogenic role due to their inactivating actions on several tumour suppressors [18,19]. The continuous expression of E7 and E6 oncogenes in αHPV-related cancers is mainly attributed to viral genomic integration into the host genome, which is considered as a key event in carcinogenesis, although it is not a requirement for cell transformation [20,21]. The precise cause of this integration event remains unknown, but it is speculated that genomic instability caused by a persistent HPV infection, eventually could promote viral genome integration into the host genome, where viral E2 gene is commonly disrupted, causing uncontrolled expression of E6 and E7, thus enhancing HPV oncogenic potential [22]. In particular, the βHPVs do not integrate into the host DNA, and its genome is lost once the cancer is established; therefore, its transforming activity may occur in the early stages of carcinogenesis [23].

Among different functions identified for E6 and E7 oncoproteins from HR-HPV types, the most studied is the targeting of tumour suppressor proteins p53 and pRb for proteasomal degradation, respectively, thus avoiding apoptosis and promoting uncontrolled cell cycle progression [24,25]. Moreover, E6 and E7 oncoproteins regulate different cell signalling pathways, which sustain proliferation and apoptosis inhibition, being also involved in immune evasion [26], all these events contribute to tumorigenic transformation [27]. The effect of αHPV oncoproteins on dysregulation of different signalling pathways has been extensively studied; including Wnt/β-Catenin [28,29], PI3K/Akt [30–33], and JAK/STAT [34] signalling pathways.

Recent findings have demonstrated that HPV E6 and E7 proteins can regulate the Hippo signalling cascade towards cervical cancer [35–38], as well as cutaneous squamous cell carcinoma [39]. The Hippo pathway controls the expression of a variety of genes implicated in cell proliferation, differentiation and apoptosis as well as in development and embryogenesis, and recent studies reveal a key role of this pathway in carcinogenesis [40,41].

This review addresses the specific participation of α and βHPVs in the dysregulation of the Hippo signalling pathway. Evidence of HPV regulation by Hippo signalling is summarized, as well as the common alteration of Hippo elements observed in HPV-related cancers.

2. Hippo signalling pathway

Numerous studies have found that the Hippo signalling pathway is dysregulated in several types of cancers including bone sarcoma [42], breast [43], colorectal [44], skin [45], cervical [46] and head and neck cancer [47], among others. The main elements of Hippo signalling are evolutionary conserved, initially described in *Drosophila* in 1995 [48,49], and further identified in mammalian cells [50]. Those elements comprise a variety of upstream regulatory proteins, a core kinase cascade and downstream transcription factors and co-regulators (Fig. 1). Yes-associated protein (YAP) and Transcriptional coactivator with PDZ-binding motif (TAZ) proteins are the main effectors in the Hippo signalling, whose stability depends on a plethora of intrinsic and extrinsic stimuli. The Hippo kinases cascade initiates when Mammalian Ste-20 like kinases 1/2 (MST1/2) are phosphorylated in Thr183 and Thr180, respectively. Then activated MST1/2 phosphorylates Salvador 1 (SAV1) and Mps one binder kinase activator-like 1 A/B (MOB1A/B), which are scaffold proteins that assist MST1/2 in the phosphorylation of the Large tumour suppressors 1/2 (LATS1/2) in the specific residues Thr1071 and Thr1079, respectively. Soon after, phospho-LATS1/2 inactivates YAP and TAZ (YAP/TAZ), through their phosphorylation in Ser127 and Ser89 residues, respectively [51]. Such event generates consensus binding sites for 14–3-3 proteins, which in turn induces YAP and TAZ cytoplasmic retention [52,53]. Nonetheless, YAP and TAZ can be further phosphorylated by Casein kinase 1 δ/ε (CK1δ/ε), which in consequence leads to YAP and TAZ ubiquitination promoting their degradation in a proteasome-dependent manner [54,55] (Fig. 1). Contrariwise, Protein phosphatase 1 catalytic subunit alpha (PP-1A) dephosphorylates YAP in Ser127 residue promoting its nuclear translocation and subsequent transcriptional activation [56]. Additionally, the Protein tyrosine phosphatase non-receptor type 14 (PTPN14) negatively regulates YAP and promotes its cytoplasmic localization through different mechanisms including direct interaction with YAP and dephosphorylation of in Tyr357 residue [57]; complexing with YAP which in turn affects YAP-mediated transcriptional activity, independently of the C-terminal phosphatase domain of PTPN14 [58–60] and stabilizing LATS1 protein in a PTPN14 C-terminus dependent manner, which could involve the participation of KIBRA [61] (Fig. 1).

Furthermore, the inactivation of core kinases induces YAP/TAZ nuclear translocation, where they mainly interact with Transcriptional enhancer factors TEF 1–4 (TEAD1-4) [62,63]. Then, TEAD1-4 is dissociated from its transcriptional co-regulators Vestigial-like proteins 1–4 (VGLL1-4), inducing the expression of target genes such as *CTGF, LATS2, CYR61, WNT5A/B, EGFR, AREG, BMP4, DKK1,* among others [64] (Fig. 1). Also, YAP/TAZ can interact with other transcription factors independently of TEAD, regulating cell survival or inducing apoptosis [65–72].

Unlike other cellular signalling pathways, the Hippo pathway does not have canonical receptors or ligands that trigger its activation; instead, several mechanisms are proposed in the regulation of this pathway, including physical cues [52,73], cell polarity and architecture [74], stress signals [75] and cell cycle regulators [76], among others. Moreover, several cellular signalling pathways cross-talk with the Hippo pathway, including Notch [77], Hedgehog [78], and Wnt/β-Catenin [79].

Particularly, in cell polarity and adhesion, apically localized proteins form different scaffold complexes that lead to an increase in MST1/2 enzymatic activity, stimulating the Hippo signalling. Some of those proteins are Kidney and brain expressed protein (KIBRA), FAT tumour suppressor homolog 1 (FAT1) and Angiomotin (AMOT). Additionally, PKC phosphorylates Ras association domain family protein1 isoform A (RASSF1A) [80], which is a scaffold protein that interacts with MST1/2, LATS1/2 and SAV1, promoting their activity [81]. Also, some members of the basolateral polarity such as Discs-large (DLG) and Scribble (SCRIB) serve as scaffold proteins that regulate the Hippo core kinases activity, mediating the phosphorylation of YAP/TAZ [82]. Also, Integrin β1 (ITGB1)-SRC signalling promotes nuclear YAP localization by inhibiting LATS1/2 [83]. In adherent junctions, α-Catenin controls YAP activity mediating its interaction with 14–3-3 [84]. Moreover, AMOT, in association with other proteins, interact with YAP/TAZ, favouring their cytoplasmic retention [82]. Suppressor of cytokine signalling 5/6 (SOCS5/6), induces YAP degradation through an ubiquitin ligase complex; nevertheless, Epidermal growth factor receptor (EGFR) promotes YAP stability through RAS, which down-regulates SOCS5/6 [85] (Fig. 1).

Importantly, crosstalk between members of the p53 family of transcriptional factors and the Hippo pathway has been described. The full-length TAp63 and truncated ΔNp63 isoforms of p63, are reported to differentially regulate the Hippo signalling pathway since TAp63 shows tumour suppressor activities while ΔNp63 acts as an oncogene [86].

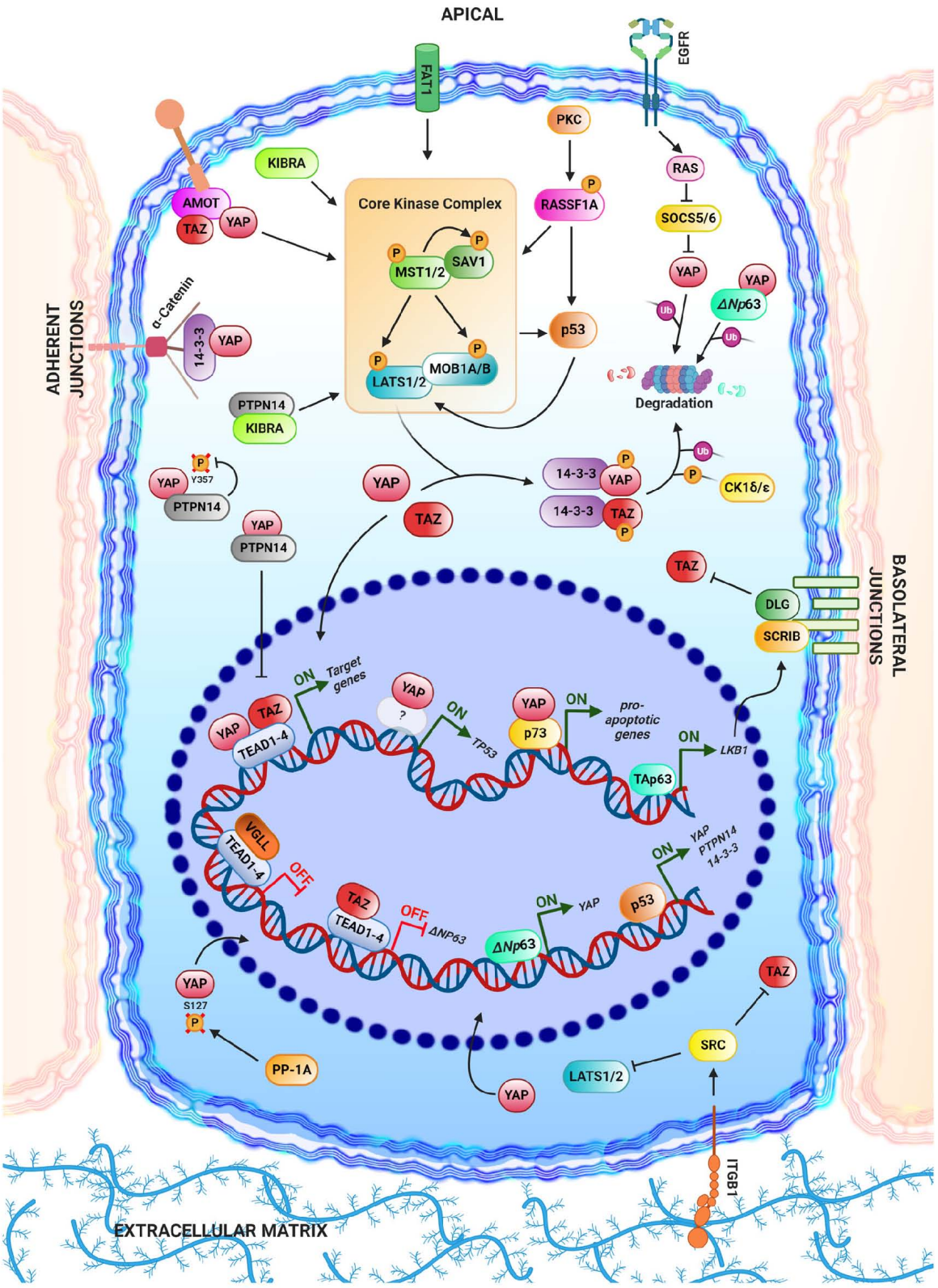

Fig. 1. Hippo signalling pathway. The Hippo signalling pathway is composed by a core kinase cascade that negatively regulates the downstream co-regulators YAP/TAZ through their phosphorylation; in the active state, YAP/TAZ bind to and activate transcriptional factors TEAD1-4 promoting the dissociation of negative co-regulators VGLL facilitating the transcription of several target genes. This main axis is regulated by a plethora of proteins at different levels, involving a great variety of mechanisms. Regulators such as KIBRA, FAT1, AMOT, PKC, RASSF1A, DLG, SCRIB, p53, p63 and LKB1 act directly promoting the activity of the core kinases; while some others such as 1β-Integrin and SRC decrease the activation of core kinases. Other proteins act directly inactivating YAP or TAZ by stimulating their cytoplasmic retention (14–3-3 family, PTPN14, AMOT and α-Catenin) or by promoting their proteasomal degradation (CK1δ/ε and SOCS5/6). Otherwise, the activation of YAP/TAZ is mediated by proteins such as PP-1A, EGFR, RAS, p53 and ΔNp63. Interestingly, ΔNp63 transcript and protein are negatively regulated by TAZ-TEAD and YAP, respectively. Meanwhile, p53 expression is positively regulated by YAP. Finally, YAP binds to p73 in DNA damage conditions promoting the transcription of pro-apoptotic target genes.

TAp63 regulates the expression of liver kinase B1 (LKB1), which increases SCRIB levels leading to the activation of Hippo core kinases, which in turn downregulate TAZ activity [87]. In contrast, ΔNp63 binds to the YAP promoter increasing its expression [88] and also interact with YAP protein inducing carcinogenesis [86]. However, TAZ-TEAD negatively regulate ΔNp63 expression [89] while YAP induces ΔNp63 proteasomal degradation [90]. Otherwise, p73 protein acts as a tumour suppressor in DNA damage conditions by binding to YAP and promoting the transcription of pro-apoptotic target genes [86,91]. Furthermore, in response to cellular stress, Hippo cooperates with p53 leading to cellular homeostasis. LATS2 is positively regulated by p53, while p53 is activated by LATS1/2, MST1/2 and RASSF1A in response to different stimuli [86,92,93]. Interestingly, YAP and p53 exhibit controversial activities over each other by switching between oncogenic and pro-apoptotic outcomes. Overexpression of YAP interferes with one of the LATS2-mediated mechanisms of p53 activation, through disruption of Apoptosis-stimulating protein of p53-1 (ASPP1)-LATS2 complex which promotes p53 proapoptotic activities under stress conditions [94]. Also, it has been demonstrated that p53 promotes transcription of YAP-negative regulator PTPN14 therefore, p53 deficiency promotes YAP activation [95]. Concordantly, p53 augments 14–3-3σ transcription [96], involved in YAP cytoplasmic localization [97]. However, it has been demonstrated that YAP binds to *TP53* promoter, inducing its expression after DNA damage conditions such as chemotherapy treatment, while in turn p53 binds to the YAP promoter, upregulating its expression [98].

In addition to the above regulation, it is important to mention that Hippo signalling is influenced by a plethora of stimuli; however, this review focuses on regulators that so far are believed to be involved in HPV-related cancers.

3. Molecular interplay between Hippo components and HPV

To elucidate the participation of HPV in YAP dysregulation, raft cultures of human foreskin keratinocytes (HFK) containing HPV16 genome were compared to HPV negative rafts; HPV positive cultures exhibited YAP overexpression with a remarked positivity in the middle and upper layers [35]. Additionally, an increase of nuclear YAP was observed in starved normal immortalized human keratinocytes (NIKS) harbouring HPV16 episomes compared to control NIKS [36], demonstrating that HPV affects YAP levels and localization. Besides, the increase of TEAD1 and TEAD4 proteins observed in HFK harbouring HPV16 or 18 genomes [99], suggests a direct activation of YAP-TEAD transcriptional complex in the presence of HPV. Furthermore, mRNA and protein levels of MST1 are decreased in HPV positive CC cells compared to those HPV negative cells; in contrast, using a model of keratinocytes, MST1 levels did not significantly change in those cells harbouring HPV18 genome compared to control cells, even when an increase in YAP levels and activity was observed. Despite this, MST1/2 overexpression promoted a decrease in cell proliferation and colony formation in HPV positive cell lines but not in HPV negative CC cells (C33A) [100] and proliferation mediated by HPV16 in mice cervical tissues was abolished when YAP was deleted [101], evidencing that Hippo is involved in HPV-mediated proliferation.

3.1. Regulation of Hippo components by E6 and E7 proteins

3.1.1. Alpha HPV types

Normal cervical cell line (HCK1T) expressing HPV16 E6 and E7 (E616 and E716) proteins showed enhanced YAP activation compared to HCK1T non-transfected cells [101]. The specific effect of E6 on YAP regulation was addressed in different works using NIKS and HFK keratinocytes [99] as well as HT3 cervical cancer cells expressing E616 and HeLa cells with HPV18 E6 (E618) knockdown. Results demonstrated that E6 proteins from both HPV types promote an increase in YAP protein levels, which at least in the case of E616, was due to a reduction of YAP proteasome-mediated degradation [35]. It was demonstrated that YAP upregulation induced by E6 is only mediated at the protein level since no effect was observed in YAP mRNA amounts [35]. According to these experiments, it was observed that cervical tissues from transgenic mice expressing E616 or E616/E716 exhibited higher YAP levels than tissues without oncoproteins expression. Furthermore, these cervical tissues exhibited increased nuclear YAP, in comparison to cervical tissues from control mice [35]. It was shown that E616 and E618, through their PDZ binding motifs (PBM), interact with different proteins that regulate YAP/TAZ localization, such as DLG1, SCRIB and AMOT [102,103], and that HR-HPV E6 proteins promote the degradation of some of these PDZ containing proteins [104]. Therefore, to evaluate whether E6-mediated nuclear YAP localization depends on E6 PBM motif, E616, E616 lacking its PBM motif or E616 harbouring the PBM motif of E618 were transduced in starved NIKS cultures, where YAP localization was evaluated. The obtained results demonstrated that nuclear YAP translocation is promoted by the PBM motif of E6 oncoproteins with a higher translocation effect produced by HPV18 PBM [36]. Additionally, it was observed that E716 also alters YAP protein localization in starved NIKS cells expressing the viral oncoprotein, where an increase in YAP nuclear translocation was detected [36]. These results are in agreement with the effect observed in cervical tissues of transgenic mice expressing E616/E716, where the observed YAP nuclear localization [35] could be due to the action of both HPV oncoproteins.

Since YAP nuclear localization correlates with its transcriptional activity, the expression of YAP target genes was evaluated in the presence of E6. Notably, it was found that the overexpression of E616 in HT3 cells increased *AREG* mRNA levels and consistently, when E618 was knocked down in HeLa cells, a reduction of *AREG* transcript levels occurred. YAP/TAZ are commonly forming a DNA-binding complex with TEAD factors, promoting transcription of their target genes [105]; interestingly, HPV has shown to be also involved in the increase of TAZ and TEAD proteins. Expression of E6 or E6/E7 oncoproteins in HFK promotes an increment of TEAD4 but not TEAD1 levels, compared to non-transfected cells [99]. Besides, the increase of TAZ, TEAD1 and TEAD4 proteins has been demonstrated in a model of NIKS cells expressing E616 [99], showing that transcription of Hippo target genes is boosted by HPV at different levels. Additionally, ablation of YAP but not TAZ in HCK1T cells expressing both E6 and E7 proteins, significantly diminished E6/E7-mediated proliferation, while YAP/TAZ silencing completely avoid the proliferative effect of HPV proteins [101]. Also, treatment with YAP-TEAD inhibitor Verteporfin, decreased the size of OSCC tumours expressing E6/E7 in mice models [106]; demonstrating the participation of Hippo signalling in HPV mediated tumorigenesis. Specifically, YAP silencing in E6-expressing HT3 cells avoids E6-mediated proliferation, demonstrating a critical role of YAP in the proliferative effect of E616 [35].

At the moment, the precise mechanisms by which the HPV oncoproteins promotes YAP activation are not completely understood. However, some studies provide information regarding this statement and demonstrate that E6 and E7 decreased the levels of a plethora of YAP/TAZ negative regulators or increase the positive ones. For instance, ablation of E6/E7 mRNA in HeLa and CaSki cells increases MST1 mRNA and protein levels which in turn decreased the levels of miR-18a, a negative regulator of MST1 [100]. In particular, the separate presence of E618 or E718 in C33A cells significantly downregulated MST1 mRNA and slightly reduced MST1 protein [100]. SOCS6 protein binds to YAP inducing its degradation via Cullin-RING-E3 ubiquitin ligase complexes [85]; interestingly, a reduction of SOCS6 protein levels was observed in HT3 cells overexpressing E616, a statement that was confirmed in HeLa cells after E618 silencing, where SOCS6 increase was evident [35]. It was shown that YAP is a direct target of miR-550a-3-5p, which in turn is downregulated by E616 but not E716 in OSCC cells. Restoration of miR-550a-3-5p in HPV positive OSCC cells significantly decreased the levels of YAP at mRNA and protein levels but did not affect TAZ levels [106]. Also, it was observed that *CCL2* expression, a YAP-TEAD transcriptional

target, was diminished when miR-550A-3-5p was overexpressed. Concordantly, the overexpression of miR-550a-3-5p in HPV positive OSCC cells-derived xenografts significantly correlated with low YAP and *CCL2* mRNA and protein levels [106]. Additionally, the overexpression of HPV16 E6/E7 in HCK1T cells decreased PTPN14 protein amounts [101]. It has been reported that E7 of different HPV types interact with and promote the proteasome-mediated degradation of PTPN14, while E7 of low-risk HPV11 did not [38,107]. The biological consequence of PTPN14 degradation mediated by E7 has been evaluated in different studies. It was shown that E718 and E716 promote the downregulation of genes involved in keratinocyte differentiation in HaCaT [108], HFK and N/TERT-1 cells, at least partially, through the degradation of PTPN14 [109,110]. Furthermore, the E7-mediated decrease of PTPN14 has shown to be involved in cell survival after cell detachment in N/TERT-1 and HFK immortalization [109], as well as the promotion of cell proliferation, migration and colony formation in HaCaT keratinocytes [108]. Collectively, these observations evidenced that the transforming activity of high-risk E7 proteins is related to the negative regulation of PTPN14 protein. Since PTPN14 acts as a negative regulator of YAP [57,61], the transforming effect of E7 could be partially due to the increase in YAP activity. Also, overexpression of a PTPN14 mutant, resistant to E7 degradation in HeLa cells, revealed a decrease of YAP transcriptional activity and its target genes such as *CTGF* and *CYR61* [108]. Contrary to these findings, experiments performed in N/TERT-1 cells demonstrated that the knockout of PTPN14, or the expression of E7 where PTPN14 is degraded, do not affect the levels of YAP targets *CTGF* and *CYR61* [109]; implying that the Hippo pathway regulation by PTPN14 could depend on the cellular context.

Different studies also demonstrate the effect of E6 and E7 oncoproteins in the modulation of p53, p63 and p73 family of transcription factors, closely related to the Hippo signalling regulation. It has been demonstrated that E7 increases DEK protein which is involved in ΔNp63 upregulation. HeLa cells with E6/E7 knocked-down and primary human keratinocytes overexpressing HPV16 E6, E7 or E6/E7 demonstrated that DEK is increased by E7 [111]. In concordance, an increment of DEK was observed in a transgenic HNSCC mice model overexpressing E716 compared to control tissues. It is important to notice that downregulation of DEK in HNSCC cells, promoted ΔNp63 decrease, which is involved in DEK-mediated proliferation and growth promotion in HNSCC tumours [112]. The ΔNp63 protein has been shown to promote YAP transcription [88]. Furthermore, the E6/E7-dependent upregulation of ΔNp63 has been evidenced through the interference of the E616/E716 mRNA in a model of HPV positive HNSCC cells, coupled with the overexpression of both oncoproteins in human keratinocytes [113].

Upregulation of ΔNp63 is also mediated by the HPV31 E7 oncoprotein through the downregulation of its negative regulator miR-203 [114]. Also, silencing of E7 but not E6 produces a significant reduction of ΔNp63 mRNA levels in CaSki cell line, surprisingly, a reduction of miR-203 was also observed in this model [115], suggestive of different mechanisms through which HPV oncoproteins promote ΔNp63 increment. It is proposed that ΔNp63 is more related to oncogenic activities [116] which high expression has been demonstrated in different types of cancer, in contrast to TAp63 isoform, which is commonly found at low amounts in cancer [117]. Experiments performed in HFK cells expressing E616 and E716 proteins exhibited overexpression of p63 which showed to drive cell invasion [118]. Besides, it was observed that E7 from HPV6 and 11 low-risk types promote a slight increment of p63 protein in comparison to E7 from types 16 and 18, which exhibit a strong effect on p63 induction [115]; however, the specific contribution of ΔNp63 and TAp63 was not assessed in these experiments therefore, results did not provide a complete scenario of E7 effect on each p63 isoform. On the other hand, experiments performed in HeLa cell line demonstrated that E618 is responsible for TAp63 protein decrease; also a decrease of TAp63 transcriptional targets, without altering ΔNp63 levels, was described in CaSki cell line which contains E6/E7 from HPV16 [119]. Due to the different effects of ΔNp63 and TAp63 isoforms on YAP activity, the positive effect of E7 on ΔNp63 and the degradation of TAp63 mediated by E6, suggest an important role of HPV in promoting YAP oncogenic activity through the modulation of p63 isoforms. Otherwise, in human keratinocytes, E7 from HPV16 increases the activity of p73 promoter in a pRB dependent manner, implying that this event is possibly through E2F1 which is negatively regulated by pRB. This upregulation promotes the increased expression of full-length p73α, p73β and p73γ isoforms; although, evaluation of small p73 isoforms needs to be performed. Moreover, HPV16 positive cervical SCC samples compared to the normal epithelium, exhibited higher proportions of p73 and p73Δ2, which lacks exon 2 of p73. Since p73Δ2 can inhibit the functions of p73, this evidence suggests a possible mechanism of p73 apoptotic functions inhibition in SCC [120]. Otherwise, E6 from HPV16 and 11 seem to interact with and inactivate p73 transcriptional activity, although, this effect is not through p73 degradation [121]. These results raise the idea that even when E7 could increase full-length p73, E6 interacts with this factor, probably interfering with the p73-YAP complex formation and blocking the transcription of pro-apoptotic genes in HPV-related cancers. Several studies demonstrate that components of the Hippo pathway mostly cooperate with wild-type p53 acting as tumour suppressors, while mutant forms of p53 cooperate with the Hippo effectors YAP and TAZ to promote tumorigenesis [86,88,122,123]. Moreover, in some tumours containing wild-type p53, the function of this factor drops due to variations in p53 regulators [124]; the latter may occur in HPV-related cancers. YAP and p53 have been shown to have an effect over each other and E6 promotes the increase of YAP protein but also has a well-documented degradation effect on p53 protein that depends on the E6 binding to the ubiquitin ligase E6-associated protein (E6AP) [125,126]. Since YAP overexpression disrupts p53 activation mediated by LATS2 and p53 deficiency promotes YAP activation [95] at least by the decrease of PTPN14 and 14–3-3σ expression, E6 activities on YAP and p53 proteins could be an important way to drive carcinogenesis through Hippo signalling dysregulation.

Taken together, all these evidence reinforces that E6 and E7 tumorigenic actions are partially mediated by Hippo components. The specific effect of HPV proteins on the Hippo signalling regulation is described in Fig. 2.

3.1.2. Beta HPV types

It has been shown that E6 proteins from βHPVs also dysregulate the Hippo pathway [39]. First, it was demonstrated that E6 proteins from βHPV8 and 5 bind to the cellular histone acetyltransferase p300 with high affinity [127]. This interaction causes destabilization of p300, which is a key regulator of gene expression, leading to a decrease in the expression of genes involved in DNA damage repair (DDR) [127,128] and to the prevention of the stabilization of p53 [129]. Interestingly, by analysing RNAseq data from cancer cell lines, Dacus et al. (2019) [39] found that in cell contexts with reduced p300 expression, similar to what happens in cells with βHPV E6 expression, canonical Hippo pathway genes were up-regulated, particularly TEAD-responsive genes. Those results were validated in HFK cells expressing βHPV8 E6, where p300 was significantly decreased while TEAD-responsive genes were upregulated, including *CTGF*, which correlated with an increase in cell proliferation. The dependence of p300 was proved through an E6 mutant disabled to bind p300, which did not show those effects. Even when nuclear YAP did not increase in this βHPV8 E6 expressing cell line, the upregulation of TEAD target genes was evident, suggesting that other Hippo pathway elements could be involved. Otherwise, during aberrant cytokinesis, LATS is activated through phosphorylation, promoting p53 accumulation [130], which in turn inhibits the proliferative activity of YAP/TAZ, inducing apoptosis [131]. It was demonstrated that during abnormal cytokinesis LATS phosphorylation is attenuated by βHPV E6 proteins, preventing p53 stabilization, provoking aneuploidy and that this effect is due in part to the interaction of E6 proteins with p300 [39]. Nevertheless, other study showed that E6/E7 from βHPV38 promote the accumulation of p53, enhancing the transcription of ΔNp73

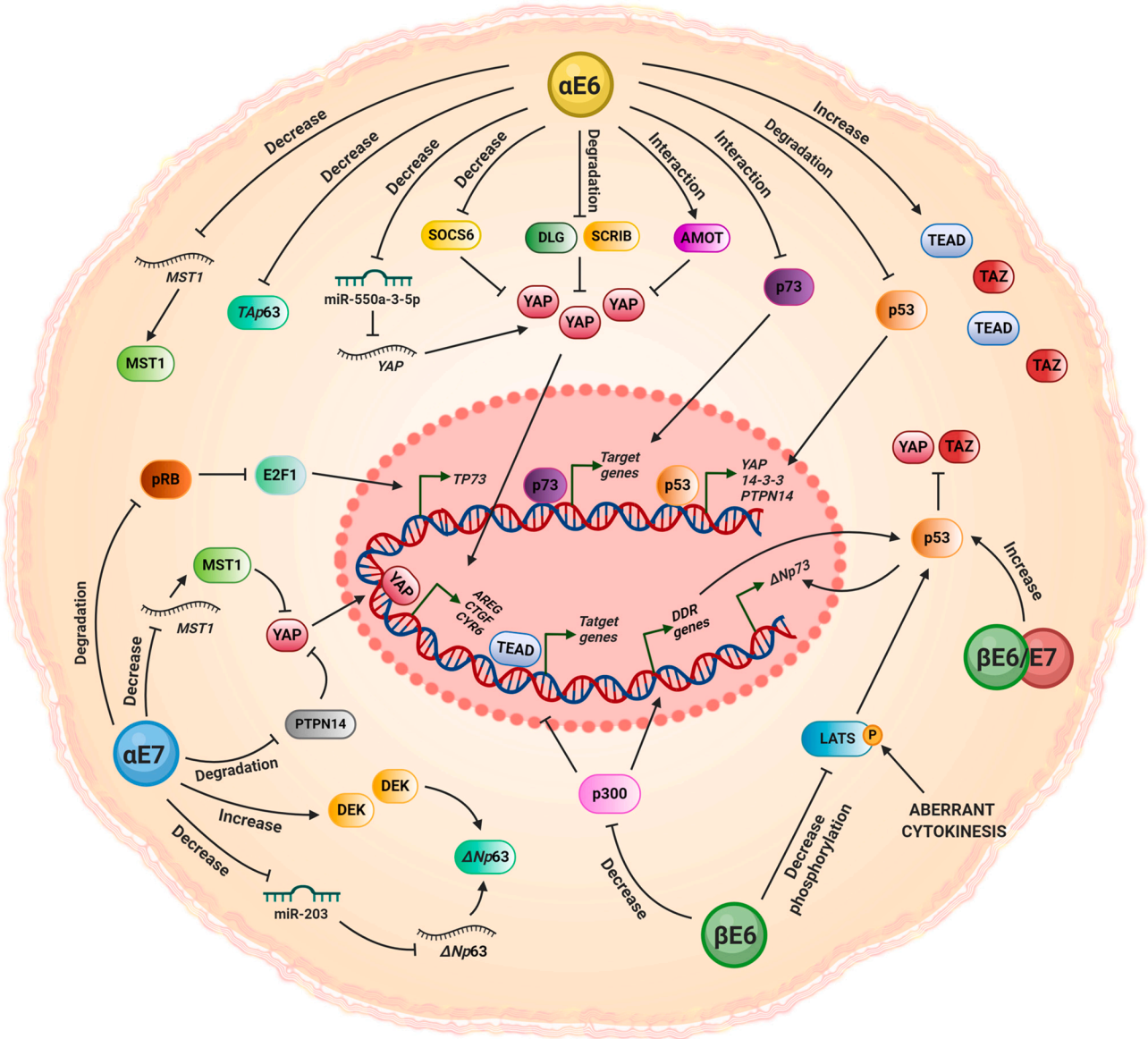

Fig. 2. Modulation of Hippo signalling components by HPV proteins. The specific mechanisms mediated by E6 and E7 oncoproteins from αHPVs, as well as oncoproteins from βHPVs, are described. E6 proteins from αHPV (αE6) affect the activation and nuclear translocation of YAP protein by different mechanisms such as downregulation of MST1, TAp63, miR-550a-3-5p, SOCS6, DLG1, SCRIB and p53; interaction with AMOT and p73 and increase of TAZ, TEAD1 and TEAD4 proteins. Otherwise, E6 from βHPV (βE6) destabilize p300, promoting upregulation of TEAD-responsive genes, as well as a decrease in transcription of DNA damage repair (DDR) genes, and consequently prevent p53 stabilization. Besides, βE6 attenuate LATS phosphorylation/activation in aberrant cytokinesis, avoiding p53 accumulation and promoting YAP/TAZ activity. Also, E6/E7 from βHPV (βE6/E7) promote the accumulation of p53 which in turn increases ΔNp73 transcription. Besides, E7 proteins from αHPV (αE7) decrease pRB promoting TP73 transcription via E2F1; decrease MST1 mRNA and protein levels; promote PTPN14 degradation; increase DEK protein, which in turn upregulates ΔNp63; and decrease the levels of miR-203, negative regulator ΔNp63.

isoform, which in turn blocks p53-apoptotic activity [132]. Moreover, experiments performed in p53 knockout mice expressing HPV38 E6/E7 demonstrated that p53 null mice did not express ΔNp73. Interestingly, it was found that E6/E7 transgenic mice evaded the cell cycle arrest mediated by UV radiation in the epidermis, in contrast, in p53 null mice expressing E6/E7 also treated with UV radiation, cell proliferation was decreased [133]. The contrasting effects on p53 could be related to differences between HPV types and/or synergic effects of the E6 and E7 oncoproteins (Fig. 2).

Table 1 summarizes the results of interactions, mRNA and protein expression of different elements of the Hippo pathway affected by HPV.

3.2. Regulation of HPV by Hippo components

From another perspective, it has been demonstrated that components of the Hippo signalling pathway can regulate HPV gene expression. Plasmid reporter assays performed in HaCaT, HeLa and SiHa cervical cell lines, demonstrated that TEAD1 activates gene transcription of the HPV16 p97 promoter [149]. Furthermore, it was shown that a non-identified transcriptional cofactor was also necessary for TEAD1 activity [150] and that such co-activator mediated, at least partially, the expression of HPV16 early genes [149]. Interestingly, it was also observed that the co-activator was a cell-specific and limiting factor for TEAD1 activity, since low concentrations of TEAD1 (that can bind to limiting cofactor amounts) stimulated HPV transcriptional activity, while high TEAD1 concentrations repressed gene expression [149,150],

Table 1
Hippo members affected by HPV.

HPV element	Hippo element	Effect	Reference
HPV genome	MST1 (STK4)	protein ↓ mRNA ↓	[134,135]
	EGFR	mRNA ↑ protein ↑	[134]
	14–3-3 (YWHAB)	mRNA ↓ protein ↓	[134]
	1β-Integrin (ITGB1)	mRNA ↓ protein ↓	[134]
	p63 (TP63)	mRNA ↑ protein ↑	[134]
	PTPN14	mRNA ↓	[135]
	BMP4	mRNA ↓	[135]
E6/E7	MST2 (STK3)	mRNA ↑	[136]
E6	SCRIB	Interaction	[137,138]
	DLG1	Interaction	[138]
	LATS1	mRNA ↑	[139]
	LATS2	Interaction	[138]
	FAT4	mRNA ↑	[139]
	CYR61	mRNA ↓	[140]
	14–3-3 (YWHAB)	Interaction	[138]
	14–3-3 (YWHAQ)	mRNA ↓	[140]
	DKK1	mRNA ↑	[141]
	SAV1	mRNA ↑	[136]
	TEAD4	Interaction	[138,142]
	TEAD2	Interaction	[138,142]
	YAP	Interaction	[138]
	KIBRA (WWC1)	Interaction	[138]
	TAOK1	Interaction	[138]
	TAOK3	Interaction	[138]
	LKB1 (STK11)	Interaction	[138]
	p63 (TP63)	Interaction	[138]
E6*	CCL2	mRNA ↑	[139]
E7	PTPN14	Interaction	[138,143,144]
	YAP	Interaction	[138,143,144]
	PP-1A (PPP1CA)	Interaction	[138]
	TEAD4	Interaction	[138,142]
	LKB1 (STK11)	Interaction	[138]
	TAOK1	Interaction	[138]
	TAOK3	Interaction	[138]
E1	AMOT	mRNA ↓	[145]
	CCL2	mRNA ↓	[145]
	FAT1	mRNA ↑	[145]
	DKK1	mRNA ↑	[145]
	CTGF	mRNA ↑	[145]
	AREG	mRNA ↑	[145]
	CYR61	mRNA ↑	[145]
	EGFR	mRNA ↑	[145]
	DLG1	Interaction	[138]
E2	14–3-3	Interaction	[144]
	TAZ	mRNA ↓	[146]
	MST1 (STK4)	mRNA ↓	[146]
	MST2 (STK3)	mRNA ↓	[147]
	Wnt5a	mRNA ↓	[147]
	AREG	Interaction	[138,148]
E5	EGFR	Interaction	[138]
	TAOK1	Interaction	[138]
	TAOK3	Interaction	[138]
	1β-Integrin (ITGB1)	Interaction	[138]
L2	MST2 (STK3)	Interaction	[138]
	LKB1 (STK11)	Interaction	[138]
	TAOK1	Interaction	[138]
	TAOK3	Interaction	[138]

↓: downregulation; ↑: upregulation.

probably because binding of TEAD1 to its DNA motifs in the absence of such co-activator interferes with the binding of the transcriptional active complex (TEAD1-cofactor). Recent experiments confirmed these findings and postulate VGLL1 transcriptional cofactor as the possible limiting actor previously described [151]. In this regard, silencing of TEAD1, but not TEAD4, promoted an evident reduction of HPV16 early and late promoters activation in undifferentiated W12 keratinocytes and CaSki cells. In contrast, silencing of either TEAD 1 or TEAD4 in HeLa cells, produced a reduction of HPV early promoter activity [151]. Otherwise, it was shown that TEAD1 binds to diverse sites on HPV16, 18 and 31 LCR-enhancers [149,151,152]. Several of these sites regulate early promoter activity at least in HPV16 and showed to bind to transcriptional cofactor VGLL1 in a TEAD1-dependent manner. Interestingly, the knockdown of VGLL1 highly reduced HPV early and late promoter activities as well as cell growth; demonstrating that VGLL1 and TEAD are strongly involved in HPV transcription (Fig. 3A). Otherwise, silencing of YAP and TAZ transcriptional cofactors showed to decrease the transcriptional activity of HPV16 early promoter, although to a lesser extent than VGLL1, while neither VGLL3 nor VGLL4 had any effect [151].

An interesting hypothesis postulated by Wang and Davis (2019) raises that hyperactivation of YAP facilitates HPV infection, which in turn promotes CC development [153]. Supporting this premise, in a mice model without HPV infection, it was demonstrated that inducible expression of activated YAP^{S127A} during two months in cervical epithelium promoted hyperplasia, and after 6–8 months invasive CC was developed [37]. Furthermore, to observe if activated YAP and E6/E7 oncoproteins possessed a synergic effect in CC development, mice models expressing YAP^{S127A} and E6 or E7 were analyzed. CC was rarely developed in mice expressing E6 or E7; however, when YAP^{S127A} was coexpressed, mice developed invasive CC in four months, less than the time necessary to develop cancer in YAP^{S127A} expressing mice [37]; so even when YAP seems to have a central role in CC, the importance of HPV oncoproteins is still evident.

HPVs infect the basal layer of stratified squamous epithelia through microlesions; later, mitotically active cells begin differentiation programs that allow HPV to complete its viral cycle from the basal to the upper layers [154,155]. It is known that tissue damage promotes a strong increment of YAP levels leading to proliferation and wound healing [156]. In concordance with this evidence, when a wound was made in a confluent culture of human cervical epithelial cells (hCerEC), wound boundaries exhibited nuclear localization of YAP, comparing to those cells far away from the wound, which showed a more homogenous YAP localization in the nucleus and cytoplasm. Interestingly, these wound-boundary cells with nuclear YAP expression were more susceptible to HPV16 pseudovirions (PV) infection, as well as cells overexpressing YAP or YAP^{S127A}. Accordingly, the ablation of YAP decreased the capacity of PV to infect [37], demonstrating a role of YAP activation during HPV infection. A plausible mechanism by which cells with activated YAP are more susceptible to HPV infection could be explained by the observed overexpression of putative HPV receptors [157], such as Syndecan-1 (SDC1), integrin-α6 (ITGA6) and EGFR in YAP-activated cells at mRNA level, and YAP^{S127A} in mice tissues at the protein level. Importantly, the silencing of ITGA6 in YAP overexpressing cells drastically decreased PV infection [37], demonstrating that overexpression of these receptors mediated by YAP favours PV infection (Fig. 3B). Moreover, it is known that in squamous epithelia YAP/TAZ are localized in the nucleus of basal layer cells while in the middle and upper layers YAP/TAZ are localized in the cytoplasm [156]. This fact could explain the idea that HPVs infect basal layer through microlesions, in those sites where YAP is hyperactivated.

Furthermore, to establish an HPV persistent infection, the virus first needs to escape from the innate immune system [158]. Some experiments strongly suggest that hyperactivation of YAP interferes with innate immunity by decreasing mRNA expression of signalling molecules involved in HPV recognition, such as Toll-like receptors (TLR2, 4), myeloid differentiation primary response gene 88 (MYD88) and TIR-domain-containing adaptor-inducing interferon-β (TRIF) [159]. Also, YAP hyperactivation seems to decrease the levels and/or nuclear localization of different immune-related factors, such as interferon regulatory factors (IRF) and the nuclear factor-κB (NF-κB) [37] (Fig. 3B), both involved in the transcription of different cytokines that counteract viral infection [160]. Released cytokines, mainly interferons, act on adjacent cells through activation of their receptors and the JAK/STAT signalling to promote transcription of genes that block viral infection

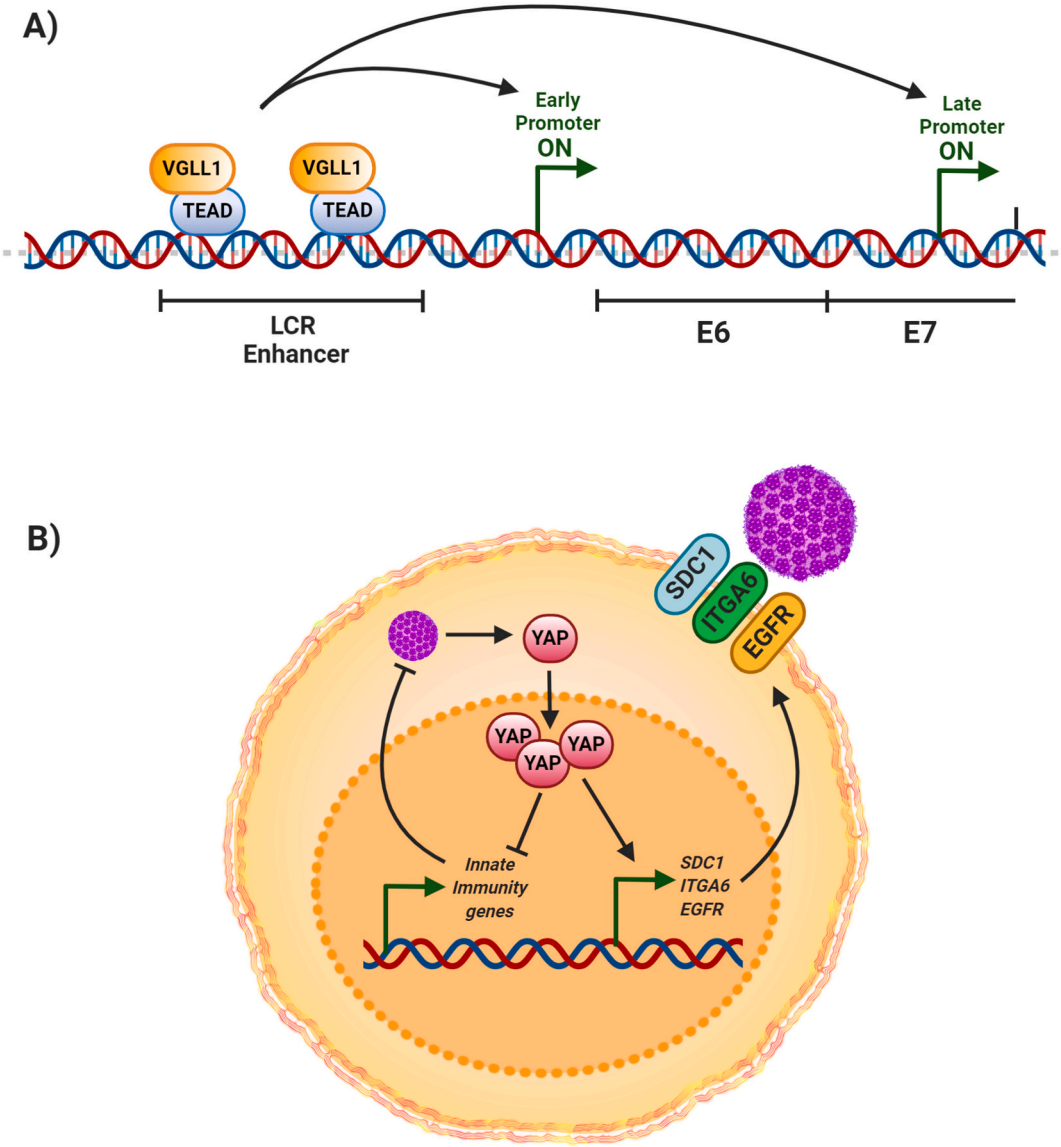

Fig. 3. Regulation of HPV by Hippo members. A) TEAD transcriptional factors associate with VGLL1 leading to their binding to several sites within the HPV LCR-enhancer, which in turn activate HPV early and late promoters; B) Hyperactivation of YAP facilitates HPV infection through overexpression of cellular HPV-entry receptors such as SDC1, ITGA6 and EGFR. The activation of YAP also interferes with innate immunity by decreasing the expression of signalling molecules involved in HPV elimination.

[161]. YAP overexpressing cells exhibit a decrease in mRNA and protein levels of elements involved in JAK/STAT signalling and its transcriptional targets [37]. Moreover, in this mice model with hyperactivated YAP, this protein is overexpressed throughout the entire cervical epithelium, an effect that is observed exclusively in cervical cancer samples, since CIN lesions exhibit YAP overexpression only in the lower third of the epithelium [162] and in normal cervical epithelia, just at the basal layer [156]. Once the virus infects the basal layer due to the increase of YAP-enhanced virus receptors, suppression of the innate immune system occurred and viral persistence is promoted. These findings suggest an important interplay between HPV and Hippo pathway.

4. The Hippo signalling pathway in HPV-related cancers

Alterations in localization, activity or levels of key proteins acting as regulators of cellular homeostasis can promote cancer progression through the modulation of different signalling pathways [163]. In HPV-related cancers, it has been demonstrated that HPV promotes the dysregulation of different genes either by HPV-genome insertion into the cellular genome [22] or by direct activity of HPV proteins [29], which in consequence modulate several signalling pathways.

Particularly, it has been described an interplay between HPV and Hippo signalling, supporting that HPV proteins regulate Hippo components [35,36] and that YAP possesses an effect on HPV infection [37]. Herein, we deeply describe data demonstrating an association of HPV with Hippo pathway modulation in HPV-related cancers; additionally, due to the involvement of HPV in the development of an important percentage of different types of cancer [7,8,164–169], we resume in Fig. 4 a wide picture of Hippo components commonly dysregulated in head and neck [106,112,170–172], cervical [35,37,46,83,173–182], penile [183], vulvar [184] and colorectal cancers [185,186]. Although some of these works have not shown a direct association between dysregulated Hippo elements and HPV, the high prevalence of the virus in these cancer types makes possible the interaction of HPV with protagonists of the Hippo pathway, a fact that deserves to be studied. Likewise, at the moment, there is no information about dysregulation of Hippo signalling in anal, vulvar and vaginal carcinomas, also highly associated with HPV.

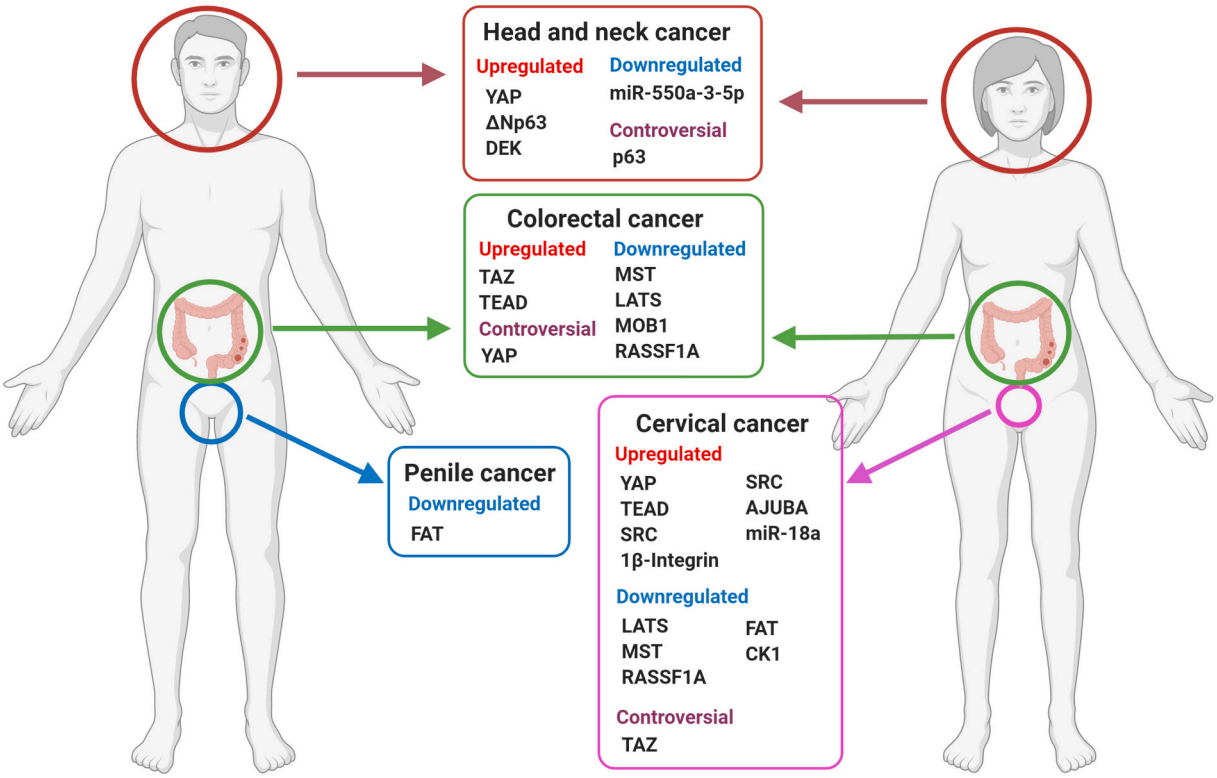

Fig. 4. Hippo signalling components dysregulated in HPV-related cancers. Commonly dysregulated elements of Hippo signalling pathway in head and neck, penile, cervical and colorectal HPV-related cancers are depicted. The Hippo members are grouped in upregulated, downregulated and those controversial.

4.1. Alteration of Hippo components in cervical cancer

HPV infection is the main risk factor for the development of cervical cancer [187], the fourth cause of women deaths by cancer worldwide [188]. The alteration of cellular signalling pathways during CC development has been described [189], and the relation of such alterations with HR-HPV has also been observed [178].

It is commonly accepted that HR-HPV DNA is found in almost all cervical cancer samples [187], and modulation of the Hippo signalling components along CC development is detected. Immunohistochemistry (IHC) analysis performed in different studies with samples including cervicitis, cervical intraepithelial neoplasias grades 1, 2 and 3 (CIN1, 2 and 3), as well as early and advanced cancer stages, demonstrated that the levels of YAP increase as cancer progresses, where the highest levels and nuclear localization are found in advanced cancer stages [37,101,162]. It is important to notice that at least an 84.2% of CIN II, III and SCC samples contain HR-HPV sequences while in cervicitis and CIN I samples HPV positivity is heterogeneous varying between negative, LR- and HR-HPV positive samples. CIN1 showed YAP expression in the basal layer or the lower third of the epithelium; while in CIN2/3, this protein is mainly expressed in the middle or upper layers [162]. Otherwise, MST1 protein levels showed a reduction during CIN progression, being higher in HPV negative normal samples when compared to HPV16 positive CIN1-3 samples; MST1 mRNA levels were also higher in normal epithelia and CIN1 compared to CIN2/3. Furthermore, the levels of the negative regulator of MST1, miR-18a, were found negatively correlated with MST1 and positively correlated with cervical disease progression [100]. Moreover, the methylation status of RASSF1A promoter, a Hippo regulator which inhibits YAP activity [190], was evaluated in a meta-analysis including data from 26 publications comprising 1820 CC, 507 CIN and 894 non-malignant samples, cytology or blood. The results showed that RASSF1A promoter methylation is elevated in CC compared to CIN and control samples [175], suggesting that its expression is downregulated, impacting in YAP activity.

Nowadays there is evidence suggesting that not all CC cases harbour HPV genomic sequences [191]; thus, it would be interesting to analyse Hippo modulation considering HPV status. Higher levels of total and phospho-YAP were found in HPV positive cell lines SiHa (HPV16+), CaSki (HPV16+), SW756 (HPV18+) and HeLa (HPV18+) compared to normal primary human keratinocytes (NHK) and HPV negative C33A cervical cancer cells [100], evidencing that HPV may be involved in YAP increase. Also, a study performed on cervicitis, CIN1/2/3 and squamous cell carcinoma (SCC) samples where HPV and YAP status were tested, demonstrated a correlation between YAP expression and HPV positivity [162]. In this study 80% of HPV-/YAP- cases corresponded to cervicitis or CIN1; 76.2% of HPV+/YAP- were CIN1/2; while 77.4% of HPV+/YAP+ were CIN2/3 or SCC, indicating an association of HPV and YAP with high-grade CIN or cancer. Furthermore, MST1 protein and mRNA, as well as phospho-MOB1 protein levels were lower in the HPV positive cell lines HeLa and CaSki compared to C33A and NHK, while miR-18a was upregulated, correlating with the pattern observed in HPV16 positive cervical lesions [100]. Interestingly, it has been demonstrated that miR-18a is a negative regulator of MST1 mRNA in HeLa and CaSki HPV positive cell lines but not in C33A, and that this miRNA acts as a promoter of cellular proliferation only in HPV positive cells [100]. Moreover, a decrease in Hippo kinases activity in HPV positive cells could also be mediated by the observed methylation of the RASSF1A promoter in these samples [175]. Together, these data suggest that HPV promotes the activation of YAP in CC through different mechanisms.

In addition, many genetic alterations in Hippo signalling components such as YAP and TAZ amplifications, LATS1/2, MST1 and FATs mutations or deletions have been commonly observed in CC [35,37,178–181]. Besides, gene and protein expression profiles demonstrated that CC samples often exhibit an upregulation in components such YAP, TAZ, TEAD1, 2, 3 or 4 [35], as well as low expression of LATS1/2 [181]. Even when these data have not been related to the presence of HPV, it seems important to notice the relevance of Hippo alterations in CC.

4.2. Deregulation of Hippo pathway by HPV in head and neck carcinoma

Among the different neoplasms induced by HPV, the group of head and neck cancer (HNC) has gained attention in the past few decades mostly due to the alarming increase in incidence and mortality [192]. Moreover, HNC patients are characterized by a poor prognosis and quality of life [193]. Almost 90% of HNC is originated from the mucosa covering the superior aerodigestive tract, thus head and neck squamous cell carcinoma (HNSCC) is the most prevalent histological type.

HNC is highly associated to alcohol and tobacco consumption; nevertheless, HPV infection has been recognized as an important etiological factor for HNSCC development with an increasing incidence over the past years mainly in young males [7,194].

The relevance of HPV in HNSCC relies on the clinical outcome exhibited by HPV positive cases, with increased OS and better response to treatment. Different experimental approaches revealed the participation of the Hippo signalling pathway either in the establishment and in the clinical outcome of HNSCC [195]; molecular aspects involved in metastatic or recurrent disease dependent on this pathway have been unveiled [196]. Since Hippo regulators and effectors are affected by HPV proteins, the alteration of the different Hippo players in HPV positive HNSCC might be influencing the clinical outcome.

Through the analysis of genomic data, Eun, et al., (2017) identified YAP amplification, which was categorized as an activation, in cohorts of HNSCC patients from different geographic regions, finding that such amplification of YAP is associated to the presence of HPV [170]. Additionally, YAP has been found in the nucleus of tumoral cells of HPV positive oropharyngeal cancers as demonstrated by a study that included in vitro analyses and clinical samples [197]. The authors found that YAP was mainly nuclear in cells with a delocalized SCRIB phenotype, a classical target of degradation of the HPV E6 oncoprotein [198]. Remarkably, direct regulation of YAP has been observed in oral squamous cell carcinoma (OSCC) through miR-550a-3-5p, wherein HPV positive OSCC samples exhibited downregulated levels of this miRNA whereas YAP was upregulated, compared to HPV negative OSCC. Also, the low expression of miR-550a-3-5p was associated with higher tumour size and the presence of metastasis [106].

On the other hand, even when several reports have evidenced the participation of YAP in laryngeal cancer, the relation with HPV is not clear, and the cases with active YAP are usually HPV negative, whilst those with inactive YAP are often HPV positive [170], thus the participation of HPV in the regulation of the Hippo signalling pathway in laryngeal carcinoma remains to be clarified.

Moreover, EGFR levels are significantly higher in HPV infected cases of laryngeal carcinoma [199] and a relationship between Hippo, EGRF and the HPV E6 oncoprotein has been demonstrated in cervical carcinoma [35]. Thus is it likely that the HPV proteins are affecting the Hippo pathway since several components result in activation of YAP. Hence, the understanding of the participation of HPV proteins in the Hippo pathway may be useful when designing and testing new drugs for HNC.

5. Concluding remarks

The Hippo pathway has recently been shown to be actively involved in the establishment, development and maintenance of HPV-related cancers. The effect of the E6 and E7 oncoproteins on the dysregulation of the Hippo elements has been identified so far, mainly related to the activation of YAP, TAZ and TEAD. However, the participation of HPV proteins other than E6 and E7 oncoproteins is not discarded, which deserves further studies. Importantly, the Hippo pathway has been described to promote both HPV infection and viral protein expression. Additionally, the Hippo pathway decreases the expression of various components of the innate immunity, favouring the establishment of an HPV infection. Hence, due to the importance of the Hippo pathway in HPV-related cancers, it becomes necessary to develop prophylactic and therapeutic strategies against key elements of this pathway, aimed at improving the clinical outcome of patients.

Author contributions

LON, JOMB, JMM and ML performed the bibliographic review and wrote the manuscript; LON generated the figures; ML conceptualized the manuscript.

Acknowledgements

LON is a doctoral student from programa de Doctorado en Ciencias Bioquímicas, Universidad Nacional Autónoma de México (UNAM) and received fellowship from PAPIIT-UNAM (IN200219) and CONACyT (404293). JOMB is a postdoctoral fellow and received a scholarship from CONACyT (741225).

This research was supported by Programa de Apoyo en Proyectos de Investigación e Innovación Tecnológica, Universidad Nacional Autónoma de México PAPIIT-UNAM (IN200219) and by Instituto Nacional de Cancerología (017/007/IBI)(CEI/1144/17).

References

[1] D. Bzhalava, C. Eklund, J. Dillner, International standardization and classification of human papillomavirus types, Virology 476 (2015) 341–344, https://doi.org/10.1016/j.virol.2014.12.028.

[2] K. Van Doorslaer, Q. Tan, S. Xirasagar, S. Bandaru, V. Gopalan, Y. Mohamoud, Y. Huyen, A.A. McBride, The Papillomavirus Episteme: a central resource for papillomavirus sequence data and analysis, Nucleic Acids Res. 41 (2013), https://doi.org/10.1093/nar/gks984.

[3] K. Van Doorslaer, Z. Li, S. Xirasagar, P. Maes, D. Kaminsky, D. Liou, Q. Sun, R. Kaur, Y. Huyen, A.A. McBride, The papillomavirus episteme: a major update to the papillomavirus sequence database, Nucleic Acids Res. 45 (2017) D499–D506, https://doi.org/10.1093/nar/gkw879.

[4] L. Bandolin, D. Borsetto, J. Fussey, M.C. Da Mosto, P. Nicolai, A. Menegaldo, L. Calabrese, M. Tommasino, P. Boscolo-Rizzo, Beta human papillomaviruses infection and skin carcinogenesis, Rev. Med. Virol. 30 (2020), https://doi.org/10.1002/rmv.2104.

[5] D. Formana, C. de Martel, C.J. Lacey, I. Soerjomataram, J. Lortet-Tieulent, L. Bruni, J. Vignat, J. Ferlay, F. Bray, M. Plummer, S. Franceschi, Global burden of human papillomavirus and related diseases, Vaccine 30 (2012), https://doi.org/10.1016/j.vaccine.2012.07.055.

[6] J.S. Smith, L. Lindsay, B. Hoots, J. Keys, S. Franceschi, R. Winer, G.M. Clifford, Human papillomavirus type distribution in invasive cervical cancer and high-grade cervical lesions: a meta-analysis update, Int. J. Cancer 121 (2007) 621–632, https://doi.org/10.1002/ijc.22527.

[7] C. de Martel, M. Plummer, J. Vignat, S. Franceschi, Worldwide burden of cancer attributable to HPV by site, country and HPV type, Int. J. Cancer 141 (2017) 664–670, https://doi.org/10.1002/ijc.30716.

[8] M. Plummer, C. de Martel, J. Vignat, J. Ferlay, F. Bray, S. Franceschi, Global burden of cancers attributable to infections in 2012: a synthetic analysis, Lancet Glob. Health 4 (2016) e609–e616, https://doi.org/10.1016/S2214-109X(16)30143-7.

[9] P. Guan, R. Howell-Jones, N. Li, L. Bruni, S. De Sanjosé, S. Franceschi, G. M. Clifford, Human papillomavirus types in 115,789 HPV-positive women: a meta-analysis from cervical infection to cancer, Int. J. Cancer 131 (2012) 2349–2359, https://doi.org/10.1002/ijc.27485.

[10] B.A. LeConte, P. Szaniszlo, S.M. Fennewald, D.I. Lou, S. Qiu, N.W. Chen, J.H. Lee, V.A. Resto, Differences in the viral genome between HPV-positive cervical and oropharyngeal cancer, PLoS One 13 (2018), https://doi.org/10.1371/journal.pone.0203403.

[11] K.J. Purdie, T. Surentheran, J.C. Sterling, L. Bell, J.M. McGregor, C.M. Proby, C. A. Harwood, J. Breuer, Human papillomavirus gene expression in cutaneous squamous cell carcinomas from immunosuppressed and immunocompetent individuals, J. Invest. Dermatol. 125 (2005) 98–107, https://doi.org/10.1111/j.0022-202X.2005.23635.x.

[12] M. Hufbauer, B. Akgül, Molecular mechanisms of human papillomavirus induced skin carcinogenesis, Viruses 9 (2017), https://doi.org/10.3390/v9070187.

[13] C. Weyn, J.M. Vanderwinden, J. Rasschaert, Y. Englert, V. Fontaine, Regulation of human papillomavirus type 16 early gene expression in trophoblastic and cervical cells, Virology 412 (2011) 146–155, https://doi.org/10.1016/j.virol.2010.12.056.

[14] Z.M. Zheng, C.C. Baker, Papillomavirus genome structure, expression, and post-transcriptional regulation, Front. Biosci. 11 (2006) 2286–2302, https://doi.org/10.2741/1971.

[15] T.H. Braunstein, B.S. Madsen, B. Gavnholt, M.W. Rosenstierne, C.K. Johnsen, B. Norrild, Identification of a new promoter in the early region of the human papillomavirus type 16 genome, J. Gen. Virol. 80 (1999) 3241–3250, https://doi.org/10.1099/0022-1317-80-12-3241.

[16] J. Sedman, A. Stenlund, Co-operative interaction between the initiator E1 and the transcriptional activator E2 is required for replicator specific DNA replication of bovine papillomavirus in vivo and in vitro, EMBO J. 14 (1995) 6218–6228, https://doi.org/10.1002/j.1460-2075.1995.tb00312.x.
[17] A.A. McBride, The papillomavirus E2 proteins, Virology 445 (2013) 57–79, https://doi.org/10.1016/j.virol.2013.06.006.
[18] S. Song, H.C. Pitot, P.F. Lambert, The human papillomavirus type 16 E6 gene alone is sufficient to induce carcinomas in transgenic animals, J. Virol. 73 (1999) 5887–5893, https://doi.org/10.1128/jvi.73.7.5887-5893.1999.
[19] S. Song, A. Liem, J.A. Miller, P.F. Lambert, Human papillomavirus types 16 E6 and E7 contribute differently to carcinogenesis, Virology 267 (2000) 141–150, https://doi.org/10.1006/viro.1999.0106.
[20] S. Vinokurova, N. Wentzensen, I. Kraus, R. Klaes, C. Driesch, P. Melsheimer, F. Kisseljov, M. Dürst, A. Schneider, M.V.K. Doeberitz, Type-dependent integration frequency of human papillomavirus genomes in cervical lesions, Cancer Res. 68 (2008) 307–313, https://doi.org/10.1158/0008-5472.CAN-07-2754.
[21] A. Chaiwongkot, S. Vinokurova, C. Pientong, T. Ekalaksananan, B. Kongyingyoes, P. Kleebkaow, B. Chumworathayi, N. Patarapadungkit, M. Reuschenbach, M. Von Knebel Doeberitz, Differential methylation of E2 binding sites in episomal and integrated HPV 16 genomes in preinvasive and invasive cervical lesions, Int. J. Cancer 132 (2013) 2087–2094, https://doi.org/10.1002/ijc.27906.
[22] Z. Hu, D. Zhu, W. Wang, W. Li, W. Jia, X. Zeng, W. Ding, L. Yu, X. Wang, L. Wang, H. Shen, C. Zhang, H. Liu, X. Liu, Y. Zhao, X. Fang, S. Li, W. Chen, T. Tang, A. Fu, Z. Wang, G. Chen, Q. Gao, S. Li, L. Xi, C. Wang, S. Liao, X. Ma, P. Wu, K. Li, S. Wang, J. Zhou, J. Wang, X. Xu, H. Wang, D. Ma, Genome-wide profiling of HPV integration in cervical cancer identifies clustered genomic hot spots and a potential microhomology-mediated integration mechanism, Nat. Genet. 47 (2015) 158–163, https://doi.org/10.1038/ng.3178.
[23] S.J. Weissenborn, I. Nindl, K. Purdie, C. Harwood, C. Proby, J. Breuer, S. Majewski, H. Pfister, U. Wieland, Human papillomavirus-DNA loads in actinic keratoses exceed those in non-melanoma skin cancers, J. Invest. Dermatol. 125 (2005) 93–97, https://doi.org/10.1111/j.0022-202X.2005.23733.x.
[24] D. Martinez-Zapien, F.X. Ruiz, J. Poirson, A. Mitschler, J. Ramirez, A. Forster, A. Cousido-Siah, M. Masson, S. Vande Pol, A. Podjarny, G. Travé, K. Zanier, Structure of the E6/E6AP/p53 complex required for HPV-mediated degradation of p53, Nature 529 (2016) 541–545, https://doi.org/10.1038/nature16481.
[25] X. Liu, A. Clements, K. Zhao, R. Marmorstein, Structure of the human papillomavirus E7 oncoprotein and its mechanism for inactivation of the retinoblastoma tumor suppressor, J. Biol. Chem. 281 (2006) 578–586, https://doi.org/10.1074/jbc.M508455200.
[26] I. Lo Cigno, F. Calati, S. Albertini, M. Gariglio, Subversion of host innate immunity by human papillomavirus oncoproteins, Pathogens 9 (2020), https://doi.org/10.3390/pathogens9040292.
[27] D. Hanahan, R.A. Weinberg, Hallmarks of cancer: the next generation, Cell 144 (2011) 646–674, https://doi.org/10.1016/j.cell.2011.02.013.
[28] H. Lichtig, D.A. Gilboa, A. Jackman, P. Gonen, Y. Levav-Cohen, Y. Haupt, L. Sherman, HPV16 E6 augments Wnt signaling in an E6AP-dependent manner, Virology 396 (2010) 47–58, https://doi.org/10.1016/j.virol.2009.10.011.
[29] J.O. Muñoz-Bello, L. Olmedo-Nieva, L.J. Castro-Muñoz, J. Manzo-Merino, A. Contreras-Paredes, C. González-Espinosa, A. López-Saavedra, M. Lizano, HPV-18 E6 oncoprotein and its spliced isoform E6*I regulate the Wnt/β-catenin cell signaling pathway through the TCF-4 transcriptional factor, Int. J. Mol. Sci. 19 (2018), https://doi.org/10.3390/ijms19103153.
[30] R. Xi, S. Pan, X. Chen, B. Hui, L. Zhang, S. Fu, X. Li, X. Zhang, T. Gong, J. Guo, X. Zhang, S. Che, HPV16 E6-E7 induces cancer stem-like cells phenotypes in esophageal squamous cell carcinoma through the activation of PI3K/Akt signaling pathway in vitro and in vivo, Oncotarget 7 (2016) 57050–57065, https://doi.org/10.18632/oncotarget.10959.
[31] S.W. Strickland, S. Vande Pol, The human papillomavirus 16 E7 oncoprotein attenuates AKT signaling to promote internal ribosome entry site-dependent translation and expression of c-MYC, J. Virol. 90 (2016) 5611–5621, https://doi.org/10.1128/jvi.00411-16.
[32] C.W. Menges, L.A. Baglia, R. Lapoint, D.J. McCance, Human papillomavirus type 16 E7 up-regulates AKT activity through the retinoblastoma protein, Cancer Res. 66 (2006) 5555–5559, https://doi.org/10.1158/0008-5472.CAN-06-0499.
[33] A. Contreras-Paredes, E. De la Cruz-Hernández, I. Martínez-Ramírez, A. Dueñas-González, M. Lizano, E6 variants of human papillomavirus 18 differentially modulate the protein kinase B/phosphatidylinositol 3-kinase (akt/PI3K) signaling pathway, Virology 383 (2009) 78–85, https://doi.org/10.1016/j.virol.2008.09.040.
[34] S. Hong, K.P. Mehta, L.A. Laimins, Suppression of STAT-1 expression by human papillomaviruses is necessary for differentiation-dependent genome amplification and plasmid maintenance, J. Virol. 85 (2011) 9486–9494, https://doi.org/10.1128/jvi.05007-11.
[35] C. He, D. Mao, G. Hua, X. Lv, X. Chen, P.C. Angeletti, J. Dong, S.W. Remmenga, K. J. Rodabaugh, J. Zhou, P.F. Lambert, P. Yang, J.S. Davis, C. Wang, The Hippo/YAP pathway interacts with EGFR signaling and HPV oncoproteins to regulate cervical cancer progression, EMBO Mol. Med. 7 (2015) 1426–1449, https://doi.org/10.15252/emmm.201404976.
[36] S. Webb Strickland, N. Brimer, C. Lyons, S.B. Vande Pol, Human papillomavirus E6 interaction with cellular PDZ domain proteins modulates YAP nuclear localization, Virology 516 (2018) 127–138, https://doi.org/10.1016/j.virol.2018.01.003.
[37] C. He, X. Lv, C. Huang, P.C. Angeletti, G. Hua, J. Dong, J. Zhou, Z. Wang, B. Ma, X. Chen, P.F. Lambert, B.R. Rueda, J.S. Davis, C. Wang, A human papillomavirus-independent cervical cancer animal model reveals unconventional mechanisms of cervical carcinogenesis, Cell Rep. 26 (2019) 2636–2650.e5, https://doi.org/10.1016/j.celrep.2019.02.004.
[38] A. Szalmás, V. Tomaić, O. Basukala, P. Massimi, S. Mittal, J. Kónya, L. Banks, The PTPN14 tumor suppressor is a degradation target of human papillomavirus E7, J. Virol. 91 (2017), https://doi.org/10.1128/jvi.00057-17.
[39] D. Dacus, C. Cotton, T.X. McCallister, N.A. Wallace, Beta human papillomavirus 8E6 attenuates LATS phosphorylation after failed cytokinesis, J. Virol. 94 (2020), https://doi.org/10.1128/jvi.02184-19.
[40] J. Mo, H.W. Park, K. Guan, The hippo signaling pathway in stem cell biology and cancer, EMBO Rep. 15 (2014) 642–656, https://doi.org/10.15252/embr.201438638.
[41] S.A. Manning, B. Kroeger, K.F. Harvey, The regulation of Yorkie, YAP and TAZ: new insights into the Hippo pathway, Dev 147 (2020), https://doi.org/10.1242/DEV.179069.
[42] C.A. Fullenkamp, S.L. Hall, O.I. Jaber, B.L. Pakalniskis, E.C. Savage, J.M. Savage, G.K. Ofori-Amanfo, A.M. Lambertz, S.D. Ivins, C.S. Stipp, B.J. Miller, M. M. Milhem, M.R. Tanas, TAZ and YAP are frequently activated oncoproteins in sarcomas, Oncotarget 7 (2016) 30094–30108, https://doi.org/10.18632/oncotarget.8979.
[43] M. Bartucci, R. Dattilo, C. Moriconi, A. Pagliuca, M. Mottolese, G. Federici, A. Di Benedetto, M. Todaro, G. Stassi, F. Sperati, M.I. Amabile, E. Pilozzi, M. Patrizii, M. Biffoni, M. Maugeri-Saccà, S. Piccolo, R. De Maria, TAZ is required for metastatic activity and chemoresistance of breast cancer stem cells, Oncogene 34 (2015) 681–690, https://doi.org/10.1038/onc.2014.5.
[44] L. Wang, S. Shi, Z. Guo, X. Zhang, S. Han, A. Yang, W. Wen, Q. Zhu, Overexpression of YAP and TAZ is an independent predictor of prognosis in colorectal cancer and related to the proliferation and metastasis of colon cancer cells, PLoS One 8 (2013), https://doi.org/10.1371/journal.pone.0065539.
[45] F. Nallet-Staub, V. Marsaud, L. Li, C. Gilbert, S. Dodier, V. Bataille, M. Sudol, M. Herlyn, A. Mauviel, Pro-invasive activity of the hippo pathway effectors YAP and TAZ in cutaneous melanoma, J. Invest. Dermatol. 134 (2014) 123–132, https://doi.org/10.1038/jid.2013.319.
[46] S. Buglioni, P. Vici, D. Sergi, L. Pizzuti, L. Di Lauro, B. Antoniani, F. Sperati, I. Terrenato, M. Carosi, T. Gamucci, C. Vincenzoni, L. Mariani, E. Vizza, A. Venuti, G. Sanguineti, A. Gadducci, M. Barba, C. Natoli, I. Vitale, M. Mottolese, R. De Maria, M. Maugeri-Saccà, Analysis of the hippo transducers TAZ and YAP in cervical cancer and its microenvironment, Oncoimmunology 5 (2016), https://doi.org/10.1080/2162402X.2016.1160187.
[47] J. Li, Z. Li, Y. Wu, Y. Wang, D. Wang, W. Zhang, H. Yuan, J. Ye, X. Song, J. Yang, H. Jiang, J. Cheng, The Hippo effector TAZ promotes cancer stemness by transcriptional activation of SOX2 in head neck squamous cell carcinoma, Cell Death Dis. 10 (2019), https://doi.org/10.1038/s41419-019-1838-0.
[48] W.Y.T. Xu, W. Wang, S. Zhang, R.A. Stewart, Identifying tumor suppressors in genetic mosaics: the drosophila lats gene encodes a putative protein kinase, Development 121 (1995) 1053–1063.
[49] R.W. Justice, O. Zilian, D.F. Woods, M. Noll, P.J. Bryant, The drosophila tumor suppressor gene warts encodes a homolog of human myotonic dystrophy kinase and is required for the control of cell shape and proliferation, Genes Dev. 9 (1995) 534–546, https://doi.org/10.1101/gad.9.5.534.
[50] J. Dong, G. Feldmann, J. Huang, S. Wu, N. Zhang, S.A. Comerford, M.F.F. Gayyed, R.A. Anders, A. Maitra, D. Pan, Elucidation of a universal size-control mechanism in drosophila and mammals, Cell 130 (2007) 1120–1133, https://doi.org/10.1016/j.cell.2007.07.019.
[51] Z. Meng, T. Moroishi, K.L. Guan, Mechanisms of Hippo pathway regulation, Genes Dev. 30 (2016) 1–17, https://doi.org/10.1101/gad.274027.115.
[52] B. Zhao, X. Wei, W. Li, R.S. Udan, Q. Yang, J. Kim, J. Xie, T. Ikenoue, J. Yu, L. Li, P. Zheng, K. Ye, A. Chinnaiyan, G. Halder, Z.C. Lai, K.L. Guan, Inactivation of YAP oncoprotein by the Hippo pathway is involved in cell contact inhibition and tissue growth control, Genes Dev. 21 (2007) 2747–2761, https://doi.org/10.1101/gad.1602907.
[53] Q.-Y. Lei, H. Zhang, B. Zhao, Z.-Y. Zha, F. Bai, X.-H. Pei, S. Zhao, Y. Xiong, K.-L. Guan, TAZ promotes cell proliferation and epithelial-mesenchymal transition and is inhibited by the hippo pathway, Mol. Cell. Biol. 28 (2008) 2426–2436, https://doi.org/10.1128/mcb.01874-07.
[54] B. Zhao, L. Li, K. Tumaneng, C.Y. Wang, K.L. Guan, A coordinated phosphorylation by Lats and CK1 regulates YAP stability through SCFβ-TRCP, Genes Dev. 24 (2010) 72–85, https://doi.org/10.1101/gad.1843810.
[55] C.Y. Liu, Z.Y. Zha, X. Zhou, H. Zhang, W. Huang, D. Zhao, T. Li, S.W. Chan, C. J. Lim, W. Hong, S. Zhao, Y. Xiong, Q.Y. Lei, K.L. Guan, The hippo tumor pathway promotes TAZ degradation by phosphorylating a phosphodegron and recruiting the SCFβ-TrCP E3 ligase, J. Biol. Chem. 285 (2010) 37159–37169, https://doi.org/10.1074/jbc.M110.152942.
[56] P. Wang, Y. Bai, B. Song, Y. Wang, D. Liu, Y. Lai, X. Bi, Z. Yuan, PP1A-mediated dephosphorylation positively regulates YAP2 activity, PLoS One 6 (2011), https://doi.org/10.1371/journal.pone.0024288.
[57] X. Liu, N. Yang, S.A. Figel, K.E. Wilson, C.D. Morrison, I.H. Gelman, J. Zhang, PTPN14 interacts with and negatively regulates the oncogenic function of YAP, Oncogene 32 (2013) 1266–1273, https://doi.org/10.1038/onc.2012.147.
[58] J.M. Huang, I. Nagatomo, E. Suzuki, T. Mizuno, T. Kumagai, A. Berezov, H. Zhang, B. Karlan, M.I. Greene, Q. Wang, YAP modifies cancer cell sensitivity to EGFR and survivin inhibitors and is negatively regulated by the non-receptor type protein tyrosine phosphatase 14, Oncogene 32 (2013) 2220–2229, https://doi.org/10.1038/onc.2012.231.
[59] C. Michaloglou, W. Lehmann, T. Martin, C. Delaunay, A. Hueber, L. Barys, H. Niu, E. Billy, M. Wartmann, M. Ito, C.J. Wilson, M.E. Digan, A. Bauer, H. Voshol,

G. Christofori, W.R. Sellers, F. Hofmann, T. Schmelzle, The tyrosine phosphatase PTPN14 is a negative regulator of YAP activity, PLoS One 8 (2013), https://doi.org/10.1371/journal.pone.0061916.
[60] W. Wang, J. Huang, X. Wang, J. Yuan, X. Li, L. Feng, J. Il Park, J. Chen, PTPN14 is required for the density-dependent control of YAP1, Genes Dev. 26 (2012) 1959–1971, https://doi.org/10.1101/gad.192955.112.
[61] K.E. Wilson, Y.W. Li, N. Yang, H. Shen, A.R. Orillion, J. Zhang, PTPN14 forms a complex with Kibra and LATS1 proteins and negatively regulates the YAP oncogenic function, J. Biol. Chem. 289 (2014) 23693–23700, https://doi.org/10.1074/jbc.M113.534701.
[62] M.B.Y.F. Kanai, P.A. Marignani, D. Sarbassova, R. Yagi, R.A. Hall, M. Donowitz, A. Hisaminato, T. Fujiwara, Y. Ito, L.C. Cantley, TAZ: a novel transcriptional co-activator regulated by interactions with 14-3-3 and PDZ domain proteins, EMBO J. 19 (2000) 6778–6791.
[63] W.M. Mahoney, J.H. Hong, M.B. Yaffe, I.K.G. Farrance, The transcriptional co-activator TAZ interacts differentially with transcriptional enhancer factor-1 (TEF-1) family members, Biochem. J. 388 (2005) 217–225, https://doi.org/10.1042/BJ20041434.
[64] H. Huh, D. Kim, H.-S. Jeong, H. Park, Regulation of TEAD transcription factors in cancer biology, Cells 8 (2019) 600, https://doi.org/10.3390/cells8060600.
[65] A. Komuro, M. Nagai, N.E. Navin, M. Sudol, WW domain-containing protein YAP associates with ErbB-4 and acts as a co-transcriptional activator for the carboxyl-terminal fragment of ErbB-4 that translocates to the nucleus, J. Biol. Chem. 278 (2003) 33334–33341, https://doi.org/10.1074/jbc.M305597200.
[66] X. Varelas, R. Sakuma, P. Samavarchi-Tehrani, R. Peerani, B.M. Rao, J. Dembowy, M.B. Yaffe, P.W. Zandstra, J.L. Wrana, TAZ controls Smad nucleocytoplasmic shuttling and regulates human embryonic stem-cell self-renewal, Nat. Cell Biol. 10 (2008) 837–848, https://doi.org/10.1038/ncb1748.
[67] O. Ferrigno, F. Lallemand, F. Verrecchia, S. L'hoste, J. Camonis, A. Atfi, A. Mauviel, Yes-associated protein (YAP65) interacts with Smad7 and potentiates its inhibitory activity against TGF-β/Smad signaling, Oncogene 21 (2002) 4879–4884, https://doi.org/10.1038/sj.onc.1205623.
[68] M. Kulkarni, T.Z. Tan, N.B.S. Sulaiman, J.M. Lamar, P. Bansal, J. Cui, Y. Qiao, Y. Ito, RUNX1 and RUNX3 protect against YAP-mediated EMT, stemness and shorter survival outcomes in breast cancer, Oncotarget 9 (2018) 14175–14192, https://doi.org/10.18632/oncotarget.24419.
[69] M. Murakami, M. Nakagawa, E.N. Olson, O. Nakagawa, A WW domain protein TAZ is a critical coactivator for TBX5, a transcription factor implicated in Holt-Oram syndrome, Proc. Natl. Acad. Sci. U. S. A. 102 (2005) 18034–18039, https://doi.org/10.1073/pnas.0509109102.
[70] J. Rosenbluh, D. Nijhawan, A.G. Cox, X. Li, J.T. Neal, E.J. Schafer, T.I. Zack, X. Wang, A. Tsherniak, A.C. Schinzel, D.D. Shao, S.E. Schumacher, B.A. Weir, F. Vazquez, G.S. Cowley, D.E. Root, J.P. Mesirov, R. Beroukhim, C.J. Kuo, W. Goessling, W.C. Hahn, β-Catenin-driven cancers require a YAP1 transcriptional complex for survival and tumorigenesis, Cell 151 (2012) 1457–1473, https://doi.org/10.1016/j.cell.2012.11.026.
[71] M. Zagurovskaya, M.M. Shareef, A. Das, A. Reeves, S. Gupta, M. Sudol, M. T. Bedford, J. Prichard, M. Mohiuddin, M.M. Ahmed, EGR-1 forms a complex with YAP-1 and upregulates Bax expression in irradiated prostate carcinoma cells, Oncogene 28 (2009) 1121–1131, https://doi.org/10.1038/onc.2008.461.
[72] S. Strano, E. Munarriz, M. Rossi, L. Castagnoli, Y. Shaul, A. Sacchi, M. Oren, M. Sudol, G. Cesareni, G. Blandino, Physical interaction with yes-associated protein enhances p73 transcriptional activity, J. Biol. Chem. 276 (2001) 15164–15173, https://doi.org/10.1074/jbc.M010484200.
[73] M. Ota, H. Sasaki, Mammalian Tead proteins regulate cell proliferation and contact inhibition as transcriptional mediators of Hippo signaling, Development 135 (2008) 4059–4069, https://doi.org/10.1242/dev.027151.
[74] C.C. Yang, H.K. Graves, I.M. Moya, C. Tao, F. Hamaratoglu, A.B. Gladden, G. Halder, Differential regulation of the hippo pathway by adherens junctions and apical- basal cell polarity modules, Proc. Natl. Acad. Sci. U. S. A. 112 (2015) 1785–1790, https://doi.org/10.1073/pnas.1420850112.
[75] M. deRan, J. Yang, C.H. Shen, E.C. Peters, J. Fitamant, P. Chan, M. Hsieh, S. Zhu, J.M. Asara, B. Zheng, N. Bardeesy, J. Liu, X. Wu, Energy stress regulates Hippo-YAP signaling involving AMPK-mediated regulation of angiomotin-like 1 protein, Cell Rep. 9 (2014) 495–503, https://doi.org/10.1016/j.celrep.2014.09.036.
[76] S. Yang, L. Zhang, M. Liu, R. Chong, S.J. Ding, Y. Chen, J. Dong, CDK1 phosphorylation of YAP promotes mitotic defects and cell motility and is essential for neoplastic transformation, Cancer Res. 73 (2013) 6722–6733, https://doi.org/10.1158/0008-5472.CAN-13-2049.
[77] A. Totaro, M. Castellan, D. Di Biagio, S. Piccolo, Crosstalk between YAP/TAZ and notch Signaling, Trends Cell Biol. 28 (2018) 560–573, https://doi.org/10.1016/j.tcb.2018.03.001.
[78] M. Tariki, P.K. Dhanyamraju, V. Fendrich, T. Borggrefe, G. Feldmann, M. Lauth, The Yes-associated protein controls the cell density regulation of Hedgehog signaling, Oncogenesis 3 (2014), https://doi.org/10.1038/oncsis.2014.27.
[79] X. Varelas, B.W. Miller, R. Sopko, S. Song, A. Gregorieff, F.A. Fellouse, R. Sakuma, T. Pawson, W. Hunziker, H. McNeill, J.L. Wrana, L. Attisano, The hippo pathway regulates Wnt/β-catenin signaling, Dev. Cell 18 (2010) 579–591, https://doi.org/10.1016/j.devcel.2010.03.007.
[80] S.K. Verma, T.S. Ganesan, P.J. Parker, The tumour suppressor RASSF1A is a novel substrate of PKC, FEBS Lett. 582 (2008) 2270–2276, https://doi.org/10.1016/j.febslet.2008.05.028.
[81] C. Guo, S. Tommasi, L. Liu, J.K. Yee, R. Dammann, G.P.P. Pfeifer, RASSF1A is part of a complex similar to the drosophila Hippo/Salvador/Lats tumor-suppressor network, Curr. Biol. 17 (2007) 700–705, https://doi.org/10.1016/j.cub.2007.02.055.
[82] M.C. Schroeder, G. Halder, Regulation of the Hippo pathway by cell architecture and mechanical signals, Semin. Cell Dev. Biol. 23 (2012) 803–811, https://doi.org/10.1016/j.semcdb.2012.06.001.
[83] A. Elbediwy, Z.I. Vincent-Mistiaen, B. Spencer-Dene, R.K. Stone, S. Boeing, S. K. Wculek, J. Cordero, E.H. Tan, R. Ridgway, V.G. Brunton, E. Sahai, H. Gerhardt, A. Behrens, I. Malanchi, O.J. Sansom, B.J. Thompson, Integrin signalling regulates YAP and TAZ to control skin homeostasis, Dev 143 (2016) 1674–1687, https://doi.org/10.1242/dev.133728.
[84] K. Schlegelmilch, M. Mohseni, O. Kirak, J. Pruszak, J.R. Rodriguez, D. Zhou, B. T. Kreger, V. Vasioukhin, J. Avruch, T.R. Brummelkamp, F.D. Camargo, Yap1 acts downstream of α-catenin to control epidermal proliferation, Cell 144 (2011) 782–795, https://doi.org/10.1016/j.cell.2011.02.031.
[85] X. Hong, H.T. Nguyen, Q. Chen, R. Zhang, Z. Hagman, P.M. Voorhoeve, S. M. Cohen, Opposing activities of the R as and H ippo pathways converge on regulation of YAP protein turnover, EMBO J. 33 (2014) 2447–2457, https://doi.org/10.15252/embj.201489385.
[86] N. Raj, R. Bam, Reciprocal crosstalk between YAP1/Hippo pathway and the p53 family proteins: mechanisms and outcomes in cancer, Front. Cell Dev. Biol. 7 (2019), https://doi.org/10.3389/fcell.2019.00159.
[87] X. Su, M. Napoli, H.A. Abbas, A. Venkatanarayan, N.H.B. Bui, C. Coarfa, Y.J. Gi, F. Kittrell, P.H. Gunaratne, D. Medina, J.M. Rosen, F. Behbod, E.R. Flores, TAp63 suppresses mammary tumorigenesis through regulation of the Hippo pathway, Oncogene 36 (2017) 2377–2393, https://doi.org/10.1038/onc.2016.388.
[88] Y. Li, F. Kong, Q. Shao, R. Wang, E. Hu, J. Liu, C. Jin, D. He, X. Xiao, YAP expression and activity are suppressed by S100A7 via p65/NFkB-mediated repression of DNp63, Mol. Cancer Res. 15 (2017) 1752–1763, https://doi.org/10.1158/1541-7786.MCR-17-0349.
[89] I. Valencia-Sama, Y. Zhao, D. Lai, H.J.J. Van Rensburg, Y. Hao, X. Yang, Hippo component TAZ functions as a co-repressor and negatively regulates ΔNp63 transcription through TEA domain (TEAD) transcription factor, J. Biol. Chem. 290 (2015) 16906–16917, https://doi.org/10.1074/jbc.M115.642363.
[90] A. Chatterjee, T. Sen, X. Chang, D. Sidransky, Yes-associated protein 1 regulates the stability of δNp63α, Cell Cycle 9 (2010) 162–167, https://doi.org/10.4161/cc.9.1.10321.
[91] H. Zhang, S. Wu, D. Xing, YAP accelerates Aβ25-35-induced apoptosis through upregulation of Bax expression by interaction with p73, Apoptosis 16 (2011) 808–821, https://doi.org/10.1007/s10495-011-0608-y.
[92] Y. Aylon, D. Michael, A. Shmueli, N. Yabuta, H. Nojima, M. Oren, A positive feedback loop between the p53 and Lats2 tumor suppressors prevents tetraploidization, Genes Dev. 20 (2006) 2687–2700, https://doi.org/10.1101/gad.1447006.
[93] N. Furth, Y. Aylon, M. Oren, P53 shades of Hippo, Cell Death Differ. 25 (2018) 81–92, https://doi.org/10.1038/cdd.2017.163.
[94] Y. Aylon, Y. Ofir-Rosenfeld, N. Yabuta, E. Lapi, H. Nojima, X. Lu, M. Oren, The Lats2 tumor suppressor augments p53-mediated apoptosis by promoting the nuclear proapoptotic function of ASPP1, Genes Dev. 24 (2010) 2420–2429, https://doi.org/10.1101/gad.1954410.
[95] S.S. Mello, L.J. Valente, N. Raj, J.A. Seoane, B.M. Flowers, J. McClendon, K. T. Bieging-Rolett, J. Lee, D. Ivanochko, M.M. Kozak, D.T. Chang, T.A. Longacre, A.C. Koong, C.H. Arrowsmith, S.K. Kim, H. Vogel, L.D. Wood, R.H. Hruban, C. Curtis, L.D. Attardi, A p53 super-tumor suppressor reveals a tumor suppressive p53-Ptpn14-Yap axis in pancreatic cancer, Cancer Cell 32 (2017) 460–473.e6, https://doi.org/10.1016/j.ccell.2017.09.007.
[96] H. Hermeking, C. Lengauer, K. Polyak, T.C. He, L. Zhang, S. Thiagalingam, K. W. Kinzler, B. Vogelstein, 14-3-3σ is a p53-regulated inhibitor of G2/M progression, Mol. Cell 1 (1997) 3–11, https://doi.org/10.1016/S1097-2765(00)80002-7.
[97] C. Wang, X. Zhu, W. Feng, Y. Yu, K. Jeong, W. Guo, Y. Lu, G.B. Mills, Verteporfin inhibits YAP function through up-regulating 14-3-3σ sequestering YAP in the cytoplasm, Am. J. Cancer Res. 6 (2016) 27–37. www.ajcr.us/ (accessed October 20, 2020).
[98] N. Bai, C. Zhang, N. Liang, Z. Zhang, A. Chang, J. Yin, Z. Li, N. Li, X. Tan, N. Luo, Y. Luo, R. Xiang, X. Li, R.A. Reisfeld, D. Stupack, D. Lv, C. Liu, Yes-associated protein (YAP) increases chemosensitivity of hepatocellular carcinoma cells by modulation of p53, Cancer Biol. Ther. 14 (2013) 511–520, https://doi.org/10.4161/cbt.24345.
[99] S. Mori, T. Takeuchi, Y. Ishii, T. Yugawa, T. Kiyono, H. Nishina, I. Kukimoto, Human papillomavirus 16 E6 upregulates APOBEC3B via the TEAD transcription factor, J. Virol. 91 (2017), https://doi.org/10.1128/jvi.02413-16.
[100] E.L. Morgan, M.R. Patterson, E.L. Ryder, S.Y. Lee, C.W. Wasson, K.L. Harper, Y. Li, S. Griffin, G.E. Blair, A. Whitehouse, A. Macdonald, MicroRNA-18a targeting of the STK4/MST1 tumour suppressor is necessary for transformation in HPV positive cervical cancer, PLoS Pathog. 16 (2020), e1008624, https://doi.org/10.1371/journal.ppat.1008624.
[101] M. Nishio, Y. To, T. Maehama, Y. Aono, J. Otani, H. Hikasa, A. Kitagawa, K. Mimori, T. Sasaki, H. Nishina, S. Toyokuni, J.P. Lydon, K. Nakao, T. Wah Mak, T. Kiyono, H. Katabuchi, H. Tashiro, A. Suzuki, Endogenous YAP1 activation drives immediate onset of cervical carcinoma in situ in mice, Cancer Sci. 111 (2020), https://doi.org/10.1111/cas.14581.
[102] M. Mohseni, J. Sun, A. Lau, S. Curtis, J. Goldsmith, V.L. Fox, C. Wei, M. Frazier, O. Samson, K.K. Wong, C. Kim, F.D. Camargo, A genetic screen identifies an LKB1-MARK signalling axis controlling the Hippo-YAP pathway, Nat. Cell Biol. 16 (2014) 108–117, https://doi.org/10.1038/ncb2884.
[103] B. Zhao, L. Li, Q. Lu, L.H. Wang, C.Y. Liu, Q. Lei, K.L. Guan, Angiomotin is a novel Hippo pathway component that inhibits YAP oncoprotein, Genes Dev. 25 (2011) 51–63, https://doi.org/10.1101/gad.2000111.

[104] C. Kranjec, L. Banks, A systematic analysis of human papillomavirus (HPV) E6 PDZ substrates identifies MAGI-1 as a major target of HPV type 16 (HPV-16) and HPV-18 whose loss accompanies disruption of tight junctions, J. Virol. 85 (2011) 1757–1764, https://doi.org/10.1128/jvi.01756-10.
[105] M.K. Kim, J.W. Jang, S.C. Bae, DNA binding partners of YAP/TAZ, BMB Rep. 51 (2018) 126–133, https://doi.org/10.5483/BMBRep.2018.51.3.015.
[106] M.X. Cao, W.L. Zhang, X.H. Yu, J.S. Wu, X.W. Qiao, M.C. Huang, K. Wang, J. B. Wu, Y.J. Tang, J. Jiang, X.H. Liang, Y.L. Tang, Interplay between cancer cells and M2 macrophages is necessary for miR-550a-3-5p down-regulation-mediated HPV-positive OSCC progression, J. Exp. Clin. Cancer Res. 39 (2020), https://doi.org/10.1186/s13046-020-01602-1.
[107] E.A. White, K. Münger, P.M. Howley, High-risk human papillomavirus E7 proteins target PTPN14 for degradation, MBio 7 (2016), https://doi.org/10.1128/mBio.01530-16.
[108] H.Y. Yun, M.W. Kim, H.S. Lee, W. Kim, J.H. Shin, H. Kim, H.C. Shin, H. Park, B. H. Oh, W.K. Kim, K.H. Bae, S.C. Lee, E.W. Lee, B. Ku, S.J. Kim, Structural basis for recognition of the tumor suppressor protein PTPN14 by the oncoprotein E7 of human papillomavirus, PLoS Biol. 17 (2019), https://doi.org/10.1371/journal.pbio.3000367.
[109] J. Hatterschide, A.E. Bohidar, M. Grace, T.J. Nulton, H.W. Kim, B. Windle, I. M. Morgan, K. Munger, E.A. White, PTPN14 degradation by high-risk human papillomavirus E7 limits keratinocyte differentiation and contributes to HPV-mediated oncogenesis, Proc. Natl. Acad. Sci. U. S. A. 116 (2019) 7033–7042, https://doi.org/10.1073/pnas.1819534116.
[110] J. Hatterschide, A.C. Brantly, M. Grace, K. Munger, E.A. White, A conserved amino acid in the C-terminus of HPV E7 mediates binding to PTPN14 and repression of epithelial differentiation, J. Virol. (2020), https://doi.org/10.1128/jvi.01024-20.
[111] T.M. Wise-Draper, H.V. Allen, M.N. Thobe, E.E. Jones, K.B. Habash, K. Münger, S. I. Wells, The human DEK proto-oncogene is a senescence inhibitor and an upregulated target of high-risk human papillomavirus E7, J. Virol. 79 (2005) 14309–14317, https://doi.org/10.1128/jvi.79.22.14309-14317.2005.
[112] A.K. Adams, G.E. Hallenbeck, K.A. Casper, Y.J. Patil, K.M. Wilson, R.J. Kimple, P. F. Lambert, D.P. Witte, W. Xiao, M.L. Gillison, K.A. Wikenheiser-Brokamp, T. M. Wise-Draper, S.I. Wells, DEK promotes HPV-positive and -negative head and neck cancer cell proliferation, Oncogene 34 (2015) 868–877, https://doi.org/10.1038/onc.2014.15.
[113] S. Citro, A. Bellini, A. Medda, M.E. Sabatini, M. Tagliabue, F. Chu, S. Chiocca, Human papilloma virus increases ΔNp63α expression in head and neck squamous cell carcinoma, Front. Cell. Infect. Microbiol. 10 (2020), https://doi.org/10.3389/fcimb.2020.00143.
[114] M. Melar-New, L.A. Laimins, Human papillomaviruses modulate expression of MicroRNA 203 upon epithelial differentiation to control levels of p63 proteins, J. Virol. 84 (2010) 5212–5221, https://doi.org/10.1128/jvi.00078-10.
[115] S. Eldakhakhny, Q. Zhou, E.J. Crosbie, B.S. Sayan, Human papillomavirus E7 induces p63 expression to modulate DNA damage response article, Cell Death Dis. 9 (2018), https://doi.org/10.1038/s41419-017-0149-6.
[116] C. Prieto-Garcia, O. Hartmann, M. Reissland, F. Braun, T. Fischer, S. Walz, C. Schülein-Völk, U. Eilers, C.P. Ade, M.A. Calzado, A. Orian, H.M. Maric, C. Münch, M. Rosenfeldt, M. Eilers, M.E. Diefenbacher, Maintaining protein stability of ΔNp63 via USP 28 is required by squamous cancer cells, EMBO Mol. Med. 12 (2020), https://doi.org/10.15252/emmm.201911101.
[117] A. Bankhead, T. McMaster, Y. Wang, P.S. Boonstra, P.L. Palmbos, TP63 isoform expression is linked with distinct clinical outcomes in cancer, EBioMedicine 51 (2020), https://doi.org/10.1016/j.ebiom.2019.11.022.
[118] K. Srivastava, A. Pickard, S. McDade, D.J. McCance, p63 drives invasion in keratinocytes expressing HPV16 E6/E7 genes through regulation of Src-FAK signalling, Oncotarget 8 (2017) 16202–16219, https://doi.org/10.18632/oncotarget.3892.
[119] Y. Khalifa, S. Teissier, M.K.M. Tan, Q.T. Phan, M. Daynac, W.Q. Wong, F. Thierry, The human papillomavirus e6 oncogene represses a cell adhesion pathway and disrupts focal adhesion through degradation of tap63β upon transformation, PLoS Pathog. 7 (2011), https://doi.org/10.1371/journal.ppat.1002256.
[120] L.A. Brooks, A. Sullivan, J. O'Nions, A. Bell, B. Dunne, J.A. Tidy, D.J. Evans, P. Osin, K.H. Vousden, B. Gusterson, P.J. Farrell, A. Storey, M. Gasco, T. Sakai, T. Crook, E7 proteins from oncogenic human papillomavirus types transactivate p73: role in cervical intraepithelial neoplasia, Br. J. Cancer 86 (2002) 263–268, https://doi.org/10.1038/sj.bjc.6600033.
[121] J.S. Park, E.J. Kim, J.Y. Lee, H.S. Sin, S.E. Namkoong, S.J. Um, Functional inactivation of p73, a homolog of p53 tumor suppressor protein, by human papillomavirus E6 proteins, Int. J. Cancer 91 (2001) 822–827, https://doi.org/10.1002/1097-0215(200002)9999:9999<::AID-IJC1130>3.0.CO;2-0.
[122] S. Di Agostino, G. Sorrentino, E. Ingallina, F. Valenti, M. Ferraiuolo, S. Bicciato, S. Piazza, S. Strano, G. Del Sal, G. Blandino, YAP enhances the pro-proliferative transcriptional activity of mutant p53 proteins, EMBO Rep. 17 (2016) 188–201, https://doi.org/10.15252/embr.201540488.
[123] M. Ferraiuolo, L. Verduci, G. Blandino, S. Strano, Mutant p53 protein and the hippo transducers YAP and TAZ: a Critical oncogenic node in human cancers, Int. J. Mol. Sci. 18 (2017), https://doi.org/10.3390/ijms18050961.
[124] A.C. Joerger, A.R. Fersht, The p53 pathway: origins, inactivation in cancer, and emerging therapeutic approaches, Annu. Rev. Biochem. 85 (2016) 375–404, https://doi.org/10.1146/annurev-biochem-060815-014710.
[125] S. Li, X. Hong, Z. Wei, M. Xie, W. Li, G. Liu, H. Guo, J. Yang, W. Wei, S. Zhang, Ubiquitination of the HPV oncoprotein E6 is critical for E6/E6AP-mediated p53 degradation, Front. Microbiol. 10 (2019), https://doi.org/10.3389/fmicb.2019.02483.
[126] Y. Masuda, Y. Saeki, N. Arai, H. Kawai, I. Kukimoto, K. Tanaka, C. Masutani, Stepwise multipolyubiquitination of p53 by the E6AP-E6 ubiquitin ligase complex, J. Biol. Chem. 294 (2019) 14860–14875, https://doi.org/10.1074/jbc.RA119.008374.
[127] N.A. Wallace, K. Robinson, H.L. Howie, D.A. Galloway, HPV 5 and 8 E6 abrogate ATR activity resulting in increased persistence of UVB induced DNA damage, PLoS Pathog. 8 (2012) 41, https://doi.org/10.1371/journal.ppat.1002807.
[128] N.A. Wallace, S.L. Gasior, Z.J. Faber, H.L. Howie, P.L. Deininger, D.A. Galloway, HPV 5 and 8 E6 expression reduces ATM protein levels and attenuates LINE-1 retrotransposition, Virology 443 (2013) 69–79, https://doi.org/10.1016/j.virol.2013.04.022.
[129] N.A. Wallace, K. Robinson, D.A. Galloway, Beta human papillomavirus E6 expression inhibits stabilization of p53 and increases tolerance of genomic instability, J. Virol. 88 (2014) 6112–6127, https://doi.org/10.1128/jvi.03808-13.
[130] N.J. Ganem, H. Cornils, S.Y. Chiu, K.P. O'Rourke, J. Arnaud, D. Yimlamai, M. Théry, F.D. Camargo, D. Pellman, Cytokinesis failure triggers hippo tumor suppressor pathway activation, Cell 158 (2014) 833–848, https://doi.org/10.1016/j.cell.2014.06.029.
[131] P.T. Stukenberg, Triggering p53 after cytokinesis failure, J. Cell Biol. 165 (2004) 607–608, https://doi.org/10.1083/jcb.200405089.
[132] R. Accardi, W. Dong, A. Smet, R. Cui, A. Hautefeuille, A.S. Gabet, B.S. Sylla, L. Gissmann, P. Hainaut, M. Tommasino, Skin human papillomavirus type 38 alters p53 functions by accumulation of ΔNp73, EMBO Rep. 7 (2006) 334–340, https://doi.org/10.1038/sj.embor.7400615.
[133] W. Dong, C. Arpin, R. Accardi, L. Gissmann, B.S. Sylla, J. Marvel, M. Tommasino, Loss of p53 or p73 in human papillomavirus type 38 E6 and E7 transgenic mice partially restores the UV-activated cell cycle checkpoints, Oncogene 27 (2008) 2923–2928, https://doi.org/10.1038/sj.onc.1210944.
[134] R. Yang, J. Klimentová, E. Göckel-Krzikalla, R. Ly, N. Gmelin, A. Hotz-Wagenblatt, H. Řehulková, J. Stulík, F. Rösl, M. Niebler, Combined Transcriptome and proteome analysis of immortalized human keratinocytes expressing human papillomavirus 16 (HPV16) oncogenes reveals novel key factors and networks in HPV-induced carcinogenesis, MSphere 4 (2019), https://doi.org/10.1128/msphere.00129-19.
[135] T. Klymenko, Q. Gu, I. Herbert, A. Stevenson, V. Iliev, G. Watkins, C. Pollock, R. Bhatia, K. Cuschieri, P. Herzyk, D. Gatherer, S.V. Graham, RNA-Seq analysis of differentiated keratinocytes reveals a massive response to late events during human papillomavirus 16 infection, including loss of epithelial barrier function, J. Virol. 91 (2017), https://doi.org/10.1128/jvi.01001-17.
[136] T. Qin, L.A. Koneva, Y. Liu, Y. Zhang, A.E. Arthur, K.R. Zarins, T.E. Carey, D. Chepeha, G.T. Wolf, L.S. Rozek, M.A. Sartor, Significant association between host transcriptome-derived HPV oncogene E6* influence score and carcinogenic pathways, tumor size, and survival in head and neck cancer, Head Neck (2020), https://doi.org/10.1002/hed.26244.
[137] E.A. White, R.E. Kramer, M.J.A. Tan, S.D. Hayes, J.W. Harper, P.M. Howley, Comprehensive analysis of host cellular interactions with human papillomavirus E6 proteins identifies New E6 binding partners and reflects viral diversity, J. Virol. 86 (2012) 13174–13186, https://doi.org/10.1128/jvi.02172-12.
[138] Q. ul A. Farooq, Z. Shaukat, T. Zhou, S. Aiman, W. Gong, C. Li, Inferring virus-host relationship between HPV and its host Homo sapiens using protein interaction network, Sci. Rep. 10 (2020), https://doi.org/10.1038/s41598-020-65837-w.
[139] P. Paget-Bailly, K. Meznad, D. Bruyère, J. Perrard, M. Herfs, A.C. Jung, C. Mougin, J.L. Prétet, A. Baguet, Comparative RNA sequencing reveals that HPV16 E6 abrogates the effect of E6*I on ROS metabolism, Sci. Rep. 9 (2019), https://doi.org/10.1038/s41598-019-42393-6.
[140] M. Jang, J.E. Rhee, D.H. Jang, S.S. Kim, Gene expression profiles are altered in human papillomavirus-16 E6 D25E-expressing cell lines, Virol. J. 8 (2011), https://doi.org/10.1186/1743-422X-8-453.
[141] V. Fragoso-Ontiveros, R. María Alvarez-García, A. Contreras-Paredes, F. Vaca-Paniagua, L. Alonso Herrera, C. López-Camarillo, N. Jacobo-Herrera, M. Lizano-Soberón, C. Pérez-Plasencia, Gene expression profiles induced by E6 from non-European HPV18 variants reveals a differential activation on cellular processes driving to carcinogenesis, Virology 432 (2012) 81–90, https://doi.org/10.1016/j.virol.2012.05.029.
[142] O. Rozenblatt-Rosen, R.C. Deo, M. Padi, G. Adelmant, M.A. Calderwood, T. Rolland, M. Grace, A. Dricot, M. Askenazi, M. Tavares, S.J. Pevzner, F. Abderazzaq, D. Byrdsong, A.R. Carvunis, A.A. Chen, J. Cheng, M. Correll, M. Duarte, C. Fan, M.C. Feltkamp, S.B. Ficarro, R. Franchi, B.K. Garg, N. Gulbahce, T. Hao, A.M. Holthaus, R. James, A. Korkhin, L. Litovchick, J. C. Mar, T.R. Pak, S. Rabello, R. Rubio, Y. Shen, S. Singh, J.M. Spangle, M. Tasan, S. Wanamaker, J.T. Webber, J. Roecklein-Canfield, E. Johannsen, A.L. Barabási, R. Beroukhim, E. Kieff, M.E. Cusick, D.E. Hill, K. Münger, J.A. Marto, J. Quackenbush, F.P. Roth, J.A. Decaprio, M. Vidal, Interpreting cancer genomes using systematic host network perturbations by tumour virus proteins, Nature 487 (2012) 491–495, https://doi.org/10.1038/nature11288.
[143] M.E. Sowa White, M.J.A. Tan, S. Jeudy, S.D. Hayes, S. Santha, K. Münger, J. W. Harper, P.M. Howley, Systematic identification of interactions between host cell proteins and E7 oncoproteins from diverse human papillomaviruses, Proc. Natl. Acad. Sci. U. S. A. 109 (2012) E.A, https://doi.org/10.1073/pnas.1116776109.
[144] M. Eckhardt, W. Zhang, A.M. Gross, J. Von Dollen, J.R. Johnson, K.E. Franks-Skiba, D.L. Swaney, T.L. Johnson, G.M. Jang, P.S. Shah, T.M. Brand, J. Archambault, J.F. Kreisberg, J.R. Grandis, T. Ideker, N.J. Krogan, Multiple routes to oncogenesis are promoted by the human papillomavirus–host protein

network, Cancer Discov. 8 (2018) 1474–1489, https://doi.org/10.1158/2159-8290.CD-17-1018.
[145] L.J. Castro-Muñoz, J. Manzo-Merino, J.O. Muñoz-Bello, L. Olmedo-Nieva, A. Cedro-Tanda, L.A. Alfaro-Ruiz, A. Hidalgo-Miranda, V. Madrid-Marina, M. Lizano, The human papillomavirus (HPV) E1 protein regulates the expression of cellular genes involved in immune response, Sci. Rep. 9 (2019), https://doi.org/10.1038/s41598-019-49886-4.
[146] E. Ramírez-Salazar, F. Centeno, K. Nieto, A. Valencia-Hernández, M. Salcedo, E. Garrido, HPV16 E2 could act as down-regulator in cellular genes implicated in apoptosis, proliferation and cell differentiation, Virol. J. 8 (2011), https://doi.org/10.1186/1743-422X-8-247.
[147] A.M. Fuentes-González, J.O. Muñoz-Bello, J. Manzo-Merino, A. Contreras-Paredes, A. Pedroza-Torres, J. Fernández-Retana, C. Pérez-Plasencia, M. Lizano, Intratype variants of the E2 protein from human papillomavirus type 18 induce different gene expression profiles associated with apoptosis and cell proliferation, Arch. Virol. 164 (2019) 1815–1827, https://doi.org/10.1007/s00705-018-04124-6.
[148] M. Muller, Y. Jacob, L. Jones, A. Weiss, L. Brino, T. Chantier, V. Lotteau, M. Favre, C. Demeret, Large scale genotype comparison of human papillomavirus E2-host interaction networks provides new insights for E2 molecular functions, PLoS Pathog. 8 (2012), https://doi.org/10.1371/journal.ppat.1002761.
[149] L.P.T.T. Ishiji, S. M J Lace, R.D. Parkkinen, T.H. Anderson, T.P. Haugen, J. H. Cripe, I. Xiao, P. Davidson, Chambon, transcriptional enhancer factor (TEF)-1 and its cell-specific co-activator activate human papillomavirus-16 E6 and E7 oncogene transcription in keratinocytes and cervical carcinoma cells, EMBO J. 11 (1992) 2271–2281.
[150] J.H. Xiao, I. Davidson, H. Matthes, J.M. Garnier, P. Chambon, Cloning, expression, and transcriptional properties of the human enhancer factor TEF-1, Cell 65 (1991) 551–568, https://doi.org/10.1016/0092-8674(91)90088-G.
[151] S. Mori, T. Takeuchi, Y. Ishii, I. Kukimoto, The transcriptional cofactor VGLL1 drives transcription of human papillomavirus early genes via TEAD1, J. Virol. 94 (2020), https://doi.org/10.1128/jvi.01945-19.
[152] T. Kanaya, S. Kyo, L.A. Laimins, The 5′ region of the human papillomavirus type 31 upstream regulatory region acts as an enhancer which augments viral early expression through the action of YY1, Virology 237 (1997) 159–169, https://doi.org/10.1006/viro.1997.8771.
[153] C. Wang, J.S. Davis, At the center of cervical carcinogenesis: synergism between high-risk HPV and the hyperactivated YAP1, Mol. Cell. Oncol. 6 (2019), https://doi.org/10.1080/23723556.2019.1612677.
[154] P.M. Day, M. Schelhaas, Concepts of papillomavirus entry into host cells, Curr. Opin. Virol. 4 (2014) 24–31, https://doi.org/10.1016/j.coviro.2013.11.002.
[155] N. Egawa, K. Egawa, H. Griffin, J. Doorbar, Human papillomaviruses; epithelial tropisms, and the development of neoplasia, Viruses 7 (2015) 3863–3890, https://doi.org/10.3390/v7072802.
[156] A. Elbediwy, Z.I. Vincent-Mistiaen, B.J. Thompson, YAP and TAZ in epithelial stem cells: a sensor for cell polarity, mechanical forces and tissue damage, BioEssays 38 (2016) 644–653, https://doi.org/10.1002/bies.201600037.
[157] Z. Surviladze, A. Dziduszko, M.A. Ozbun, Essential roles for soluble virion-associated heparan sulfonated proteoglycans and growth factors in human papillomavirus infections, PLoS Pathog. 8 (2012), https://doi.org/10.1371/journal.ppat.1002519.
[158] A. Amador-Molina, J.F. Hernández-Valencia, E. Lamoyi, A. Contreras-Paredes, M. Lizano, Role of innate immunity against human papillomavirus (HPV) infections and effect of adjuvants in promoting specific immune response, Viruses 5 (2013) 2624–2642, https://doi.org/10.3390/v5112624.
[159] Q. Zhou, K. Zhu, H. Cheng, Toll-like receptors in human papillomavirus infection, Arch. Immunol. Ther. Exp. 61 (2013) 203–215, https://doi.org/10.1007/s00005-013-0220-7.
[160] M. Iwanaszko, M. Kimmel, NF-KB and IRF pathways: cross-regulation on target genes promoter level, BMC Genomics 16 (2015), https://doi.org/10.1186/s12864-015-1511-7.
[161] E. Platanitis, D. Demiroz, A. Schneller, K. Fischer, C. Capelle, M. Hartl, T. Gossenreiter, M. Müller, M. Novatchkova, T. Decker, A molecular switch from STAT2-IRF9 to ISGF3 underlies interferon-induced gene transcription, Nat. Commun. 10 (2019), https://doi.org/10.1038/s41467-019-10970-y.
[162] H. Xiao, L. Wu, H. Zheng, N. Li, H. Wan, G. Liang, Y. Zhao, J. Liang, Expression of yes-associated protein in cervical squamous epithelium lesions, Int. J. Gynecol. Cancer 24 (2014) 1575–1582, https://doi.org/10.1097/IGC.0000000000000259.
[163] R. Sever, J.S. Brugge, Signal transduction in cancer, Cold Spring Harb. Perspect. Med. 5 (2015), https://doi.org/10.1101/cshperspect.a006098.
[164] Y.B. Yu, Y.H. Wang, X.C. Yang, Y. Zhao, M.L. Wang, Y. Liang, H.T. Niu, The relationship between human papillomavirus and penile cancer over the past decade: a systematic review and meta-analysis, Asian J. Androl. 21 (2019) 375–380, https://doi.org/10.4103/aja.aja_39_19.
[165] M.K. Ibragimova, M.M. Tsyganov, N.V. Litviakov, Human papillomavirus and colorectal cancer, Med. Oncol. 35 (2018), https://doi.org/10.1007/s12032-018-1201-9.
[166] N. Buyru, A. Tezol, N. Dalay, Coexistence of K-ras mutations and HPV infection in colon cancer, BMC Cancer 6 (2006), https://doi.org/10.1186/1471-2407-6-115.
[167] D.C. Damin, M.B. Caetano, M.A. Rosito, G. Schwartsmann, A.S. Damin, A. P. Frazzon, R.D. Ruppenthal, C.O.P. Alexandre, Evidence for an association of human papillomavirus infection and colorectal cancer, Eur. J. Surg. Oncol. 33 (2007) 569–574, https://doi.org/10.1016/j.ejso.2007.01.014.
[168] D.C. Damin, P.K. Ziegelmann, A.P. Damin, Human papillomavirus infection and colorectal cancer risk: a meta-analysis, Color. Dis. 15 (2013), https://doi.org/10.1111/codi.12257.
[169] X.H. Zhang, W. Wang, Y.Q. Wang, D.F. Jia, L. Zhu, Human papillomavirus infection and colorectal cancer in the Chinese population: a meta-analysis, Color. Dis. 20 (2018) 961–969, https://doi.org/10.1111/codi.14416.
[170] Y.G. Eun, D. Lee, Y.C. Lee, B.H. Sohn, E.H. Kim, S.Y. Yim, K.H. Kwon, J.S. Lee, Clinical significance of YAP1 activation in head and neck squamous cell carcinoma, Oncotarget 8 (2017) 111130–111143, https://doi.org/10.18632/oncotarget.22666.
[171] L. Ge, M. Smail, W. Meng, Y. Shyr, F. Ye, K.H. Fan, X. Li, H.M. Zhou, N. A. Bhowmick, Yes-associated protein expression in head and neck squamous cell carcinoma nodal metastasis, PLoS One 6 (2011), https://doi.org/10.1371/journal.pone.0027529.
[172] S. Ono, K. Nakano, K. Takabatake, H. Kawai, H. Nagatsuka, Immunohistochemistry of YAP and dNp63 and survival analysis of patients bearing precancerous lesion and oral squamous cell carcinoma, Int. J. Med. Sci. 16 (2019) 766–773, https://doi.org/10.7150/ijms.29995.
[173] L. Bi, F. Ma, R. Tian, Y. Zhou, W. Lan, Q. Song, X. Cheng, AJUBA increases the cisplatin resistance through hippo pathway in cervical cancer, Gene 644 (2018) 148–154, https://doi.org/10.1016/j.gene.2017.11.017.
[174] K.I. Pappa, P. Christou, A. Xholi, G. Mermelekas, G. Kontostathi, V. Lygirou, M. Makridakis, J. Zoidakis, N.P. Anagnou, Membrane proteomics of cervical cancer cell lines reveal insights on the process of cervical carcinogenesis, Int. J. Oncol. 53 (2018) 2111–2122, https://doi.org/10.3892/ijo.2018.4518.
[175] F. Zheng, H. Yu, RASSF1A promoter methylation was associated with the development, progression and metastasis of cervical carcinoma: a meta-analysis with trial sequential analysis, Arch. Gynecol. Obstet. 297 (2018) 467–477, https://doi.org/10.1007/s00404-017-4639-7.
[176] A.M. Poma, L. Torregrossa, R. Bruno, F. Basolo, G. Fontanini, Hippo pathway affects survival of cancer patients: extensive analysis of TCGA data and review of literature, Sci. Rep. 8 (2018), https://doi.org/10.1038/s41598-018-28928-3.
[177] F. Sanchez-Vega, M. Mina, J. Armenia, W.K. Chatila, A. Luna, K.C. La, S. Dimitriadoy, D.L. Liu, H.S. Kantheti, S. Saghafinia, D. Chakravarty, F. Daian, Q. Gao, M.H. Bailey, W.W. Liang, S.M. Foltz, I. Shmulevich, L. Ding, Z. Heins, A. Ochoa, B. Gross, J. Gao, H. Zhang, R. Kundra, C. Kandoth, I. Bahceci, L. Dervishi, U. Dogrusoz, W. Zhou, H. Shen, P.W. Laird, G.P. Way, C.S. Greene, H. Liang, Y. Xiao, C. Wang, A. Iavarone, A.H. Berger, T.G. Bivona, A.J. Lazar, G. D. Hammer, T. Giordano, L.N. Kwong, G. McArthur, C. Huang, A.D. Tward, M. J. Frederick, F. McCormick, M. Meyerson, S.J. Caesar-Johnson, J.A. Demchok, I. Felau, M. Kasapi, M.L. Ferguson, C.M. Hutter, H.J. Sofia, R. Tarnuzzer, Z. Wang, L. Yang, J.C. Zenklusen, J. Julia Zhang, S. Chudamani, J. Liu, L. Lolla, R. Naresh, T. Pihl, Q. Sun, Y. Wan, Y. Wu, J. Cho, T. DeFreitas, S. Frazer, N. Gehlenborg, G. Getz, D.I. Heiman, J. Kim, M.S. Lawrence, P. Lin, S. Meier, M.S. Noble, G. Saksena, D. Voet, H. Zhang, B. Bernard, N. Chambwe, V. Dhankani, T. Knijnenburg, R. Kramer, K. Leinonen, Y. Liu, M. Miller, S. Reynolds, I. Shmulevich, V. Thorsson, W. Zhang, R. Akbani, B.M. Broom, A.M. Hegde, Z. Ju, R.S. Kanchi, A. Korkut, J. Li, H. Liang, S. Ling, W. Liu, Y. Lu, G.B. Mills, K.S. Ng, A. Rao, M. Ryan, J. Wang, J.N. Weinstein, J. Zhang, A. Abeshouse, J. Armenia, D. Chakravarty, W.K. Chatila, I. de Bruijn, J. Gao, B.E. Gross, Z.J. Heins, R. Kundra, K. La, M. Ladanyi, A. Luna, M.G. Nissan, A. Ochoa, S.M. Phillips, E. Reznik, F. Sanchez-Vega, C. Sander, N. Schultz, R. Sheridan, S.O. Sumer, Y. Sun, B.S. Taylor, J. Wang, H. Zhang, P. Anur, M. Peto, P. Spellman, C. Benz, J. M. Stuart, C.K. Wong, C. Yau, D.N. Hayes, J.S. Parker, M.D. Wilkerson, A. Ally, M. Balasundaram, R. Bowlby, D. Brooks, R. Carlsen, E. Chuah, N. Dhalla, R. Holt, S.J.M. Jones, K. Kasaian, D. Lee, Y. Ma, M.A. Marra, M. Mayo, R.A. Moore, A. J. Mungall, K. Mungall, A.G. Robertson, S. Sadeghi, J.E. Schein, P. Sipahimalani, A. Tam, N. Thiessen, K. Tse, T. Wong, A.C. Berger, R. Beroukhim, A.D. Cherniack, C. Cibulskis, S.B. Gabriel, G.F. Gao, G. Ha, M. Meyerson, S.E. Schumacher, J. Shih, M.H. Kucherlapati, R.S. Kucherlapati, S. Baylin, L. Cope, L. Danilova, M. S. Bootwalla, P.H. Lai, D.T. Maglinte, D.J. Van Den Berg, D.J. Weisenberger, J. T. Auman, S. Balu, T. Bodenheimer, C. Fan, K.A. Hoadley, A.P. Hoyle, S. R. Jefferys, C.D. Jones, S. Meng, P.A. Mieczkowski, L.E. Mose, A.H. Perou, C. M. Perou, J. Roach, Y. Shi, J.V. Simons, T. Skelly, M.G. Soloway, D. Tan, U. Veluvolu, H. Fan, T. Hinoue, P.W. Laird, H. Shen, W. Zhou, M. Bellair, K. Chang, K. Covington, C.J. Creighton, H. Dinh, H.V. Doddapaneni, L. A. Donehower, J. Drummond, R.A. Gibbs, R. Glenn, W. Hale, Y. Han, J. Hu, V. Korchina, S. Lee, L. Lewis, W. Li, X. Liu, M. Morgan, D. Morton, D. Muzny, J. Santibanez, M. Sheth, E. Shinbrot, L. Wang, M. Wang, D.A. Wheeler, L. Xi, F. Zhao, J. Hess, E.L. Appelbaum, M. Bailey, M.G. Cordes, L. Ding, C.C. Fronick, L. A. Fulton, R.S. Fulton, C. Kandoth, E.R. Mardis, M.D. McLellan, C.A. Miller, H. K. Schmidt, R.K. Wilson, D. Crain, E. Curley, J. Gardner, K. Lau, D. Mallery, S. Morris, J. Paulauskis, R. Penny, C. Shelton, T. Shelton, M. Sherman, E. Thompson, P. Yena, J. Bowen, J.M. Gastier-Foster, M. Gerken, K.M. Leraas, T. M. Lichtenberg, N.C. Ramirez, L. Wise, E. Zmuda, N. Corcoran, T. Costello, C. Hovens, A.L. Carvalho, A.C. de Carvalho, J.H. Fregnani, A. Longatto-Filho, R. M. Reis, C. Scapulatempo-Neto, H.C.S. Silveira, D.O. Vidal, A. Burnette, J. Eschbacher, B. Hermes, A. Noss, R. Singh, M.L. Anderson, P.D. Castro, M. Ittmann, D. Huntsman, B. Kohl, X. Le, R. Thorp, C. Andry, E.R. Duffy, V. Lyadov, O. Paklina, G. Setdikova, A. Shabunin, M. Tavobilov, C. McPherson, R. Warnick, R. Berkowitz, D. Cramer, C. Feltmate, N. Horowitz, A. Kibel, M. Muto, C.P. Raut, A. Malykh, J.S. Barnholtz-Sloan, W. Barrett, K. Devine, J. Fulop, Q. T. Ostrom, K. Shimmel, Y. Wolinsky, A.E. Sloan, A. De Rose, F. Giuliante, M. Goodman, B.Y. Karlan, C.H. Hagedorn, J. Eckman, J. Harr, J. Myers, K. Tucker, L.A. Zach, B. Deyarmin, H. Hu, L. Kvecher, C. Larson, R.J. Mural, S. Somiari, A. Vicha, T. Zelinka, J. Bennett, M. Iacocca, B. Rabeno, P. Swanson, M. Latour, L. Lacombe, B. Têtu, A. Bergeron, M. McGraw, S.M. Staugaitis, J. Chabot, H. Hibshoosh, A. Sepulveda, T. Su, T. Wang, O. Potapova, O. Voronina, L. Desjardins, O. Mariani, S. Roman-Roman, X. Sastre, M.H. Stern, F. Cheng,

S. Signoretti, A. Berchuck, D. Bigner, E. Lipp, J. Marks, S. McCall, R. McLendon, A. Secord, A. Sharp, M. Behera, D.J. Brat, A. Chen, K. Delman, S. Force, F. Khuri, K. Magliocca, S. Maithel, J.J. Olson, T. Owonikoko, A. Pickens, S. Ramalingam, D. M. Shin, G. Sica, E.G. Van Meir, H. Zhang, W. Eijckenboom, A. Gillis, E. Korpershoek, L. Looijenga, W. Oosterhuis, H. Stoop, K.E. van Kessel, E. C. Zwarthoff, C. Calatozzolo, L. Cuppini, S. Cuzzubbo, F. DiMeco, G. Finocchiaro, L. Mattei, A. Perin, B. Pollo, C. Chen, J. Houck, P. Lohavanichbutr, A. Hartmann, C. Stoehr, R. Stoehr, H. Taubert, S. Wach, B. Wullich, W. Kycler, D. Murawa, M. Wiznerowicz, K. Chung, W.J. Edenfield, J. Martin, E. Baudin, G. Bubley, R. Bueno, A. De Rienzo, W.G. Richards, S. Kalkanis, T. Mikkelsen, H. Noushmehr, L. Scarpace, N. Girard, M. Aymerich, E. Campo, E. Giné, A.L. Guillermo, N. Van Bang, P.T. Hanh, B.D. Phu, Y. Tang, H. Colman, K. Evason, P.R. Dottino, J. A. Martignetti, H. Gabra, H. Juhl, T. Akeredolu, S. Stepa, D. Hoon, K. Ahn, K. J. Kang, F. Beuschlein, A. Breggia, M. Birrer, D. Bell, M. Borad, A.H. Bryce, E. Castle, V. Chandan, J. Cheville, J.A. Copland, M. Farnell, T. Flotte, N. Giama, T. Ho, M. Kendrick, J.P. Kocher, K. Kopp, C. Moser, D. Nagorney, D. O'Brien, B. P. O'Neill, T. Patel, G. Petersen, F. Que, M. Rivera, L. Roberts, R. Smallridge, T. Smyrk, M. Stanton, R.H. Thompson, M. Torbenson, J.D. Yang, L. Zhang, F. Brimo, J.A. Ajani, A.M.A. Gonzalez, C. Behrens, J. Bondaruk, R. Broaddus, B. Czerniak, B. Esmaeli, J. Fujimoto, J. Gershenwald, C. Guo, C. Logothetis, F. Meric-Bernstam, C. Moran, L. Ramondetta, D. Rice, A. Sood, P. Tamboli, T. Thompson, P. Troncoso, A. Tsao, I. Wistuba, C. Carter, L. Haydu, P. Hersey, V. Jakrot, H. Kakavand, R. Kefford, K. Lee, G. Long, G. Mann, M. Quinn, R. Saw, R. Scolyer, K. Shannon, A. Spillane, J. Stretch, M. Synott, J. Thompson, J. Wilmott, H. Al-Ahmadie, T.A. Chan, R. Ghossein, A. Gopalan, D.A. Levine, V. Reuter, S. Singer, B. Singh, N.V. Tien, T. Broudy, C. Mirsaidi, P. Nair, P. Drwiega, J. Miller, J. Smith, H. Zaren, J.W. Park, N.P. Hung, E. Kebebew, W. M. Linehan, A.R. Metwalli, K. Pacak, P.A. Pinto, M. Schiffman, L.S. Schmidt, C. D. Vocke, N. Wentzensen, R. Worrell, H. Yang, M. Moncrieff, C. Goparaju, J. Melamed, H. Pass, N. Botnariuc, I. Caraman, M. Cernat, I. Chemencedji, A. Clipca, S. Doruc, G. Gorincioi, S. Mura, M. Pirtac, I. Stancul, D. Tcaciuc, M. Albert, I. Alexopoulou, A. Arnaout, J. Bartlett, J. Engel, S. Gilbert, J. Parfitt, H. Sekhon, G. Thomas, D.M. Rassl, R.C. Rintoul, C. Bifulco, R. Tamakawa, W. Urba, N. Hayward, H. Timmers, A. Antenucci, F. Facciolo, G. Grazi, M. Marino, R. Merola, R. de Krijger, A.P. Gimenez-Roqueplo, A. Piché, S. Chevalier, G. McKercher, K. Birsoy, G. Barnett, C. Brewer, C. Farver, T. Naska, N.A. Pennell, D. Raymond, C. Schilero, K. Smolenski, F. Williams, C. Morrison, J.A. Borgia, M. J. Liptay, M. Pool, C.W. Seder, K. Junker, L. Omberg, M. Dinkin, G. Manikhas, D. Alvaro, M.C. Bragazzi, V. Cardinale, G. Carpino, E. Gaudio, D. Chesla, S. Cottingham, M. Dubina, F. Moiseenko, R. Dhanasekaran, K.F. Becker, K. P. Janssen, J. Slotta-Huspenina, M.H. Abdel-Rahman, D. Aziz, S. Bell, C. M. Cebulla, A. Davis, R. Duell, J.B. Elder, J. Hilty, B. Kumar, J. Lang, N. L. Lehman, R. Mandt, P. Nguyen, R. Pilarski, K. Rai, L. Schoenfield, K. Senecal, P. Wakely, P. Hansen, R. Lechan, J. Powers, A. Tischler, W.E. Grizzle, K.C. Sexton, A. Kastl, J. Henderson, S. Porten, J. Waldmann, M. Fassnacht, S.L. Asa, D. Schadendorf, M. Couce, M. Graefen, H. Huland, G. Sauter, T. Schlomm, R. Simon, P. Tennstedt, O. Olabode, M. Nelson, O. Bathe, P.R. Carroll, J.M. Chan, P. Disaia, P. Glenn, R.K. Kelley, C.N. Landen, J. Phillips, M. Prados, J. Simko, K. Smith-McCune, S. VandenBerg, K. Roggin, A. Fehrenbach, A. Kendler, S. Sifri, R. Steele, A. Jimeno, F. Carey, I. Forgie, M. Mannelli, M. Carney, B. Hernandez, B. Campos, C. Herold-Mende, C. Jungk, A. Unterberg, A. von Deimling, A. Bossler, J. Galbraith, L. Jacobus, M. Knudson, T. Knutson, D. Ma, M. Milhem, R. Sigmund, A.K. Godwin, R. Madan, H.G. Rosenthal, C. Adebamowo, S.N. Adebamowo, A. Boussiotas, D. Beer, T. Giordano, A.M. Mes-Masson, F. Saad, T. Bocklage, L. Landrum, R. Mannel, K. Moore, K. Moxley, R. Postier, J. Walker, R. Zuna, M. Feldman, F. Valdivieso, R. Dhir, J. Luketich, E.M.M. Pinero, M. Quintero-Aguilo, C.G. Carlotti, J.S. Dos Santos, R. Kemp, A. Sankarankuty, D. Tirapelli, J. Catto, K. Agnew, E. Swisher, J. Creaney, B. Robinson, C.S. Shelley, E. M. Godwin, S. Kendall, C. Shipman, C. Bradford, T. Carey, A. Haddad, J. Moyer, L. Peterson, M. Prince, L. Rozek, G. Wolf, R. Bowman, K.M. Fong, I. Yang, R. Korst, W.K. Rathmell, J.L. Fantacone-Campbell, J.A. Hooke, A.J. Kovatich, C. D. Shriver, J. DiPersio, B. Drake, R. Govindan, S. Heath, T. Ley, B. Van Tine, P. Westervelt, M.A. Rubin, J. Il Lee, N.D. Aredes, A. Mariamidze, E.M. Van Allen, A.D. Cherniack, G. Ciriello, C. Sander, N. Schultz, Oncogenic signaling pathways in the cancer genome atlas, Cell 173 (2018) 321, 337.e10, https://doi.org/10.1016/j.cell.2018.03.035.

[178] R.D. Burk, Z. Chen, C. Saller, K. Tarvin, A.L. Carvalho, C. Scapulatempo-Neto, H. C. Silveira, J.H. Fregnani, C.J. Creighton, M.L. Anderson, P. Castro, S.S. Wang, C. Yau, C. Benz, A. Gordon Robertson, K. Mungall, L. Lim, R. Bowlby, S. Sadeghi, D. Brooks, P. Sipahimalani, R. Mar, A. Ally, A. Clarke, A.J. Mungall, A. Tam, D. Lee, E. Chuah, J.E. Schein, K. Tse, K. Kasaian, Y. Ma, M.A. Marra, M. Mayo, M. Balasundaram, N. Thiessen, N. Dhalla, R. Carlsen, R.A. Moore, R.A. Holt, S.J. M. Jones, T. Wong, A. Pantazi, M. Parfenov, R. Kucherlapati, A. Hadjipanayis, J. Seidman, M. Kucherlapati, X. Ren, A.W. Xu, L. Yang, P.J. Park, S. Lee, B. Rabeno, L. Huelsenbeck-Dill, M. Borowsky, M. Cadungog, M. Iacocca, N. Petrelli, P. Swanson, A.I. Ojesina, A.I. Ojesina, A.I. Ojesina, X. Le, G. Sandusky, S.N. Adebamowo, T. Akeredolu, C. Adebamowo, S.M. Reynolds, I. Shmulevich, C. Shelton, D. Crain, D. Mallery, E. Curley, J. Gardner, R. Penny, S. Morris, T. Shelton, J. Liu, L. Lolla, S. Chudamani, Y. Wu, M. Birrer, M.D. McLellan, M. H. Bailey, C.A. Miller, M.A. Wyczalkowski, R.S. Fulton, C.C. Fronick, C. Lu, E. R. Mardis, E.L. Appelbaum, H.K. Schmidt, L.A. Fulton, M.G. Cordes, T. Li, L. Ding, R.K. Wilson, J.S. Rader, B. Behmaram, D. Uyar, W. Bradley, J. Wrangle, A. Pastore, D.A. Levine, F. Dao, J. Gao, N. Schultz, C. Sander, M. Ladanyi, M. Einstein, R. Teeter, S. Benz, N. Wentzensen, I. Felau, J.C. Zenklusen, C. Bodelon, J.A. Demchok, L. Yang, M. Sheth, M.L. Ferguson, R. Tarnuzzer, H. Yang, M. Schiffman, J. Zhang, Z. Wang, T. Davidsen, O. Olaniyan, C.M. Hutter, H.J. Sofia, D.A. Gordenin, K. Chan, S.A. Roberts, L.J. Klimczak, C. Van Waes, Z. Chen, A.D. Saleh, H. Cheng, J. Parfitt, J. Bartlett, M. Albert, A. Arnaout, H. Sekhon, S. Gilbert, M. Peto, J. Myers, J. Harr, J. Eckman, J. Bergsten, K. Tucker, L. Anne Zach, B.Y. Karlan, J. Lester, S. Orsulic, Q. Sun, R. Naresh, T. Pihl, Y. Wan, H. Zaren, J. Sapp, J. Miller, P. Drwiega, B.A. Murray, H. Zhang, A. D. Cherniack, C. Sougnez, C. Sekhar Pedamallu, L. Lichtenstein, M. Meyerson, M. S. Noble, D.I. Heiman, D. Voet, G. Getz, G. Saksena, J. Kim, J. Shih, J. Cho, M. S. Lawrence, N. Gehlenborg, P. Lin, R. Beroukhim, S. Frazer, S.B. Gabriel, S. E. Schumacher, K.M. Leraas, T.M. Lichtenberg, E. Zmuda, J. Bowen, J. Frick, J. M. Gastier-Foster, L. Wise, M. Gerken, N.C. Ramirez, L. Danilova, L. Cope, S. B. Baylin, H.B. Salvesen, C.P. Vellano, Z. Ju, L. Diao, H. Zhao, Z. Chong, M. C. Ryan, E. Martinez-Ledesma, R.G. Verhaak, L. Averett Byers, Y. Yuan, K. Chen, S. Ling, G.B. Mills, Y. Lu, R. Akbani, S. Seth, H. Liang, J. Wang, L. Han, J. N. Weinstein, C.A. Bristow, W. Zhang, H.S. Mahadeshwar, H. Sun, J. Tang, J. Zhang, X. Song, A. Protopopov, K.R. Mills Shaw, L. Chin, O. Olabode, P. DiSaia, A. Radenbaugh, D. Haussler, J. Zhu, J. Stuart, P. Chalise, D. Koestler, B.L. Fridley, A.K. Godwin, R. Madan, G. Ciriello, C. Martinez, K. Higgins, T. Bocklage, J. Todd Auman, C.M. Perou, D. Tan, J.S. Parker, K.A. Hoadley, M.D. Wilkerson, P. A. Mieczkowski, T. Skelly, U. Veluvolu, D. Neil Hayes, W. Kimryn Rathmell, A. P. Hoyle, J.V. Simons, J. Wu, L.E. Mose, M.G. Soloway, S. Balu, S. Meng, S. R. Jefferys, T. Bodenheimer, Y. Shi, J. Roach, L.B. Thorne, L. Boice, M. Huang, C. D. Jones, R. Zuna, J. Walker, C. Gunderson, C. Snowbarger, D. Brown, K. Moxley, K. Moore, K. Andrade, L. Landrum, R. Mannel, S. McMeekin, S. Johnson, T. Nelson, E. Elishaev, R. Dhir, R. Edwards, R. Bhargava, D.G. Tiezzi, J. M. Andrade, H. Noushmehr, C. Gilberto Carlotti, D.P. da Cunha Tirapelli, D. J. Weisenberger, D.J. Van Den Berg, D.T. Maglinte, M.S. Bootwalla, P.H. Lai, T. Triche, E.M. Swisher, K.J. Agnew, C. Simon Shelley, P.W. Laird, J. Schwarz, P. Grigsby, D. Mutch, Integrated genomic and molecular characterization of cervical cancer, Nature 543 (2017) 378–384, https://doi.org/10.1038/nature21386.

[179] E. Lorenzetto, M. Brenca, M. Boeri, C. Verri, E. Piccinin, P. Gasparini, F. Facchinetti, S. Rossi, G. Salvatore, M. Massimino, G. Sozzi, R. Maestro, P. Modena, YAP1 acts as oncogenic target of 11q22 amplification in multiple cancer subtypes, Oncotarget 5 (2014) 2608–2621, https://doi.org/10.18632/oncotarget.1844.

[180] S. Yang, Y. Wu, S. Wang, P. Xu, Y. Deng, M. Wang, K. Liu, T. Tian, Y. Zhu, N. Li, L. Zhou, Z. Dai, H. Kang, HPV-related methylation-based reclassification and risk stratification of cervical cancer, Mol. Oncol. (2020), https://doi.org/10.1002/1878-0261.12709.

[181] D. Wang, J. He, J. Dong, T.F. Meyer, T. Xu, The HIPPO pathway in gynecological malignancies, Am. J. Cancer Res. 10 (2020) 610–629. http://www.ncbi.nlm.nih.gov/pubmed/32195031 (accessed July 29, 2020).

[182] Y. Liu, M. Ren, X. Tan, L. Hu, Distinct changes in the expression TAZ are associated with normal cervix and human cervical cancer, J. Cancer 9 (2018) 4263–4270, https://doi.org/10.7150/jca.26623.

[183] Y. Wang, K. Wang, Y. Chen, J. Zhou, Y. Liang, X. Yang, X. Li, Y. Cao, D. Wang, L. Luo, B. Li, D. Li, L. Wang, Z. Liang, C. Gao, Q. Wang, Q. Lv, Z. Li, Y. Shi, H. Niu, Mutational landscape of penile squamous cell carcinoma in a Chinese population, Int. J. Cancer 145 (2019) 1280–1289, https://doi.org/10.1002/ijc.32373.

[184] J. O'Nions, L.A. Brooks, A. Sullivan, A. Bell, B. Dunne, M. Rozycka, A. Reddy, J. A. Tidy, D. Evans, P.J. Farrell, A. Evans, M. Gasco, B. Gusterson, T. Crook, p73 is over-expressed in vulval cancer principally as the δ2 isoform, Br. J. Cancer 85 (2001) 1551–1556, https://doi.org/10.1054/bjoc.2001.2138.

[185] P.M. Wierzbicki, A. Rybarczyk, The hippo pathway in colorectal cancer, Folia Histochem. Cytobiol. 53 (2015) 105–119, https://doi.org/10.5603/FHC.a2015.0015.

[186] M.L. Wan, Y. Wang, Z. Zeng, B. Deng, B.S. Zhu, T. Cao, Y.K. Li, J. Xiao, Q. Han, Q. Wu, Colorectal cancer (CRC) as a multifactorial disease and its causal correlations with multiple signaling pathways, Biosci. Rep. 40 (2020), https://doi.org/10.1042/BSR20200265.

[187] J.M.M. Walboomers, M.V. Jacobs, M.M. Manos, F.X. Bosch, J.A. Kummer, K. V. Shah, P.J.F. Snijders, J. Peto, C.J.L.M. Meijer, N. Muñoz, Human papillomavirus is a necessary cause of invasive cervical cancer worldwide, J. Pathol. 189 (1999) 12–19, https://doi.org/10.1002/(SICI)1096-9896(199909)189:1<12::AID-PATH431>3.0.CO;2-F.

[188] F. Bray, J. Ferlay, I. Soerjomataram, R.L. Siegel, L.A. Torre, A. Jemal, Global cancer statistics 2018: GLOBOCAN estimates of incidence and mortality worldwide for 36 cancers in 185 countries, CA Cancer J. Clin. 68 (2018) 394–424, https://doi.org/10.3322/caac.21492.

[189] J. Manzo-Merino, A. Contreras-Paredes, E. Vázquez-Ulloa, L. Rocha-Zavaleta, A. M. Fuentes-Gonzalez, M. Lizano, The role of Signaling pathways in cervical cancer and molecular therapeutic targets, Arch. Med. Res. 45 (2014) 525–539, https://doi.org/10.1016/j.arcmed.2014.10.008.

[190] N. Vlahov, S. Scrace, M.S. Soto, A.M. Grawenda, L. Bradley, D. Pankova, A. Papaspyropoulos, K.S. Yee, F. Buffa, C.R. Goding, P. Timpson, N. Sibson, E. O'Neill, Alternate RASSF1 transcripts control SRC activity, E-cadherin contacts, and YAP-mediated invasion, Curr. Biol. 25 (2015) 3019–3034, https://doi.org/10.1016/j.cub.2015.09.072.

[191] I. Nicolás, L. Marimon, E. Barnadas, A. Saco, L. Rodríguez-Carunchio, P. Fusté, C. Martí, A. Rodriguez-Trujillo, A. Torne, M. del Pino, J. Ordi, HPV-negative tumors of the uterine cervix, Mod. Pathol. 32 (2019) 1189–1196, https://doi.org/10.1038/s41379-019-0249-1.

[192] E.P. Simard, L.A. Torre, A. Jemal, International trends in head and neck cancer incidence rates: differences by country, sex and anatomic site, Oral Oncol. 50 (2014) 387–403, https://doi.org/10.1016/j.oraloncology.2014.01.016.

[193] L.J. Liao, W.L. Hsu, W.C. Lo, P.W. Cheng, P.W. Shueng, C.H. Hsieh, Health-related quality of life and utility in head and neck cancer survivors, BMC Cancer 19 (2019), https://doi.org/10.1186/s12885-019-5614-4.

[194] A.K. Chaturvedi, E.A. Engels, R.M. Pfeiffer, B.Y. Hernandez, W. Xiao, E. Kim, B. Jiang, M.T. Goodman, M. Sibug-Saber, W. Cozen, L. Liu, C.F. Lynch, N. Wentzensen, R.C. Jordan, S. Altekruse, W.F. Anderson, P.S. Rosenberg, M. L. Gillison, Human papillomavirus and rising oropharyngeal cancer incidence in the United States, J. Clin. Oncol. 29 (2011) 4294–4301, https://doi.org/10.1200/JCO.2011.36.4596.

[195] M.S. Lawrence, C. Sougnez, L. Lichtenstein, K. Cibulskis, E. Lander, S.B. Gabriel, G. Getz, A. Ally, M. Balasundaram, I. Birol, R. Bowlby, D. Brooks, Y.S. N. Butterfield, R. Carlsen, D. Cheng, A. Chu, N. Dhalla, R. Guin, R.A. Holt, S.J. M. Jones, D. Lee, H.I. Li, M.A. Marra, M. Mayo, R.A. Moore, A.J. Mungall, A. G. Robertson, J.E. Schein, P. Sipahimalani, A. Tam, N. Thiessen, T. Wong, A. Protopopov, N. Santoso, S. Lee, M. Parfenov, J. Zhang, H.S. Mahadeshwar, J. Tang, X. Ren, S. Seth, P. Haseley, D. Zeng, L. Yang, A.W. Xu, X. Song, A. Pantazi, C.A. Bristow, A. Hadjipanayis, J. Seidman, L. Chin, P.J. Park, R. Kucherlapati, R. Akbani, T. Casasent, W. Liu, Y. Lu, G. Mills, T. Motter, J. Weinstein, L. Diao, J. Wang, Y. Hong Fan, J. Liu, K. Wang, J.T. Auman, S. Balu, T. Bodenheimer, E. Buda, D.N. Hayes, K.A. Hoadley, A.P. Hoyle, S.R. Jefferys, C. D. Jones, P.K. Kimes, Y. Liu, J.S. Marron, S. Meng, P.A. Mieczkowski, L.E. Mose, J. S. Parker, C.M. Perou, J.F. Prins, J. Roach, Y. Shi, J.V. Simons, D. Singh, M. G. Soloway, D. Tan, U. Veluvolu, V. Walter, S. Waring, M.D. Wilkerson, J. Wu, N. Zhao, A.D. Cherniack, P.S. Hammerman, A.D. Tward, C.S. Pedamallu, G. Saksena, J. Jung, A.I. Ojesina, S.L. Carter, T.I. Zack, S.E. Schumacher, R. Beroukhim, S.S. Freeman, M. Meyerson, J. Cho, M.S. Noble, D. DiCara, H. Zhang, D.I. Heiman, N. Gehlenborg, D. Voet, P. Lin, S. Frazer, P. Stojanov, Y. Liu, L. Zou, J. Kim, D. Muzny, H.V. Doddapaneni, C. Kovar, J. Reid, D. Morton, Y. Han, W. Hale, H. Chao, K. Chang, J.A. Drummond, R.A. Gibbs, N. Kakkar, D. Wheeler, L. Xi, G. Ciriello, M. Ladanyi, W. Lee, R. Ramirez, C. Sander, R. Shen, R. Sinha, N. Weinhold, B.S. Taylor, B.A. Aksoy, G. Dresdner, J. Gao, B. Gross, A. Jacobsen, B. Reva, N. Schultz, S.O. Sumer, Y. Sun, T.A. Chan, L.G. Morris, J. Stuart, S. Benz, S. Ng, C. Benz, C. Yau, S.B. Baylin, L. Cope, L. Danilova, J. G. Herman, M. Bootwalla, D.T. Maglinte, P.W. Laird, T. Triche, D. J. Weisenberger, D.J. Van Den Berg, N. Agrawal, J. Bishop, P.C. Boutros, J. P. Bruce, L.A. Byers, J. Califano, T.E. Carey, Z. Chen, H. Cheng, S.I. Chiosea, E. Cohen, B. Diergaarde, A.M. Egloff, A.K. El-Naggar, R.L. Ferris, M.J. Frederick, J.R. Grandis, Y. Guo, R.I. Haddad, T. Harris, A.B.Y. Hui, J.J. Lee, S.M. Lippman, F. F. Liu, J.B. McHugh, J. Myers, P.K.S. Ng, B. Perez-Ordonez, C.R. Pickering, M. Prystowsky, M. Romkes, A.D. Saleh, M.A. Sartor, R. Seethala, T.Y. Seiwert, H. Si, C. Van Waes, D.M. Waggott, M. Wiznerowicz, W.G. Yarbrough, J. Zhang, Z. Zuo, K. Burnett, D. Crain, J. Gardner, K. Lau, D. Mallery, S. Morris, J. Paulauskis, R. Penny, C. Shelton, T. Shelton, M. Sherman, P. Yena, A.D. Black, J. Bowen, J. Frick, J.M. Gastier-Foster, H.A. Harper, K. Leraas, T.M. Lichtenberg, N.C. Ramirez, L. Wise, E. Zmuda, J. Baboud, M.A. Jensen, A.B. Kahn, T.D. Pihl, D. A. Pot, D. Srinivasan, J.S. Walton, Y. Wan, R.A. Burton, T. Davidsen, J. A. Demchok, G. Eley, M.L. Ferguson, K.R. Mills Shaw, B.A. Ozenberger, M. Sheth, H.J. Sofia, R. Tarnuzzer, Z. Wang, L. Yang, J.C. Zenklusen, C. Saller, K. Tarvin, C. Chen, R. Bollag, P. Weinberger, W. Golusiński, P. Golusiński, M. Ibbs, K. Korski, A. Mackiewicz, W. Suchorska, B. Szybiak, E. Curley, C. Beard, C. Mitchell, G. Sandusky, J. Ahn, Z. Khan, J. Irish, J. Waldron, W.N. William, S. Egea, C. Gomez-Fernandez, L. Herbert, C.R. Bradford, D.B. Chepeha, A.S. Haddad, T. R. Jones, C.M. Komarck, M. Malakh, J.S. Moyer, A. Nguyen, L.A. Peterson, M. E. Prince, L.S. Rozek, E.G. Taylor, H.M. Walline, G.T. Wolf, L. Boice, B.S. Chera, W.K. Funkhouser, M.L. Gulley, T.G. Hackman, M.C. Hayward, M. Huang, W. K. Rathmell, A.H. Salazar, W.W. Shockley, C.G. Shores, L. Thorne, M.C. Weissler, S. Wrenn, A.M. Zanation, B.T. Brown, M. Pham, Comprehensive genomic characterization of head and neck squamous cell carcinomas, Nature 517 (2015) 576–582, https://doi.org/10.1038/nature14129.

[196] L. Nisa, D. Barras, M. Medova, D.M. Aebersold, M. Medo, M. Poliakova, J. Koch, B. Bojaxhiu, O. Eliçin, M.S. Dettmer, P. Angelino, R. Giger, U. Borner, M. D. Caversaccio, T.E. Carey, L. Ho, T.A. McKee, M. Delorenzi, Y. Zimmer, Comprehensive genomic profiling of patient-matched head and neck cancer cells: a preclinical pipeline for metastatic and recurrent disease, Mol. Cancer Res. 16 (2018) 1912–1926, https://doi.org/10.1158/1541-7786.MCR-18-0056.

[197] F. Alzahrani, L. Clattenburg, S. Muruganandan, M. Bullock, K. MacIsaac, M. Wigerius, B.A. Williams, M.E.R. Graham, M.H. Rigby, J.R.B. Trites, S. M. Taylor, C.J. Sinal, J.P. Fawcett, R.D. Hart, The Hippo component YAP localizes in the nucleus of human papilloma virus positive oropharyngeal squamous cell carcinoma, J. Otolaryngol. Head Neck Surg. 46 (2017), https://doi.org/10.1186/s40463-017-0187-1.

[198] S. Nakagawa, J.M. Huibregtse, Human scribble (Vartul) is targeted for ubiquitin-mediated degradation by the high-risk papillomavirus E6 proteins and the E6AP ubiquitin-protein ligase, Mol. Cell. Biol. 20 (2000) 8244–8253, https://doi.org/10.1128/mcb.20.21.8244-8253.2000.

[199] G. Almadori, G. Cadoni, P. Cattani, J. Galli, F. Bussu, G. Ferrandina, G. Scambia, G. Fadda, M. Maurizi, Human papillomavirus infection and epidermal growth factor receptor expression in primary laryngeal squamous cell carcinoma, Clin. Cancer Res. 7 (2001) 3988–3993.

International Journal of
Molecular Sciences

MDPI

Article

HPV-18 E6 Oncoprotein and Its Spliced Isoform E6*I Regulate the Wnt/β-Catenin Cell Signaling Pathway through the TCF-4 Transcriptional Factor

J. Omar Muñoz-Bello [1,2], Leslie Olmedo-Nieva [1], Leonardo Josué Castro-Muñoz [1], Joaquín Manzo-Merino [3], Adriana Contreras-Paredes [1], Claudia González-Espinosa [4], Alejandro López-Saavedra [1] and Marcela Lizano [1,5,*]

1 Unidad de Investigación Biomédica en Cáncer, Instituto Nacional de Cancerología-Instituto de Investigaciones Biomédicas, Universidad Nacional Autónoma de México, Mexico City 14080, Mexico; omarmube@gmail.com (J.O.M.-B.); leslie_azul25@hotmail.com (L.O.-N.); joscasmunoz@gmail.com (L.J.C.-M.); adrycont@yahoo.com.mx (A.C.-P.); alexlosaav@gmail.com (A.L.-S.)
2 Programa de Doctorado en Ciencias Biomédicas, Universidad Nacional Autónoma de México, Mexico City 04510, Mexico
3 CONACyT-Instituto Nacional de Cancerología, Mexico City 14080, Mexico; jmanzome@conacyt.mx
4 Departamento de Farmacobiología, Centro de Investigación y Estudios Avanzados del Instituto Politécnico Nacional, Sede sur, Mexico City 14330, Mexico; cgonzal@cinvestav.mx
5 Departamento de Medicina Genómica y Toxicología Ambiental, Instituto de Investigaciones Biomédicas, Universidad Nacional Autónoma de México (UNAM), Mexico City 04510, Mexico
* Correspondence: lizanosoberon@gmail.com; Tel.: +52-5556280400 (ext. 31035)

Received: 6 August 2018; Accepted: 9 October 2018; Published: 13 October 2018

Abstract: The Wnt/β-catenin signaling pathway regulates cell proliferation and differentiation and its aberrant activation in cervical cancer has been described. Persistent infection with high risk human papillomavirus (HR-HPV) is the most important factor for the development of this neoplasia, since E6 and E7 viral oncoproteins alter cellular processes, promoting cervical cancer development. A role of HPV-16 E6 in Wnt/β-catenin signaling has been proposed, although the participation of HPV-18 E6 has not been previously studied. The aim of this work was to investigate the participation of HPV-18 E6 and E6*I, in the regulation of the Wnt/β-catenin signaling pathway. Here, we show that E6 proteins up-regulate TCF-4 transcriptional activity and promote overexpression of Wnt target genes. In addition, it was demonstrated that E6 and E6*I bind to the TCF-4 (T cell factor 4) and β-catenin, impacting TCF-4 stabilization. We found that both E6 and E6*I proteins interact with the promoter of *Sp5*, in vitro and in vivo. Moreover, although differences in TCF-4 transcriptional activation were found among E6 intratype variants, no changes were observed in the levels of regulated genes. Furthermore, our data support that E6 proteins cooperate with β-catenin to promote cell proliferation.

Keywords: HPV-18 E6; HPV-18 E6*I; TCF-4 transcription factor; Wnt/β-catenin signaling

1. Introduction

The Wnt signaling pathway regulates a variety of processes, including cell proliferation and differentiation [1]. Briefly, in the off-state of the canonical pathway, the effector protein, β-catenin, is associated to a multiprotein complex that promotes its phosphorylation in specific residues in a GSK3β (Glycogen synthase kinase 3β) and CK1 (Casein kinase 1) kinase-dependent fashion. Those residues are recognized by the ubiquitin-ligase β-TrCP, allowing β-catenin ubiquitylation and subsequent degradation via the proteasome, whilst in the nucleus, the co-repressor, Groucho/TLE

(Transducin-like enhancer), suppresses transcriptional activation through the inhibition of TCF/LEF (Lymphoid enhancer binding factor) transcriptional factors. In the on-state, the Wnt ligands bind to the Frizzled receptor and the LRP 5/6 co-receptor, which dimerize, leading to disassembly of the destruction complex. Subsequently, β-catenin is released in the cytoplasm and translocated into the nucleus, where it binds to TCF/LEF and replaces the repressor protein, Groucho/TLE [2]. This event induces TCF/LEF transcriptional activation and expression of genes, such as *Axin2*, *Jun*, *Myc*, *Ccnd1*, and *Sp5* (Specificity protein transcription factor 5) [3]. It has been demonstrated that alterations in the Wnt cell signaling pathway contribute to the development of several types of cancer [4], including colorectal [5], hepatocarcinoma [6], breast [7], and HPV-related cancers [8–10].

The persistent infection with high risk human papillomavirus (HR-HPV) is the main risk factor associated to cervical cancer development [11]. HPV-16 and HPV-18 are the most prevalent types, found in almost 70% of cervical cancer cases worldwide [12]. HR-HPV transformation capacity is mainly due to the overexpression of the E6 and E7 viral oncoproteins, which interact with many cellular proteins, thus affecting their functions [13]. E6 is implicated in the modulation of several cell signaling pathways involved in cell adhesion, proliferation, and apoptosis, such as RAF (Rapidly accelerated fibrosarcoma)/MEK (MAPK/ERK kinase)/ERK (Extracellular signal-regulated kinase) and PI3K (Phosphoinositide 3 kinase), among others [14].

The E6–E7 open reading frames (ORFs) contain spliced donor and acceptor sites, highly conserved among the HR-HPV. Those sites are recognized by the spliceosome complex, promoting the removal of a small intron and the generation of a premature stop codon, giving place to short forms of E6, termed E6*. In HPV-16, at least four isoforms of E6* (I–IV) have been identified, whereas in HPV-18, only one has been reported hitherto, termed E6*I [15]. Although these E6 small isoforms are highly expressed in premalignant lesions and cervical cancer biopsies [16,17], their functions are poorly understood [18].

The abnormal activation of the Wnt cell signaling pathway has been reported in HPV-related tumors [8,19,20]. In cervical tumor biopsies and HPV positive cell lines, β-catenin is mainly located in the cytoplasm and nucleus, while in normal tissue, it is mainly distributed at the cell membrane [9,20]. In vitro assays have demonstrated that HPV-16 E6 induces TCF-4 transcriptional activation, whereas β-catenin is not stabilized. Moreover, E6AP ubiquitin ligase contributes to the increase in the TCF transcriptional activation mediated by E6, in a proteasome-dependent manner, without affecting β-catenin levels [21,22].

No interactions of HPV-18 E6 protein with members of the Wnt activation complex (TCF-4, β-catenin) have been identified so far, and the mechanisms by which E6 induces TCF transcriptional activation are poorly understood. Moreover, the effect of E6* proteins in this pathway remains unknown. Therefore, the aim of this study was to investigate the role of HPV-18 E6 and E6*I proteins in the Wnt/β-catenin signaling regulation. Through a TCF-4-dependent luciferase reporter plasmid, we show that E6 and E6*I up-regulate TCF-4 transcriptional activity, which is enhanced with the expression of exogenous β-catenin. Moreover, Wnt target genes are overexpressed in E6 and E6*I transfected cells. We also found that E6 and E6*I increase β-catenin and TCF-4 protein levels, but they do not alter their subcellular distribution. Immunoprecipitation and pull-down assays revealed an interaction of TCF-4 and β-catenin with E6 and E6*I proteins and those interactions impact in TCF-4 stabilization. We found that E6 and E6*I interact with the *Sp5* gene promoter, in vivo and in vitro. Furthermore, proliferation induced by β-catenin is enhanced by E6 and E6*I proteins. Finally, although E6 intratype variants differentially affected TCF-4 transcriptional activation, no differences appeared in their ability to bind TCF-4 or β-catenin.

2. Results

*2.1. HPV-18 E6 and E6*I Proteins Enhance β-Catenin/TCF-4 Transcription*

C33A cells were transiently transfected with a TCF-4-dependent luciferase reporter plasmid (TOPFLASH) and FLAG-tagged versions of 18E6WT, 18E6SM, 18E6*I, or 16E6 expressing plasmids. All experiments were performed co-transfecting the empty vector (p3X) or the β-catenin expressing plasmid, as indicated. After 48 h of transfection, immunoblot assays were performed for each experiment, confirming the expression of FLAG-tagged E6 proteins (Figure 1A). It is worth mentioning that the relation of protein expression of E6 full length and E6*I in the 18E6WT transfected cells is around 20% and 80%, respectively; while in 18E6SM transfected cells, such a relation is inverted, being around 80% and 20%, respectively. This effect is because 18E6SM harbors an A233G mutation in the donor splicing site that promotes a decrease in the expression of E6*I. Therefore, 18E6SM was used to compare a condition with a higher expression of E6 full length. Ectopic expression of both 18E6WT and 18E6*I increased 1.5-fold TCF-4 transcriptional activity (Figure 1B), compared with the empty vector. 18E6SM showed a similar effect in the TCF4 transcriptional activation as observed for the other E6 expressing plasmids, although non-significant. A 2.9-fold induction of TCF-4 activity was observed in 16E6 transfected cells, similar to the effect of ectopically expressed β-catenin. Subsequently, when the Wnt pathway was over activated through the co-transfection of β-catenin and E6 expressing plasmids, an enhancement of TCF-4 activity occurred in all tested conditions, above the β-catenin response (around 1.6-fold). As shown in Figure 1B, the 18E6 full-length or E6*I continued showing an increase in TCF response, with a consistent higher effect for 16E6 (3-fold).

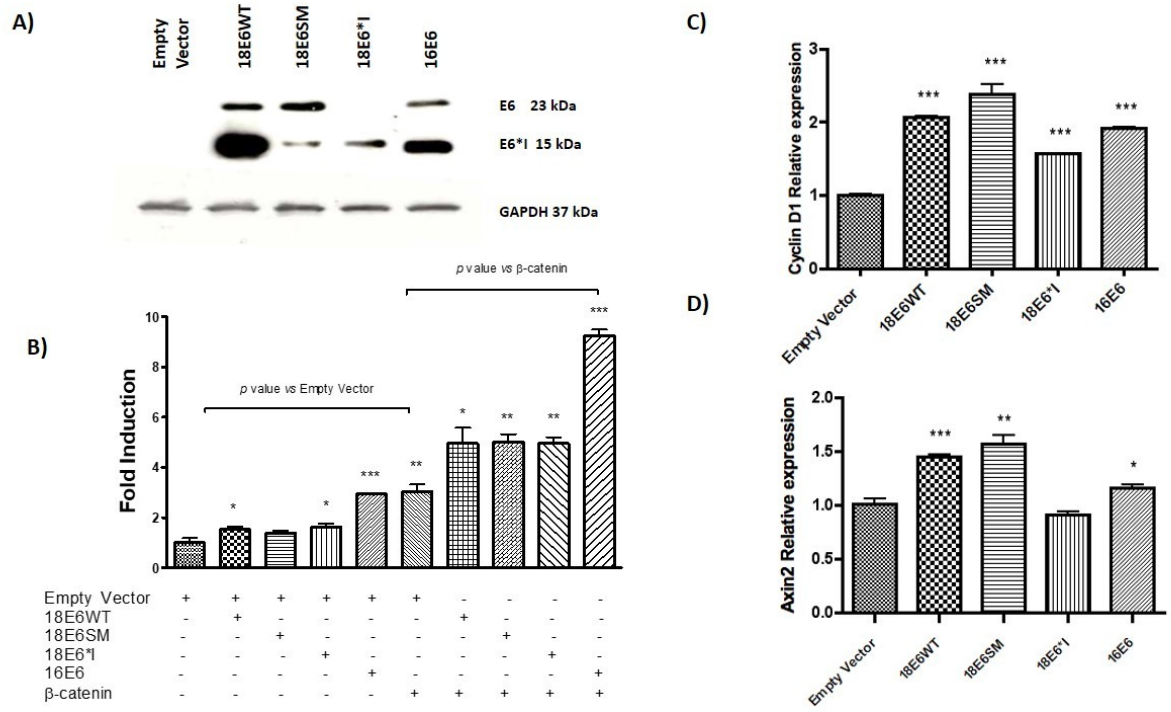

Figure 1. E6 and E6*I proteins induce TCF-4 transcriptional activity. (**A**) Expression of E6 and E6*I proteins was analyzed 48 h post-transfection in C33A cells, by western blot. (**B**) 18E6WT, 18E6SM, 18E6*I, 16E6, and β-catenin expressing vectors were transfected as indicated, with TOPFLASH (TCF-4 reporter plasmid) and β-galactosidase reporter plasmids in C33A cells. Luciferase reporter activity was measured 48 h post-transfection. Luciferase activities were compared with the empty vector or β-catenin plasmid. (**C**) *Cyclin D1* and (**D**) *Axin2* gene expression was evaluated by qPCR in E6 transfected cells. The means and ±SD of three independent experiments are depicted in each graph. Student t test was performed to evaluate the significant differences, the values are represented as * $p < 0.05$, ** $p < 0.001$, *** $p < 0.0001$.

Overexpression of E6 proteins also stimulate native promoters containing TCF-4 responsive elements, as evidenced by the expression of the Wnt target genes, *Axin2* and *Cyclin D1*, evaluated by qPCR assay. As observed in Figure 1C,D, E6 proteins enhanced the expression of *Cyclin D1* (up to 2-fold, compared to the control vector), while *Axin2* reached up to a 1.5-fold increase; although 18E6*I had no effect on *Axin2* expression. Taken together, these findings suggest that HPV-18 E6 and E6*I cooperate in the activation of the canonical Wnt/β-catenin cell signaling.

2.2. E6 Proteins Increase β-Catenin and TCF-4 Protein Levels, But Do Not Alter Their Subcellular Localization

To determine the effect of E6 proteins on β-catenin and TCF-4 levels, we performed immunoblot assays using total cell lysates. We observed that both E6 and E6*I proteins significantly increase β-catenin (Figure 2A,B) and TCF-4 (Figure 2C,D) levels. Therefore, immunofluorescence assays were performed to investigate whether HPV-18 E6 full length and E6*I proteins alter β-catenin or TCF-4 localization. C33A cells were transfected with 18E6WT, 18E6SM, or 18E6*I expressing plasmids and after 48 h, cells were fixed and analyzed. As shown in Figure 3A,B, all the E6 proteins were detected in the cytosol and nuclei. On the other hand, β-catenin was found mainly at the cellular membrane and cytosol, which was unaffected by the presence of E6 proteins (Figure 3A). Similar results were obtained in HaCaT E6-transfected cells, a keratinocyte-derived model (Figure S1). Concordantly with previous reports carried out with 16E6, we observed that E6 and E6*I of HPV-18 do not alter β-catenin subcellular distribution [21]. As shown in Figure 3B, TCF-4 subcellular localization was also unaltered in the presence of the transfected E6 isoforms.

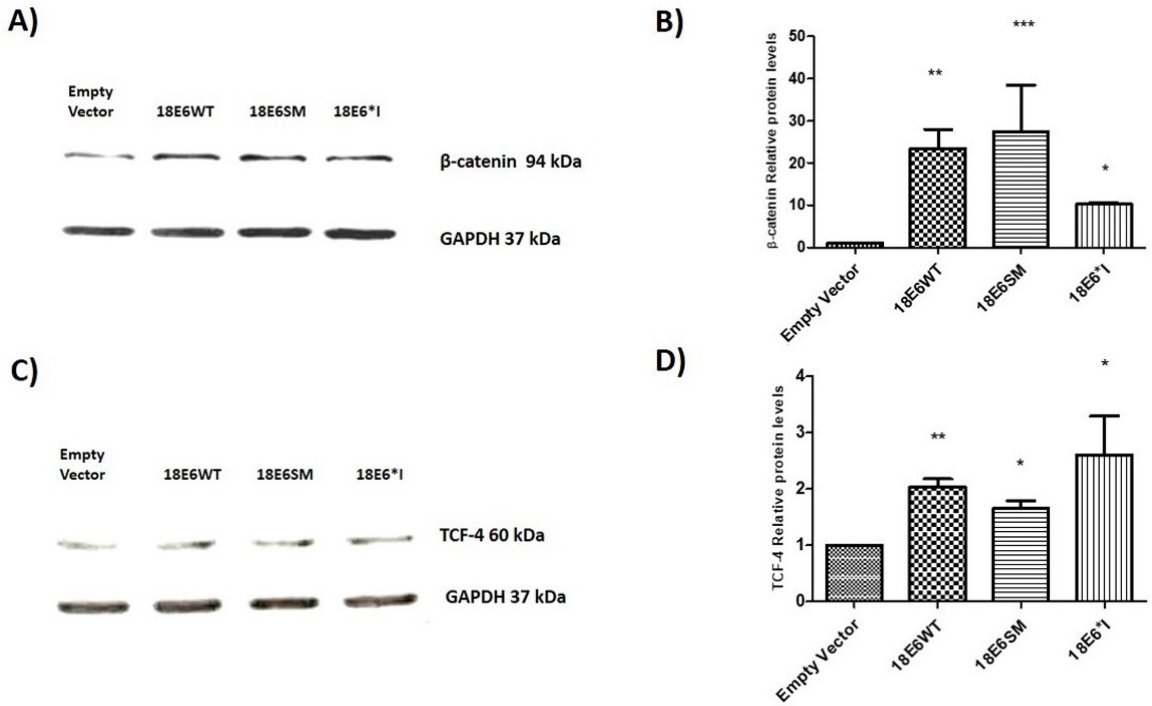

Figure 2. HPV-18 E6 and E6*I increase β-catenin and TCF-4 total protein levels. C33A cells were transfected with E6WT, E6SM, and E6*I expressing vectors. 48 h post-transfection, total cell lysates were analyzed by western blot. (**A**) β-catenin immunoblot and (**B**) densitometric analysis; (**C**) TCF-4 immunoblot; and (**D**) densitometric analysis. Data from three independent experiments were collected and graphed showing the mean and ±SD. *t* student analysis was performed, * $p < 0.05$, ** $p < 0.001$ and *** $p < 0.0001$ vs. empty vector values.

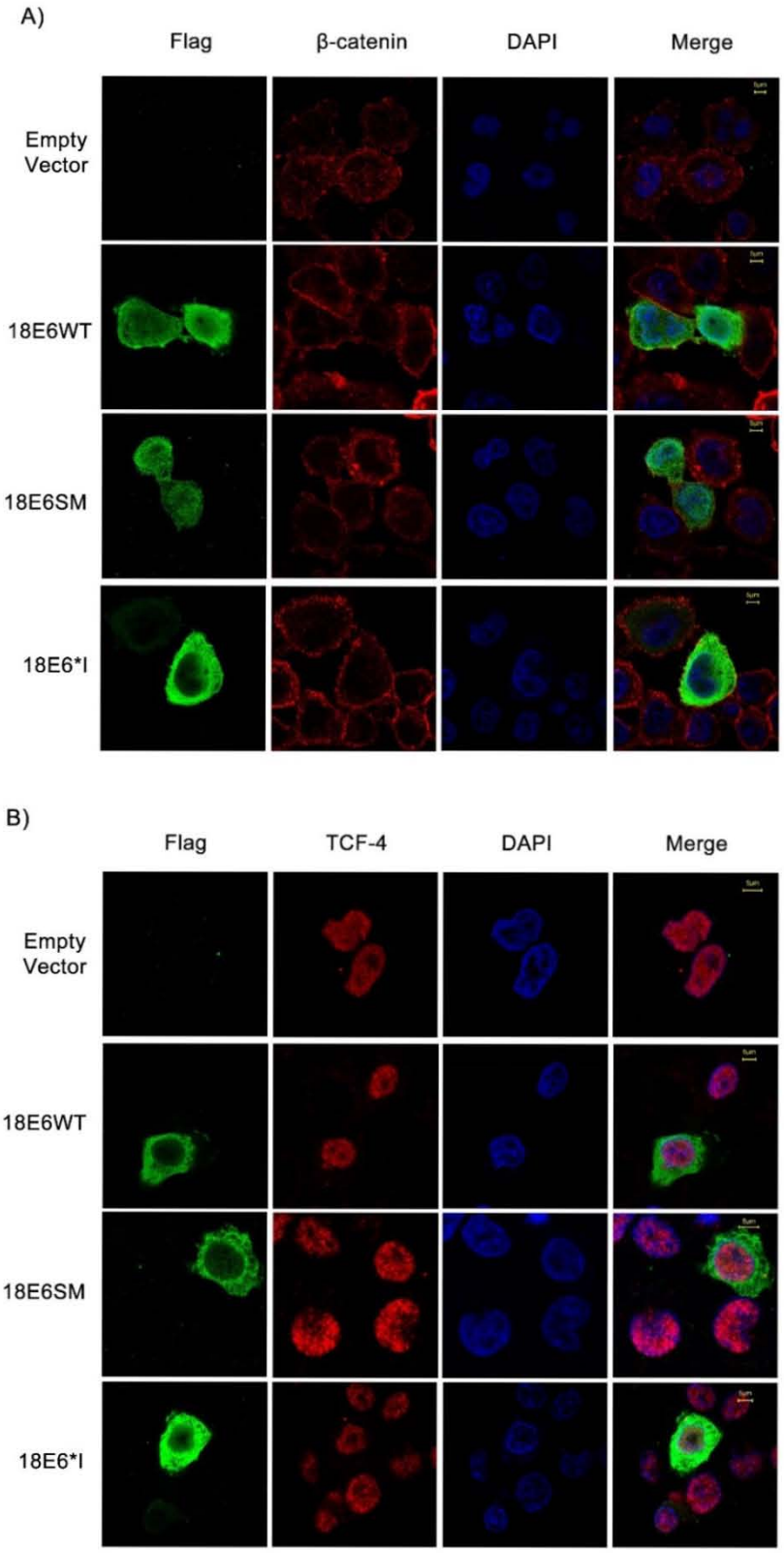

Figure 3. E6 proteins do not alter subcellular distribution of β-catenin or TCF-4. C33A cells were transfected with plasmids encoding 18E6WT, 18E6SM, or 18E6*I as indicated. 48 h post-transfection cells were fixed, and immunofluorescence stain was performed using specific antibodies against β-catenin (**A**) or TCF-4 (**B**) (Red) and FLAG (Green). Cells were also stained with DAPI (Blue) to visualize the nuclei. Images were acquired by confocal microscope. Data from three independent experiments were collected with a 63× objective oil immersion lens. Scale bar size 5 μm.

Figure 3. E6 proteins do not alter subcellular distribution of β-catenin or TCF-4. C33A cells were transfected with plasmids encoding 18E6WT, 18E6SM, or 18E6*I as indicated. 48 h post-transfection cells were fixed, and immunofluorescence stain was performed using specific antibodies against β-catenin (**A**) or TCF-4 (**B**) (Red) and FLAG (Green). Cells were also stained with DAPI (Blue) to visualize the nuclei. Images were acquired by confocal microscope. Data from three independent experiments were collected with a 63× objective oil immersion lens. Scale bar size 5 μm.

2.3. E6 Proteins Interact with the Wnt Activation Complex In Vivo and In Vitro

Previous reports demonstrate that HPV-16 E6 interacts with members of the Wnt signaling pathway, such as Dvl2 (Dishevelled Segment Polarity Protein 2) [23]. To investigate a further interaction with β-catenin and TCF-4, immunoprecipitation, assays were performed in C33A cells transfected with the different E6 expressing plasmids. After 48 h post-transfection, cell protein lysates were obtained and incubated with anti-β-catenin or anti-TCF-4 specific antibodies to immunoprecipitate these proteins. Afterwards, a western blot with anti-FLAG antibody was performed to assess the binding of the E6 proteins with β-catenin or TCF-4. As observed in Figure 4A,B, the immunoblot revealed that 16E6, 18E6 full-length, and 18E6*I proteins were able to bind to β-catenin (94 kDa band) and TCF-4 (60 kDa band), respectively.

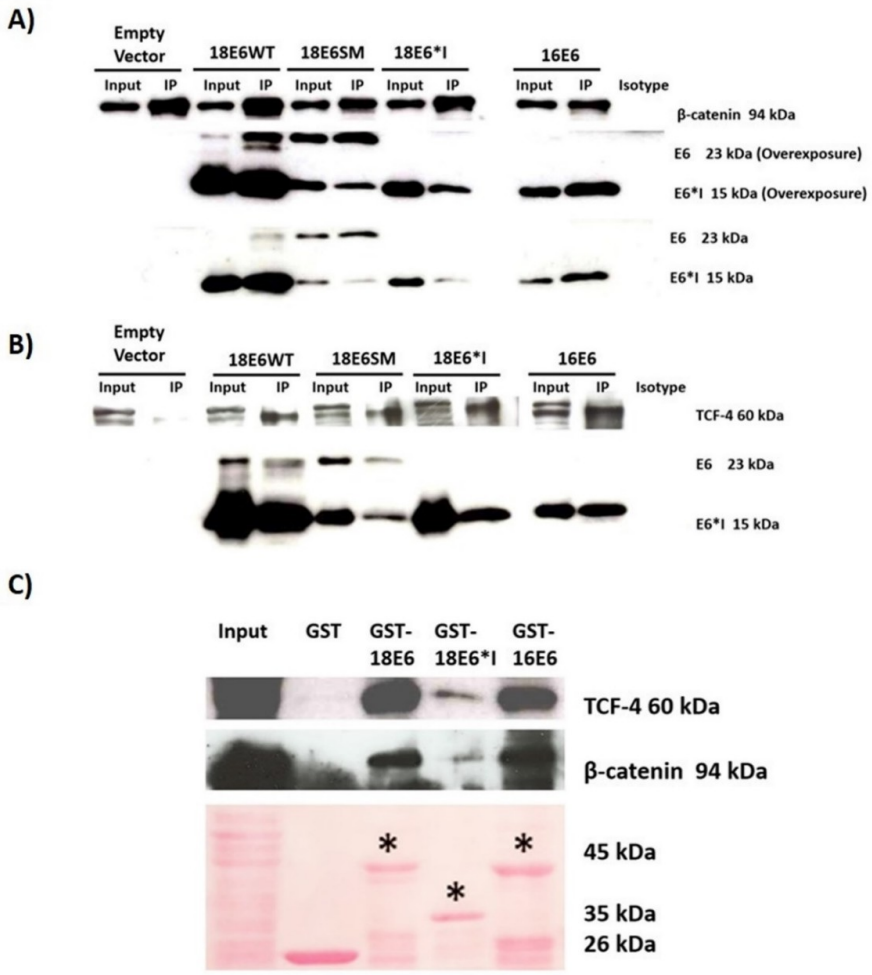

Figure 4. E6 and E6*I proteins interact with β-catenin and the transcriptional factor, TCF-4, in vivo and in vitro. C33A cells were transfected with different E6 expressing vectors, and 48 h post-transfection, protein lysates were obtained. (**A**) β-catenin and (**B**) TCF-4 were immunoprecipitated with the appropriate antibodies. The immuno-complexes were analyzed by Western blot using anti-β-catenin and anti-TCF-4 antibodies to detect the immunoprecipitated protein, and with an anti-FLAG to detect E6 proteins. Image shows a representative experiment of three performed. For comparison, 10% of protein used for immunoprecipitation (input) and the precipitation with an irrelevant IgG antibody (isotype) are shown. An overexposure of E6 proteins in shown in panel A. (**C**) Purified GST-18E6, GST-18E6*I, and GST-16E6 recombinant proteins were incubated with C33A protein extracts, while GST purified protein was used as a control. Immunoblots were performed using anti-β-catenin and anti-TCF-4 antibodies. 10% of protein extract was used as input. Lower panel shows Ponceau S red staining of a representative nitrocellulose membrane. Asterisks (*) show the E6 recombinant proteins.

These results were further confirmed by GST pull down assays using C33A lysates and GST-E6 fusion proteins (Figure 4C), where recombinant proteins bound to β-catenin and TCF-4. These data suggest that the E6 proteins regulate the Wnt/β-catenin cell signaling pathway through the interaction with the TCF-4 activation complex.

*2.4. E6 and E6*I from HPV-18 Increase TCF-4 Protein Stability*

To further determine the effect of the interaction of HPV-18 E6 and E6*I with TCF-4, we evaluated the TCF-4 stability through half-life determination assay. C33A cells were transfected with E6 or E6*I expressing plasmids, and 48 h post-transfection, cells were treated with 200 μg/mL of cycloheximide and the TCF-4 degradation rate was evaluated at 0, 6, and 12 h post-treatment. Overtime, it was observed that TCF-4 protein levels decreased considerably in E6 non-transfected cells after 6 and 12 h (Figure 5A,B). Interestingly, TCF-4 protein levels were maintained in the presence of E6 and E6*I proteins after 6 h, reaching up to 4.37- to 7.25-fold, compared to cells transfected with the empty vector. Finally, TCF-4 protein levels were higher at 12 h in 18E6WT expressing cells compared to those transfected with the control vector. These data strongly suggest that the half-life of TCF-4 is elongated in E6 and E6*I expressing cells, and that such an effect could be explained through the E6/E6*I-TCF-4 interaction.

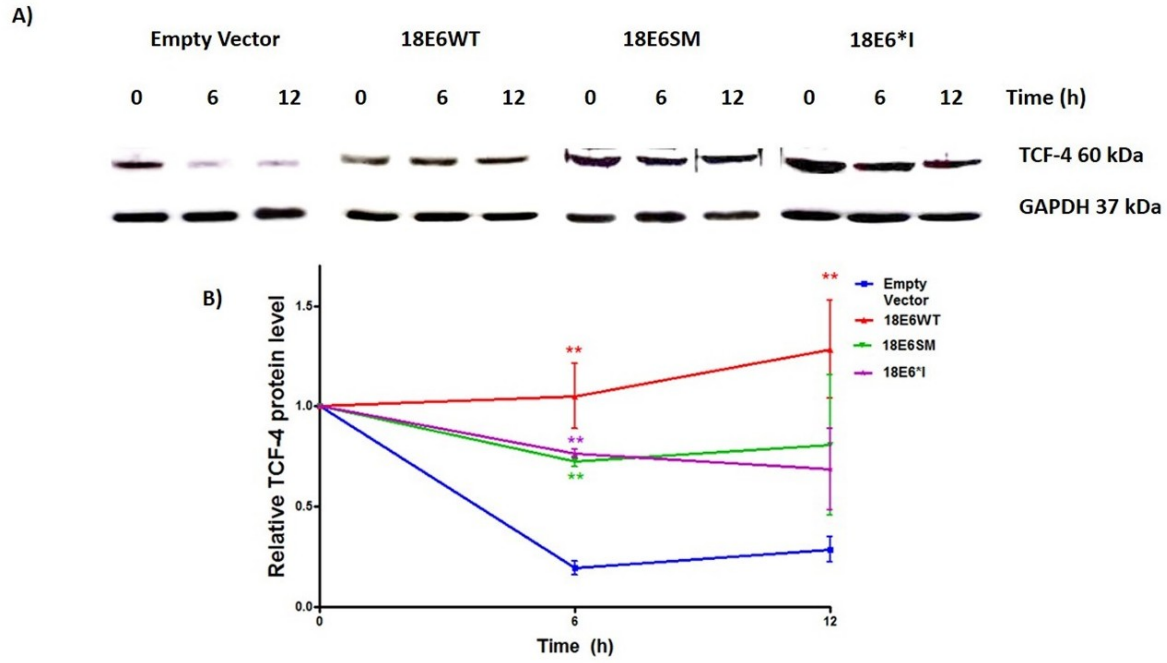

Figure 5. HPV-18 E6 proteins augment TCF-4 stability. C33A cells were transfected with E6 expressing plasmids. 48 h post-transfection, 200 μg/mL of cycloheximide was added to the culture medium. Protein extracts were obtained at 0, 6, and 12 h after treatment. (**A**) A representative immunoblot is shown with the different treatments. In non-E6 transfected cells, the TCF-4 levels were diminished at 6 and 12 h post-treatment, in contrast to E6 expressing cells, where TCF-4 levels remained without change at 6 and 12 h. (**B**) Graph showing the data as the mean and ± SD of three independent experiments. One-way ANOVA and a Tukey's post-hoc test, ** $p < 0.001$ versus empty vector values.

*2.5. HPV-18 E6 and E6*I Increase Nuclear TCF-4 Protein Levels*

To further determine the effect of E6 proteins on nuclear TCF-4 levels, soluble cellular fractionation was performed. As is shown in Figure 6A, full-length E6 is mainly located in the nucleus while E6*I is found in both the nucleus and cytoplasm. Interestingly, TCF-4 was significantly increased in the nucleus in both E6 and E6*I expressing cells (Figure 6A,B). This supports our data showing an increase in TCF-4 stability, which may lead to an enrichment of nuclear TCF-4.

Int. J. Mol. Sci. **2018**, *19*, 3153 8 of 20

increased in the nucleus in both E6 and E6*I expressing cells (Figure 6A,B). This supports our data showing an increase in TCF-4 stability, which may lead to an enrichment of nuclear TCF-4.

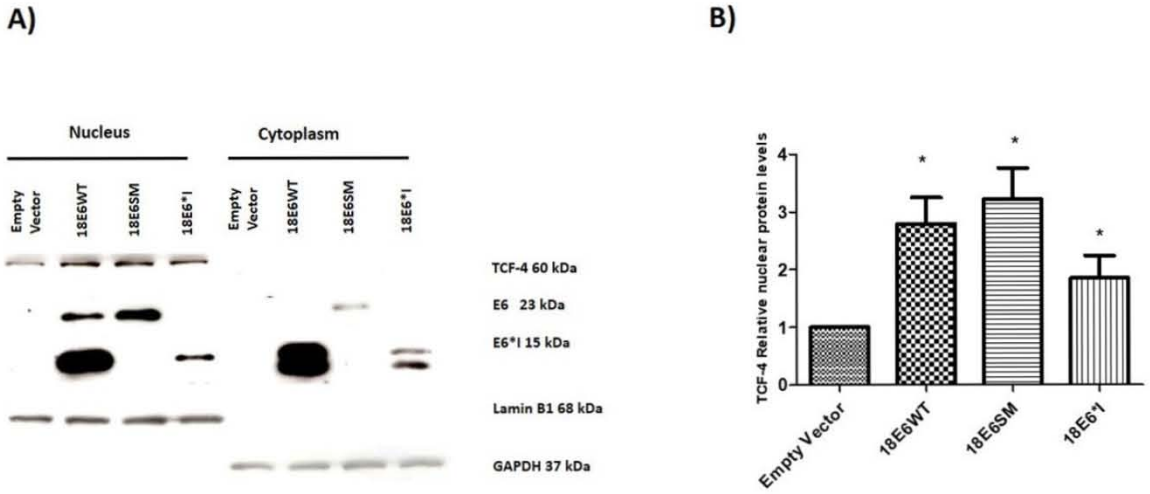

Figure 6. E6 proteins increase nuclear TCF-4 protein levels. (**A**) Representative immunoblot of TCF-4 and E6 proteins in nuclear and cytoplasmic soluble fractions of C33A cells transfected with E6 expressing plasmids. Lamin B1 and GAPDH proteins were used as nuclear and cytoplasmic load controls, respectively. (**B**) A densitometric analysis of relative nuclear TCF-4 levels shows an increase of TCF-4 protein levels in the presence of the E6 proteins. Data from three independent experiments were collected and graphed showing the mean and SD. Student's *t*-test analysis was performed, * $p < 0.05$ vs. empty vector values.

Figure 6. E6 proteins increase nuclear TCF-4 protein levels. (**A**) Representative immunoblot of TCF-4 and E6 proteins in nuclear and cytoplasmic soluble fractions of C33A cells transfected with E6 expressing plasmids. Lamin B1 and GAPDH proteins were used as nuclear and cytoplasmic load control, respectively. (**B**) A densitometric analysis of relative nuclear TCF-4 levels shows an increase of TCF-4 protein levels in the presence of the E6 proteins. Data from three independent experiments were collected and graphed showing the mean and SD. Student's *t*-test analysis was performed, * $p < 0.05$ vs. empty vector values.

*2.6. HPV-18 E6 and E6*I Proteins Bins to a TCF-4 Dependent Promoter In Vivo and In Vitro*

The effect of E6 proteins in *Sp5* expression was analyzed by qPCR. Figure 7A demonstrates that E6 proteins increase *Sp5* mRNA levels in C33A cells co-transfected with β-catenin. Therefore, we further analyzed whether E6 proteins could interact with the *Sp5* promoter, which is TCF-4-dependent. It was previously demonstrated that TCF-4 binds to a conserved sequence, A-C/G-A/T-C-A-A-A-G, found in TCF-4/β-catenin-dependent promoters, such as the *Sp5* gene promoter [24,25]. We used a pair of primers to amplify a *Sp5* promoter sequence flanking the −326 to −129 nucleotides, since this region contains two TCF-4 binding sites located at nucleotides, −303 to −296, and −149 to −142. Those binding sites were confirmed when the fragment was analyzed in silico using the informatics tool, Tfsitescan [26]. Co-transfections of E6-HA-tagged and β-catenin plasmids were performed in C33A cells. Chromatin immunoprecipitation assay (ChIP) revealed that 18E6 binds to the *Sp5* promoter (Figure 7B). TCF-4 also bound to this promoter, either in cells with the empty vector or 18E6-HA transfected cells. It is worth mentioning that the binding of 18E6 to the *Sp5* promoter is overwhelming, since virtually no amplification is seen when the immunoprecipitation is carried out with anti-HA in cells transfected with the empty vector.

The effect of E6 proteins in *Sp5* expression was analyzed by qPCR. Figure 7A demonstrates that E6 proteins increase *Sp5* mRNA levels in C33A cells co-transfected with β-catenin. Therefore, we further analyzed whether E6 proteins could interact with the *Sp5* promoter, which is TCF-4-dependent. It was previously demonstrated that TCF-4 binds to a conserved sequence, A-C/G-A/T-C-A-A-A-G, found in TCF-4/β-catenin-dependent promoters, such as the *Sp5* gene promoter [24,25]. We used a pair of primers to amplify a *Sp5* promoter sequence flanking the −326 to −129 nucleotides, since this region contains two TCF-4 binding sites located at nucleotides, −303 to −296, and −149 to −142. Those binding sites were confirmed when the fragment was analyzed in silico using the informatics tool, Tfsitescan [26]. Co-transfections of E6-HA-tagged and β-catenin plasmids were performed in C33A cells. Chromatin immunoprecipitation assay (ChIP) revealed that 18E6 binds to the *Sp5* promoter (Figure 7B). TCF-4 also bound to this promoter, either in cells with the empty vector or 18E6-HA transfected cells. It is worth mentioning that the binding of 18E6 to the *Sp5* promoter is overwhelming, since virtually no amplification is seen when the immunoprecipitation is carried out with anti-HA in cells transfected with the empty vector.

In order to confirm the obtained results, C33A cells were transfected with 18E6WT, 18E6SM, or 18E6*I expressing plasmids, and 48 h post-transfection, the DNA pull-down assay was performed. As expected, TCF-4 interacted with the *Sp5* promoter in all the tested samples (Figure 7C). Interestingly, E6 full-length as well as E6*I were also able to interact with the *Sp5* promoter, as a complex in the *Sp5* fragment (Figure 7D). Taken together these results indicate that E6 and E6*I proteins from HPV-18 interact with a TCF-4 dependent promoter, suggesting that such binding could be performed through TCF-4/E6/E6*I interactions, which may allow the up-regulation of the Wnt/β-catenin signaling pathway (Figure 7D).

In order to confirm the obtained results, C33A cells were transfected with 18E6WT, 18E6SM, or 18E6*I expressing plasmids, and 48 h post-transfection, the DNA pull-down assay was performed. As expected, TCF-4 interacted with the *Sp5* promoter in all the tested samples (Figure 7C). Interestingly, E6 full-length as well as E6*I were also able to interact with the *Sp5* promoter, as a complex in the *Sp5* fragment (Figure 7D). Taken together these results indicate that E6 and E6*I proteins from HPV-18 interact with a TCF-4 dependent promoter, suggesting that such binding could be performed through TCF-4/E6/E6*I interactions, which may allow the up-regulation of the Wnt/β-catenin signaling pathway (Figure 7D).

Int. J. Mol. Sci. **2018**, *19*, x FOR PEER REVIEW 9 of 20

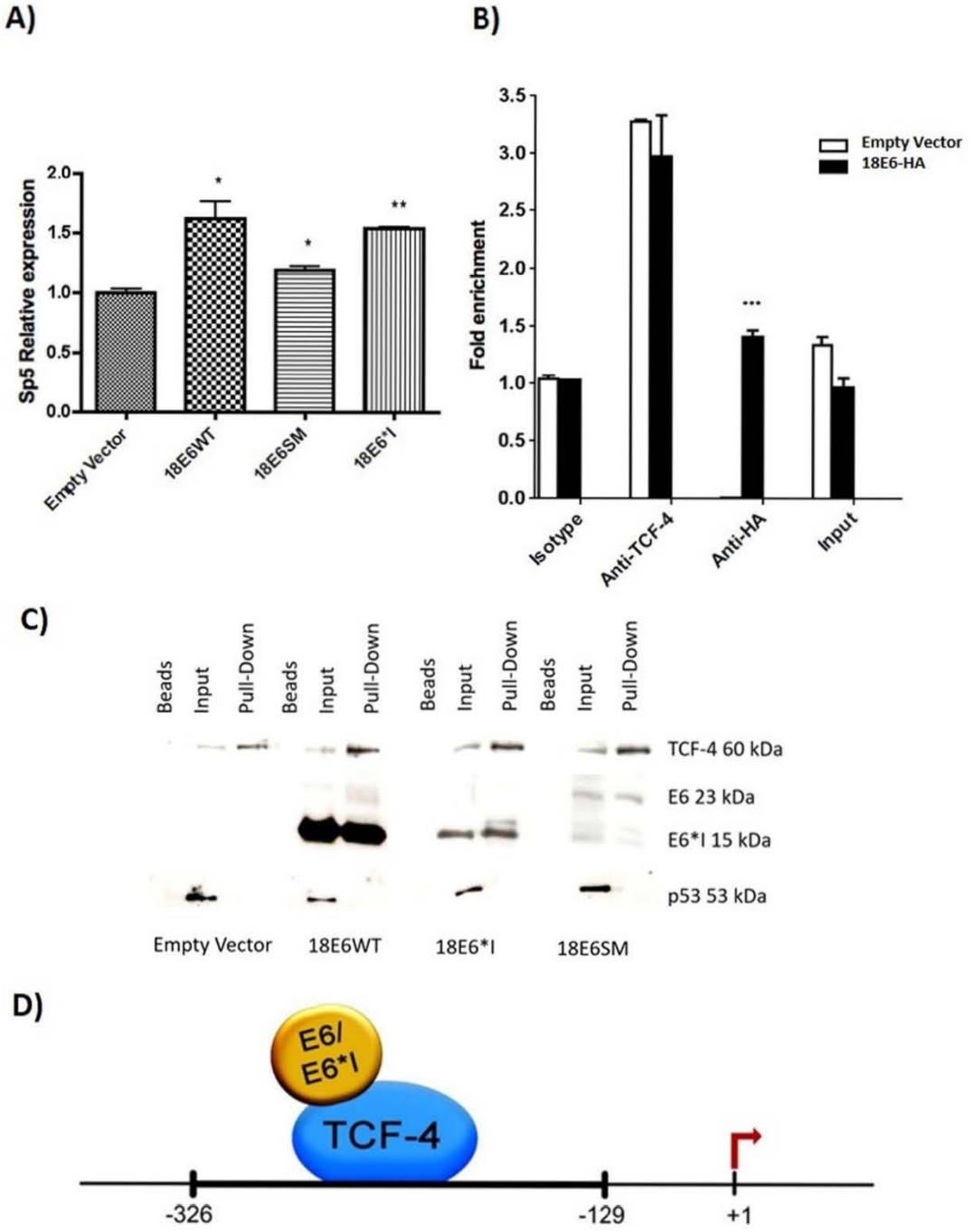

Figure 7. E6 and E6*I of HPV-18 interact with the *Sp5* promoter. C33A cells were co-transfected with β-catenin and E6 expressing plasmids as indicated: **(A)** E6 proteins increase *Sp5* relative expression as shown by qPCR analysis; * $p < 0.05$, ** $p < 0.01$, compared to the empty vector; **(B)** Chromatin immunoprecipitation assay (ChIP) shows that 18E6 binds to the *Sp5* promoter in vivo. Anti-HA antibody was used to detect E6-HA tagged protein, and anti-TCF-4 and anti-IgG antibodies were used as positive and isotype controls, respectively. 10% of input was analyzed. *** $p < 0.001$, of E6-HA compared to the empty vector. **(C)** C33A cells were transfected with 18E6WT, 18E6SM, or 18E6*I expressing plasmids, and 48 h post-transfection, a DNA pull-down assay was performed as indicated, in which TCF-4 interacts with the *Sp5* promoter only in the presence of both E6 and E6*I of HPV-18 with the *Sp5* promoter. The p53 transcription factor was used as a negative control as it does not bind to the *Sp5* promoter. **(D)** Schematic showing the suggested interactions of E6 and E6*I of HPV-18 with TCF-4 dependent promoter, proposing a possible mechanism of Wnt signaling regulation by E6 proteins.

2.7. HPV-18 E6 and E6*I Proteins Induce Cell Proliferation in Cooperation with β-Catenin Overexpression

*2.7. HPV-18 E6 and E6*I Proteins Induce Cell Proliferation in Cooperation with β-Catenin Overexpression*

Finally, to determine the contribution of E6 proteins in the Wnt/β catenin signaling pathway, MTS and crystal violet proliferation assays were performed in C33A cells co-transfected with β-catenin. As shown in Figure 8A,B, when E6 proteins were transfected alone, there was an increase in proliferation of between 70 and 85% in MTS assays, while crystal violet assays showed an increase of only 20–30% in relation to the empty vector. Additionally, transfection of β-catenin alone showed an increase in proliferation of 97% in MTS assays and 51% in crystal violet assays. Furthermore, when both E6 and E6*I and β-catenin were co-transfected, there was a further increase in proliferation of 40–50% in MTS assays, as compared to β-catenin alone, while the increase found using crystal violet was of 15–30%. This suggests that E6 proteins cooperate with β-catenin to promote the proliferation of these cells.

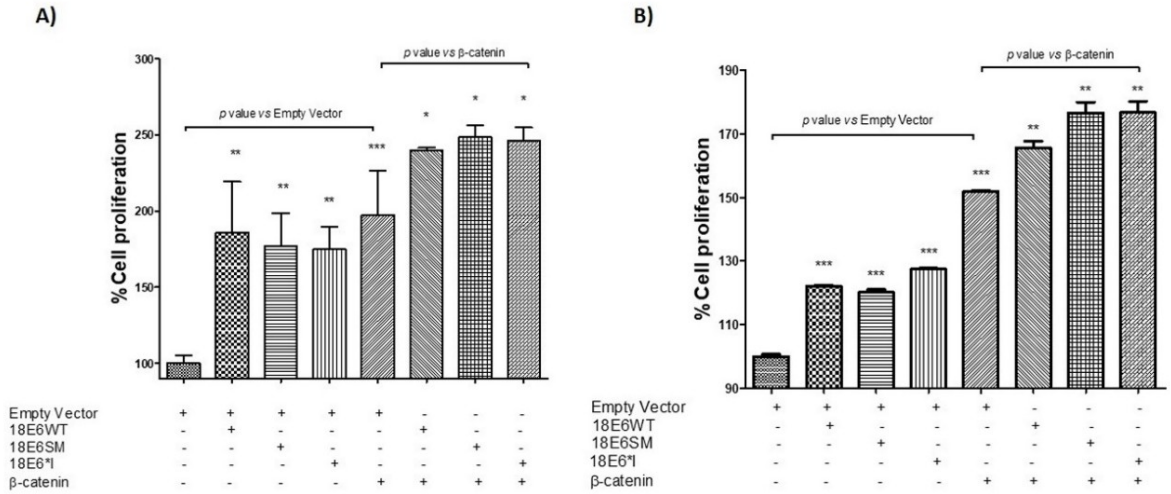

Figure 8. HPV-18 E6 and E6*I alone or in combination with β-catenin increase cell proliferation. C33A cells were transfected with the indicated plasmids, and 24 h post-transfection were seeded into a 96 well plate. Then, experiments were assessed after 72 h either by (**A**) MTS (3-(4,5-dimethylthiazol-2-yl)-5-(3-carboxymethoxyphenyl)-2-(4-sulfophenyl)-2H-tetrazolium, inner salt) or (**B**) Crystal violet assays. Data from three independent experiments were collected and graphed showing the mean and ± SD. *t* student analysis was performed, * $p < 0.05$, ** $p < 0.001$ and *** $p < 0.0001$ vs. empty vector values.

2.8. HPV-18 E6 Variants Differentially Modulate TCF-4-Mediated Transcription

It has been proposed that HPV variants of the same type may present distinct biological behaviors conferring different pathogenic risks [17,27,28]. To determine whether HPV-18 E6 variations differentially induce TCF-4 transcriptional activity, we tested the E6Af variant belonging to the African phylogenetic branch and harbors genomic variations that lead to amino acidic changes, compared to the reference variant, E6AsAi, that in this study, is also shown as 18E6WT [17]. HPV-18 E6Af and E6AsAi expressing plasmids were transfected in C33A cells and co-transfected with the TCF-4-dependent luciferase reporter plasmid (TOPFLASH), β-galactosidase reporter, and, in some cases, with β-catenin plasmids, as indicated. Protein expression of E6 variants was evaluated by immunoblot as shown in Figure 9A. E6Af was able to augment TCF-4 transcriptional activity up to 2.8-fold, higher than the 1.5-fold induction observed for E6AsAi. These effects were also evident when β-catenin was added, where E6Af reached up to 2.25-fold induction, while E6AsAi showed a 1.6-fold induction above exogenous β-catenin. These results show that HPV-18 E6 variants differentially induce TCF-4 transcriptional activation (Figure 9B). However, when the levels of Wnt target native genes were analyzed by qPCR, both E6 variants were able to enhance the expression of *Axin2* and *Cyclin D1*, with no significant differences among them, as shown in (Figure 9C,D).

Int. J. Mol. Sci. **2018**, *19*, x FOR PEER REVIEW 11 of 20
Int. J. Mol. Sci. **2018**, *19*, x FOR PEER REVIEW 11 of 20

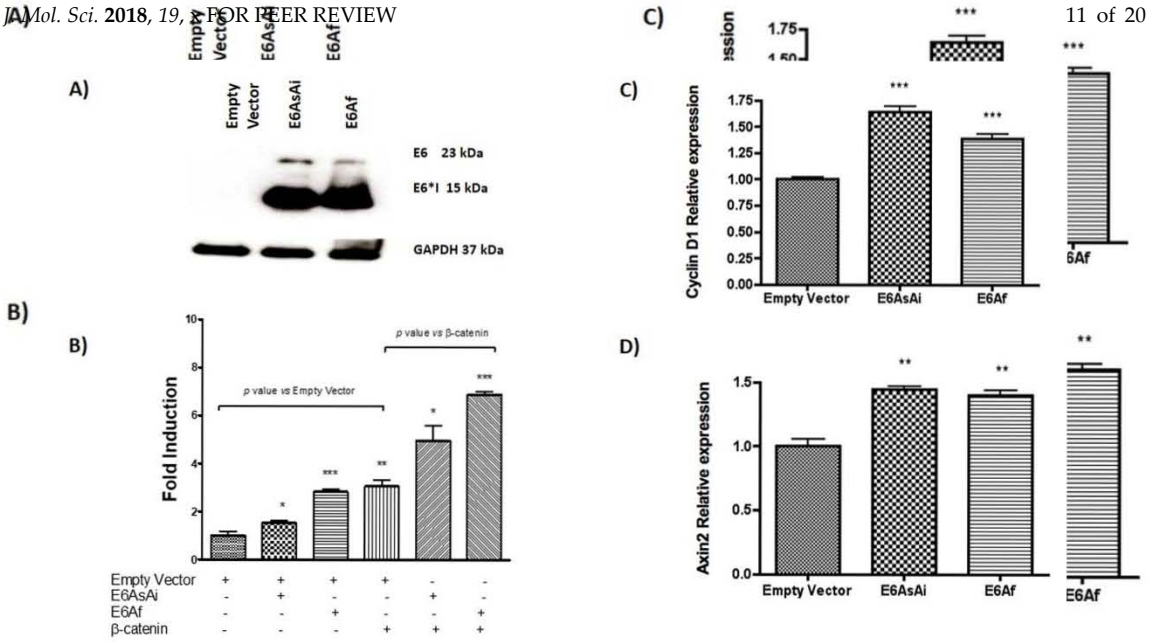

Figure 9. HPV-18 E6AsAi and E6Af variants modulate TCF4 transcriptional activity. (**A**) HPV-18 E6AsAi and E6Af protein expression in C33A transfected cells. (**B**) C33A cells were transfected with E6AsAi, E6Af, alone or combined with β-catenin expressing plasmids, and co-transfected with TCF-4 transcriptional reporter plasmid (TOPFLASH) and β-galactosidase reporter vector as indicated. Cyclin D1 and D1 mRNA (**C**) and protein (**D**) expression was analyzed by qPCR and Western blot, respectively. The means and SD of three independent experiments are depicted in each graph. Student *t* test was performed to evaluate the significant differences, the values are represented as $^{*}p < 0.05$; $^{**}p < 0.0001$; $^{***}p < 0.00001$.

2.9. HPV-18 Intratype Variants Interact with β-Catenin and TCF-4

In order to demonstrate the interaction of β-catenin and TCF-4 proteins with E6AsAi or E6Af variants, immunoprecipitation assays were done. C33A cells were transfected with E6AsAi and E6Af expressing plasmids, and 48 h post-transfection cells were lysed and incubated with anti-TCF-4 and anti-β-catenin specific antibodies. Immunoblot analysis revealed that both E6 variants were able to interact with both β-catenin (Figure 10A,B) and TCF-4 (Figure 10C,D), respectively. Therefore, although the tested E6 variants showed a differential effect in other cellular pathways [29], no changes were observed in the ability to bind TCF-4/β-catenin nor in the levels of the regulated genes.

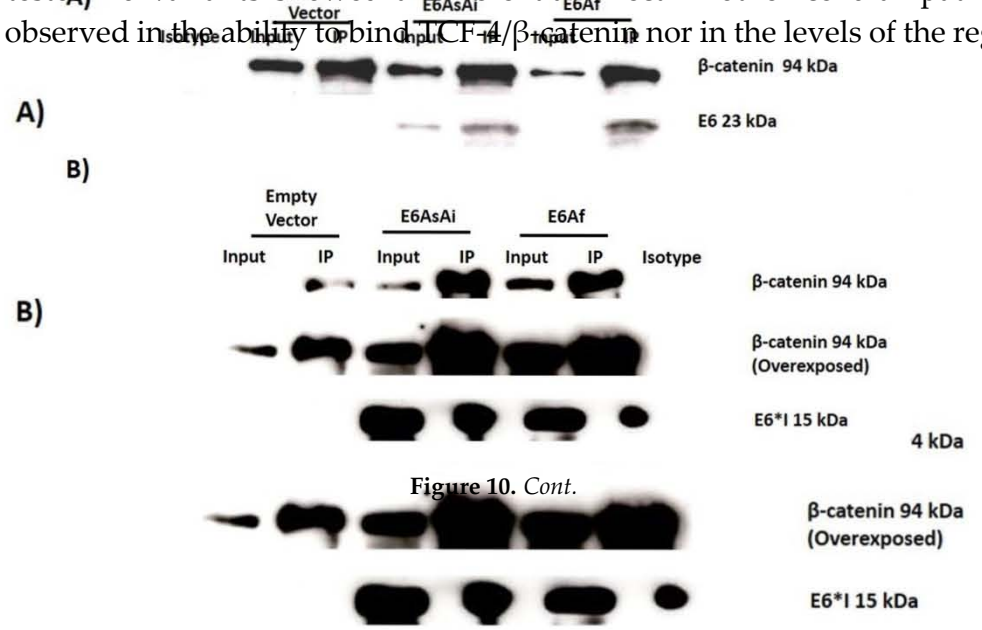

Figure 10. *Cont.*

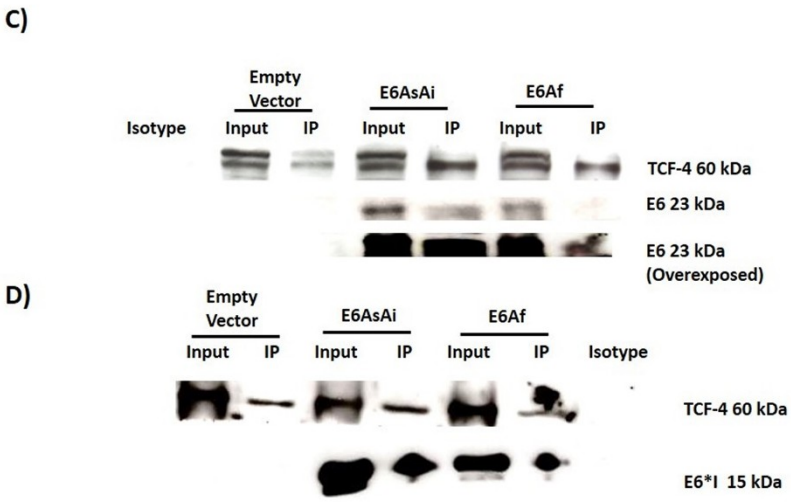

Figure 10. HPV-18 E6 variants interact in vivo with β-catenin and TCF-4. C33A cells were transfected with the E6 variant plasmids. 48 h post-transfection, cell lysates were collected and immunoprecipitated with anti-β-catenin (**A**,**B**) and anti-TCF-4 (**C**,**D**). Immunoblots show an interaction of E6 (**A**,**C**) and E6*I (**B**,**D**) with both proteins. Overexposures of β-catenin and E6 proteins are shown in panel B and C, respectively. Representative images are shown from three experiments performed. 10% of protein used for immunoprecipitation is indicated as input, and an irrelevant antibody was used (isotype).

3. Discussion

The continuous expression of the E6 and E7 oncoproteins is necessary for cellular transformation and immortalization in HPV-related cancers. E6 oncoprotein contributes to malignant progression through targeting a set of cellular proteins [30]. A common feature of E6-E7 mRNA from HR-HPV is to produce small isoforms termed E6*, whose cellular functions are poorly understood [18]. It is proposed that HPV-18 E6*I antagonizes the effects of full-length E6 [31], while some studies show that E6* has proper E6-independent functions [32–35]. E6* interacts with E6 and E6AP [31], and also downregulates PDZ domain containing proteins, such as hDlg, Scrib, MAGI-1, and MAGI-2 [32]. It has also been demonstrated that E6* modulates apoptosis related-proteins, since it binds to procaspase 8, affecting its stability [36]. Our research group previously showed that E6* induces the activation and nuclear translocation of the procaspase 8, without inducing cell death [33]. These findings suggest that E6* isoforms may, in a way that has not yet been described, cooperate with E6 in the malignant progression.

An aberrant activation of the Wnt cell signaling pathway has been described during cervical carcinogenesis [9,20,37] and a role of HPV-16 E6 in this activation has been proposed in cellular models [8,21,22,38]. Nevertheless, the effect of HPV-18 E6 and E6*I in this pathway has not yet been analyzed.

In the present study, we demonstrate that E6*I hyperactivates the Wnt/β-catenin pathway. HPV-18 E6*I by itself enhanced the TCF-4 transcriptional activity in C33A-transfected cells in 1.5-fold compared to the control, and a similar effect was observed when 18E6WT was expressed. This suggests that E6*I cooperates with E6 full length in the TCF-4 response. In an attempt to increase the expression of E6 over E6*I, we used an E6 expressing plasmid whose expression is enriched with full-length E6 (18E6SM). The mutation in the 18E6SM plasmid allows the expression of higher amounts of E6 full-length, although some E6*I is still produced since another donor site not yet described could be used during the splicing process. When transfecting this plasmid there was a slight increment in the TCF-4 transcriptional regulation, although non-significant, in relation to the control vector.

Interestingly, when the Wnt pathway was over activated with the co-transfection of β-catenin, TCF-4 transcriptional activation was enhanced in the presence of E6 or E6*I proteins, supporting that E6*I and E6 collaborate in Wnt/β-catenin pathway activation. We also found that 16E6 induced a

higher response in TCF-4 activation, reaching up to a 2.5-fold induction, and this effect was slightly enhanced in the presence of exogenous β-catenin (3-fold). Our results are in agreement with previous reports, where three-fold-induction of the TCF-4 luciferase reporter was obtained in HEK293T cells ectopically expressing HPV-16 E6, the Wnt receptor HFz1, and the Wnt3a ligand [21]. Additionally, Bonilla-Delgado et al. (2012) [23] reported a 50-fold induction of the TCF-4-dependent response in COS-7 cells where HPV-16 E6 in combination with Dvl-2 and β-catenin were expressed. These data suggest that the cellular context and/or the method used for Wnt pathway activation play an important role in the effect induced by HPV E6.

The expression of TCF-4 target genes was evaluated in the presence of E6 and E6*I. In HPV-18, E6WT and E6SM expressing cells increased *Cyclin D1*, *Axin2*, and *Sp5* expression, in agreement with a previous report where E6 from HPV-16 was able to activate the Cyclin D1 promoter [21]. Moreover, in a transgenic mice model expressing HPV-16 E6, *Cyclin D1* was also up-regulated [23].

Among the Wnt target genes, *Axin2* is considered a tumor suppressor and mutations within this gene are associated to cancer development [39,40]. Axin2 is involved in a Wnt negative feedback loop that may limit the duration intensity or the spread of Wnt signaling [41,42]. It is interesting that even though E6*I increased *Cyclin D1* expression, it failed in promoting an up-regulation of *Axin2*. It is possible that E6 recruits co-regulators that are distinct to those recruited by E6*I that could be necessary for *Axin2* expression.

It has been previously demonstrated that HPV-16 E6 induces TCF-4 transcriptional activation without affecting β-catenin localization [21]. Consistent with this result, our findings revealed that although E6 and E6*I increase β-catenin and TCF-4 protein levels, they do not alter their subcellular localization. Moreover, our results demonstrate that both E6 and E6*I are able to complex with β-catenin and TCF-4 in vivo and in vitro, which are the main proteins involved in the TCF-4-dependent transcriptional activation.

We demonstrate that E6 and E6*I from HPV-18 not only interact with TCF-4, but are also able to induce the TCF-4 stabilization. Further studies are needed to elucidate whether the interaction of TCF-4 with E6 proteins is responsible for TCF-4 stabilization. Previous studies have shown that HPV-16 E6 together with the E3 ubiquitin ligase E6AP, and induce stabilization of other members of the canonical Wnt pathway, such as β-catenin, impacting in the activation of the pathway [22].

Furthermore, it is well known that when Wnt signaling is activated, β-catenin complexes with TCF-4 in the nucleus, inducing the TCF-4 transcriptional response [43]. Our findings revealed that both E6 and E6*I increased nuclear TCF-4 protein levels, which may directly impact in TCF-4 transcriptional activation. Remarkably, the DNA pull-down as well as the ChIP results revealed that both E6 and E6*I interact with a TCF-4 dependent promoter. This interaction could be explained through complexes formed by E6/E6*I and TCF-4 that recognize specific sequences located at the *Sp5* promoter or other TCF-4 response promoters. Additionally, in concordance with previous studies [44,45], we found an enhancement in proliferation in E6 expressing cells. Interestingly, proliferation enhanced by β-catenin was increased when E6 and E6*I were co-transfected. Therefore, our findings support a new mechanism by which E6 and also E6*I could modulate the Wnt/β-catenin pathway.

Since HPV intratype variations have been proposed to affect the HPV biological behavior, we were also interested in determining if HPV-18 E6 variants could differentially affect the Wnt/β-catenin signaling pathway. HPV intratype variants are defined as those containing less than 1% of nucleotide changes in coding regions [46,47]. Our group has previously reported that HPV-18 variants exhibit differences in E6 full-length/E6*I transcript proportions, impacting on p53 levels [17]. Moreover, E6 variants differentially modulate the Akt/PI3K signaling pathway [29]. Previous studies demonstrated that E6 variants from HPV-16 exert different abilities in the activation of the Wnt/β-catenin signaling pathway [48]. Luciferase assays described herein showed that HPV-18 E6 variants have a different ability to augment TCF-4 dependent transcription, showing that E6Af promoted at least a 2.8-fold induction of the reporter gene transcription compared with 1.5-fold of E6AsAi. In addition, when E6 variants where co-transfected with β-catenin, E6-Af and E6AsAi reached

up to a 2.25-fold and a 1.6- fold TCF-4 induction, respectively, compared to that obtained with β-catenin exogenous expression. Nevertheless, even though E6 variants displayed different levels of TCF-4 activation, both E6Af and E6AsAi enhanced the expression of *Axin2* and *Cyclin D1*, with no differences among them. This effect could be due to a distinct capacity of E6 variants to regulate or interact with other untested proteins involved in the activation of the Wnt signaling pathway. However, we observed that both E6 variants interact with TCF-4 and β-catenin in a similar manner, which reveals that aminoacidic changes in E6 variants do not influence at least in such a binding capacity.

In this study, we demonstrated that not only E6, but also E6*I from HPV-18 are able to up-regulate Wnt/β-catenin signaling, involving their interaction with the TCF-4 activation complex. Additional effects on members of the Wnt pathway should be analyzed in order to determine the specific contribution of E6 and the spliced isoform E6*I in cell transformation induced by the Wnt/β-catenin pathway.

4. Materials and Methods

4.1. Cell Culture and Transfection

C33A epithelial cells were acquired from ATCC and HaCaT were kindly provided by A. García-Carrancá (Instituto Nacional de Cancerología, Mexico City, Mexico) and were maintained in Dulbecco's modified Eagle medium (DMEM) supplemented with 10% of fetal bovine serum (FBS) in a humidified incubator with 5% CO_2. Transfections were performed using Lipofectamine 2000 reagent (Invitrogen, Carlsbad, CA, USA) according to the manufacturer's instructions.

4.2. Plasmids

18E6WT Open Reading Frame (ORF) was obtained and PCR-amplified from an HPV-18 positive cervical cancer biopsy, 18E6*I ORF was obtained by RT-PCR amplification from HeLa cells (HPV-18 positive), and 16E6 ORF was amplified by PCR from CaSki cells (HPV-16 positive). The HPV-18 E6 spliced mutant (18E6SM) sequence was amplified from the plasmid, pCAHPV18-E6sm [32]. 18E6SM harbors a mutation at the donor splicing site (G233A), favoring the expression of the E6 full-length. The HPV-18 E6Af variant (from African phylogenetic branch) and the E6AsAi variant (from Asian-Amerindian phylogenetic branch), which is the canonical reference variant, were PCR-amplified from DNA previously obtained from tumor biopsies [27]. All these fragments were purified and cloned into the p3x-FLAG CMV.10 expression vector (Sigma Aldrich, Sant Louis, MO, USA) Constructs were verified by DNA-sequencing. β-catenin, pCAHPV18-E6sm, and pGW1-18E6-HA (hemagglutinin-tagged) expressing plasmids were kindly provided by Lawrence Banks (ICGEB, Trieste, Italy). The TCF-4 reporter plasmid (TOPFLASH) containing two sets of 3 copies of TCF-4 binding sites upstream of Thymidine Kinase minimal promoter and luciferase ORF (Merck-Millipore, Burlington, MA, USA) was used to perform luciferase assays, and pCMV-β-galactosidase plasmid (Promega, Madison, WI, USA) was used to evaluate the efficiency of transfection.

4.3. Luciferase Reporter Activity Assays

C33A cells were seeded in a 24 well plate and transfected with a mix containing 50 ng of appropriate E6 expressing plasmid, 100 ng of TOPFLASH, and 1 ng of β-galactosidase reporter plasmid, either with 50 ng of empty vector or β-catenin, as indicated. Cell extracts were obtained 48 h post-transfection and assayed for luciferase and β-galactosidase activities (Tropix Inc, Bedford, MA, USA) using a Glomax 96-well plate luminometer (Promega, Madison, WI, USA) The presented data are shown as relative luciferase readouts comparing the E6 expressing cells vs the control vector, where luciferase readouts in empty vector condition were adjusted to 1 after normalizing with β-galactosidase activity. At least three independent experiments were performed, each by triplicate.

4.4. Quantitative Polymerase Chain Reaction (qPCR)

C33A cells were seeded in a 60 mm culture dish and transfected with 3 μg of each E6 plasmid. After 48 h post-transfection, cells were collected, and total RNA extraction was performed using the RNeasy mini kit (Qiagen, Hilden, Germany). The isolated RNA was treated with the DNAse Free DNA removal kit (Thermo Fisher Scientific, Waltham, MA, USA) and 400 μg of RNA was reverse-transcribed with random hexamers utilizing the GeneAmp RNA PCR Core Kit (Applied Biosystems, Foster City, CA, USA) For the *Cyclin D1* amplification, forward 5′-ACAAACAGATCATCCGCAAACAC-3′ and reverse 5′-TGTTGGGGCTCCTCAGGTTC-3′ primers were used. For *Sp5* amplification, forward 5′-TCGGACATAGGGACCCAGTT-3′ and reverse 5′-CTGACGGTGGGAACGGTTTA-3′. As a house keeping control, 18S mRNA was amplified with forward 5′-AACCCGTTGAACCCATT-3′ and reverse 5′-CCATCCAATCGGTAGTAGCG-3′ primers. SYBER select Master Mix (Applied Biosystems, Foster City, CA, USA) was utilized for qPCR reactions. For Axin2 amplification, Taqman probes were used (Applied Biosystems, Foster City, CA, USA): *Axin2* FAM (Hs00610344_m1) and 18S VIC (Hs99999901_s1) probes, with Taqman Gene Expression Master Mix for qPCR analysis (Applied Biosystems, Foster City, CA, USA). The results are presented as relative quantification using the $^{\Delta\Delta Ct}$ method.

4.5. Western Blotting

C33A cells were cultured in 60 mm dishes and transfected with 3 μg of the indicated plasmid. 48 h post-transfection, cells were lysed using 300 μL of RIPA buffer (100 mM Tris pH 8.0, 50 mM $NaCl_2$, 0.5% Nonidet P-40, and protease inhibitor cocktail (Roche, Basel, Switzerland)). 20 μg of cell protein extracts were analyzed by SDS-PAGE gels (10–12%) and transferred in a 0.22 μm nitrocellulose membrane (Bio-Rad). Membranes were blocked with 10% skimmed milk in TBS-0.1% Tween 20 per 1 h at room temperature, followed by incubation with the indicated primary antibody diluted 1:1000: anti-FLAG M2 (Sigma Aldrich, Sant Louis, MO, USA); anti-TCF-4 (Santa Cruz Biotechnologies, Dallas, TX, USA); anti-β-catenin (Santa Cruz Biotechnologies, Dallas, TX, USA). After washing three times with TBS-0.1% Tween 20, membranes were incubated with HPR-conjugated secondary anti-mouse antibody in a dilution 1:10000 (Santa Cruz, Biotechnologies, Dallas, TX, USA). Proteins were visualized utilizing the Immobilon Western (Millipore) according to the manufacturer's instructions. Western blots were performed at least three times each to assure result reproducibility.

4.6. Immunoprecipitation Assay

After 48 h of transfection with the indicated plasmid, 400 μg of protein extracts were incubated with 1μg of anti-β-catenin (Santa Cruz Biotechnologies, Dallas, TX, USA), anti-TCF-4 (Santa Cruz Biotechnologies, Dallas, TX, USA) antibodies, or IgG isotype control (Santa Cruz Biotechnologies, Dallas, TX, USA) overnight at 4 °C. A total of 20 μL of protein G-agarose beads (Upstate) were added to each sample and incubated at 4 °C, for 3 h. Complexes were washed three times with PBS-0.1% NP-40, resuspended in Laemmli sample buffer, and submitted to immunoblot analysis with anti-FLAG M2 (Sigma Aldrich, Sant Louis, MO, USA), anti-β-catenin (Santa Cruz Biotechnologies, Dallas, TX, USA), and anti-TCF-4 antibodies (Santa Cruz Biotechnologies, Dallas, TX, USA).

4.7. Analysis of TCF-4 Stability

C33A cells were seeded in 60 mm dishes and transfected with 3 μg of the indicated plasmid. 48 h post-transfection, cells were treated with 200 μg/mL of cycloheximide (an inhibitor of protein biosynthesis) (Sigma Aldrich, Sant Louis, MO, USA). After 0, 6, and 12 h post-treatment protein extracts were isolated using 2× Laemmli sample buffer (Bio-Rad, Hercules, CA, USA). Western blot assays were carried out in order to analyze the TCF-4 protein stability.

4.8. Immunofluorescence Staining and Cell Imaging

C33A and HaCaT cells were seeded over slides in 6 well plates and transfected with the indicated plasmids. After 48 h post-transfection cells were fixed with 3.7% paraformaldehyde in PBS for 10 min and permeabilized with PBS-0.1% Triton X-100. Then, cells were incubated with anti-FLAG M2 (Sigma Aldrich, Sant Louis, MO, USA) and anti-β-catenin (Cell Signaling) or anti-TCF-4 (Santa Cruz Biotechnologies, Dallas, TX, USA) antibodies overnight at 4 °C, after blocking with a 0.3% BSA solution. Cells were washed extensively with PBS and later incubated with anti-rabbit or anti-mouse antibodies conjugated to Rhodamine or Alexa-488 (Invitrogen, Carlsbad, CA, USA), respectively. Slides were washed and mounted with Prolong Diamond Antifade Mounting (Molecular Probes, Eugene, OR, USA) and then analyzed with a confocal microscope (Zeiss LSM 710 DUO, Oberkochen, Germany), with lasers giving excitation lines at 488 and 594 nm. Around twenty fields were observed for each treatment and representative images were acquired. The data of three independent experiments were collected with a 63× objective oil immersion lens.

4.9. GST- Fusion Protein Purification

E6 coding sequences were cloned into the pGEX-2T (GE) expression plasmid and the identity of each plasmid was verified by DNA-sequencing. GST-fusion protein production was induced in DH5-α *E. coli* strain with 10 mM IPTG. After three hours of induction, proteins were purified by lysing the cells using 1% triton/PBS and separating the insoluble fraction by centrifugation. Supernatant was then incubated with glutathione sepharose beads (Sigma Aldrich, Sant Louis, MO, USA), washed several times, and then re-suspended in 1 mL of 1% triton/PBS and analyzed by SDS-PAGE. Similar amounts of GST-fusion proteins were incubated overnight with 40 μg of C33A cellular protein extract, beads were then washed several times, and bound protein was analyzed by western blot using anti-TCF-4 and β-catenin antibodies.

4.10. Soluble Cell Fractionation Assay

C33A cells were seeded into a 60 mm dish and transfected with 3 μg of the indicated plasmid. 48 h post-transfection, cells were pelleted and washed with PBS (Phosphate-Buffered Saline). Cells were resuspended in 300 μL of lysis buffer (10 mm Tris pH 6.5, 27 mM $Na_2S_2O_5$, 1% Triton X-100, 10 mM $MgCl_2$, 25 mM Sucrose, and protease inhibitor cocktail) and incubated for 10 min at 4 °C with gentle agitation. The samples were centrifuged and the supernatants were collected (Cytoplasmic fraction). The pellets were resuspended in extraction buffer (10 mM HEPES pH 7.9, 10 mM KCl, 0.1 mM EDTA pH 8.0, 0.1 mM EGTA pH 8.0, and protease inhibitor cocktail) and centrifuged through a 0.34 M sucrose gradient. Then, the pellets were resuspended in RIPA buffer (100 mM Tris pH 8.0, 50 mM $NaCl_2$, 0.5% Nonidet P-40, and protease inhibitor cocktail (Roche, Basel, Switzerland)) (Nuclear fraction). The samples were analysed by immunoblot using anti-TCF-4 (Santa Cruz Biotechnologies, Dallas, TX, USA), anti-Lamin B1 (Abcam, Cambridge, UK), anti-GAPDH (Santa Cruz Biotechnologies, Dallas, TX, USA), and anti-FLAG M2 (Sigma Aldrich, Sant Louis, MO, USA) antibodies.

4.11. DNA Pull-Down Assay

A fragment of the *Sp5* promoter was amplified using the biotin labelled forward primer, 5′Bio-GGGTCTCCAGGCGGCAAG3′, and reverse specific primer, 5′-AGCGAAAGCAAATCCTTTGAATCC-3′. The probe was purified with the QIAquick PCR purification kit (Qiagen, Hilden, Germany) according to the manufacturer's protocol. C33A cells were seeded and transfected with 10 μg of each plasmid as indicated. 48 h post-transfection cells were lysed using the HKMG buffer (10mM HEPES pH 7.9, 100 mM KCl, 5 mM $MgCl_2$,1 mM DTT, 1 mM Na_3VO_4, 10% glycerol, 0.5% NP-40, and protease inhibitor cocktail), incubated 20 min at 4 °C, and then passed through a 25-gauge needle attached to a 1 mL syringe for 20 times. The lysates were centrifuged, and the supernatant were collected. The protein extracts were pre-cleared with 60 μL of Streptavidin

agarose beads (Invitrogen, Carlsbad, CA, USA) during 30 min at 4 °C and then were centrifuged and the supernatants were collected. For each sample, a total amount of 4 µg of biotin probes and 2.5 µg of Poly dI-dC (Sigma Aldrich, Sant Louis, MO, USA) were added and incubated overnight. 60 µL of Streptavidin agarose beads were added to each sample and incubated during 30 min at 4 °C. The samples were centrifuged, and the supernatants were discarded. The obtained beads were washed five times with the HKMG buffer and finally resuspended with 2× Laemmli sample buffer (Bio-Rad, Hercules, CA, USA). Then, Western blot assays were carried out.

4.12. Chromatin Immunoprecipitation Assay

C33A cells were seeded in a 100 mm plates and co-transfected with 7 µg of each 18E6HA and β-catenin expressing plasmids. 48 h post-transfection, cells were cross-linked with 1% of formaldehyde and quenched with 0.125 M of glycine. Cell lysates were obtained using a Lysis Buffer (1% SDS, 10 mM EDTA pH 8, 50 mM Tris HCl pH 8, and protease inhibitor cocktail) and sonicated with a Bioruptor Pico (Diagenode, Denville, NJ, USA), obtaining DNA fragments ranging from 200 to 500 bp. A total of 20 µg of chromatin per sample was used and diluted 1:5 with a Dilution Buffer (1% Triton X-100, 150 mM NaCl, 2 mM EDTA pH 8, 20 mM Tris HCl pH 8, and protease inhibitor cocktail). Then, all samples were precleared with 50 µL of protein G agarose/Salmon Sperm DNA beads (Millipore) during 3 h at 4 °C and centrifuged. Supernatants were incubated using anti-HA (Cell Signaling), anti-TCF-4 (Abcam, Cambridge, UK), or anti-IgG (Santa Cruz Biotechnologies, Dallas, TX, USA) rabbit antibodies overnight at 4 °C. Further, 50 µL of protein G agarose/Salmon Sperm DNA (Millipore) was added and incubated during 3 h at 4 °C. Samples were centrifuged, and the beads were washed four times with Wash Buffer I (1% Triton X-100, 0.1% SDS, 150 mM NaCl, 2 mM EDTA pH 8, 20 mM Tris-HCl pH 8, and protease inhibitor cocktail) and once with Wash Buffer II (1% Triton X-100, 0.1% SDS, 500 mM NaCl, 2 mM EDTA pH 8, 20 mM Tris-HCl pH 8, and protease inhibitor cocktail). Immunoprecipitated complexes were eluted with the Elution Buffer (1% SDS, 100 mM $NaHCO_3$) and de-crosslinked with 200 mM NaCl for 5 h at 65 °C. All samples were treated with RNAse (200 µg) and Proteinase K (160 µg). DNA fragments were obtained using the phenol/chloroform protocol. Further, qPCR was performed to evaluated proteins interaction with *Sp5* promoter using specific primers: Forward 5′-GGGTCTCCAGGCGGCAAG-3′ and Reverse 5′-AGCGAAAGCAAATCCTTTGAATCC-3′. To analyze the data, the fold enrichment method was performed.

4.13. Proliferation Assays

C33A cells were seeded in a 60 mm dishes and transfected with 3 µg of E6 and β-catenin expressing plasmids, as indicated. After 24 h post-transfection, cells were harvested and seeded in a 96-well plate for 72 h. The MTS (3-(4,5-dimethylthiazol-2-yl)-5-(3-carboxymethoxyphenyl)-2-(4-sulfophenyl)-2*H*-tetrazolium, inner salt) assays were performed using the CellTiter 96 Aqueous One Solution Cell Proliferation kit (Promega, Madison, WI, USA), according to the manufacturer's instructions.

For crystal violet assays, cells were fixed with 10% of formol/PBS for 30 min at room temperature while shaking. Cells were then stained with crystal violet/PBS for 15 min. After several washes, cells were treated with acetic acid/PBS and then measured at 490 nm. The data were graphed to determine the percentage of cell proliferation for each assay condition.

4.14. Statistical Analysis

Data showing the effects of HPV-18 E6 and E6*I and HPV-16 E6 on TCF-4 in the different assays are presented as mean ± SD. p was calculated by Student's t-test or ANOVA Tuckey's post-hoc analysis. Significance differences were accepted at $p \leq 0.05$, as indicated.

Supplementary Materials: Supplementary materials can be found at http://www.mdpi.com/1422-0067/19/10/3153/s1.

Author Contributions: J.O.M.-B., L.O.-N., L.J.C.-M. carried out the experiments and analyzed the data. A.L.-S. performed the confocal microscopy acquisition and analysis of the images. A.C.-P., J.M.-M. and C.G.-E. critically revised the manuscript and participated in data interpretation. M.L. conceived and designed the study, directed and wrote the manuscript.

Funding: This work was partially supported by CONACyT grant CB-166808 and by Instituto Nacional de Cancerología, México (017/007/IBI) (CEI/1144/17).

Acknowledgments: J. Omar Muñoz-Bello is a Ph.D. student from Programa de Doctorado en Ciencias Biomédicas, Universidad Nacional Autónoma de México (UNAM), and received a fellowship from CONACyT (Scholarship No. 269303). We acknowledge Dr. Miguel Tapia from Unidad de Microscopía, MSc. Patricia de la Torre from Unidad de Secuenciación, Instituto de Investigaciones Biomédicas, UNAM, for technical support, and Rocío Morales-Bárcenas (INCan) for citometry technical support.

Conflicts of Interest: The authors declare no conflict of interest.

References

1. Clevers, H.; Nusse, R. Wnt/β-catenin signaling and disease. *Cell* **2012**, *149*, 1192–1205. [CrossRef] [PubMed]
2. Nusse, R. Wnt signaling. *Cold Spring Harb. Perspect. Biol.* **2012**, *4*. [CrossRef] [PubMed]
3. Nusse, R. The Wnt Homepage. Available online: http://web.stanford.edu/group/nusselab/cgi-bin/wnt/ (accessed on 9 April 2017).
4. Zhan, T.; Rindtorff, N.; Boutros, M. Wnt signaling in cancer. *Oncogene* **2017**, *36*, 1461–1473. [CrossRef] [PubMed]
5. Deitrick, J.; Pruitt, W.M. Wnt/β Catenin-Mediated Signaling Commonly Altered in Colorectal Cancer. *Prog. Mol. Biol. Transl. Sci.* **2016**, *144*, 49–68. [CrossRef] [PubMed]
6. Takigawa, Y.; Brown, A.M.C. Wnt signaling in liver cancer. *Curr. Drug Targets* **2008**, *9*, 1013–1024. [CrossRef] [PubMed]
7. Khramtsov, A.I.; Khramtsova, G.F.; Tretiakova, M.; Huo, D.; Olopade, O.I.; Goss, K.H. Wnt/beta-catenin pathway activation is enriched in basal-like breast cancers and predicts poor outcome. *Am. J. Pathol.* **2010**, *176*, 2911–2920. [CrossRef] [PubMed]
8. Rampias, T.; Boutati, E.; Pectasides, E.; Sasaki, C.; Kountourakis, P.; Weinberger, P.; Psyrri, A. Activation of Wnt signaling pathway by human papillomavirus E6 and E7 oncogenes in HPV16-positive oropharyngeal squamous carcinoma cells. *Mol. Cancer Res.* **2010**, *8*, 433–443. [CrossRef] [PubMed]
9. Rodríguez-Sastre, M.A.; González-Maya, L.; Delgado, R.; Lizano, M.; Tsubaki, G.; Mohar, A.; García-Carrancá, A. Abnormal distribution of E-cadherin and beta-catenin in different histologic types of cancer of the uterine cervix. *Gynecol. Oncol.* **2005**, *97*, 330–336. [CrossRef] [PubMed]
10. Bello, J.O.M.; Nieva, L.O.; Paredes, A.C.; Gonzalez, A.M.F.; Zavaleta, L.R.; Lizano, M. Regulation of the Wnt/β-Catenin Signaling Pathway by Human Papillomavirus E6 and E7 Oncoproteins. *Viruses* **2015**, *7*, 4734–4755. [CrossRef] [PubMed]
11. zur Hausen, H. Papillomaviruses and cancer: From basic studies to clinical application. *Nat. Rev. Cancer* **2002**, *2*, 342–350. [CrossRef] [PubMed]
12. Smith, J.S.; Lindsay, L.; Hoots, B.; Keys, J.; Franceschi, S.; Winer, R.; Clifford, G.M. Human papillomavirus type distribution in invasive cervical cancer and high-grade cervical lesions: A meta-analysis update. *Int. J. Cancer* **2007**, *121*, 621–632. [CrossRef] [PubMed]
13. McLaughlin-Drubin, M.E.; Münger, K. Oncogenic activities of human papillomaviruses. *Virus Res.* **2009**, *143*, 195–208. [CrossRef] [PubMed]
14. Manzo-Merino, J.; Contreras-Paredes, A.; Vázquez-Ulloa, E.; Rocha-Zavaleta, L.; Fuentes-Gonzalez, A.M.; Lizano, M. The role of signaling pathways in cervical cancer and molecular therapeutic targets. *Arch. Med. Res.* **2014**, *45*, 525–539. [CrossRef] [PubMed]
15. Tang, S.; Tao, M.; McCoy, J.P.; Zheng, Z.-M. The E7 oncoprotein is translated from spliced E6*I transcripts in high-risk human papillomavirus type 16- or type 18-positive cervical cancer cell lines via translation reinitiation. *J. Virol.* **2006**, *80*, 4249–4263. [CrossRef] [PubMed]
16. Shirasawa, H.; Tanzawa, H.; Matsunaga, T.; Simizu, B. Quantitative detection of spliced E6-E7 transcripts of human papillomavirus type 16 in cervical premalignant lesions. *Virology* **1991**, *184*, 795–798. [CrossRef]

17. De la Cruz-Hernández, E.; García-Carrancá, A.; Mohar-Betancourt, A.; Dueñas-González, A.; Contreras-Paredes, A.; Pérez-Cardenas, E.; Herrera-Goepfert, R.; Lizano-Soberón, M. Differential splicing of E6 within human papillomavirus type 18 variants and functional consequences. *J. Gen. Virol.* **2005**, *86*, 2459–2468. [CrossRef] [PubMed]
18. Olmedo-Nieva, L.; Muñoz-Bello, J.; Contreras-Paredes, A.; Lizano, M. The Role of E6 Spliced Isoforms (E6*) in Human Papillomavirus-Induced Carcinogenesis. *Viruses* **2018**, *10*. [CrossRef] [PubMed]
19. Al-Shabanah, O.A.; Hafez, M.M.; Hassan, Z.K.; Sayed-Ahmed, M.M.; Abozeed, W.N.; Alsheikh, A.; Al-Rejaie, S.S. Methylation of SFRPs and *APC* genes in ovarian cancer infected with high risk human papillomavirus. *Asian Pac. J. Cancer Prev.* **2014**, *15*, 2719–2725. [CrossRef] [PubMed]
20. Uren, A.; Fallen, S.; Yuan, H.; Usubütün, A.; Küçükali, T.; Schlegel, R.; Toretsky, J.A. Activation of the canonical Wnt pathway during genital keratinocyte transformation: A model for cervical cancer progression. *Cancer Res.* **2005**, *65*, 6199–6206. [CrossRef] [PubMed]
21. Lichtig, H.; Gilboa, D.A.; Jackman, A.; Gonen, P.; Levav-Cohen, Y.; Haupt, Y.; Sherman, L. HPV16 E6 augments Wnt signaling in an E6AP-dependent manner. *Virology* **2010**, *396*, 47–58. [CrossRef] [PubMed]
22. Sominsky, S.; Kuslansky, Y.; Shapiro, B.; Jackman, A.; Haupt, Y.; Rosin-Arbesfeld, R.; Sherman, L. HPV16 E6 and E6AP differentially cooperate to stimulate or augment Wnt signaling. *Virology* **2014**, *468–470*, 510–523. [CrossRef] [PubMed]
23. Bonilla-Delgado, J.; Bulut, G.; Liu, X.; Cortés-Malagón, E.M.; Schlegel, R.; Flores-Maldonado, C.; Contreras, R.G.; Chung, S.-H.; Lambert, P.F.; Uren, A.; et al. The E6 oncoprotein from HPV16 enhances the canonical Wnt/β-catenin pathway in skin epidermis in vivo. *Mol. Cancer Res.* **2012**, *10*, 250–258. [CrossRef] [PubMed]
24. Takahashi, M.; Nakamura, Y.; Obama, K.; Furukawa, Y. Identification of SP5 as a downstream gene of the beta-catenin/Tcf pathway and its enhanced expression in human colon cancer. *Int. J. Oncol.* **2005**, *27*, 1483–1487. [PubMed]
25. Hatzis, P.; van der Flier, L.G.; van Driel, M.A.; Guryev, V.; Nielsen, F.; Denissov, S.; Nijman, I.J.; Koster, J.; Santo, E.E.; Welboren, W.; et al. Genome-wide pattern of TCF7L2/TCF4 chromatin occupancy in colorectal cancer cells. *Mol. Cell. Biol.* **2008**, *28*, 2732–2744. [CrossRef] [PubMed]
26. TFSiteScan. Available online: http://www.ifti.org/cgi-bin/ifti/Tfsitescan.pl (accessed on 5 August 2018).
27. Lizano, M.; Berumen, J.; Guido, M.C.; Casas, L.; García-Carrancá, A. Association between human papillomavirus type 18 variants and histopathology of cervical cancer. *J. Natl. Cancer Inst.* **1997**, *89*, 1227–1231. [CrossRef] [PubMed]
28. Lizano, M.; De la Cruz-Hernández, E.; Carrillo-García, A.; García-Carrancá, A.; Ponce de Leon-Rosales, S.; Dueñas-González, A.; Hernández-Hernández, D.M.; Mohar, A. Distribution of HPV16 and 18 intratypic variants in normal cytology, intraepithelial lesions, and cervical cancer in a Mexican population. *Gynecol. Oncol.* **2006**, *102*, 230–235. [CrossRef] [PubMed]
29. Contreras-Paredes, A.; De la Cruz-Hernández, E.; Martínez-Ramírez, I.; Dueñas-González, A.; Lizano, M. E6 variants of human papillomavirus 18 differentially modulate the protein kinase B/phosphatidylinositol 3-kinase (akt/PI3K) signaling pathway. *Virology* **2009**, *383*, 78–85. [CrossRef] [PubMed]
30. Moody, C.A.; Laimins, L.A. Human papillomavirus oncoproteins: Pathways to transformation. *Nat. Rev. Cancer* **2010**, *10*, 550–560. [CrossRef] [PubMed]
31. Pim, D.; Massimi, P.; Banks, L. Alternatively spliced HPV-18 E6* protein inhibits E6 mediated degradation of p53 and suppresses transformed cell growth. *Oncogene* **1997**, *15*, 257–264. [CrossRef] [PubMed]
32. Pim, D.; Tomaic, V.; Banks, L. The human papillomavirus (HPV) E6* proteins from high-risk, mucosal HPVs can direct degradation of cellular proteins in the absence of full-length E6 protein. *J. Virol.* **2009**, *83*, 9863–9874. [CrossRef] [PubMed]
33. Manzo-Merino, J.; Massimi, P.; Lizano, M.; Banks, L. The human papillomavirus (HPV) E6 oncoproteins promotes nuclear localization of active caspase 8. *Virology* **2014**, *450–451*, 146–152. [CrossRef] [PubMed]
34. Evans, W.; Filippova, M.; Filippov, V.; Bashkirova, S.; Zhang, G.; Reeves, M.E.; Duerksen-Hughes, P. Overexpression of HPV16 E6* Alters β-Integrin and Mitochondrial Dysfunction Pathways in Cervical Cancer Cells. *Cancer Genomics Proteomics* **2016**, *13*, 259–273. [PubMed]
35. Tungteakkhun, S.S.; Filippova, M.; Fodor, N.; Duerksen-Hughes, P.J. The full-length isoform of human papillomavirus 16 E6 and its splice variant E6* bind to different sites on the procaspase 8 death effector domain. *J. Virol.* **2010**, *84*, 1453–1463. [CrossRef] [PubMed]

36. Filippova, M.; Johnson, M.M.; Bautista, M.; Filippov, V.; Fodor, N.; Tungteakkhun, S.S.; Williams, K.; Duerksen-Hughes, P.J. The large and small isoforms of human papillomavirus type 16 E6 bind to and differentially affect procaspase 8 stability and activity. *J. Virol.* **2007**, *81*, 4116–4129. [CrossRef] [PubMed]
37. Ramos-Solano, M.; Meza-Canales, I.D.; Torres-Reyes, L.A.; Alvarez-Zavala, M.; Alvarado-Ruíz, L.; Rincon-Orozco, B.; Garcia-Chagollan, M.; Ochoa-Hernández, A.B.; Ortiz-Lazareno, P.C.; Rösl, F.; et al. Expression of WNT genes in cervical cancer-derived cells: Implication of WNT7A in cell proliferation and migration. *Exp. Cell Res.* **2015**, *335*, 39–50. [CrossRef] [PubMed]
38. Kuslansky, Y.; Sominsky, S.; Jackman, A.; Gamell, C.; Monahan, B.J.; Haupt, Y.; Rosin-Arbesfeld, R.; Sherman, L. Ubiquitin ligase E6AP mediates nonproteolytic polyubiquitylation of β-catenin independent of the E6 oncoprotein. *J. Gen. Virol.* **2016**, *97*, 3313–3330. [CrossRef] [PubMed]
39. Koch, A.; Hrychyk, A.; Hartmann, W.; Waha, A.; Mikeska, T.; Waha, A.; Schüller, U.; Sörensen, N.; Berthold, F.; Goodyer, C.G.; et al. Mutations of the Wnt antagonist AXIN2 (Conductin) result in TCF-dependent transcription in medulloblastomas. *Int. J. Cancer* **2007**, *121*, 284–291. [CrossRef] [PubMed]
40. Liu, W.; Dong, X.; Mai, M.; Seelan, R.S.; Taniguchi, K.; Krishnadath, K.K.; Halling, K.C.; Cunningham, J.M.; Boardman, L.A.; Qian, C.; et al. Mutations in AXIN2 cause colorectal cancer with defective mismatch repair by activating beta-catenin/TCF signalling. *Nat. Genet.* **2000**, *26*, 146–147. [CrossRef] [PubMed]
41. Leung, J.Y.; Kolligs, F.T.; Wu, R.; Zhai, Y.; Kuick, R.; Hanash, S.; Cho, K.R.; Fearon, E.R. Activation of AXIN2 expression by beta-catenin-T. cell factor. A feedback repressor pathway regulating Wnt signaling. *J. Biol. Chem.* **2002**, *277*, 21657–21665. [CrossRef] [PubMed]
42. Lustig, B.; Jerchow, B.; Sachs, M.; Weiler, S.; Pietsch, T.; Karsten, U.; van de Wetering, M.; Clevers, H.; Schlag, P.M.; Birchmeier, W.; et al. Negative feedback loop of Wnt signaling through upregulation of conductin/axin2 in colorectal and liver tumors. *Mol. Cell. Biol.* **2002**, *22*, 1184–1193. [CrossRef] [PubMed]
43. Shitashige, M.; Hirohashi, S.; Yamada, T. Wnt signaling inside the nucleus. *Cancer Sci.* **2008**, *99*, 631–637. [CrossRef] [PubMed]
44. Wang, S.; Pang, T.; Gao, M.; Kang, H.; Ding, W.; Sun, X.; Zhao, Y.; Zhu, W.; Tang, X.; Yao, Y.; et al. HPV E6 induces eIF4E transcription to promote the proliferation and migration of cervical cancer. *FEBS Lett.* **2013**, *587*, 690–697. [CrossRef] [PubMed]
45. Ben, W.; Yang, Y.; Yuan, J.; Sun, J.; Huang, M.; Zhang, D.; Zheng, J. Human papillomavirus 16 E6 modulates the expression of host microRNAs in cervical cancer. *Taiwan. J. Obstet. Gynecol.* **2015**, *54*, 364–370. [CrossRef] [PubMed]
46. Lizano, M.; Berumen, J.; García-Carrancá, A. HPV-related carcinogenesis: Basic concepts, viral types and variants. *Arch. Med. Res.* **2009**, *40*, 428–434. [CrossRef] [PubMed]
47. Burk, R.D.; Harari, A.; Chen, Z. Human papillomavirus genome variants. *Virology* **2013**, *445*, 232–243. [CrossRef] [PubMed]
48. Zehbe, I.; Lichtig, H.; Westerback, A.; Lambert, P.F.; Tommasino, M.; Sherman, L. Rare human papillomavirus 16 E6 variants reveal significant oncogenic potential. *Mol. Cancer* **2011**, *10*. [CrossRef] [PubMed]